UNIVERSIDADE DA BEIRA INTERIOR
Engenharia

Numerical analysis of slope failure in granitic soil slopes

Main types of instability and remediation measures

Manuel João Niza das Neves

Tese para obtenção do Grau de Doutor em

Engenharia Civil

(3º ciclo de estudos)

Orientador: Professor Catedrático Victor Manuel Pissarra Cavaleiro
Co-orientador: Professor Auxiliar Alexandre da Luz Pinto

Covilhã, Julho de 2015

“When calculating the stability of a slope,
one uses the ‘wrong’ slip circle
with the ‘wrong’ shear strength
to arrive to the satisfactory answer.”

Clayton, Mathews, & Simons (1995)

Acknowledgement

The work presented in this thesis has been carried out at the Geotechnical Division, Department of Civil Engineering and Architecture, Faculty of Engineering, Universidade da Beira Interior (UBI) under the supervision of Full Professor Dr. Victor Cavaleiro, as the main adviser, and Assistant Professor Alexandre Pinto as co-adviser. I am very grateful to their valuable guidance, discussions and encouragement throughout the study period and especially all contributions to this investigation. Appreciation by words is not sufficient to adviser Victor Cavaleiro who not only encouraged me to apply, but also made it possible for me to successfully complete this study.

I would also like to thank Assistant Professor Luís Pais for his valuable feedbacks, suggestions and comments during the study period, as well as my PhD colleagues in the Geotechnical Division, including Filipe Nunes, António Carvalho and José Riscado, for all their assistance and valuable inputs.

I am also very thankful to my colleagues within Jacobs UK, in particular Chris Currie, for all the help with the SLOPE/W modelling and to the company itself for facilitating me the use of their offices and resources to undertake this research.

Finally, a huge thank you note to my family. Their patience, encouragement and invaluable help and support through this journey have made it possible for me to complete this research despite of the distance that separates us.

Manuel João Niza das Neves

Covilhã, Portugal

July 2015

Abstract

Slope stability is a worldwide problem which above all affects people's safety. However, in tropical or temperate regions (such as the Mediterranean), a combination of their topographic, geologic and climate settings contributes to an increased landslide hazard. A full understanding of this topic, and what it entails, requires an accurate knowledge of its triggers and awareness to the different instability mechanisms that may occur. Furthermore, the instability phenomenon may present different particularities for distinct ground conditions, being of major significance in civil engineering, as it forms part of most construction works and mining activities, particularly in large scale geotechnical schemes, such as highways/railways, canals, tunnels, embankment dams and open pit mines.

This thesis is primarily focused on the stability assessment of slopes in granitic residual soils resorting to both limit equilibrium (LEM) and finite element (FEM) approaches. In order to do so, it makes use of one LEM based software (SLOPE/W) and one FEM based software (PLAXIS 2D). The LEM approach comprises three different formulations of the method of slices, which despite being based on the static of equilibrium of the soil mass, are constructed on different sets of assumptions which only allows them to partially fulfil the static equilibrium conditions. The FEM method, on the other hand, is based on the stress-strain relationship and constitutive law of the soils.

One of the aims of the study is to establish a comparison between not only different LEM methods but also between LEM and FEM approaches, whilst varying surcharge values and groundwater levels. The LEM methods that have been selected for use are the Bishop's simplified, Janbu's simplified and Fellenius' methods, which have all been well established for many years and are still commonly used in practice for stability analysis. Simplicity and relatively good results are their main advantages. These are then compared with the results of the Hardening Soil Model (available within the PLAXIS 2D software) with and without remedial measures.

However, the key objective of this study is to produce a design chart that allows for an expedite assessment of the stability of granitic residual soil slopes, considering different soil properties, geometries, groundwater levels and applied surcharges. The relevant geotechnical soil parameters required for the LEM and FEM simulations have been primarily based on laboratory testing undertaken by other PhD students at UBI and complemented by historical data.

The parametric study of the pre-set range of conditions reveals that changes in groundwater levels are more detrimental to the stability of the slope than increases in the applied surcharge at its crest. However, the results from the different LEM methods do not entirely converge, as the Bishop's and Janbu's simplified methods appear to be more critical when

groundwater level rises in steeper slopes, whereas the Fellenius' method returns greater reductions in the FoS for slacker slopes. The FEM approach reveals some similarities to the above, with also greater reductions on the least steep configuration.

From an overall perspective, reductions in FoS using LEM methods due to rises in groundwater levels appear to be inversely proportional to the cohesion of the intersected materials, i.e., the greater the c' of the soil, the lesser the consequences of rises in groundwater appear to be. Results also show that, albeit both approaches reveal the FoS to be more sensitive to changes in groundwater levels than to the surcharge applied on the crest, the latter appears to have a more critical effect on the LEM analyses.

A direct comparison between FEM and LEM approaches reveals a significant divergence in the obtained FoS for purely granular materials, with all LEM methods overestimating the safety of the slope by up to circa 40%. These differences are more expressive for greater heights and increased applied surcharges.

When comparing the outcomes of the Fellenius' method, the FoS presents a better correlation to the FEM results with both over and underestimates, but generally under circa 5%. No tendency is apparent for changes in either groundwater levels or applied surcharges.

In soils with a given effective cohesion, the results of the Bishop's simplified method are circa 5% to 10% higher than the FEM outcomes. These differences appear to accentuate with the slope's gradient and height and with rising groundwater levels. However, no noticeable differences are reported for variations in surcharge.

The majority of the FoS obtained with the Janbu's simplified method present the best correlation with the FEM approach (from between all three LEM formulations), with differences predominantly under 5%. The best correlations seem to be obtained for greater surcharge values and in slacker slopes.

Nevertheless, the differences in FoS between LEM methods and between FEM and FEM approaches may have little interest if there is a large uncertainty in the input parameters of the soils. Therefore, priority should be given to investigating their shear strength parameters and precise mapping of the slope geometry before undertaking a stability analysis. Furthermore, the stability charts provided within this thesis are only to be perceived as indicative and shall only be used as a preliminary tool to help corroborate site observations. A detailed design will necessarily require further analysis to be undertaken.

Similarly, the remedial options discussed and analysed in this thesis are to be interpreted as concept ideas as their gain in terms of FoS will likely vary on a case to case basis. Also, the topography and existing restraints at a site can often lead the Designer to opt between a limited number of feasible choices. Finally, the assessment of the benefits of combining more than one remedial option are excluded from this study.

Keywords: Slope stability charts, Limit equilibrium, Finite elements, Remedial measures

Extended Abstract (in Portuguese) [1]

1 Introdução

A estabilidade de taludes é um problema global, particularmente importante em regiões do globo de maior perigosidade dada a sua topografia e condições geológicas e climáticas, como é o caso, por exemplo, da área Mediterrânica. A compreensão deste fenómeno requer um entendimento tanto das suas causas como dos seus possíveis mecanismos de rotura.

Este trabalho aborda a estabilidade de taludes em solos residuais de granito tirando partido dos correntes métodos de equilíbrio limite (LEM) e de elementos finitos (FEM) para a sua análise. Para tal, são utilizados dois softwares comerciais vocacionados para este problema, nomeadamente SLOPE/W (LEM) e PLAXIS 2D (FEM). Os métodos de equilíbrio limite, no caso desta tese Fellenius e Bishop e Janbu simplificados, embora baseados no equilíbrio estático de uma massa de solo, partem de diferentes premissas/simplificações que lhes permitem apenas cumprir parcialmente as condições estáticas de equilíbrio. Por contraste, o método de elementos finitos baseia-se na relação tensão-deformação do solo e nas suas leis constitutivas.

Este documento insere-se no estudo que a Universidade da Beira Interior (UBI) tem vindo a desenvolver para caracterização dos solos residuais de granito, um abundante recurso natural da região, comummente utilizado na construção de infra-estruturas rodoviárias. Como tal, o seu comportamento do ponto de vista da estabilidade de taludes é aqui analisado. As suas propriedades geotécnicas, embora tipicamente dentro de determinados intervalos de valores, são analisadas para permitir uma avaliação expedita da segurança de um talude composto por estes materiais através de abacos de dimensionamento.

Para tal, um estudo paramétrico relativo a estabilidade de taludes é aqui efectuado, usando várias combinações de posições do nível freático, valores de parâmetros do solo, geometrias de talude e sobrecargas, através dos métodos de Fellenius e de Bishop e Janbu simplificados (LEM) e do modelo Hardening Soil (FEM). São adicionalmente abordadas algumas das mais comuns técnicas de remediação de taludes e quantificada a sua eficácia através de ambas as abordagens.

2 Factores que influenciam a estabilidade de taludes

Os movimentos em taludes são geralmente processos complexos que envolvem uma série de eventos, desde a sua causa até ao derradeiro efeito, sendo frequentemente difícil de apontar

[1] Por decisão pessoal, o autor do texto não escreve segundo o novo Acordo Ortográfico.

apenas um motivo para a sua ocorrência. São geralmente função da litologia e geometria, bem como das condições hidrológicas e hidrogeológicas locais. Dos diferentes factores que afectam a estabilidade de taludes, a saturação do solo, particularmente devido a períodos de intensa ou prolongada pluviosidade, aparenta ser a principal causa de rotura. Contudo, a escala deste fenómeno está intrinsecamente relacionada com a topografia e as propriedades geotécnicas dos materiais intersectados. Eventos sísmicos, embora igualmente precursores de instabilidade em taludes, particularmente em zonas de elevada sismicidade, saem fora do âmbito desta tese e os seus efeitos não são aqui abordados.

Por último, é igualmente importante referir que acções humanas são muitas vezes responsáveis pela ocorrência deste tipo de fenómenos, como é o caso de alterações de padrões de drenagem, deficiente funcionamento de estruturas de drenagem, remoção de vegetação, alterações na geometria de taludes ou imposição de sobrecargas adicionais.

3 Parâmetros geotécnicos

Os mais importantes parâmetros geotécnicos que governam a estabilidade de taludes são o ângulo de atrito em tensões efectivas (φ') e a coesão em tensões efectivas (c') dos materiais. Estas grandezas reflectem a relação entre tensões normais e de corte, como ilustrado na Figura A1.

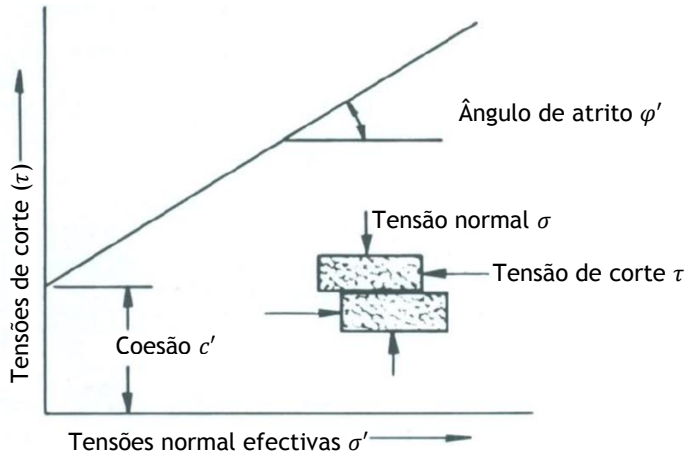

Figura A1. Relação entre tensões normais e de corte para induzir movimento, adaptado de Guidicini & Nieble (1984).

Esta relação pode ser descrita através do critério de rotura de Mohr-Coulomb (Equação A1).

$$\tau = c' + \sigma' \, tg\varphi' \quad \text{(A1)}$$

Contudo, a dependência linear entre τ e σ' pode sofrer variações e, por outro lado, a coesão efectiva dos solos é tipicamente considerada nula para materiais granulares, o que simplifica esta relação e descreve este comportamento como puramente atrítico.

4 Tipos de instabilização de taludes

De acordo com Mencl & Záruba (1982), os fenómenos de deslizamento envolvem tal variedade de processos e de causas que oferecem ilimitadas possibilidades de classificação. Contudo, em termos técnicos um deslizamento é descrito como um movimento gravítico, em direcção ao sopé de um talude, de uma dada massa de solo, rocha e outros materiais. São geralmente classificados com base no tipo de movimento (escorregamentos rotacionais e translacionais, despreendimentos, torrentes e creeping).

5 Solos residuais

Por definição, um solo residual é aquele que se formou *in situ*, por alteração da rocha-mãe, e que não foi transportado até distâncias significativas. Significa isso que o seu processo de decomposição ocorreu mais rapidamente que a erosão e transporte das partículas de solo, como ilustrado na Figura A2. Contudo, estes solos também se podem formar através de processos erosivos, desde que não sejam transportados posteriormente. Este fenómeno ocorre frequentement nos solos residuais de granito portugueses (Figura A3).

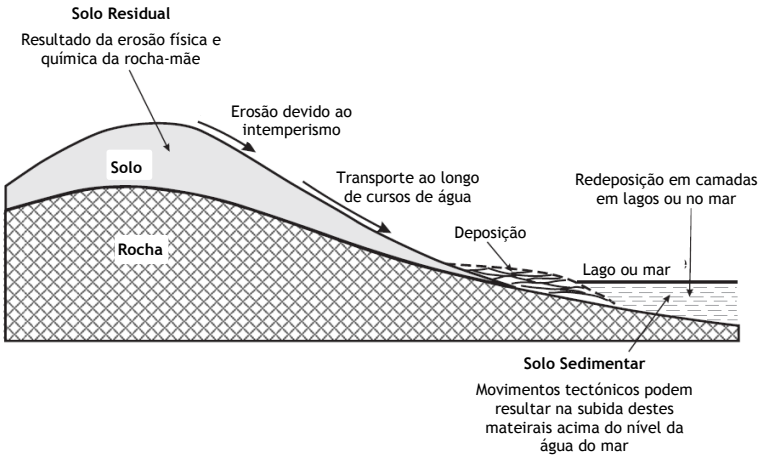

Figura A2. Formação de solos residuais e sedimentares, adaptado de Wesley (2010).

Figura A3. Exemplo de talude em solo residual de granito com a rocha-mãe visível na base.

Por sua vez, os solos sedimentares sofrem um sistemático e contínuo processo durante a sua formação (erosão, transporte e sedimentação). Como resultado, as partículas mais finas são separadas da fracção mais grosseira do solo, acabando depositadas em diferentes localizações

e/ou camadas. Consequentemente, e ao contrário dos solos residuais, estes materiais tendem a ser razoavelmente homogéneos.

Com efeito, e embora os solos residuais cubram uma parte significativa da crusta terrestre, a Mecânica dos Solos focou principalmente a sua atenção nos solos sedimentares como resultado da sua abundância nos países onde os princípios que governam o comportamento do solo foram inicialmente estudados. Contudo, os solos residuais apresentam algumas particularidades complexas, podendo apresentar diferentes comportamentos e propriedades relativamente a solos sedimentares com a mesma granulometria e índice de vazios.

A explicação para este fenómeno aparenta estar relacionada com as ligações interpartículas "herdadas" da rocha-mãe ou que se estabelecem aquando do processo de erosão (Fernandes, 2011). Como tal, é questionável a representatividade das curvas granulométricas nestes materiais e se as suas propriedades geotécnicas podem ser extrapoladas a partir das mesmas, uma vez que a peneiração quebra/afecta estas ligações.

Os solos residuais são comuns em zonas tropicais ou sub-tropicais, uma vez que as temperaturas relativamente altas, combinadas com a abundância de água, favorecem a ocorrência das reacções químicas que permitem a decomposição da rocha-mãe. Por outro lado, a abundância de vegetação protege os solos dos fenómenos erosivos, facilitando assim a formação de solos residuais. Podem igualmente formar-se em outras zonas climáticas, tal como em climas temperados (como é o caso de Portugal), tipicamente fruto de movimentos tectónicos seguidos de processos erosivos.

Na zona norte de Portugal e junto ao complexo da Serra da Estrela as rochas magmáticas predominam, nomeadamente o granito. Os resultantes solos residuais são abundantes e estendem-se usualmente até profundidades entre 5 e 10m, podendo em algumas instâncias prolongar-se até cerca de 20m de profundidade (Fernandes, 2011). Na zona da Covilhã este tipo de solos cobre mais de 50% da superfície, estendendo-se até profundidades máximas de cerca de 18m (Cavaleiro, 2001).

Um perfil típico de alteração de um solo residual é apresentado na Figura A4, ilustrando o arranjo vertical dos diferentes horizontes, desde a rocha-mãe até ao solo, e que reflecte as etapas progressivas de transformação/decomposição. De uma maneira geral, é espectável a seguinte evolução nas propriedades da rocha/solo à medida que nos aproximamos da superfície:

- Aumento de porosidade e do índice de vazios;
- Aumento do teor em água;
- Redução do peso volúmico, tanto húmido como seco;
- Redução do tamanho médio das partículas.

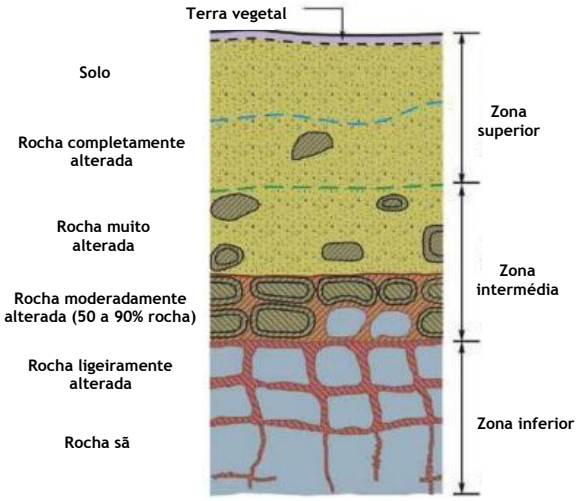

Figura A4. Perfil de alteração de um solo residual, adaptado de Aung & Leong (2011).

A Figura A4 apresenta ainda uma escala tipicamente usada para descrever, com a menor ambiguidade possível, o estado de alteração de uma dada rocha/solo residual. Cada um dos horizontes apresentados é descrito em algum detalhe na Tabela A1 abaixo.

Tabela A1. Classificação do perfil de alteração de um solo/rocha, adaptado de Fernandes (2011) e Huat (2012).

Estado de alteração			Descrição
	Termo	Zone	
Solo residual	Solo residual	VI	Todo o material rochoso foi convertido em solo e a textura da rocha não é reconhecível. O material apresenta geralmente fracções finas e grosseiras e tem uma cor homogénea.
	Rocha completamente alterada	V	Toda a rocha se decompôs mas a textura original ainda é visível. Dada a sua composição, amostras não podem ser recuperadas por métodos normais de rotação em furos de sondagens. O material é bastante arenoso e pode ser usado como material de aterro. Quando em taludes pode requer protecção contra a erosão.
	Rocha muito alterada	IV	O material rochoso encontra-se na fase de transição entre rocha e solo. Geralmente contem menos de 50% de rocha e esta, dado o seu estado de alteração, é desagrega-se.
Rocha/Solo semi-residual	Rocha moderadamente alterada (rocha a 50 a 90%)	III	O material rochoso apresenta alguma coloração e a alteração estende-se a toda a rocha. O material oferece grande resistência à escavação e requer o uso de explosivos. A percentagem de rocha varia entre 50 e 90%.
	Rocha pouco alterada	II	Coloração ao longo de descontinuidades e de parte do maciço rochoso. A textura da rocha encontra-se ainda completamente preservada e nos granitos os feldspatos começam a alterar-se. A resistência é idêntica à da rocha sã e a percentagem de rocha excede os 90%.
	Rocha sã	I	Rocha sem sinais visíveis de alteração. Pode no entanto apresentar alguma coloração nas superfícies de descontinuidade.

Os solos residuais são geralmente uma combinação de areia, silte e argila em diferentes proporções, dependendo das condições geológicas da sua génese. Os tipos mais comuns, quer em zonas tropicais quer em zonas temperadas, resultam da alteração do granito e de rochas sedimentares ou metassedimentares (Salih, 2012).

Para além da envolvente geológica, a topografia pode igualmente influenciar as propriedades dos solos residuais, uma vez que pode ter interferência no tipo de minerais argilosos que se formam. Em regiões montanhosas, por exemplo, os solos tendem a ser bem drenados, percolando as águas infiltradas em profundidade (Figura A5) até a um nível freático profundo. Este fenómeno, nas devidas condições geológicas, condiciona a formação de minerais argilosos de baixa actividade, especialmente a caulinite (Wesley, 2010). Solos residuais contendo estes minerais têm geralmente boas propriedades geotécnicas.

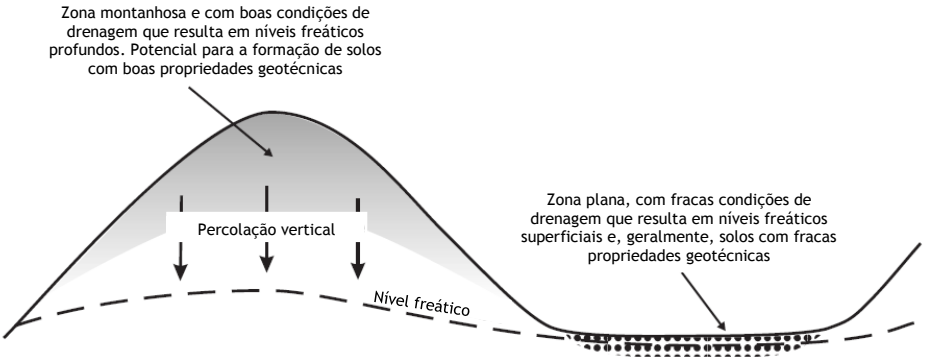

Figura A5. Influência da topografia na formação de solos residuais, adaptado de Wesley (2010).

Por contraste, em regiões planas a drenagem é limitada e o teor em água varia consideravelmente durante o ano, evaporando nos meses secos e ganhando água na altura das chuvas. Consequentemente, existe uma tendência para que a montmorilonite e outros minerais de alta actividade sejam produzidos (caso as condições geológicas o permitam), o que torna estes solos menos interessantes do ponto de vista geotécnico.

De um modo geral, a permeabilidade de um solo residual tende a ser superior à de um solo sedimentar com a mesma granulometria, dadas a sua estrutura (herdada da rocha-mãe). Contudo, se se tratar de um solo residual remoldado, este efeito deixa de se sentir.

6 Solo residual granítico da Covilhã

A composição típica dos solos residuais de granito da região da Covilhã (Figura A6) contém caulinite como o mineral argiloso predominante (Cavaleiro, 2001).

Figura A6. Exemplos de taludes de solos residuais de granito na Covilhã.

A fracção fina destes solos é variável, embora frequentemente reduzida, predominando as areias na sua constituição, o que resulta na sua classificação como areias siltosas ou siltes arenosas. A Figura A7 ilustra o fuso granulométrico de cerca de 80 amostras de solos residuais de granito da Covilhã (a cinzento no gráfico). Estas indicam que a percentagem de areias e seixo correspondem a cerca de 60 a 95% do seu peso, com uma percentagem de finos entre os 7 e os 38%.

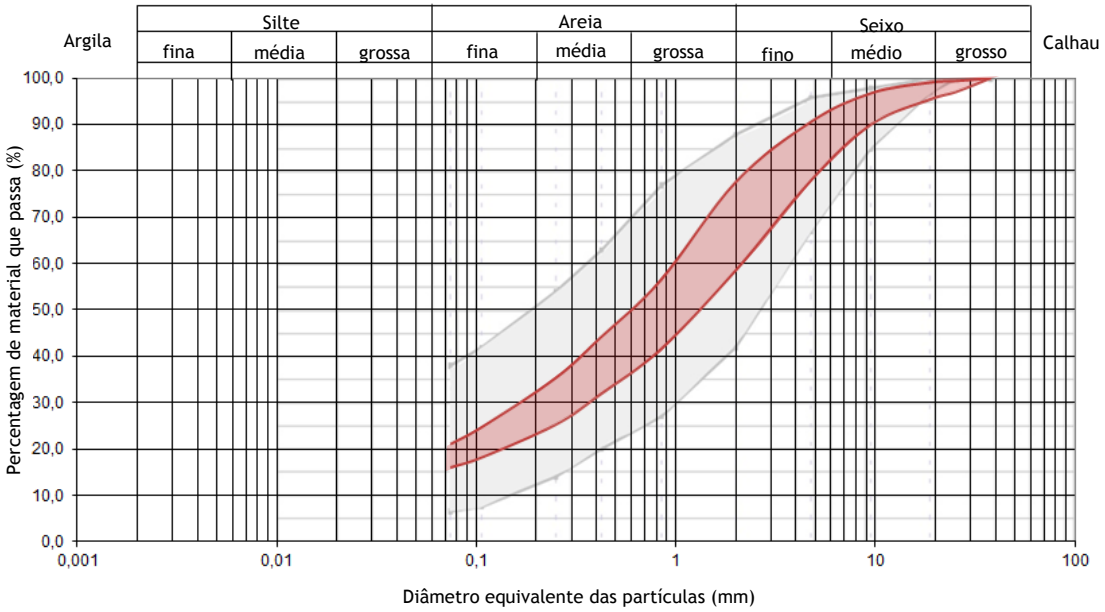

Figura A7. Fusos granulométricos de solos residuais de granito da Covilhã. A cinzento dados históricos (Cavaleiro, 2001) e a vermelho resultados da campanha experimental no solo analisado neste estudo.

Como tal, estes materiais são classificados como bem graduados, com partículas desde argilas até seixos e com areia como o principal componente. As argilas são predominantemente caulinite e ilite (Cavaleiro, 2001), subprodutos da alteração da moscovite e feldspatos.

Uma vez que a fracção argilosa destes solos geralmente não é significativa, e que os seus minerais constituintes exibem baixa plasticidade, são geralmente classificados como não plásticos. Contudo, a matriz argilosa pode revelar valores do Índice de Plasticidade inferiores a 20% (Cavaleiro, 2001).

Sobreposto ao fuso granulométrico anterior, é também possível observar na Figura A7 o fuso granulométrico do solo residual analisado neste trabalho, resultante de cerca de 15 amostras e classificado como uma areia fina a grosseira, siltosa e com grande percentagem de seixo (>20%). Uma percentagem de finos inferior a 20% é igualmente reportada. Os resultados obtidos são relativamente homogéneos, sem grandes variações, e enquadram-se na campanha experimental anterior (Cavaleiro, 2001).

A campanha experimental na qual este estudo se baseia incluiu a realização de ensaios triaxiais drenados e não drenados em amostras remoldadas do solo em análise. Estes ensaios permitiram obter estimativas dos módulos de deformação drenados e não drenados tangentes ($E_t{}'$ and E_{u_t}) e secantes ($E_s{}'$ and E_{u_s}), bem como dos ângulos de atrito de pico e residuais. Os resultados obtidos estão resumidos em seguida na Tabela A2, juntamente com os valores medidos para os pesos volúmicos seco e saturado.

Tabela A2. Parâmetros geotécnicos realizados durante a campanha de ensaios triaxiais.

E_{u_s} (MPa)	E_{u_t} (MPa)	$E_s{}'$ (MPa)	$E_t{}'$ (MPa)	γ_d (kN/m^3)	γ_{sat} (kN/m^3)	φ'_{pico} (°)	$\varphi'_{residual}$ (°)
16,6 – 23,3 (18,5)	25,2 – 37,0 (29,4)	12,0 – 34,5 (25,8)	21,8 – 46,0 (34,3)	19,3 – 19,8 (19,5)	21,0-21,9 (21,5)	37,5 – 43,6 (40,6)	35,3 – 36,9 (36,1)

Nota: Os valores dentro de parêntesis correspondem à média dos valores obtidos, resultantes de cerca de 15 amostras.

Os valores reportados excedem os obtidos na campanha histórica mais alargada aos solos graníticos da região (Cavaleiro, 2001), que reporta ângulos de atrito entre 26,7° e 37,7°. Contudo, estes valores foram obtidos considerando que estes materiais possuíam valores de coesão até 20kPa, enquanto que os valores na Tabela A2 foram obtidos para valores de coesão nula. A aplicação deste mesmo princípio aos valores históricos do ângulo de atrito resulta em valores para esta grandeza entre 31,3° e 42,5°, que por sua vez concordam com os valores reportados na Tabela A2.

Ensaios de corte directo em amostras indeformadas dos mesmos materiais (Cavaleiro, 2001), resumidos na Figura A8 abaixo, reportam valores de coesão entre 4kPa e 42kPa e ângulos de atrito entre 35° e 45°.

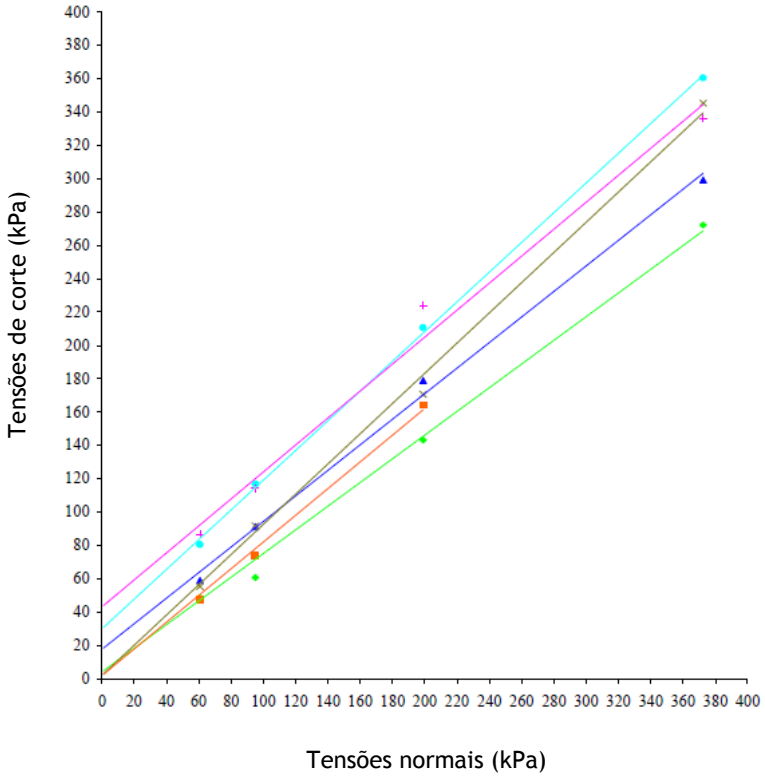

Figura A8. Resultados dos ensaios de corte directo, adaptado de Cavaleiro (2001).

A mesma fonte classifica todas as amostras ensaiadas como não plásticas de acordo com os Limites de Atterberg.

A caracterização destes materiais envolveu igualmente uma componente mais prática, através da construção de um aterro experimental utilizando o solo em análise, e cuja execução foi supervisionada por alunos de doutoramento da UBI. Este aterro experimental foi concluído em Novembro de 2010 com uma largura máxima de 16,0m na base e com um desenvolvimento de 20,0m (Figura A9).

O perfil final do terreno em redor deste aterro controlado foi reperfilado utilizando o mesmo solo residual granítico. Contudo, a sua execução não foi supervisionada como no caso do aterro experimental.

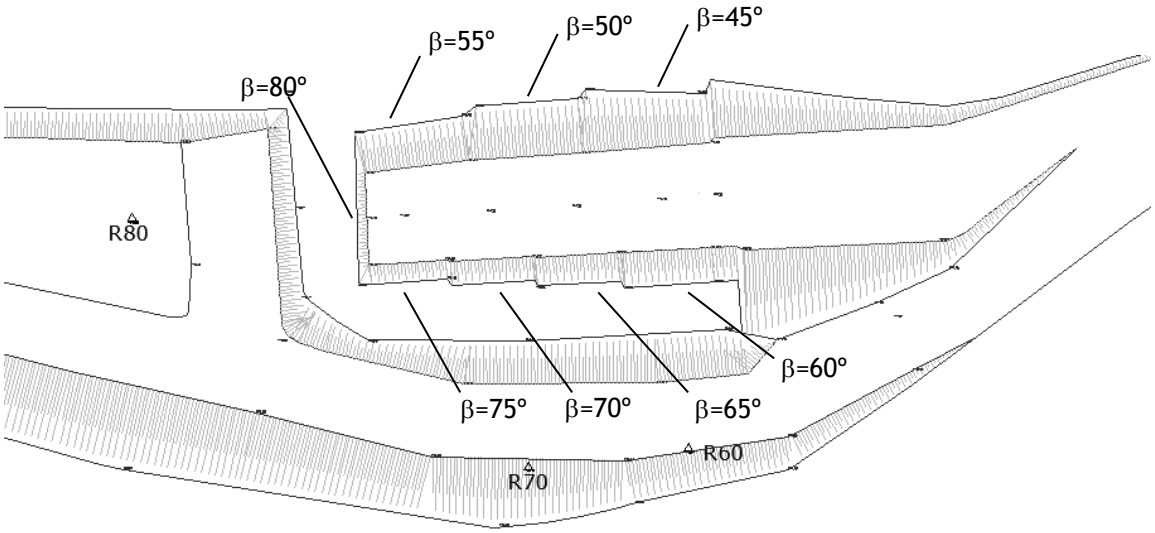

PLANTA

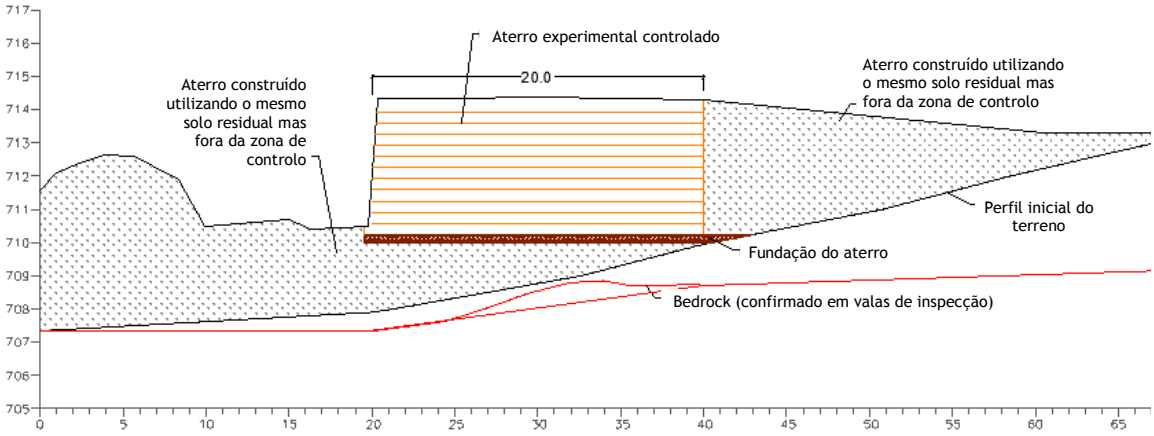

ALÇADO

Figura A9. Planta e alçado do aterro experimental, reproduzido com permissão de Filipe Nunes (aluno de doutoramento D716 na UBI).

A altura do aterro foi mantida constante ao longo do seu desenvolvimento (4.0m) enquanto que os seus taludes foram construídos com diferentes ângulos, a fim de estabelecer experimentalmente qual seria a configuração estável mais íngreme. O ângulo dos taludes variou entre 45° e 80° com a horizontal, crescendo em incrementos de 5° (Figura A9).

Adicionalmente, uma sobrecarga de 10kPa foi aplicada, em Agosto de 2011, no topo do talude e perto da sua face mais íngreme. Cerca de 4 anos após a sua aplicação, ainda não são visíveis quaisquer sinais de instabilidade. O talude foi inicialmente protegido dos agentes erosivos

através do uso de uma película plástica que se deteriorou com o tempo deixando o talude exposto nesta fase (Figuras A10 e A11).

Figura A10. Vista de um dos alçados do aterro pouco tempo depois da sua construção.

Figura A11. Vista do aterro actualmente.

O ponto de partida das análises numéricas efectuadas nesta tese foi o de tentar corroborar, numericamente, a aparente estabilidade deste aterro construído a partir do solo residual de granito da região. Numa fase posterior as análises numéricas foram generalizadas de modo a poder tirar partido das mesmas em condições geotécnicas mais genéricas.

7 Análise da estabilidade de taludes

Os solos residuais de granito apresentam geralmente boas propriedades geotécnicas, o que poderá ajudar a explicar a existência de encostas íngremes neste tipo de materiais.

No entanto, a avaliação da estabilidade de um talude natural não pode nunca ser um exercício puramente analítico, uma vez que existem sempre limitações para aplicação de métodos analíticos a estes taludes. Como tal, é recomendável que os seguintes métodos complementares sejam igualmente seguidos:

- Inspecção visual do talude;
- Utilização de fotografia aérea;
- Inspecção de outros taludes em materiais semelhantes ao talude em análise.

Uma atenta inspecção de um talude em solos residuais, juntamente com conhecimento da geologia local, pode providenciar boas indicações relativas à sua estabilidade. Uma topografia regular e pouco acidentada tende a indicar que o talude se formou por processos erosivos e sem escorregamentos de material, enquanto que uma topografia irregular pode sugerir que algum movimento pode ter tido lugar anteriormente (Figura A12).

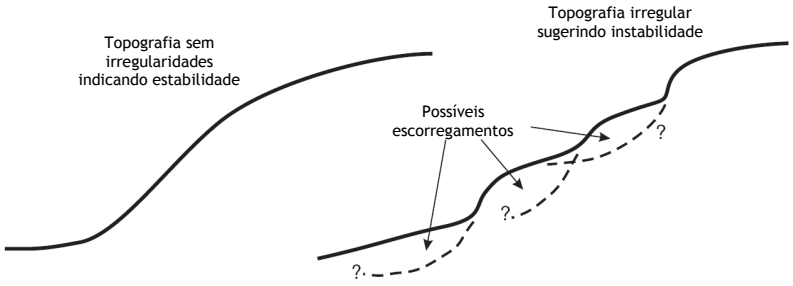

Figura A12. Possíveis conclusões de observações *in situ* da morfologia de taludes em solos residuais, adaptado de Wesley (2010).

8 Estabilidade de taludes de acordo com o EC7

O Eurocódigo 7 (EC7) prescreve três diferentes Abordagens de Cálculo (AC 1, AC 2 e AC 3) utilizando diferentes conjuntos de valores de coeficientes parciais para acções, propriedades dos materiais/solos e capacidades resistentes. A escolha de qual a abordagem a seguir para cada estrutura geotécnica é feita por cada país (Figura A13) no seu respectivo Anexo Nacional.

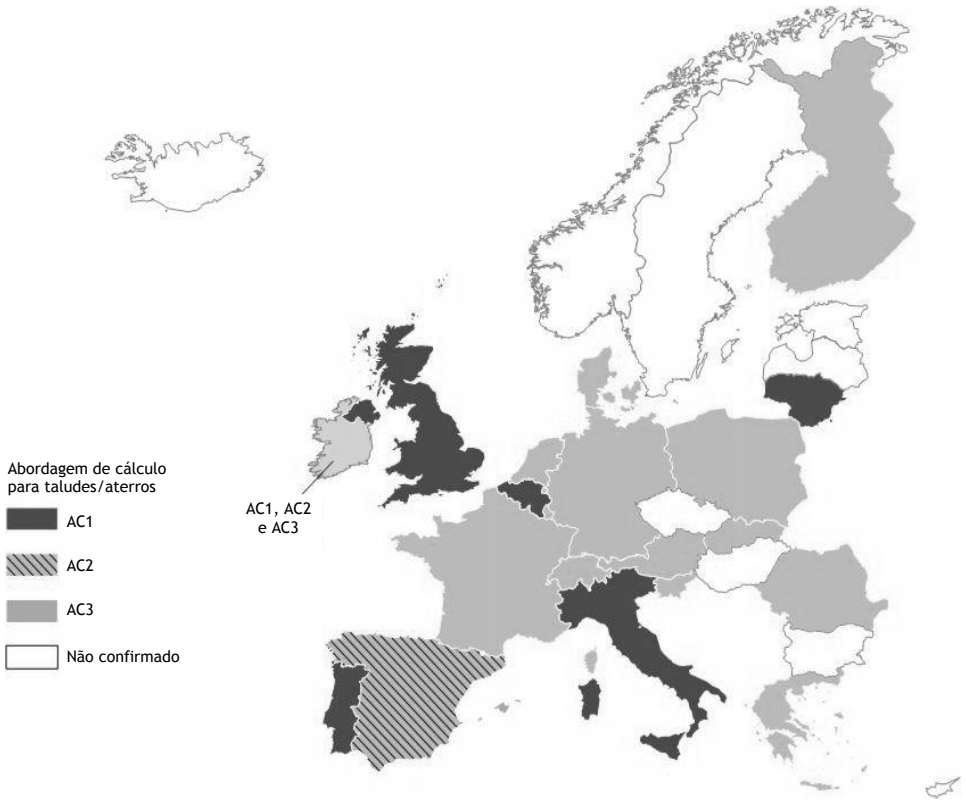

Figura A13. Escolha das Abordagens de Cálculo de cada país para o dimensionamento de taludes, adaptado de Bond & Harris (2008).

A Abordagem de Cálculo escolhida pelo Anexo Nacional Português do EC7 é a Abordagem de Cálculo 1, uma vez que na sua essência, este é um problema em que o solo é responsável por uma parte significativa da resistência total.

Dentro desta Abordagem de Cálculo duas diferentes combinações têm de ser verificadas (Combinações 1 e 2). Na primeira, coeficientes parciais de segurança superiores à unidade são aplicados a acções desfavoráveis ou efeitos de acções, enquanto que na Combinação 2 o inverso dos coeficientes parciais de segurança maiores que a unidade são aplicados às propriedades do solo. Ou seja, em termos gerais a Combinação 1 resulta num incremento dos efeitos das acções enquanto que na Combinação 2 a resistência do solo é diminuída.

Dadas as diferenças entre combinações, é intuitivo que a Combinação 1 é especialmente relevante quando a carga aplicada ao talude (excluindo o peso próprio do solo) controla a sua rotura. Por outro lado, quando esta combinação é utilizada, um coeficiente parcial de segurança para acções permanentes deve ser aplicado ao peso volúmico do solo, o que resulta no seguinte:

- Em tensões efectivas, o efeito do coeficiente é o de aumentar as acções destabilizantes. Contudo, a resistência ao corte do solo é também incrementada o que parcialmente anula o efeito anterior;
- Em tensões totais, o aumento do peso volúmico do solo resulta num aumento das acções desfavoráveis sem aumento da resistência ao corte do solo. Contudo, um maior coeficiente parcial de segurança é aplicado à resistência não drenada do solo na Combinação 2 que às acções desfavoráveis permanentes na Combinação 1.

Em ambos os casos, a Combinação 1 tende a ser menos crítica que a Combinação 2 na maioria das situações.

Aquando da avaliação da estabilidade de taludes naturais, o EC7 recomenda ainda que qualquer incerteza relativa ao peso volúmico do solo seja tida em consideração estabelecendo valores máximos e mínimos para esta grandeza.

9 Análises numéricas

Provavelmente não existe outra análise conduzida por engenheiros geotécnicos que tenha sido alvo de mais atenção, em termos de programação, que os métodos de fatias de equilíbrio limite, usados para estimar o factor (FoS) ou margem (MoS) de segurança de taludes à rotura. A explicação para isto reside no facto de estes métodos requererem diversas iterações que são usualmente realizadas automaticamente e num curto espaço de tempo. Por outro lado, o actual software disponível no mercado apresenta a vantagem de ter um output gráfico que

ilustra todas as potenciais superfícies de deslizamento consideradas e qual o/a FoS/MoS de cada uma delas.

No entanto, estes métodos consideram que as forças actuam num ou em vários pontos da superfície de deslizamento, assumindo que a rotura ocorre instantaneamente e que toda a resistência ao corte disponível é mobilizada ao longo de toda a superfície e em simultâneo. Em alternativa, os métodos baseados na relação tensão-deformação dos solos podem ser utilizados para superar estas simplificações. Ao considerar esta relação durante a deformação e rotura de um talude, passa também a ser possível estimar as deformações ao longo do mesmo. O software vocacionado para este tipo de análises possibilita ainda que se estabeleça o FoS de um determinado talude, embora este valor seja diferente do valor estimado pelos métodos de equilíbrio limite uma vez que a superfície de rotura não é completamente definida. Neste trabalho tanto os métodos LEM como FEM são utilizados.

A validação do software LEM foi efectuada manualmente para apurar a fiabilidade do programa. Os programas comerciais utilizados nas análises são SLOPE/W, especialmente vocacionado para lidar com a estabilidade de taludes utilizando os métodos das fatias, e PLAXIS 2D, vocacionado para análises tensão-deformação em solos e rochas. Os métodos das fatias utilizados neste estudo são o método de Fellenius e os métodos simplificados de Bishop e Janbu.

9.1 Implicações do EC7 no dimensionamento

O dimensionamento de taludes e aterros utilizando ambos os métodos LEM e FEM não é tão directo como pode parecer à primeira vista dados os coeficientes de segurança envolvidos. Isto resulta do facto de o EC7 prescrever diferentes coeficientes de segurança para acções favoráveis e desfavoráveis, o que não é possível no cálculo de estabilidade de taludes correntes, uma vez que a separação entre acções favoráveis e desfavoráveis é muitas vezes impossível.

Como tal, dado que a Abordagem de Cálculo 1 requere que as acções permanentes sejam multiplicadas por um determinado coeficiente parcial de segurança, a solução passa por aplicar o mesmo ao peso volúmico do solo, o que resulta em tratar os seus efeitos favoráveis e desfavoráveis da mesma forma, uma vez que resultam da mesma origem.

9.2 Dificuldades numéricas dos métodos LEM

Os métodos das fatias não requerem vastos inputs, conseguindo rapidamente realizar uma extensa e iterativa procura pela superfície de deslizamento crítica. Contudo, a resistência ao corte dos materiais baseia-se na mecânica dos solos saturados, e a contribuição da sucção matricial acima do nível freático é geralmente ignorada (Rahardjo & Fredlund, 1991).

Como resultado, e uma vez que a maioria do software disponível se foca apenas em solos saturados, esta contribuição pode contudo ser contabilizada através de um aumento da coesão do solo. Isto é, esta metodologia permite que a expressão geral que governa a resistência ao corte dos solos possa continuar a ser usada. Na modelação efectuada neste estudo a quantificação da contribuição da sucção matricial não foi estabelecida. Contudo, uma vez que esta pode ser "convertida" em valores de coesão, as análises efectuadas poderão, em certas situações, ser consideradas apropriadas em casos onde este fenómeno tenha de ser contabilizado.

9.3 Campanha numérica

Dado que o principal objectivo deste estudo requer o output de inúmeras simulações em LEM, um procedimento manual de cálculo não seria suficiente e, como tal, um software comercial vocacionado para a estabilidade de taludes for utilizado. Antes de iniciar o procedimento numérico, estabeleceram-se quais os parâmetros a variar e os intervalos de valores para cada um deles, conforme resumido na Tabela A3.

Tabela A3. Intervalo de valores considerados nas análises LEM.

Parâmetros		Intervalo de valores			
Geometria	Ângulo	1(V):2(H)	1(V):1,5(H)	1(V):1(H)	2(V):1(H)
	Altura	2,0m – 8,0m, com incrementos de 1.0m			
Valor característico do ângulo de atrito efectivo		35º, 36º, 37º e 38º			
Valor característico da coesão efectiva		0kPa, 5kPa e 10kPa			
Nível freático		Não presente Nível freático baixo Nível freático elevado			
Sobrecarga aplicada		0kPa, 5kPa e 10kPa			

Após a conclusão das análises LEM, e com o intuito de comparar os seus resultados com a formulação FEM, os seguintes modelos foram igualmente analisados no software PLAXIS 2D (Tabela A4), considerados suficientes para estabelecer uma relação entre as MoS obtidas por ambas as metodologias.

Tabela A4. Intervalo de valores considerados nas análises FEM.

Parâmetros		Intervalo de valores		
Geometria	Ângulo	1(V):2(H)	1(V):1,5(H)	1(V):1(H)
	Altura	5,0m e 8,0m		
Valor característico do ângulo de atrito efectivo		35º		
Valor característico da coesão efectiva		0kPa, 5kPa e 10kPa		
Nível freático		Não presente Nível freático baixo Nível freático elevado		
Sobrecarga aplicada		0kPa, 5kPa e 10kPa		

Os modelos com a configuração mais íngreme dos taludes, 2(V):1(H), foram excluídos das análises FEM uma vez que apresentam FoS significativamente abaixo da unidade. Adicionalmente, modelos com uma inclinação de 1(V):1(H) só puderam ser analisados para valores de coesão de 10kPa.

9.4 Análise comparativa dos resultados LEM

Efeitos da aplicação de sobrecargas no topo do talude

No que toca à aplicação de sobrecargas no topo do talude, constatou-se que, em solos graníticos residuais compactados e puramente atríticos, aumentos de sobrecarga para 5kPa e 10kPa tipicamente resultam em reduções máximas na MoS de cerca de 5% a 10%, respectivamente, e frequentemente sem grande consequência na sua estabilidade. Por outro lado, estes resultados aparentam ser relativamente constantes ,independentemente do ângulo do talude e da posição do nível freático. As superfícies de deslizamento críticas tendem a ser superficiais e ao longo da face do talude o que faz com que não sejam muito afectadas pela aplicação de sobrecargas.

Quando é considerada uma coesão de 5kPa, o efeito da sobrecarga é mais pronunciado. Na ausência de nível freático a redução na MoS é de no máximo 15%, para uma sobrecarga de 5kPa, aumentando para valores máximos de 20% (Bishop) e 25% (Fellenius e Janbu) para uma sobrecarga de 10kPa. Contudo, estes valores extremos apenas ocorrem para taludes de altura reduzida (2 a 3m). Ignorando estes últimos, as diferenças na MoS reduzem-se a máximos de cerca 5% e 10% para sobrecargas de 5kPa e 10kPa, respectivamente. Ilações semelhantes são retiradas da análise dos resultados para os diferentes níveis freáticos. Contrariamente ao caso anterior (coesão nula), as diferenças na MoS são reportadas em toda a gama de alturas analisadas, enquanto que anteriormente, e a partir de alturas de 5m a 6m, estas eram mínimas.

Para valores de coesão de 10kPa, e independentemente da posição do nível freático, as reduções na MoS são de até 15%, para uma sobrecarga de 5kPa, e 25% para uma sobrecarga de 10kPa. Mais uma vez estes valores extremos ocorrem para taludes de pequena altura (2m a 3m). Ignorando estes valores, as diferenças na MoS cifram-se a máximos de cerca 10% e 15% para sobrecargas de 5kPa e 10kPa, respectivamente.

Em todos os métodos das fatias analisados, e considerando todos os cenários e variáveis abordadas nesta tese, aumentos de sobrecarga em taludes compostos por materiais com coesão aparentam ser mais desfavoráveis do que em taludes com materiais puramente atríticos. Para estes últimos, em taludes com alturas superiores a 3m, as diferenças são frequentemente insignificantes. Por último, e embora as reduções sejam da mesma ordem de grandeza independentemente da posição do nível freático, a presença de um nível freático elevado é ligeiramente mais penalizadora do ponto de vista de um aumento da sobrecarga aplicada.

Efeitos de subidas no nível freático

Quando se analisa somente variações no nível freático nos modelos considerados, as variações na MoS são significativamente mais expressivas. Contudo, em solos atríticos a ausência de nível freático ou a existência de um nível freático baixo não aparenta afectar a estabilidade dos taludes. Porém, com a sua subida para níveis elevados, são registadas reduções de até 50%.

Em todos os casos, as reduções na MoS aparentam ser pouco sensíveis à sobrecarga aplicada ao topo do talude, embora directamente relacionadas com a inclinação deste. Para os métodos de Bishop e Janbu as reduções são idênticas para os taludes menos inclinados, 1(V):2(H) e 1(V):1,5(H), com as maiores reduções na configuração mais íngreme 2(V):1(H).

Uma tendência diferente emerge da análise dos resultados do método de Fellenius, onde as reduções máximas ocorrem para taludes menos inclinados, até máximos de 35%.

Conclusões similares são retiradas para solos com coesões de 5kPa e 10kPa, com a diferença de que nestas circunstâncias e para os taludes menos inclinados, 1(V):2(H) e 1(V):1,5(H), a passagem de ausência de nível freático para um nível freático baixo produz reduções na MoS, aumentando com a altura do talude até máximos de 15%. Este comportamento aparenta resultar do facto de, em materiais coesivos, as superfícies de deslizamento serem mais profundas o que, em taludes menos inclinados, potencía que estas intersectem o nível freático.

Por último, as reduções na MoS com a subida do nível freático aparentam ser inversamente proporcionais à coesão dos materiais intersectados, isto é, maiores reduções são reportadas para valores inferiores de coesão.

Comparação entre métodos LEM

Esta comparação foi efectuada tomando como referência os resultados do método de Bishop. Como tal, as observações que se seguem comparam os dois restantes métodos testados com o anterior.

Os valores das MoS aparentam convergir, em materiais puramente atríticos, para taludes menos inclinados e para maiores alturas. Adicionalmente, e em linha com as observações anteriores acerca da sensibilidade da MoS a subidas no nível freático, os resultados mostram que para taludes mais íngremes, 1(V):1(H) e 2(V):1(H), o método de Fellenius apresenta valores da MoS significativamente superiores ao do método de Bishop (até cerca de 70%) para níveis freáticos altos. Isto contrasta com os resultados do método de Janbu, que reportam reduções na MoS (em relação ao método de Bishop) nestes mesmos modelos de até 25%.

De uma maneira geral, para taludes menos inclinados, 1(V):2(H) e 1(V):1,5(H), uma boa correlação é obtida entre todos os métodos, com diferenças máximas de cerca de 10% e frequentemente abaixo dos 5%.

Diferentes ilações são retiradas para solos coesivos, com excepção do método de Fellenius continuar a reportar MoS significativamente superiores aos de Bishop para altos níveis freáticos e geometrias mais íngremes. Nos restantes casos, o método de Fellenius é mais gravoso que o método de Bishop, com diferenças até 10%.

Quando comparando os resultados do método de Janbu, é claro que de uma forma geral estes são mais próximos dos valores obtidos para o método de Bishop que os resultados do método de Fellenius.

9.5 Análise comparativa dos resultados FEM

A utilização do modelo Hardening Soil no software PLAXIS 2D permitiu obter as seguintes conclusões.

Efeitos da aplicação de sobrecargas no topo do talude

Em materiais puramente atríticos, reduções significativas na MoS são obtidas para sobrecargas de 5kPa e 10kPa, respectivamente 20% e 30%. As maiores reduções são registadas para os modelos de 5m de altura e o aumento de sobrecarga aparenta ser menos crítico quando para modelos com um nível freático elevado.

Quando considerando que os materiais possuem coesão, as consequências do aumento de sobrecarga são menos gravosas (por oposição às análises LEM), com reduções geralmente abaixo dos 5% e com um valor máximo de 6,3%. O efeito do aumento da sobrecarga aparenta ser similar para situações em que o nível freático é baixo ou está ausente e, tal como anteriormente, com menores consequências para níveis freáticos elevados.

As consequências do aumento de sobrecarga aparentam ainda ser menos gravosas à medida que o ângulo do talude aumenta, embora a amostra de resultados recolhida não seja suficientemente extensa para confirmar este padrão.

Efeitos de subidas no nível freático

Contrariamente ao ponto anterior, subidas no nível freático aparentam ser mais críticas em materiais coesivos do que não-coesivos, embora seja de destacar que apenas dois modelos com solos puramente atríticos tenham sido analisados e que nestes não foi possível por razões numéricas simular um nível freático elevado.

Em materiais coesivos reduções pouco significativas na MoS são reportadas para taludes mais íngremes, 1(V):1(H). Já configurações menos inclinadas, 1(V):2(H) e 1(V):1,5(H), apresentam reduções na MoS de cerca de 30% e 35% para níveis freáticos elevados, respectivamente para alturas de 5m e 8m.

Ao considerar um nível freático reduzido, as reduções cifram-se até 10% e 15%, respectivamente para alturas de 5m e 8m em taludes 1(V):2(H). Para taludes mais inclinados, 1(V):1,5(H), as diferenças reduzem-se a 5% e 10% respectivamente para taludes entre 5m e 8m de altura.

Não se registam diferenças significativas com o aumento de sobrecarga, o que leva a concluir que variações no nível freático são substancialmente mais gravosas que variações nas sobrecargas aplicadas.

Comparação entre os métodos LEM e FEM

A comparação entre as abordagens LEM e FEM revela uma significativa divergência nas MoS obtidas para materiais não coesivos, com todos os métodos LEM a sobrestimarem a estabilidade dos taludes, até máximos de 40%, em relação aos resultados das análises FEM. Estas diferenças são mais expressivas para maiores alturas e maiores sobrecargas.

Em solos com coesão os resultados do método de Bishop revelam MoS cerca de 5% a 10% superiores aos obtidos através de FEM. Estas diferenças aparentam ser mais expressivas com o aumento da inclinação do talude e para subidas no nível freático e razoavelmente independentes da sobrecarga aplicada.

O método de Fellenius apresenta valores da MoS tanto acima como abaixo dos valores das análises FEM, com a maioria das diferenças relativas até 5% mas alguns valores entre 5% e 10%. Não é possível discernir nenhuma tendência para diferenças de sobrecarga ou posição de nível freático.

A maioria dos valores obtidos com o método de Janbu simplificado apresenta a melhor correlação com a abordagem FEM (em solos coesivos). Diferenças predominantemente abaixo

dos 5% e com as melhores correlações a estabelecerem-se para maiores valores de sobrecarga e taludes menos inclinados.

10 Medidas de remediação

Medidas de remediação, como o nome indica, são formas de após uma rotura ocorrer num talude ou de excessivas deformações serem registadas (sugerindo risco de deslizamento), aumentar as forças que resistem a estes fenómenos. Isto pode ser conseguido aumentando a resistência ao corte dos materiais existentes, alterando a geometria do talude ou providenciando elementos que forneçam uma resistência adicional a potenciais superfícies de rotura.

O seu dimensionamento requer não só uma estimativa dos relevantes parâmetros geotécnicos do solo e de potenciais geometrias das superfícies de deslizamento mas especialmente uma análise atenta dos factores que despoletaram o movimento. Este processo é geralmente o resultado de retro-análises, a fim de para estabelecer os "verdadeiros" parâmetros do solo. Adicionalmente, a escala, urgência e equipamento disponível acabam por frequentemente limitar as alternativas possíveis.

De uma forma geral, a MoS de um talude pode ser melhorada reduzindo as acções instabilizantes ou aumentando os efeitos benéficos. Tal é normalmente consigo à custa de uma ou de uma combinação das seguintes opções (Figura A14):

- Modificando a geometria do talude;
- Instalando/promovendo drenagem;
- Instalando elementos resistentes ao longo do talude;
- Construindo contenções na base do talude.

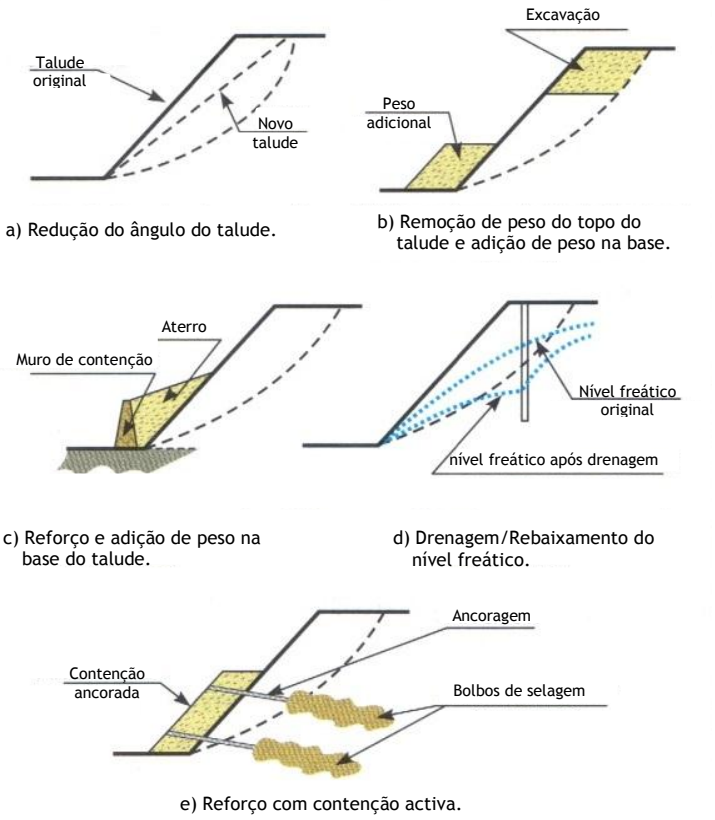

Figura A14. Técnicas comuns de estabilização e reforço de taludes, adaptado de Vallejo, Ferrer et al. (2004).

10.1 Análises de técnicas de remediação em LEM e FEM

As análises efectuadas anteriormente permitem analisar os benefícios tanto da redução da inclinação do talude como do nível freático na sua MoS. Contudo, com vista a quantificar o mérito das diferentes opções de estabilização que resultam da instalação/construção de elementos resistentes, análises adicionais foram efectuadas para ambas as abordagens LEM e FEM. Para tal, seis diferentes modelos (Tabela A5), todos com diferentes particularidades, foram seleccionados para avaliar a eficácia de cada técnica em cada caso.

Tabela A5. Modelos utilizados na análise das técnicas de remediação.

Modelos		1	2	3	4	5	6
Parâmetros		Intervalo de valores					
Geometria	Ângulo	1(V):1(H)	1(V):1,5(H)	1(V):1,5(H)	1(V):2(H)	1(V):2(H)	1(V):2(H)
	Altura	8,0m	5,0m	5,0m	5,0m	8,0m	8,0m
Valor característico do ângulo de atrito		35º					
Valor característico da coesão efectiva		10kPa	5kPa	10kPa	0kPa	0kPa	10kPa
Nível freático		NF baixo	NF baixo	NF elevado	NF ausente	NF ausente	NF elevado
Sobrecarga aplicada		0kPa, 5kPa e 10kPa					

Para cada um dos modelos apresentados acima, o resultado da inserção/construção dos seguintes elementos resistentes foi analisado nas abordagens LEM e FEM.

- Estacas-pranchas (Figura A15);
- Pregagens (Figura A16); e
- Muro de gabiões (Figura A17).

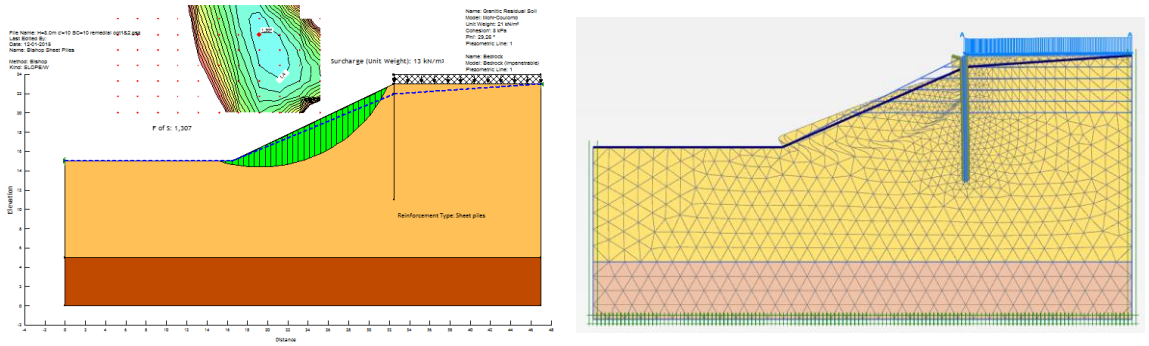

Figura A15 Exemplo da modelação de um reforço com estacas prancha nas abordagens LEM e FEM e respectivos mecanismos de rotura.

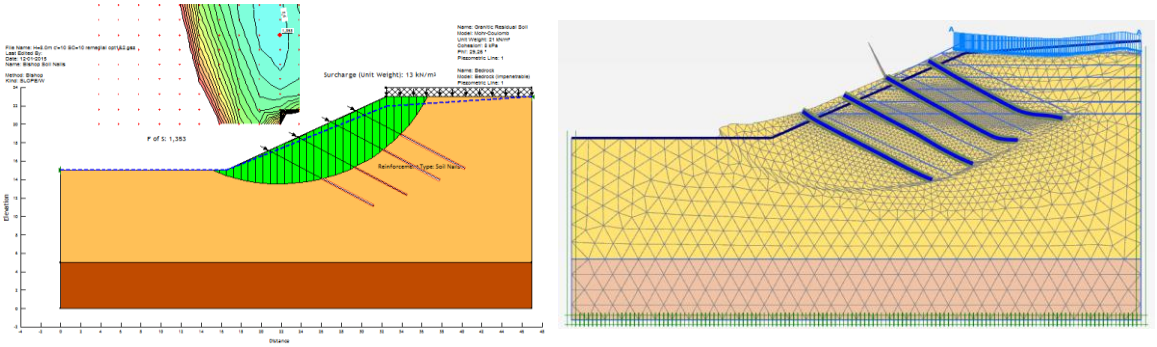

Figura A16 Exemplo da modelação de um reforço com pregagens nas abordagens LEM e FEM e respectivos mecanismos de rotura.

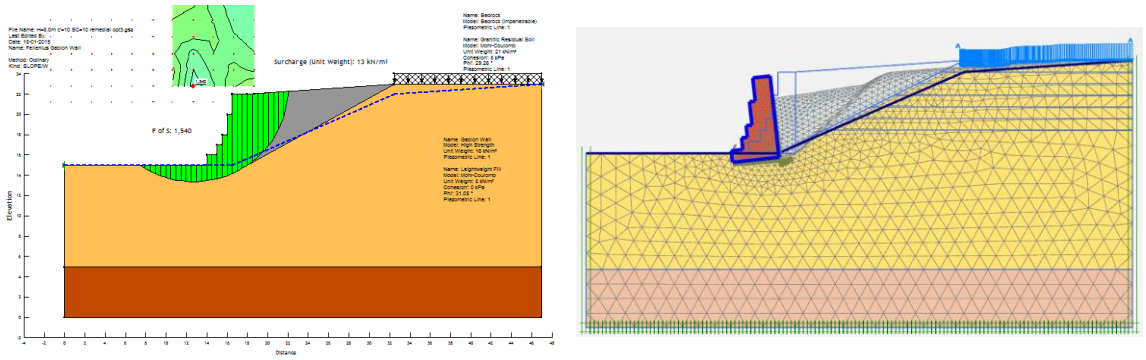

Figura A17 Exemplo da modelação de um reforço com um muro de gabiões nas abordagens LEM e FEM e respectivos mecanismos de rotura.

É de realçar contudo que o procedimento embebido no software PLAXIS 2D para determinação da MoS requer uma inspecção atenta do mecanismo de rotura, por forma a assegurar que este é realístico. Esta metodologia revelou que o software aparenta ser incapaz de avaliar correctamente o FoS em taludes sem coesão.

Para o propósito destes cálculos foram tomadas as seguintes premissas:

- Estacas-pranchas com uma secção PU18-a e aço S355GP, instaladas no topo do talude e prelongando-se até 3m abaixo da base do mesmo (embora a sua cravação em solos residuais graníticos possa ser difícil, em função da sua granulometria);
- Pregagens com 12m de comprimento, 25mm de diâmetro, instaladas e injectadas em furações de 100mm de diâmetro. Instaladas com um espaçamento horizontal de 1,5m e em 3 ou 4 níveis, respectivamente para alturas de 5m e 8m. Em solos granulares é usual adaptar-se um reforço entre pregagens para prevenir erosão superficial que não foi considerado na modelação numérica;
- A geometria dos muros de gabiões foi obtida através do manual de dimensionamento da empresa Maccaferri (Maccaferri Ltd., 1995), considerando um rácio H/B≥2. Um peso volúmico de 16kN/m^3 foi adoptado para o muro e o material de aterro no tardoz da contenção foi agregado leve com um peso volúmico de 8kN/m^3 e a φ'_k de 37°.

Para os modelos apresentados acima, e como mencionado anteriormente, o benefício da redução da inclinação do talude e rebaixamento do nível freático apenas foi obtido na abordagem LEM.

10.2 Análise comparativa dos resultados

A Tabela A6 resume os resultados de cada uma das medidas de remediação com base nas análises LEM e FEM.

Tabela A6. Melhoria na MoS (percentual) das diferentes medidas de remediação.

Medida de remedição	Coesão = 0kPa	Coesão = 5kPa	Coesão = 10kPa
Estacas-pranchas	Reduzida	5 - 10% (LE) <5% (FE)	10 - 20% (LE) 5 - 10% (FE)
Pregagens	5 - 20% (LE)	20 - 30% (LE) 25% (FE)	5 - 30% (LE) 40 - 45% (FE)
Muro de gabiões	30 - >50% (LE) 15 - 35% (FE)	30% (LE) 20% (FE)	25 - >40% (LE) 25 - 40% (FE)
Rebaixamento do nível freático [(1)]	Não avaliado	Não avaliado	20 - >30% (LE)
Rebatimento do talude	Não avaliado	15% (LE)	15 - 25% (LE)

[(1)] Apenas válido quando o nível freático é rebaixado de elevado para baixo. Diferenças na MoS entre ter um nível freático baixo e a sua ausência são desprezáveis.

Desta análise foram retirados as seguintes conclusões. A instalação de estacas-pranchas no topo do talude aparenta não resultar num ganho significativo no que toca à MoS do talude. Contudo, a sua presença força a que a superfície de deslizamento crítica seja mais superficial e não afecte o topo do talude. Como tal, e embora a MoS global não seja significativamente aumentada, se a prioridade é apenas assegurar que o topo do talude permanece estável, esta aparente ser uma solução adequada. A modelação FEM revela contudo que os movimentos ao longo do talude não são significativamente reduzidos com esta alternativa.

O uso de pregagens aparenta ser uma solução mais eficaz que a anterior, particularmente em solos coesivos e para taludes de menor altura. Todavia, a sua eficácia depende do seu comprimento e espaçamento (tanto horizontal como vertical). No que toca aos deslocamentos espectáveis ao longo do talude, esta opção prevê reduções entre 30% a 50%. A modelação FEM resulta nestes casos numa MoS superior às análises LEM, o que possivelmente se deve às diferenças no mecanismo de rotura, uma vez que no software PLAXIS 2D, as superfícies críticas formam-se no tardoz das pregagens e, não as atravessando, como ocorre nas análises LEM.

A opção de construir uma contenção da base do talude, neste caso um muro de gabiões, provou ter um efeito similar em todos cenários e registando na maioria dos casos os maiores ganhos em termos de MoS (25 - >40%). Com efeito, o mecanismo crítico de rotura nestes casos passa a depender das propriedades do material de aterro utilizado. Análises adicionais revelam ainda que, quando o material de aterro utilizado não corresponde a agregado leve, os ganhos desta solução cifram-se entre o uso de estacas-pranchas e de pregagens.

No que toca ao rebaixamento do nível freático, as análises LEM revelam que passar de um nível elevado para um nível baixo resulta em ganhos de 20% a 30% na segurança do talude. Quanto à configuração do talude, a redução do seu ângulo pode resultar em aumentos de 15% a 25% no seu FoS.

11 Conclusão

A maioria das análises de estabilidade de taludes efectuadas actualmente continuam a utilizar a abordagem de equilíbrio limite (LEM) através de métodos de fatias. A sua simplicidade e comprovada fiabilidade torna-os uma ferramenta muito útil contra o uso de mais complexas simulações em elementos finitos (FEM). Os últimos contudo, conseguem prever pontos de concentração de tensões e deformações ao longo dos taludes que são impossíveis de identificar em LEM. Como tal, há uma tendência de hoje em dia complementar os resultados LEM com análises FEM visto que deformação excessiva é um dos motivos pelos quais as medidas de remediação são instaladas.

Todavia, os métodos LEM são especialmente úteis quando o talude a analisar possui uma MoS abaixo da unidade. Nestes casos, o benefício das diferentes medidas de reforço pode ser estimado em análises LEM, enquanto que a abordagem FEM raramente consegue analisar situações onde a MoS é significativamente inferior à unidade.

O intuito desta tese foi o de comparar diferentes métodos de cálculo para estabilidade de taludes e de efectuar um estudo paramétrico aos mais importantes inputs geotécnicos neste tipo de problemas, concentrando-se em particular nos solos residuais graníticos da Covilhã. Uma análise de sensibilidade foi igualmente efectuada para a sobrecarga aplicada no topo do talude e para subidas no nível freático, ambos vistos como factores que induzem instabilidade. Os métodos de Fellenius e métodos simplificados de Bishop e Janbu foram utilizados na abordagem LEM, enquanto que o modelo Hardening Soil for escolhido na abordagem FEM.

Adicionalmente a este estudo paramétrico, as mais comuns técnicas de remedição foram abordadas nesta tese, bem como quantificada a sua contribuição para a melhoria da segurança do talude.

Por último, os ábacos de estabilidade produzidos devem apenas ser considerados como indicativos e usados apenas numa análise preliminar de estabilidade. Por outro lado, no que toca à remediação de taludes, a escolha da alternativa a seguir é muitas vezes influenciada por condicionantes locais e pode inclusivamente resultar de uma combinação de efeitos, cuja quantificação sai fora do âmbito deste trabalho.

Table of Contents

List of Figures

List of Tables

List of Symbols and Abbreviations

Greek symbols

α_i	angle between base of slice and horizontal (°)
β	slope angle (°)
Δ_u	excess pore pressures (kPa)
ϕ'	angle of shearing resistance of a rock mass/rock discontinuity (°)
ϕ^b	angle of shearing resistance introduced to relate the shear strength contribution from the matric suction stress state variable
γ	bulk unit weight (kN/m³)
$\gamma_{c'}$	partial factor for the effective cohesion
γ_{cu}	partial factor for the undrained shear strength
γ_d	dry unit weight (kN/m³)
γ_f	partial factor for an actions
γ_G	partial factor for a permanent action
γ_Q	partial factor for a variable action
γ_{qu}	partial factor for unconfined strength
γ_m	partial factor for a soil parameter
γ_R	partial factor for a resistance
γ_S	unit weight of solid particles (kN/m³)
γ_{sat}	saturated unit weight (kN/m³)
γ_w	unit weight of water (kN/m³)
$\gamma_{\phi'}$	partial factor for the angle of shearing resistance ($tan\ \phi'$)
γ_γ	partial factor for weight density
φ'	angle of shearing resistance of a soil (°)
$\varphi'_{critical}$	critical angle of shearing resistance of a soil (°)
φ'_{peak}	peak angle of shearing resistance of a soil (°)
φ'_r	residual angle of shearing resistance of a soil (°)
σ	total normal stress (kPa)
σ'	effective normal stress (kPa)
$\sigma_n - u_a$	net normal stress (kPa)

τ	shear stress (kPa)
τ_f	available shear strength (kPa)
τ_{mob}	mobilised shear strength (kPa)

Roman symbols

A	cross-sectional area (m²)
c	cohesion intercept of the Mohr-Coulomb failure envelope which includes the contribution of matric suction on shear strength (kPa)
C	capacity
C	constant related to the shape of the grains and the surface impurities
C_c	coefficient of curvature
c'	effective cohesion (kPa)
C_u	coefficient of uniformity
D	demand
d	diameter of the capillary tube (m)
D_{10}	grain size that correspond to 10% of passing material (mm)
D_{30}	grain size that correspond to 30% of passing material (mm)
D_{60}	grain size that correspond to 60% of passing material (mm)
$E_{d,dts}$	design destabilising actions
$E_{d,stb}$	design stabilising actions
E_s'	drained secant deformability modulus (MPa)
E_t'	drained tangent deformability modulus (MPa)
E_{u_s}	undrained secant deformability modulus (MPa)
E_{u_t}	undrained tangent deformability modulus (MPa)
f_0	correction factor for FoS
F_d	design value of actions
F_k	characteristic value of actions
F_x	force in horizontal direction (kN)
F_y	force in vertical direction (kN)
FoS_0	factor of safety without correction factor

h	piezometric head (m)
H	slope height (m)
$h_{c\,min}$	minimum height of the capillary fringe (m)
$h_{c\,max}$	maximum height of the capillary fringe (m)
h_w	height of the column of water
i	hydraulic gradient
I_P	plasticity index (%)
l	length (m)
K	Permeability (m/s)
L	slip surface length (m)
M	moment (kNm/m)
N_i	normal force at the base of a slice (kN)
Q	flow (m^3/s)
P_w	hydrostatic pressure in tension crack (kN/m)
R	slip radius (m)
w_L	Liquid limit (%)
u	pore water pressure (kPa)
u_a	pore air pressure
$u_a - u_w$	matric suction (kPa)
V	Volume (m^3)
W	weight of soil block (kN/m)
X_d	design values of geotechnical parameters
X_k	characteristic values of geotechnical parameters
y_c	lever arm for hydrostatic pressure in tension crack (m)
z	slip plane depth (m)
z_w	depth of water table (m)

Abbreviations

BS	British Standard
CBR	California Bearing Ratio
CEN/TC	European Committee for Standardization/Technical Committee

CPT	Cone Penetration Test
DA	Design Approach
EC	Eurocode
EN	European Standard
FEM	Finite Elements
FHWA	Federal Highway Administration (U.S. Department of Transportation)
FoS	Factor(s) of Safety
LEM	Limit Equilibrium
SLS	Serviceability Limit States
min	minimum
max	maximum
MoS	Margin(s) of Safety
NF	Norme Française
NP	Norma Portuguesa
PSD	Particle Size Distribution
SPT	Standard Penetration Test
UBI	Universidade da Beira Interior
ULS	Ultimate Limit States
USACE	U.S. Army Corps of Engineers

1. Introduction

The record of the first use of soil as a construction material is lost in antiquity. However, for years, the art of soil engineering was based almost entirely on past experience, until the need for better and more cost effective designs became crucial from a financial point of view.

Slope instability represents a significant threat to people's safety, especially in regions with an increased landslide hazard given their topographic, geologic and climate settings, such as the Mediterranean area, for example. In fact, landslides occur almost every year in nearly all regions of the world, albeit the number of occurrences and their consequences can be difficult to ascertain. This is due to a significant percentage of them taking place during hurricanes or storm events or even as a by-product of earthquakes.

There is however at least one country in the world where these statistics are accurately kept. Japanese authorities maintain a register of the annual number of human casualties due to landslide incidents, earthquake disasters and volcanic events. These figures (Figure 1) highlight the importance of slope stability, more so given that these occurrences can be prevented or, as a minimum, mitigated.

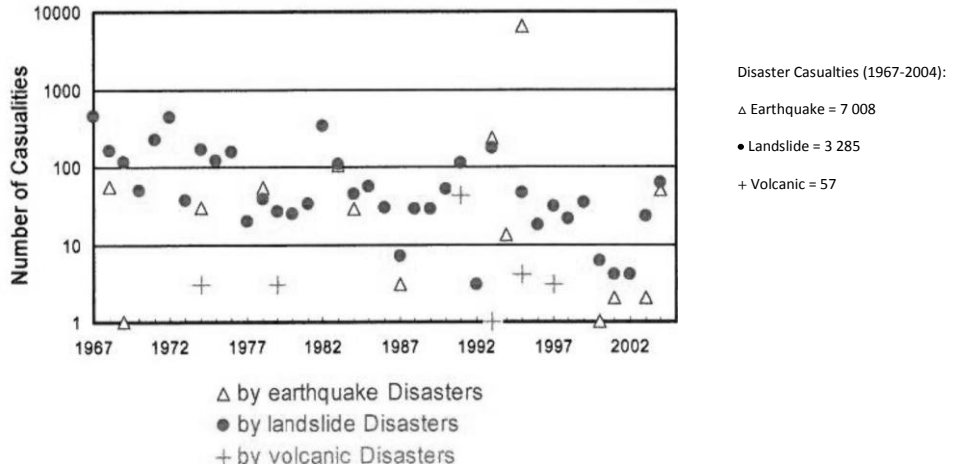

Figure 1. Disaster Casualties in Japan, adapted from Sassa K., Fukuoka et al. (2007).

If the plot shown above is cross referenced with the scale/size of the affected area by each of these type of events, it helps emphasize the importance of accurately mapping the areas in risk of being affected by slope failures. This can work as a very effective prevention tool in the mitigation of this phenomenon.

1.1 Motivation and choice of subject

Slope stability is a worldwide issue which can occur not only due to natural conditions but often triggered by human activities. It can present itself in a vast range of sizes and time scales and with a variety of possible movements. At one extreme a gravitational sliding on a continental scale may occur at a rate of only a few centimetres per year, whereas a relatively localised and sudden failure can take place in highway cuttings or open-cut mines.

Much data has been collected over time during the undertaking of civil and mining works, motivated by the economic impact of slope failures. The continuous study of the problem has also led to a refinement in calculation methods to ensure compliance with design standards.

Regardless of the design approach used, the full understanding of the problem and what it entails requires an accurate knowledge of its likely causes and an awareness of the different instability mechanisms that may occur. Simultaneously, a slope stability assessment requires an understanding of the relevant geological and geotechnical properties of soils and rocks that govern the resisting (shearing) forces. Furthermore, the instability phenomenon may present different particularities for distinct ground conditions, and is of major significance in large scale geotechnical works, such as highways/railways, canals, open pit mines, tunnels and even embankment dams. However, a distinction should be made amongst the previous examples, as permanent slopes excavated for infrastructure are typically designed for long-term stability whereas in mining operations they are generally temporary, having to remain stable for only several months or a few years, until mineral extraction ceases.

Although the latter are perceived as temporary, its stability must still be addressed, especially due to the continuous geometry changes that slopes undergo during mining operations. Taking this issue lightly may result in serious consequences, as the exemplified by the recent Tumbi Quarry landslide in Papua New Guinea (Figures 2 and 3). At the time of writing the causes for the incident were still yet to be determined (Fox, Liam; ABC News, 2012).

Figure 2. Global view of the landslide in Tumbi Quarry in Papua New Guinea (Fox, Liam; ABC News, 2012).

Figure 3. Closer perspective of the landslide in Tumbi Quarry in Papua New Guinea (Fox, Liam; ABC News, 2012).

Further examples of slope stability problems near transport infrastructures are the recent landslides that occurred in both Leiria, Portugal, along the IC36 (Figure 4) and in Taranaki, New Zealand, near the Manawatu Gorge (Figure 5). The first incident was most likely a result of a lack of drainage along the slope, which had not yet been installed at that time, whilst the second one was potentially a result of intense rainfall in the area (Petley, The Landslide Blog, 2010).

Figure 4. Landslide along Highway IC36, Leiria, Portugal.

Figure 5. Landslide in Taranaki, near the Manawatu Gorge, New Zealand (Petley, 2010).

The construction of the well-known Panama Canal, and especially one of its sections, known as the Culebra Cut (Figures 6 and 7), turned up to be particularly challenging from a geotechnical perspective as a result of continued landslides. In fact, the canal was filled with water in 1913, but had to undergo several dredging operations along that section of the route, and it was not opened until August 1914 (Rogers, J.; Missouri S&T, 2008).

Figure 6. Dredging operations at Culebra Cut 1913 (Rogers, J.; Missouri S&T, 2008).

Figure 7. Present day look of the Culebra Cut (Rogers, J.; Missouri S&T, 2008).

Slope stability analysis also serves as a supplement to tunnel design. In fact, portals form one of the most critical parts of the tunnel as they are generally sited on slopes with thin overburden and where active mass movements can occur. This is particularly relevant if the tunnel excavation intersects unstable discontinuities, allowing them to daylight onto a free face (Figure 8). The portal zones can also comprise particularly weathered and/or highly fractured materials (Figure 9).

Figure 8. Landslide-blocked west portal of tunnel near the Yamakoshi Village, Japan (Rathje, Jibson et al, 2004).

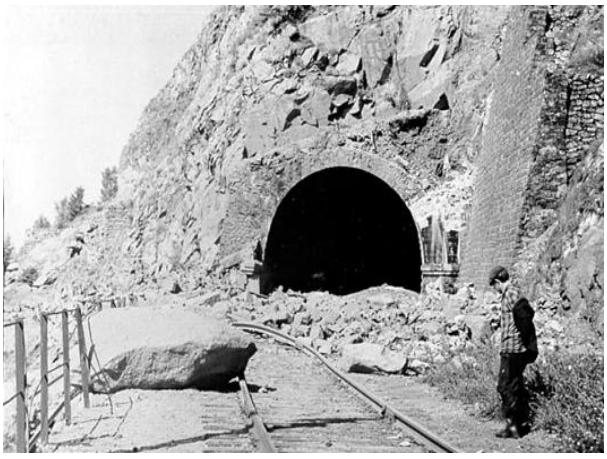

Figure 9. Landslide that demolished the western portal a tunnel of the Trans-Siberian Railway, in the vicinity of the Beryozovaya creek in the Irkutsk region, Russia (Mikhail, 1998).

As mentioned earlier, slope stability can be a decisive factor in the stability of a dam and regardless of its construction stage. This has been emphasized by the Vajont catastrophe in 1963 in Italy, which culminated in around 2000 deaths. The incident was the result of a

massive landslide which projected itself into the reservoir and generated a high wave that overtopped and breached the dam (Petley, 2008), as shown in Figures 10 and 11.

Figure 10. View of the Vajont Damn, Italy, before the landslide accident (Petley, 2008).

Figure 11. View of the Vajont Damn, Italy, after failure (Petley, 2008).

Although the cause of the movement is still not entirely known, it seems likely that the rising in reservoir levels resulted in excessive pore pressures within existing clay layers. This in turn, may have contributed to a reduction of its effective normal stress along the slip plane and, consequently, its shear resistance (Petley, 2010).

As previously stated, and illustrated by some of the earlier examples, slope stability is of particular importance in mountainous regions due their irregular topography. However, in some of these areas another problem has to be dealt with, the repeated freeze-thaw cycles (Figure 12). This situation is of particular interest in rocky zones, where the formation of ice along discontinuities can trigger slope movements. This phenomenon can be witnessed in the scree deposits at the base of some fiords in Norway (Figure 13).

Figure 12. Example of a freeze/thaw phenomenon (Wooten, Rick; NCGS).

Figure 13. Talus cones on the north shore of Ifjorden, Svalbard, Norway (Wilson, Mark A.; The College of Wooster, 2009).

Yet, slope stability is not confined to difficult terrains and also presents itself as a key feature in the design of temporary and permanent slopes for civil works (Figure 14), where usually stabilisation measures are installed due to geometrical constraints that unable the desired slope height or angle to be achieved.

Figure 14. Slope failure within a residential development in Lisbon and a sketch of its failure mechanism (Schuster & Highland, 2001).

Regardless of the context where slope stability analyses are being undertaken, and considering the disastrous consequences of landslides, it is crucial to evaluate the need for monitoring plans to be put into place during and post construction. These can monitor not only the soil/rock mass, but also any nearby structures. Such plans typically include the definition of alert and alarm criteria in advance of the commencement of the works, as well as strengthening measures should these values be exceeded.

The current standard which regulates geotechnical design in Europe is the Eurocode 7, also known as EC7 (NP EN 1997-1:2010, 2010). It stipulates the design requirements for capacity, stability, serviceability and durability of geotechnical structures. This is meant to be used in conjunction with both Eurocode 0 (NP EN 1990:2009, 2009), which establishes the basic design principles, and Eurocode 1 (NP EN 1991-1-1:2009, 2009), which prescribes the factors of safety that are applied to actions on buildings and civil engineering works. All loads and actions, deriving exclusively from the existing ground conditions, are defined exclusively in EC7.

These standards set out, for each (geotechnical) design, the relevant limit states to be checked and separates Ultimate Limit States (ULS) from Serviceability Limit States (SLS). Nevertheless, both are required to comply with the fundamental inequality (Equation 1) considering the appropriate design values for actions, resistances and strengths:

$$E_{d,dts} \leq E_{d,stb} \quad (1)$$

in which $E_{d,dts}$ represents the design destabilising actions and $E_{d,stb}$ the design stabilising actions.

Besides these new European standards (EN 1990 to EN 1999) and their national annexes, which focus primarily on actions and design considerations, there are other relevant norms that also provide guidance and recommendations on the design and construction procedures of earthworks, materials' specification or geotechnical investigation procedures. Useful examples are the following:

- FHWA-NHI-10-024 - Geotechnical Engineering Circular No. 11 - Design and Construction Guidelines of Mechanically Stabilized Earth Walls and Reinforced Soil Slopes;
- FHWA-SA-97-075 & -076 – Geotechnical Engineering Circular No. 3 - Earthquake Engineering for Highways, Design Principles, Vols. 1 & 2;
- USACE EM 1110-2-1912 - Stability of Excavated and Natural Slopes in Soils and Clay Shales;
- BS 6031:2009 - Code of practice for earthworks;
- BS 5930:1999+A1:2007 - Code of practice for site investigations;
- Manual of Contract Documents for Highway Works, Volume 1 – Specification for Highway Works (Department for Transport - Highways Agency);
- NF P 11-300:1992 – Earthworks, Classification of materials for use in the construction of embankments and capping layers of road infrastructures;
- NF P 94-290 (P94-290) - Geotechnical Design, Earthworks;
- Practical Manual for the Use of Soils and Rocky Materials in Embankment Construction (Laboratoire Central des Ponts et Chaussées).

In slope stability problems it is common to make use of structural/resistant elements within the soil/rock mass to enhance the overall shear resistance. Therefore, and since the Eurocodes are design orientated and not specifically focused on construction details, additional standards from the European Committee for Standardization (CEN/TC 288) on the execution of special geotechnical work should also be referred to. These cover a wide variety of techniques such as:

- Bored piles (BS EN 1536:2010+A1:2015);
- Ground anchors (BS EN 1537:2013);
- Diaphragm walls (BS EN 1538:2010+A1:2015);
- Sheet piling (BS EN 12063:1999);
- Micro pilling (BS EN 14199:2015);
- Soil nailing (BS EN 14490:2010);
- Reinforced fill (BS EN 14475:2006).

1.2 Objectives

This thesis is part of the on-going study, currently being undertaken at UBI, of one of the region's most abundant resource, its granitic residual soil. This is a very common construction material in the area, particularly in highway schemes, which has raised the interest on its behaviour from a slope stability perspective (Figure 15).

Figure 15. Cutting through granitic residual soils of the Covilhã region and embankment constructed along the same road alignment reusing these materials.

This particular type of soil and its properties, although usually falling within a rather well-defined range of values, have been the subject of significant analysis in order to expedite the design and stability assessment of future and existing earthworks.

An experimental embankment was completed in November 2010 (Figures 16 and 17) using the granitic residual soil of the area to help with the study of its geotechnical properties. The embankment shoulders were constructed with varying gradients, from 45º to 80º to the horizontal, having remained stable since its construction. In addition, a surcharge of 10kPa was applied to the crest of the slope, near its steepest section, without any evidence of instability.

Figure 16. View of the experimental embankment.

Figure 17. Steepest slope face (80º).

The relevant soil parameters of the materials used in this construction have been derived through published data and by means of laboratory testing and incorporated in the numerical modelling. To better understand the potential of this residual soil, this study has primarily focused on assessing its slope stability using two different calculation approaches, Limit Equilibrium (LEM) and Finite Elements (FEM).

The ultimate goal has been to produce a design chart that enables an expedite stability assessment of granitic residual soil slopes, considering different soil parameters, slope geometries, applied surcharges and groundwater levels.

Finally, this research has also sought to illustrate the most suitable remediation measures when addressing slope failures in these materials. This has also considered both LEM and FEM approaches.

1.3 Methodology

The methodology adopted in this study has begun with an extensive bibliographic research on the topic, covering previous doctoral theses on similar topics, guidelines and standards of several geotechnical organisations and government agencies, a clear indicator of the global extend of the problem, as well as numerous published articles on conferences and congresses.

Naturally, a significant part of the literature reviewed has consisted of technical publications whose authors are well-known experts on the subject.

The inputs required for the numerical simulations have been derived from laboratory testing undertaken by other PhD candidates at UBI, and published data on the subject.

Following a review of the appropriate soil parameters, the numerical analyses have been progressed, initially making use of a LEM commercial software especially designed to address slope stability (SLOPE/W – GeoStudio 2012, May 2014 Release version 8.13.0.9042, under Jacobs UK Ltd. licence). Prior to its use a hand validation of the software's outputs has been undertaken to confirm its accuracy.

Among the most common LEM based methods, which are incorporated in SLOPE/W, the Bishop's and Janbu's simplified methods, and Fellenius' method have been used in this study. The findings of the previous methods have also been compared with the results from the FEM analysis using the commercial software PLAXIS 2D (Release version 1012.1.12068.7096, under Jacobs UK Ltd. licence). The comparisons are based on the obtained Margins of Safety (MoS) for different combinations of soil parameters, applied surcharges and groundwater profiles.

Finally, and in order to illustrate the suitability of the proposed remediation measures an estimation of their effectiveness has also been undertaken using both LEM and FEM approaches.

1.4 Structure of the thesis

This thesis consists of seven chapters and has been developed as another step of the on-going study of the Covilhã's granitic residual soil at UBI. It intends to not only provide useful information for geotechnical and other civil engineering professionals, but also steer the way into additional research.

Initially, in Chapter 2, a review of the state of art regarding slope stability is undertaken, covering the main factors influencing slope stability as well as the most common failure mechanisms.

Then, in Chapter 3, granitic residual soil are introduced, along with an overview of the published data and laboratory test results and their findings, which are used in this study.

Chapter 4 focuses on slope stability per se, the soil principles behind it and the classic (LEM) and FEM formulations for the problem. Reference is also made to the commercial software used and the difficulties associated with numerical modelling.

Gathered all of the analyses outputs, Chapter 5 is devoted to presenting and summarising them, for both LEM and FEM approaches, including the presentation of the proposed design charts.

In Chapter 6 the most common remedial measures to stabilise failed, or marginally stable, slopes are presented, including a quantification of their benefits (increase in MoS).

Finally, in Chapter 7 some conclusions and critics about the work that has been undertaken are presented, along with proposals for future investigation/development on the subject.

2. State of the art

In a state of the art article, Duncan (1996) stated that "the first prerequisite for performing effective slope stability analysis is to formulate the right problem, and to formulate it correctly". However, the number of parameters involved in slope stability and their estimation lead to the conclusion that an exact solution to this type of problems is often unattainable. As such, methods of analysis have been sought and developed which have enabled engineers to assess the disturbance of man-made slopes on the existing ground stability. This typically results from either removing or placing new soil, thus varying the pre-existing stresses, or by applying additional surcharges (Figure 18).

Figure 18. Examples of additional surcharge from buildings along slopes (Wattie, 2008).

The refinement of these tools, which started off as a by-product of direct observation/experience, has been closely accompanied by field and laboratory research, always balancing commercial interests and safety requirements. In broad terms, the aims of slope stability analysis are as follows:

- Assessment of the stability of natural and man-made slopes based on geotechnical investigations, historical data, and a sound mechanistic approach complemented by empirical observations and experience;
- Analysis of landslides to understand failure mechanisms, verify the accuracy of stability analysis techniques and assess the potential for future landslides;
- Development of remedial measures and planning for preventive measures for failed and marginally stable slopes, respectively;
- Evaluation of the effects of seismic loading and environmental conditions.

A crucial aspect of slope stability is its required design life, as permanent slopes require a long term stability analysis, whereas temporary works or with mining operations only need to remain stable for a short period of time.

Regardless of the time factor, slope stability focuses on assessing a lump Factor of Safety (FoS) which provides a simplistic way of establishing the need for and ranking any stabilising measures. The FoS is nothing more than a deterministic measure of the ratio between the resisting forces (capacity, C) and the driving forces (demand, D), as shown in Equation 2.

$$FoS = \frac{C}{D} \quad (2)$$

When this ratio is unitary a limit equilibrium state is, in theory, reached. In reality, given the uncertainty about the likely performance of the slope under such critical conditions, a more robust design acceptance criterion is usually adopted. This may vary with the importance of the slope and the severity of the consequences of failure. As a result, a minimum FoS is established, which relates to a Probability of Failure (PoF), for each scenario. This may take into account the effects of dynamic loading (typically a seismic event), as showed in Table 1.

Table 1. Typical FoS and PoF acceptance criteria values (Read & Stacey, 2009).

Consequences of Failure	Acceptance criteria		
	FoS (min) (static)	FoS (min) (dynamic)	PoF (max) P [FoS≤1]
Low	1.2 – 1.3	1.0	15 - 20%
Moderate	1.3	1.05	10%
High	1.3 – 1.5	1.1	5%

This deterministic approach has however been superseded by the use of the Eurocodes and the concept of Margins of Safety (MoS) as opposed to the use of a lump FoS. But regardless of the approach to be used, the FoS/MoS should always reflect the degree of confidence in the input parameters.

Thus, an understanding of the relevant geotechnical parameters, the most likely failure mechanisms and a correct assessment of the factors conditioning or triggering instability is crucial. For example, a thorough stability assessment of a slope is largely dependent on the identification and understanding of its drainage conditions, the correct choice of shear strength (drained or undrained) and the use of the appropriate type of analysis (total or effective stress). However, prior to the design stage, site investigations, intended for geotechnical, environment and hydrogeological purposes, are typically undertaken. Their findings are then used to establish a conceptual ground model and the relevant geotechnical parameters to use in design.

The usual laboratory work includes classification and shear strength testing in soils, direct shear strength evaluation on discontinuities and compressive strength tests in rocks.

To sum up, slope stability fundamentally involves undertaking analysis against predicted failure modes that could affect the slope and then comparing the obtained results with the agreed/established acceptance criteria.

2.1 Factors influencing slope stability

Slope movement often is a complex process which involves a continuous series of events from cause to effect, making it rather difficult to pinpoint a single trigger to the movement. It is largely determined by lithology and stratigraphy (influencing strength, deformability and permeability), as well as the hydrogeological conditions, the topography of the terrain and the weather conditions. A combination of these may trigger a failure event along one or more sliding surfaces, which induces the movement of the unstable mass.

Of the different factors influencing slope stability, which are detailed in the next Subsections, saturation appears to be the primary cause of landslides, especially if resulting from rainfall. Its magnitude depends on both weather conditions (distribution and duration of precipitation and changes in temperatures) and topography.

This helps to explain the reason behind the majority of slope movements typically occurring in a specific period of the year: in summer (June and July), after heavy and prolonged rains. Also, studies have concluded that the interval between the beginning of above-normal rainfall and the start of slope movement depends on the permeability of the soils but also on the type and form of the landslide induced (Mencl & Záruba, 1982). Nevertheless, the influence of weather conditions on slope movements across Central Europe, where precipitation is distributed throughout the year, cannot be compared with zones where rainfall is seasonal and restricted to shorter periods of time.

Besides the influence of water there is another key factor commonly accepted to have a great influence in the occurrence of landslides; seismic events. When discussing seismically active regions of the world, it is clear that earthquakes are one of the most important landslide-inducing agents. The intensity required to trigger slope instability depends on several factors, from which the geological structure, geometry of the slope and amount of precipitation preceding the event stand out (Mencl & Záruba, 1982).

Lastly, and in addition to natural occurrences, human activities play a crucial role in slope stability. Disturbing or changing drainage patterns, destabilising slopes and removing vegetation are common human-induced factors that may trigger instability. Other examples

include steepening of slopes by undercutting its toe, placing loads on its crest or even the presence of leaking pipes.

In fact, the abundant variety of slope movements somehow reflects the diversity of factors that may disrupt its stability. The most relevant are listed over the next sections, focusing primarily on soil slopes. These are subdivided in internal causes (acting within the slope), external factors (acting outwith of the slope) and the effects of groundwater.

2.1.1 Internal causes

The type of materials comprising a slope is intrinsically related to the modes of failure that may occur, as different lithologies present a distinct susceptibility to potential slippage or failure. However, the location of the failure surfaces is also dependent on the spatial arrangement of the different strata.

In situ stresses also play an important role in slope stability, particularly when they are relieved due to excavation works. This may lead to a change in the slope materials' properties and their behaviour. Particularly in deep excavations, the tension relief can result in a significant change in the ratio between vertical and horizontal stresses at rest (K_0). The new state of equilibrium may be responsible for developing high stresses at the slope's toe and inducing significant displacements.

2.1.2 External causes

The most common external causes of slope stability are often a by-product of human activity, although they may also be a consequence of natural events. Seasonal temperature and humidity variations can lead to superficial shrinkage cracks that, in turn, facilitate water infiltration (Guerra, 2008).

2.1.2.1 Geometry changes

The most recurrent external trigger is a change in geometry, usually due to excavation works near the slope's toe. In general, geometry changes are a result of one, or a combination, of the following options:

i. *Changes in gradient:* caused by natural or man-made events or, in singular cases, as result of tectonic activity. An increase in gradient leads to a change in stresses within the affected mass, increasing shear stresses and disturbing the existing equilibrium;

ii. *Changes in height:* which can result from vertical erosion or excavation works. The most common example of the former is the deepening of a valley due to weathering and the associated relief in lateral stresses.

At this stage it is worth mentioning that reprofiling slopes is often the preferred remedial option to stabilise them. However, this often results not only in a decrease of the disturbing forces but also in the lessening of the acting normal pressures along the failure surface which, in turn, reduces the resisting forces.

2.1.2.2 Vibrations and overloading

Other sources of disturbance to the existing equilibrium within a slope are induced vibrations and overloading. The former are usually caused by earthquakes, explosions, heavy traffic or even the impact of sea waves. During a seismic event, a soil element within a slope is subjected to a series of alternate shear stresses which are added to those it already bears. As such, depending on the original shear stresses and the magnitude of the cyclic action, slope movement may be induced. Also, when dealing with sandy saturated materials, their stability will also be affected if the porewater pressures reach a critical limit, when all resistance is suddenly lost and the sandy materials act as a fluid (liquefaction). The phenomenon affects not only sands, but also a variety of well-graded soils that contain a significant coarse fraction (Dawson, Morgenstern et al., 1998).

As for overloading, and especially when the load increment is applied at the crest, it results in additional shear stresses and porewater pressures, especially in clayey soils, which reduces shear resistance.

2.1.2.3 Weathering and erosion

There is a significant degradation in the strength properties of both rock and soil slopes due to weathering. In soils, the soluble mineral constituents and/or the cementing elements can be gradually washed away, which may result in a loss of cohesion and a reduction of the angle of shearing resistance.

The weathering process is a mechanism of continuous degradation (either physical or chemical) that can affect geotechnical structures which have remained stable for a long period of time. It leads to a gradual reduction in the FoS until the critical limit equilibrium is reached and collapse occurs. This phenomenon assumes however a greater importance on rock masses than on soils as it results in greater substantial reductions in strength and

deformability parameters, ultimately transforming the rock mass into a complex mixture of bedrock, weathered rock and residual soil.

Commonly associated with weathering is the erosion (undercutting) at the toe of slopes, which may result, in extreme cases, in unsupported overlying material and which can be responsible for landslides or rock falls. Nonetheless, erosion can also be internal, with the formation and subsequent collapse of cavities in karsic areas as an example (Vallejo, Ferrer et al., 2004).

Erosion is also often related to deforestation, being commonly accepted that forests play a crucial role in the protection of the soil and prevention of landslides. They lessen the weathering effects on the slope surface and their shielding effect can be split into three different components, namely the treetops, the accumulated plant debris at ground level and the root system. Treetops are responsible for shielding the slope from direct sun exposure, as well as wind and rain, thus preventing sudden variations in temperature and water content. They are also responsible for eliminating a substantial portion of the water in the ground by evapotranspiration.

As for the plant debris, it retains a part of the water that hits the ground surface (the thicker the more significant the effect) and promotes a subsurface flow, along with the root system, which helps prevent potentially erosive surface runoff (Figure 19). The root system also contributes to an improvement in the overall shear resistance, not only from a mechanical point of view, but also from a hydraulic perspective (Guidicini & Nieble, 1984). However, it should be noted that the tree system also acts a surcharge along the slope face.

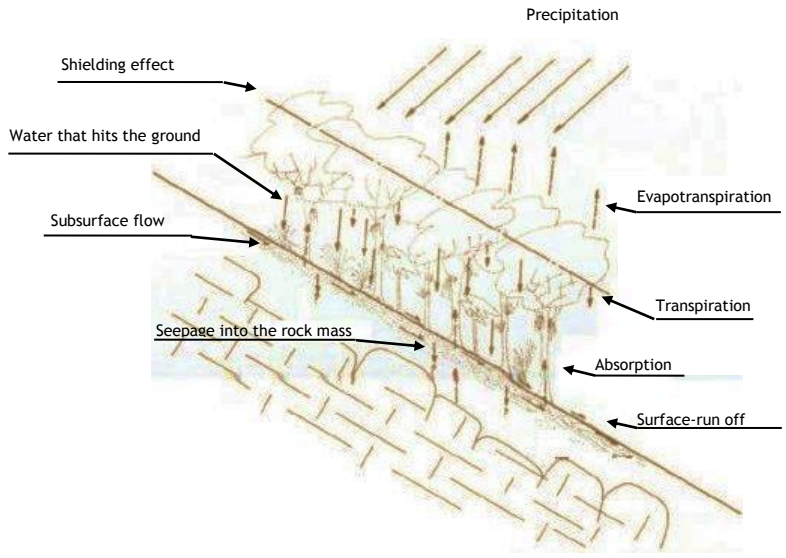

Figure 19. Main components of the water balance of a forested slope, adapted from Guidicini & Nieble (1984).

2.1.3 Presence of water

Most failures are triggered, or at the very least worsened, by the presence of groundwater. Its principal effects are as follows:

i. *Changes in porewater pressures:* Rain and melted water infiltrate through joints and/or cracks increasing porewater pressure and reducing shear resistance. In fact, measurements taken during rainfall periods have confirmed that recurrent slope movements occur in exceptionally high rainfall events. This is especially damaging in clayey soils when it succeeds a long dry period, as the soils become desiccated and superficial cracks are formed;
ii. *Liquefaction:* Abrupt changes in porewater pressures (typically associated with seismic events) may lead to the liquefaction of sandy soils (McRoberts & Sladen, 1985);
iii. *Frost effects:* Especially relevant in rock masses, water in fissures and joints expands when it freezes and reduces the acting normal pressures. Alternatively, the freezing of water in superficial layer of soil along a slope face may prevent drainage, thus disturbing the existing equilibrium and leading to a build-up in porewater pressures.

In soils or intensely fractured rock masses, shear resistance can be expressed in accordance with Equations 3 and 4, either for cohesive or non-cohesive materials respectively:

$$\tau = c' + (\sigma - \gamma_w h)\, tg\varphi' \quad (3)$$

$$\tau = (\sigma - \gamma_w h)\, tg\varphi' \quad (4)$$

- σ – normal stress on a given point P of a possible slip surface;
- h - piezometric head at the same point;
- γ_w – unit weight of water;
- φ' - angle of shearing resistance of the slip surface.

These equations will be analysed in more detail in Chapter 4, and are only presented at this stage to illustrate how a rise in groundwater levels contributes to the reduction of shear resistance.

The shape of a water table within a slope is determined both by the permeability of the materials and its geometry (Figure 20). It is also influenced by the presence of materials with sharply different permeabilities, as illustrated below.

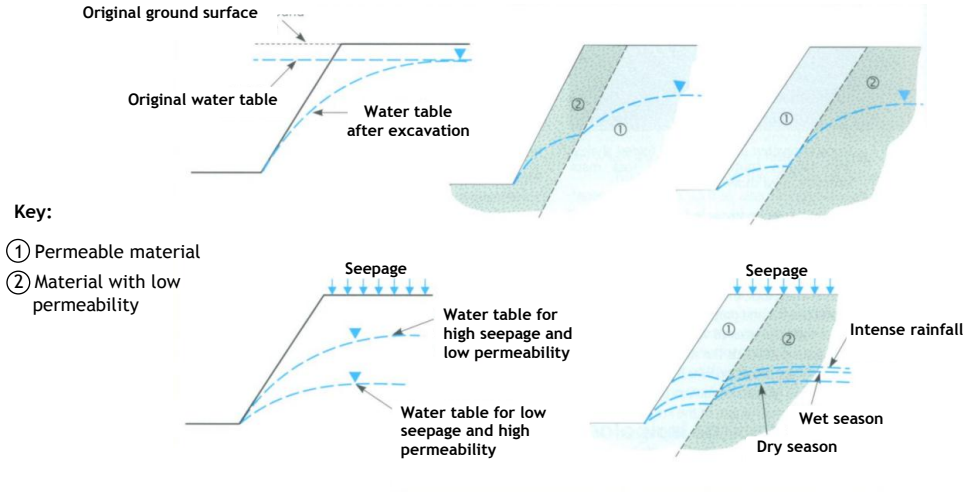

Figure 20. Diagrams of the water table in a slope as a function of the distribution of materials and presence of infiltration, adapted from Vallejo, Ferrer et al. (2004).

Provided that a given water table is unconfined and that its position is known, the water pressure, u, at a given point can be approximately estimated from the weight of column of water above it (Equation 5):

$$u = h_w . \gamma_w \quad (5)$$

- h_w – height of the column of water;
- γ_w – unit weight of water.

However, this expression does not account for a non-horizontal water flow within a slope, and therefore becomes less rigorous as the angle of flow increases from the horizontal. As such, the definition of the pore pressures within a slope is complex and usually requires assumptions to be made. The common hypothesis adopted for estimating pressures (flow parallel to the slopes, hydrostatic conditions, etc.) do not take into account the parameters controlling the hydraulic regime of the slope, which may lead to error.

In simple situations, the porewater pressures along on a planar slip plane (with or without the formation of tension cracks) can be approximately estimated by assuming triangular distributions of hydrostatic pressure on these surfaces (Figure 21). In the figures below, the height of the triangle corresponds to the maximum water pressure value along the failure plane (Vallejo, Ferrer et al., 2004).

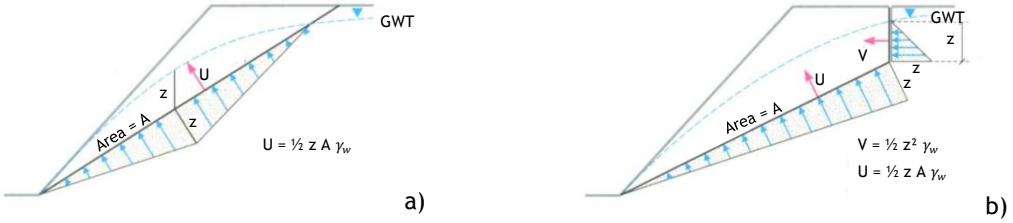

Figure 21. a) Resultant hydrostatic force along a planar slip plane in a soil slope , adapted from Vallejo, Ferrer et al. (2004);

b) Pressure distribution when a tension crack develops at the top of the slope (U and V are the resultant hydrostatic forces along the slip plane and tension crack, respectively), adapted from Vallejo, Ferrer et al. (2004).

When dealing with low permeability rock masses with families of joints and fractures, the existing water pressures can often present steep variation in consecutive discontinuities (Figure 22, Guidicini & Nieble, 1984).

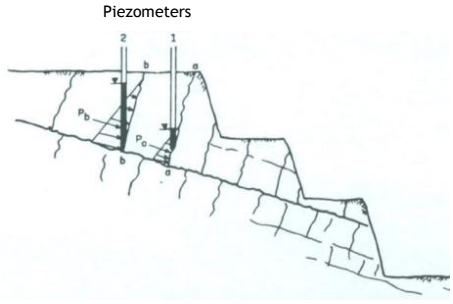

Figure 22. Example of pore pressure distribution within a rock mass (Guidicini & Nieble, 1984).

Changes in the water table are usually either seasonal or the result of long periods of rainfall or drought. However, and although these changes typically occur during relatively long periods of time, it may happen that, after intense rainfall, the water table will quickly rise within very permeable materials. In such situations, or whenever the groundwater table within a slope is not horizontal (Figure 23 a), Equation 3 should be re-written as Equation 6.

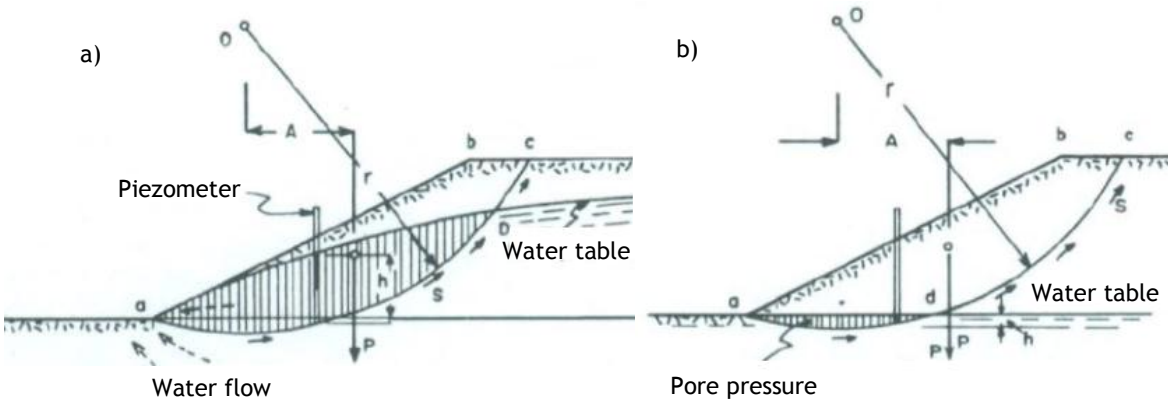

Figure 23. Differences in porewater pressures distributions after a quick rise in groundwater levels, adapted from (Guidicini & Nieble, 1984).

$$\tau = c' + \sum(\sigma_i - \gamma_w h_i)\, tg\varphi' \quad (6)$$

Where $(\sigma_i - \gamma_w h_i)$ is the effective normal pressure on each unitary surface element. The expression is valid in both scenarios however, the pore pressures along the slip surface are much higher on the first instance, which will have a negative impact on the resisting shear forces. This can help to explain how a slope, having remained stable throughout several seasons, with slow changes in the water table, can fail after a quick rise in levels.

When groundwater flows through the soil it applies, due to its viscosity, a certain pressure on the soil particles, which acts in the direction of the flow and is proportional to the speed of the fluid. If we assume a laminar flow within the soil, Darcy's law (Equation 7) is the basic equation governing the flow of groundwater through it and states that the volume rate of saturated flow (Q) of groundwater is directly proportional to the cross-sectional area (A) through which flow is occurring, the hydraulic gradient (i) and the permeability of the soil layer (K).

$$Q = KiA \quad (7)$$

For groundwater to flow it needs to overcome the resistance produced by its own viscosity and by the soil fabric, which results in a loss of energy (piezometric head Δh) which is transferred into the soil grains (Figure 24). As this transfer occurs within a determined length Δl, loss of energy per metre $\Delta h/\Delta l$ is known as the hydraulic gradient (i). Within a slope, if flow occurs it is likely to have a vertical component (Figure 25).

Figure 24. Water pressures on the soil grains as water flows through (Guidicini & Nieble, 1984).

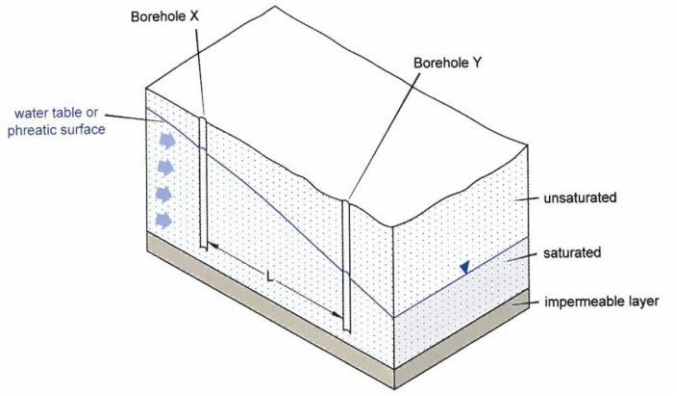

Figure 25. Typical groundwater flow within a soil (Read & Stacey, 2009).

According to Darcy's law, the magnitude of the flow, and therefore of the water pressures, is proportional to the loss of piezometric head. Therefore, this is of greater importance at the toe of a slope, where particle movement along the flow net may be induced.

This erosive process can potentially lead to an unstable situation by dragging away soil particles, particularly in granular materials. And ultimately, if the toe is to fail, the remainder of the slope top will surely follow by lack of support.

However, most slopes are heterogeneous and anisotropic, which makes it easier for water to flow in one direction than another. In the example illustrated in Figure 26 the permeability in the direction parallel to the bedding is greater than in the perpendicular direction. This is often the result of the compaction of the soil or the presence of strata with remarkably heterogeneous permeability.

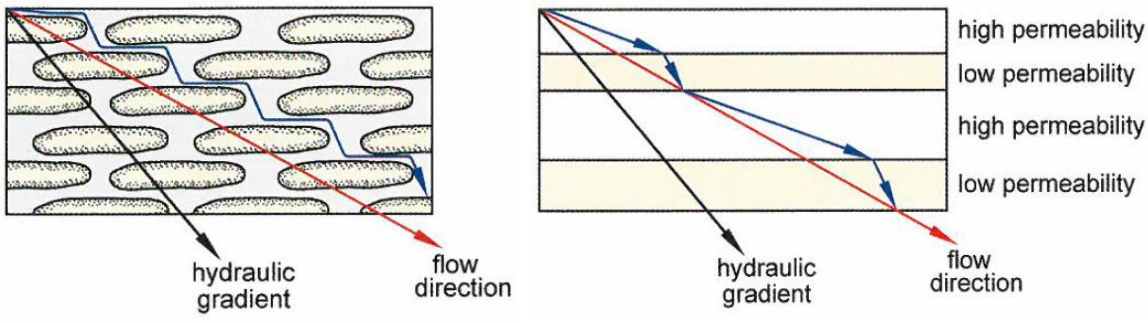

Figure 26. Anisotropy of permeability (Read & Stacey, 2009).

Moreover, the presence of interstitial water in soils, even in non-cohesive materials, can generate, by means of matric suction and due the specific surface area, cohesive features. Yet, these properties tend to disappear with soil saturation or drying. Therefore, in the right

settings, it is possible to obtain a vertical slope in slightly humid sandy soils, as suction is generated by the large contact area between air and water particles.

This phenomenon takes place because the soil is generally hydrophilic, tending to absorb and hold moisture on its surface. When desaturating a soil, small interfaces or menisci tend to form between the air, moving into the pores of the soil, and the water fraction. The air pressure is usually assumed to be atmospheric or "zero gauge" relatively to atmospheric pressure.

2.1.3.1 Capillarity.

Due to capillary action, water is drawn up from the water table into the interstices of the soils above it. This region is known as capillary fringe and is of particular importance in fine-grained soils where the interconnected voids act like capillary tubes, partially saturating the soil within this height (Smith, 1990).

Water in this fringe (Figure 27) can be regarded as being in a state of negative pressure, i.e., pressure values below atmospheric.

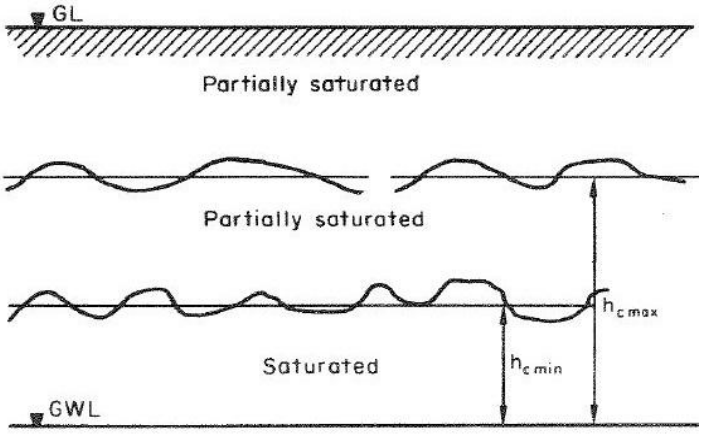

Figure 27. Diagram of capillary fringe (Smith, 1990).

The minimum height of the fringe ($h_{c\,min}$) is dependent on the maximum size of the voids within the soil. Up to this height the soil can be considered as fully saturated. Within the range $h_{c\,min}$ and $h_{c\,max}$ the soil can only be considered as partially saturated (Smith, 1990).

An approximate relationship between $h_{c\,max}$ and the grain size for a granular soil is presented in Equation 8 (Terzaghi & Peck, 1948). Since the diameter of the capillary tube (d) is approximately one fifth of D_{10} (refer to Section 3.3) the capillary rise formula can be simplified (Das, 2011).

$$h_{c\,max} = \frac{C}{e\,D_{10}} \approx \frac{150}{D_{10}} \quad (8)$$

The constant C is related to the shape of the grains and the surface impurities. Should be noted that the expression above is only valid for granular soils.

2.2 Physical and mechanical parameters

The most relevant parameters in the long term stability of slopes are the angle of shearing resistance (φ') and effective cohesion (c') of soils and rocks. These parameters are used to describe how normal and shear stresses relate, as illustrated in Figure 28. The shear stress needed to induce movement is proportional to the applied normal stress and this relationship is defined by two parameters mentioned above.

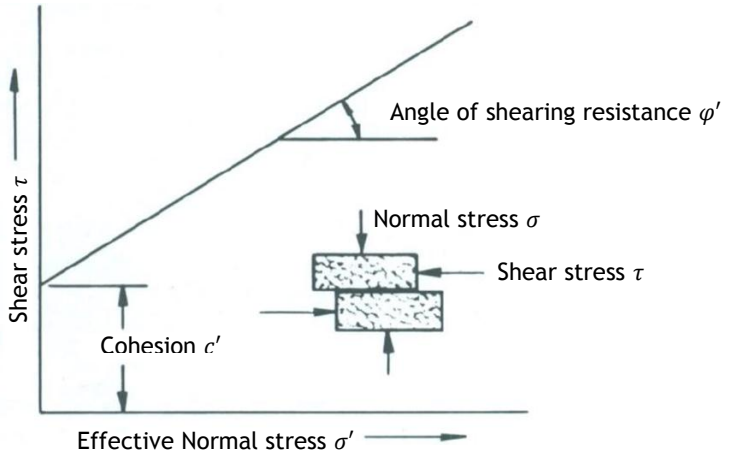

Figure 28. Correlation between the shear stress needed to induce movement on a slip surface and the applied normal stress, adapted from Guidicini & Nieble (1984).

From a mathematically point of view, the shear stress required to induce movement, in absence of null normal stresses, is defined as the effective cohesion of the material/slip surface. Consequently, and condensing the term $(\sigma - \gamma_w h)$ from Equation 3, Equation 9 can be written which governs soil or rock (discontinuities) behaviour.

$$\tau = c' + \sigma' \, tg\varphi' \quad (9)$$

Typical values, or ranges of values for the parameters mentioned above are presented in Table 2 below. This also includes estimates for unit weights.

Table 2. Typical soil parameters for rocks and soils (Guidicini & Nieble, 1984).

TYPICAL PROPRIETIES OF ROCKS AND SOILS							
DESCRIPTION		UNIT WEIGHT(γ)		FRICTION ANGLE (φ', for soils & ϕ', for rocks)		COHESION (c')	
		MATERIAL	[kN/m^3]	MATERIAL	[°]	MATERIAL	[kPa]
NON-COHESIVE	SAND	Dry gravel	14.4	Compact, well graded and uniform sand	40 – 45	-	
		Dry fine sand	16.0				
		Humid	18.4	Loose and well graded sand	35 -40		
		Very Humid	19.2				
				Dry and fine sand	30 -35		
	BOULDER	Common	17.6	Common	35 – 40	-	
		Fluvial	22.4	Sandy and compact	40 – 45		
		Loose	18.4	Sandy and loose	35 - 40		
		Sandy	19.2				
NON-COHESIVE	LOOSE ROCK	Granite	16.0 - 20.0	Crushed or fragmented rock	35 – 45	-	
		Basalt	17.6 - 22.4	Crushed or fragmented chalk	35 - 45		
		Limestone	12.8 - 19.2	-	-		
		Chalk	10.0 - 12.8				
COHESIVE	CLAY	Dry	17.6	Dry clay	30	Very hard clay	175
		Humid	18.4	Humid clay	40	Hard clay	100
		Wet	19.2	Hard clay	10 - 20	Regular clay	50
		Sandy loam	16.0	Soft clay	5 – 7	-	
		Loam	17.6	Clay filing	10 – 20		
		With boulders	20.0	Breccia or angular rocky fragments	14 – 27		
	INTACT ROCK	Granite	26.1	Granite	30 – 50	Hard rock masses (e. .g granite)	100 – 300
		Quartzite	26.1	Quartzite	30 – 45		
		Sandstone	19.5	Sandstone	30 – 45	Sandstone or Limestone masses	150
		Limestone	21.7	Limestone	30 – 50		25
		Chalk	17.6	Chalk	30 - 40	Soft rock masses	25 - 100

However, the linear dependence between τ and σ can often suffer variations, and the effective cohesion is often considered null in granular materials, which implies that shear resistance in these is a purely frictional phenomenon.

Additionally, it is worth noting that the shear resistance of soil-rock interfaces is typically inferior to the shear strength of the soils above it, further decreasing with the smoothness and absence of undulation along the rock surface.

2.2.1 Pre-existing movement

It is common to witness cracks on the crest of slopes, some of which have been monitored for dozens of years without any noticeable unstable behaviour. According to some researchers

(Guidicini & Nieble, 1984), these cracks are often a result of minor shear movements within the slope. These, although individually small, when accumulated may lead to significant slope movement, sufficient to cause a vertical separation on the materials at the top of the slope, thus forming tension cracks.

The fact that these structures are a result of shear movements is extremely relevant, as when a tension crack becomes visible it can be an indicator that a slip surface may have already been formed within the slope and that a shear failure process is underway.

However, it is nearly impossible to quantify just how hazardous this phenomenon is, since it represents the beginning of a complex and progressive failure mechanism. Moreover, there is also the possibility that, in some cases, the appearance of tension cracks is purely associated with a relief in porewater pressure (Guidicini & Nieble, 1984).

2.3 Types of slope failure

According to Mencl & Záruba (1982) "Sliding phenomena involve such a variety of processes and disturbing factors that they afford unlimited possibilities of classification".

Technically, a landslide is the general term used to describe the downslope movement of soil, rock, and organic materials under the effects of gravity and also the landform that results from such movement (IAEG, 1990). Landslides can be classified into different types on the basis of the type of movement that takes place: fall, topple, slide, flow, etc. (IAEG, 1979).

Considering the scope of this document, only failure mechanisms associated with soil slopes will be presented in the following sections.

2.3.1 Rotational slides

Instability in soil slopes typically occurs along curved slip planes (Figure 29) and, according to Terzaghi and Peck (1948), they can be classified as "slope failure", "toe failure" or "base failure" (Sassa K. , Fukuoka, Wang, & Wang, 2007). These designations are dependent on where the slip surface daylights in relation to the slope face, i.e., somewhere along the slope face, at its toe or, if sufficiently deep-seated, emerging beyond this point (Terzaghi & Peck, 1948).

Nevertheless, when a slope consists either of homogeneous soil or different strata with homogeneous geotechnical properties, the most usual slip surface is roughly circular with its lower end cutting the slope at its toe (Figure 29).

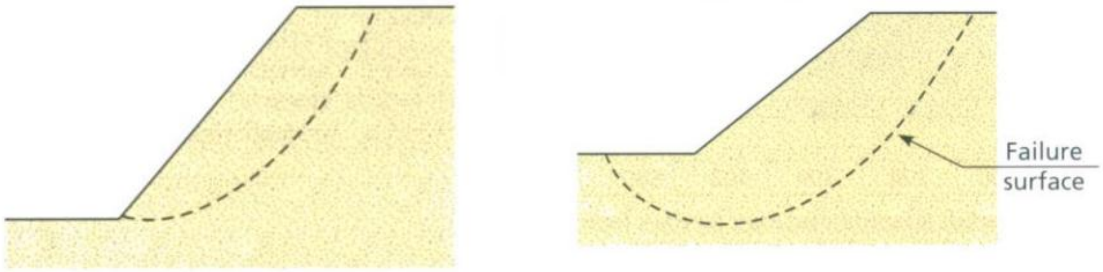

Toe failure

Deep / base failure

Figure 29. Examples of rotational failures in soils, adapted from Vallejo, Ferrer et al. (2004).

In this type of failure, movement does not tend to occur simultaneously over the whole of what eventually becomes the slip surface. However, under certain circumstances, the triggered mass may move in a relatively coherent manner and with little internal deformation (Bobrowsky & Highland, 2008). The displaced mass slides in a more or less rotational movement about an axis parallel to the slope (Figure 30).

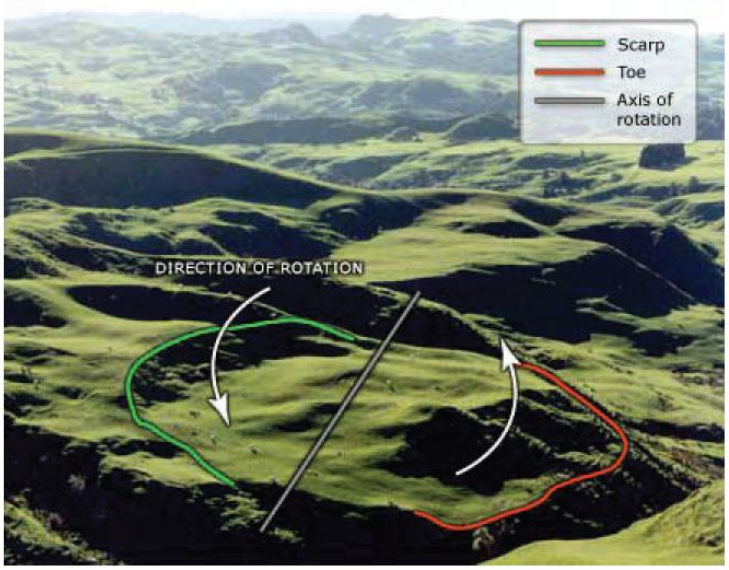

Figure 30. Example of a rotational slide (Bobrowsky & Highland, 2008).

The head of the displaced material moves almost vertically downward, as exemplified in Figure 31. The triggering mechanisms, as mentioned earlier, are often associated with intense and/or sustained rainfall leading to the saturation of slopes and rises in the water table.

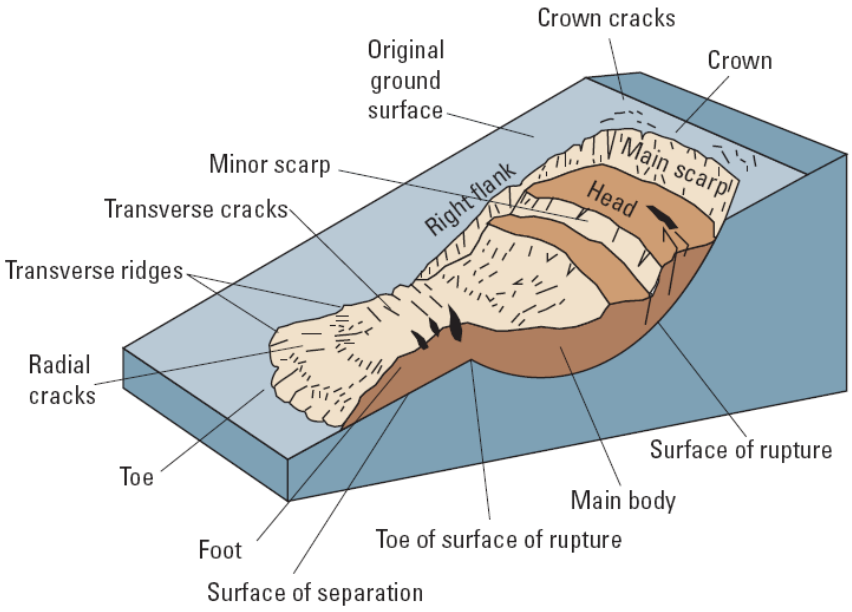

Figure 31. Schematic of a rotational landslide (Bobrowsky & Highland, 2008).

2.3.2 Translational slides

In certain conditions, i.e. where there are strata or layers with distinct proprieties, slope failure may occur along a plane surface or a polygonal surface made up of several planes (Figure 32).

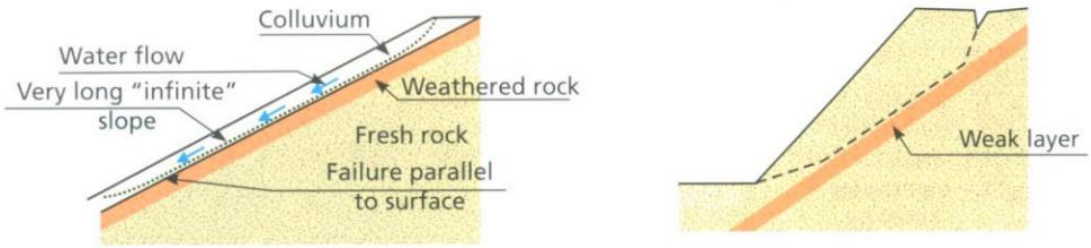

Figure 32. Types of translational failures in soils (Vallejo, Ferrer et al., 2004).

Slope failure that occurs along a single plane, parallel to the slope, is not as common as rotational slips. This "infinite" slope situation is harder to come across in natural slopes, apart from shallow rock slopes which are covered with residual soil or debris.

In this type of landslide, the soil mass moves out, or down and outward along a relatively planar surface with little rotational movement (Figure 33). This movement may progress over considerable distances if the failure surface is sufficiently steep (Figure 34), and usually takes

place over geologic discontinuities such as faults, joints, bedding surfaces, or the contact between rock and soil. Its triggering mechanisms are identical to rotational movements.

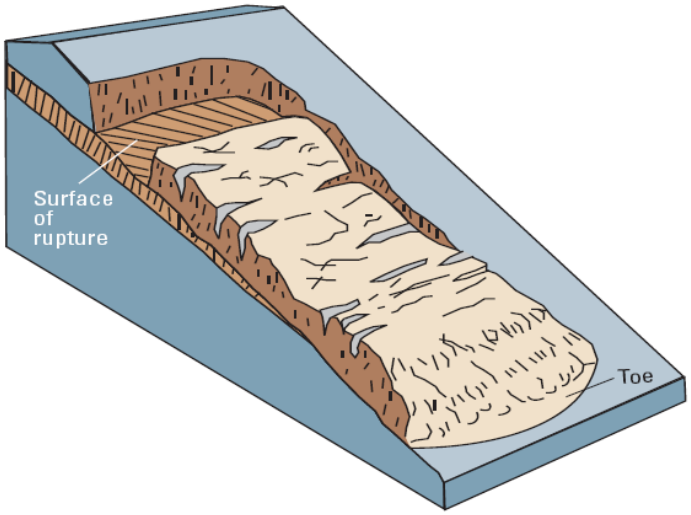

Figure 33. Schematic of a translational landslide (Bobrowsky & Highland, 2008).

Figure 34. Example of a translational landslide (Bobrowsky & Highland, 2008).

2.3.3 Lateral spreads

Lateral spreads usually occur on very gentle slopes or essentially flat terrain, when a stronger upper layer of cohesive materials undergoes extension and moves above an underlying softer and weaker layer. This is commonly followed by some general subsidence into the weaker underlying stratum (Figure 35).

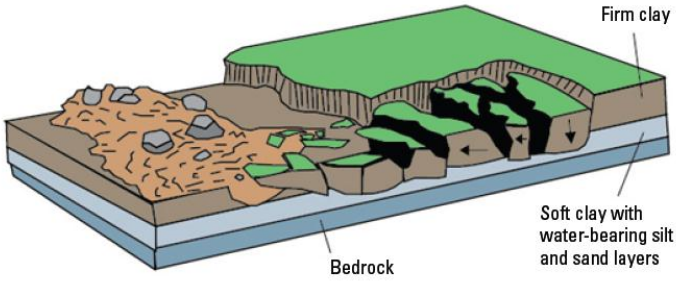

Figure 35. Schematic of a lateral spread (Bobrowsky & Highland, 2008).

According to (Bobrowsky & Highland, 2008) this phenomenon is usually precipitated by:

i. Liquefaction of lower weak layer by earthquake shaking (Figure 36);
ii. Overloading of the ground above an unstable slope;
iii. Saturation of the underlying weaker stratum;

Figure 36. Example of a lateral spread damage to a roadway as a result of an earthquake (Bobrowsky & Highland, 2008).

2.3.4 Flows

A flow is a spatially continuous movement in which the shear failure surfaces are closely spaced and are usually not preserved. The velocity of the displacing mass in a flow resembles a viscous liquid, in which loose soil, rock and even organic matter combine with water to form a slurry that moves downslope (Figure 37).

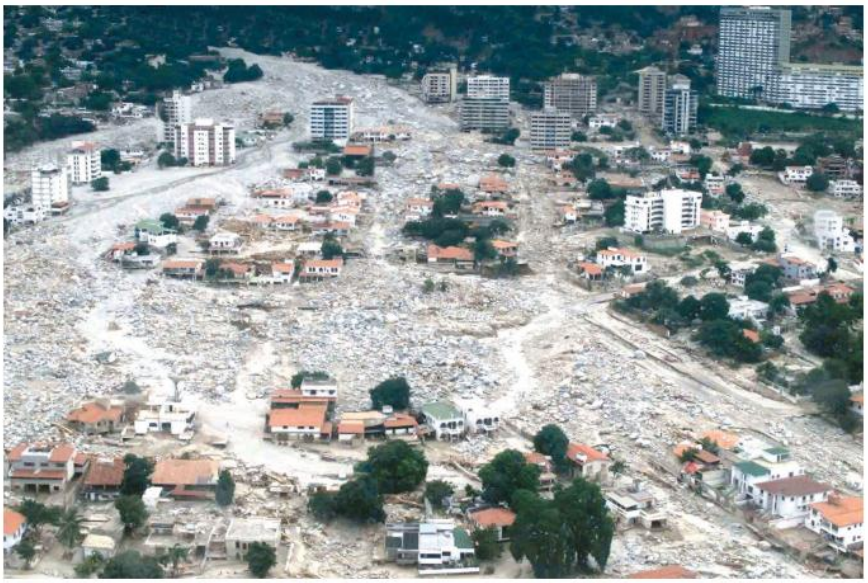

Figure 37. Example of a debris-flow damage (Bobrowsky & Highland, 2008).

Occasionally, as a rotational or transactional slide gains velocity and as the internal mass loses cohesion or gains water, it may evolve into a flow. These events are often triggered by intense surface-water flow, due to heavy rain (Figure 38) or rapid snowmelt, that erodes loose soil on steep slopes.

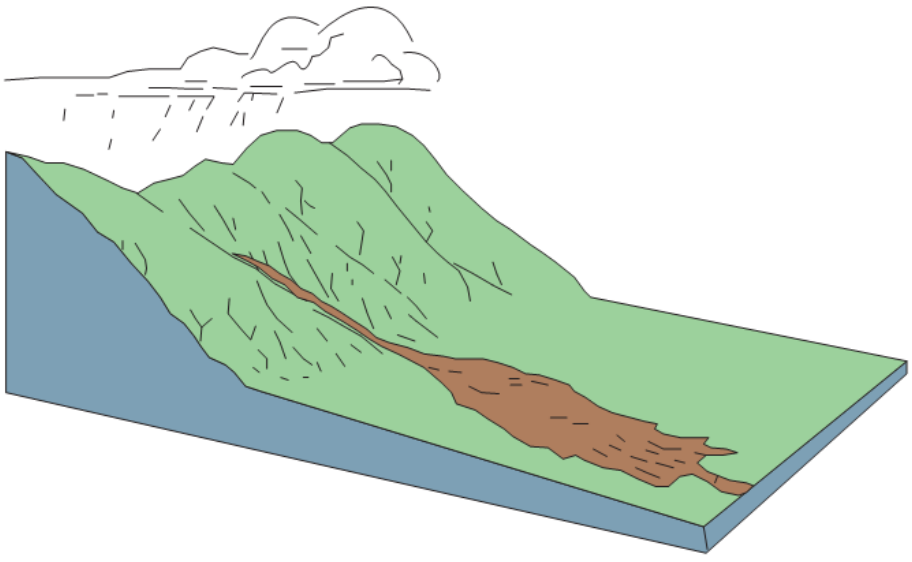

Figure 38. Schematic of a debris flow (Bobrowsky & Highland, 2008).

The destructive potential of a flow depends on its velocity, and the ones "particular dangerous" to human life are those which achieve or surpass a velocity of the order of 5 m s^{-1}. Slower movements are usually only responsible for material damage. The limit of 5 m s^{-1}

roughly corresponds to the speed of a person running and it known as “catastrophic velocity”. Landslides capable of reaching these velocities are classified as “extremely rapid” (Cruden & Varnes, 1996).

2.3.5 Slow flow (creep)

This particular type of slope movement, typically referred to as creep, consists of an imperceptibly slow, yet steady downward movement. This is caused by an internal shear stress which is sufficient to cause deformation but not enough to generate failure. Generally falls within three categories (Bobrowsky & Highland, 2008):

i. Seasonal, where movement occurs within the depth of soil affected by seasonal changes in soil moisture and temperature;
ii. Continuous, when shear stress continuously exceeds the strength of the material;
iii. Progressive, when the slope’s mass reaches a point in which a sudden failure event might take place.

Creep can often be identified by curved tree trunks, bent fences and/or retaining walls, tilted poles (Figure 39) and small soil ripples or ridges on the surface (Figure 40). The travelling velocity of the dislocated mass is usually less than 1 meter per decade (Bobrowsky & Highland, 2008).

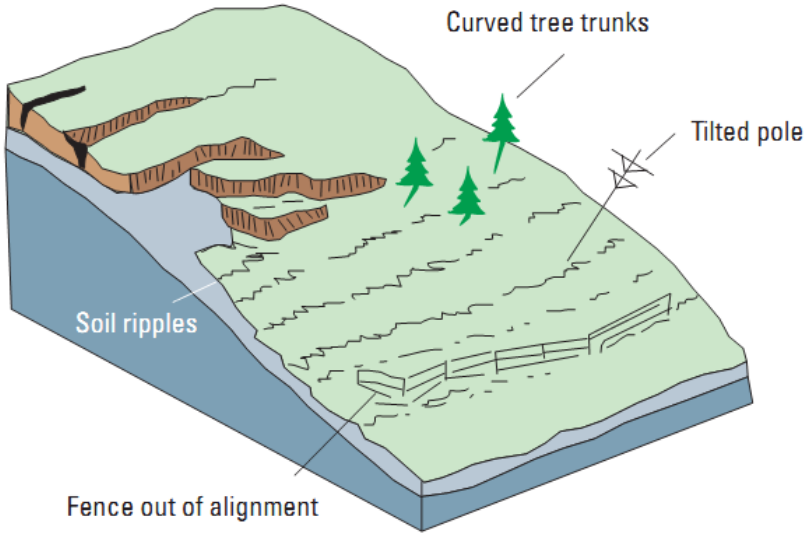

Figure 39. Schematic of a slow earthflow, also referred to as creep (Bobrowsky & Highland, 2008).

Figure 40. Example of the effects of creep (Bobrowsky & Highland, 2008).

2.3.6 Non-planar failure

Although this type of failure mechanism is associated with rock masses, it has been considered to include within this section, as it takes place in very weathered or heavily jointed rock masses (presenting an almost isotropic behaviour), precursors of the formation of residual soils.

In these situations, non-planar and even circular failures may take place, as the rock mass begins to alter its original response, behaving increasingly more like a soil (Figure 41).

Figure 41. Diagram of a curved failure surface in heavily jointed rock (Vallejo, Ferrer et al., 2004).

3. Geotechnical characterization of a residual soil

3.1 Introduction

Unlike other civil engineering materials, soils can present a significant variability. In fact, their proprieties can vary considerably within just a few meters in a site. A thorough and comprehensive site investigation is therefore a fundamental prerequisite for any design work, allowing for a better understanding of the existing geological conditions and the estimation of any relevant soil parameters.

A typical site investigation may include preliminary studies, which comprise a desk study and site reconnaissance, geophysical surveys, the undertaking of exploratory holes, *in situ* testing, sampling and associated laboratory testing, as well as groundwater observations and monitoring. Common procedures include:

- A preliminary geological survey, using geological maps with a scale relevant to the type of project;
- Trial pits to inspect the materials and take disturbed samples;
- Boreholes sunken to recover disturbed and undisturbed samples, which then undergo laboratory testing;
- *In situ* testing, including permeability tests, in both trial pit and borehole locations.

The relevant soil parameters are usually derived by a combination of laboratory and/or *in situ* findings, as both have advantages and limitations in their applicability. Consideration should be given to the fact that the sampling, transportation and specimen preparation procedures usually subject the samples to strains that affect their structure.

Furthermore, it is important to ensure that the laboratory testing is carried out on samples which are truly representative of the existing material at the site. This is ensured by undertaking complementary field tests, more relevant when in soils which are sensitive to any disturbance (The Government of the Hong Kong Special Administrative Region, 2000).

When trying to characterise a given soil a wide range of tests is available. Table 3 below summarises some of the most common options.

Table 3. Most common *in situ* and laboratory tests on soil samples.

Category of test	Name of test	Remarks/Objectives
In situ	Hand shear vane	The Vane Shear Test is mainly used to determine the in situ undrained shear strength of a cohesive soil. The test works by inserting a vane and rotating it until the soil fails, being the undrained shear strength assessed by analysing the torque and knowing the diameter of the vane used.
	Standard penetration test (SPT)	Penetration test used to determine the density of a soil. Given its popularity and wide spread use its results are usually correlated to obtain different soil parameters.
	Cone penetration test (CPT)	Penetration test used to measure the force required to push a "cone" into the ground, thus providing information on the friction generated in each stratum between the cone and the soil. As opposed to the SPT, the CPT is a continuous test which allows the soil stratigraphy to be delineated. Given its popularity and wide spread use its results are usually used in correlations to obtain different soil parameters. A variation, the $CPT_{(u)}$, is also capable of measuring the porewater pressures of the intersected strata.
	California bearing ratio (CBR) *	Penetration test used to determine the aptitude of a soil or aggregate sample as a road subgrade. The harder the stratum the test in conducted in, the higher the CBR rating.
	Pressuremeter test	Commonly used to test hard clays, dense sands and weathered rock to measure the "at-rest horizontal earth pressure" by means of a flexible membrane which applies even pressure to the walls of the borehole as it expands.
	Dynamic probing	A cylindrical steel sacrificial or fixed cone which is driven vertically into the ground using a high frequency percussive hammer using a given drop weight and height. Blows are recorded every 100mm and the results can be directly correlated to a standard penetration test 'N' value.
	Flat dilatometer test	Generally used to determine the soil in-situ lateral stress and soil lateral stiffness by driving a steel blade into the ground, inflating it and measuring the corresponding pressure and deformation.
	Permeability test**	There are a vast number of laboratory and in situ tests to determine the permeability coefficient of soils. For sandy silts and silty sands, the Khafagi probe, Menard probe, water filtration method, constant head laboratory test and falling head laboratory test are the most accurate (Nagy, Tábacks et al., 2013).
Laboratory	Moisture content	Used in the determination of basic soil properties, e.g. dry density, water content and degree of saturation.
	Atterberg limits	Used to determine the consistency boundaries of a soil (Atterberg limits – liquid and plastic limit), which are defined by the amount of water a soil needs to reach those boundaries. These results are often used in correlations to establish other engineering properties.
	Particle size distribution: • Sieving • Sedimentation	Commonly used classification test that allows an understanding of which properties govern the behaviour of a given soil. Sieving allows the grading of the soil coarser than silt. The proportion of soil passing the finest sieve (163 μm) represents the combined silt and clay fraction. The relative proportions of silt and clay are then determined by sedimentation, which is often prescribed only if the percentage of fines is found to be greater than 10 to 15%.
	Triaxial compression and consolidation tests	Conducted in order to assess soil strength and deformation parameters and permeability. Values of the deformation moduli of the soil samples are obtained from the stress strain curves.
	One-dimensional consolidation (oedometer test)	Allows for a reasonable assessment of how a soil sample behaves (settles) under compression and for a range of different stresses. Tests can also be used to determine how the samples respond to unloading.
	Direct shear tests	A useful and practical alternative to the consolidated drained triaxial test for shear strength measurements. Although when coarse material is present it may require a large sample for the test to be undertaken.

Note:

* CBR testing can also be undertaken in a laboratory using a remoulded sample.

** Permeability tests can be carried out both *in situ* and in a laboratory.

3.2 Residual soils

The definition of a residual soil is one which has been formed *in situ* by decomposition of a parent rock and which has not been transported to any significant distance. This occurs when the decomposition processes are quicker than the erosion and transport of the resulting soil grains, as illustrated by Figure 42 below. However, these soils can also result from erosive processes, as long as they are not transported afterwards. This occurs frequently in the Portuguese granitic residual soils (Figure 43).

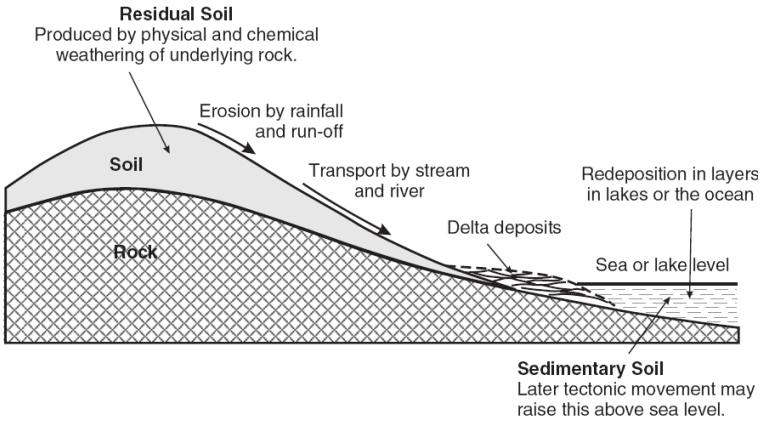

Figure 42. Formation of sedimentary and residual soils (Wesley, 2010).

Figure 43. Example of granitic residual soil slope with parent rock visible at the bottom.

Sedimentary soils, on the other hand, undergo a systematic and continuous sorting process during the stages illustrated above (erosion, transportation and deposition). As a result, finer particles are separated from the coarser fraction of the soil and deposit themselves in different locations and/or layers.

Another difference between the two is that, according to Wesley (2010), the concepts of stress history and of normal and overconsolidation are of little relevance in residual soils. "There is no such thing as the virgin consolidation line of a residual soil, a fact that is not always appreciated by those investigating their properties. The "virginal state" of a residual soil is the parent rock from which it is formed, not a soft sediment at the bottom of the sea or a lake (as is the case with sedimentary soils)".

In fact, and although residual soils cover a very significant extent of the Earth's surface, Soil Mechanics has paid much less attention to them then to sedimentary soils, as its principles were mainly studied and defined in countries where the latter were the most common and

problematic. Nevertheless, residual soils can present some particularly complex features, exhibiting a significantly different behaviour from sedimentary soils with similar grading, void ratio and moisture content.

This is thought to be the result of interparticle connections, inherited from the original parent rock, or due to the chemical reactions that occur through the weathering process (Fernandes, 2011). As such, it is questionable just how representative are grading curves for these soils and whether their geotechnical parameters should be extrapolated from them, given that sieving necessarily affects and/or breaks this bond.

Residual soils are most common in tropical or subtropical climate areas, as the relatively high temperatures, combined with an abundance of water, allow the chemical reactions involved in the decomposition of rocks to occur. Also, the abundant vegetation in these regions shields the soils from erosion, thus facilitating the formation of residual soils.

Granite rock masses are predominant in the northern part of Portugal and in the surroundings of the Serra da Estrela mountain complex. Here, granitic residual soils are abundant and typically extend to depths between 5.0m and 10.0m, albeit they can reach in some instances a maximum depth of circa 20m (Fernandes, 2011). In the Covilhã area these materials cover more than 50% of the surface and can extend to maximum depths of over 18.0m (Cavaleiro, 2001).

However, the transition between granite and its residual soil is not abrupt and typical follows the weathering profile of presented in Figure 44. This illustrates the progressive stages of transformation/weathering from fresh rock to its correspondent residual soil.

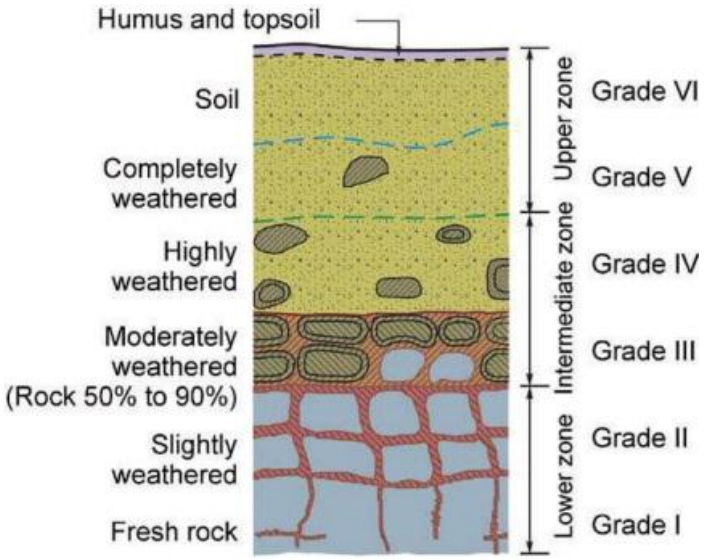

Figure 44. Typical weathering profile of residual soil (Aung & Leong, 2011).

Naturally, as we get closer to the surface the following changes in properties are expected:

- An increase in porosity and void ratio;
- An increase in water content;
- A reduction in the bulk and dry unit weights;
- Smaller mean particle size.

Figure 44 also presents a scale (right hand side) which is typically used when describing the weathering state of a given material, in order to reduce ambiguity. Each of the grades is described to some detail in Table 4 below.

Table 4. Classification of the engineering weathering profile, adapted from Fernandes (2011) and Huat (2012).

Weathering classification			Description
	Term	Zone	
Residual soil	Residual soil	VI	All rock material is converted to soil. The rock mass structure and material fabric (texture) are completely destroyed. The material generally presents both a coarse and a finer fractions and has an homogenous colour.
	Completely weathered	V	All rock material is decomposed to soil but the original texture is still visible. Material partially preserved, although samples cannot be recovered by normal rotary boring techniques. The material is very sandy and friable if soaked in water or squeezed by hand. Can be used as backfill material and, when in slopes, requires protection against erosion.
	Highly weathered	IV	The rock material is in the transitional stage to form soil. Material condition is either soil or rock with the fabric completely preserved and is often presents some coloration. Mass structure is partially preserved, although it usually contains less than 50% rock. Can be partially recovered using traditional rotary boring techniques.
Semi-residual soil	Moderately weathered	III	The rock material shows a partial coloration and the mass structure and material texture are completely preserved. Discontinuity is commonly filled by iron-rich material. Offers considerable resistance to digging without the use of explosives and the percentage of rock varies between 50 and 90%.
	Slightly weathered	II	Some coloration along discontinuities and on part of the rock mass. The mass structure and material texture are completely preserved. In granite, some of the feldspar starts to decompose. The resistance is almost the same as fresh rock and the percentage of rock is over 90%. Requires explosives for excavation works.
	Fresh rock	I	No visible sign of rock material weathering. Some coloration on major discontinuity surfaces.

Residual soils are usually a combination of sand, silt and clay size particles, in varying proportions, depending on the geological setting where they have been formed. The most

recurrent types on tropical and temperate areas are a product of the decomposition of granitic, sedimentary and meta-sedimentary rocks (Salih, 2012).

Besides the geological setting, topography can also influence the properties of a residual soil, as it may interfere in the type of clay minerals formed. In mountainous areas for example, the soil is typically well drained and seepage tends to occur downwards (Figure 44). This phenomenon, in the right geological setting, is associated with the formation of low-activity clay minerals, especially kaolinite (Wesley, 2010). Soils containing these generally have good engineering properties.

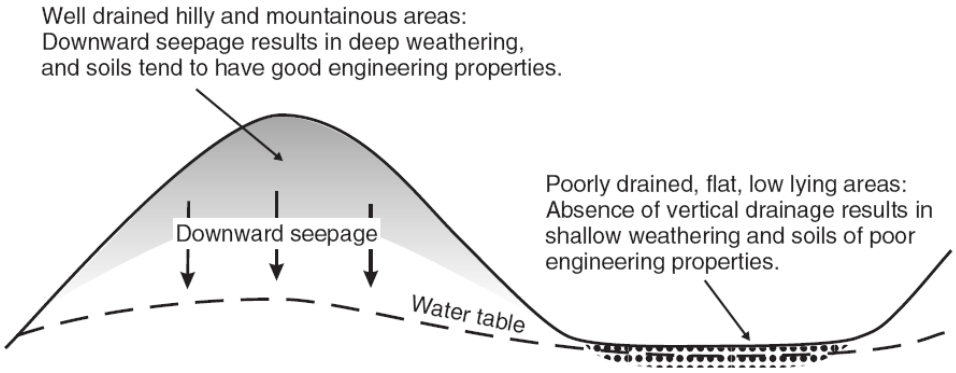

Figure 45. Influence of topography on residual soil formation (Wesley, 2010).

In contrast, in wide and flat areas, where drainage is limited and changes in groundwater levels occur primarily as a result of seasonal changes, there is a tendency for montmorillinite and associated high-activity clay minerals (smectites) to be formed (Wesley, 2010). However, once again this will depend on the existing geological setting. Regardless, soils containing these minerals generally have poor or undesirable geotechnical properties.

In general, residual soils tend to be substantially more permeable than sedimentary soils. This is due to both their microstructural features, such as the aggregation of clay particles into clusters, and the ability of creating bonds between particles that lead to a very open structure. However, the remoulding and compacting of residual soil samples tends to destroy its fabric, which may significantly decrease its permeability.

Furthermore, the permeability of a young residual soil , i.e. a material that both physically and chemically can be classified as a soil but that retains the structure and matrix of the original parent rock, tends to be greater than of a mature residual soil where continuous weathering has eroded this ‘inheritance’ (Fonseca, 1996).

3.3 Granitic residual soils of the Covilhã region

The typical composition of a granitic residual soil from this region (Figure 46) contains kaolinite as the most common clay mineral (Pais, 2007).

Figure 46. Location of the Covilhã region (Europa Turismo) and example of granitic residual soil slopes in Covilhã.

The fine fraction in these soils varies, although predominantly low, with sand typically being the predominant fraction. This classified them as mostly silty gravelly sands or sandy gravelly silts.

Figure 47 below illustrates the grading envelope obtained from circa 80 different samples of granitic residual soils of the Covilhã region. These historical results show the percentage of sand and gravel to total circa 60% to 95% of its weight, with a percentage of fines between 7% and 38%.

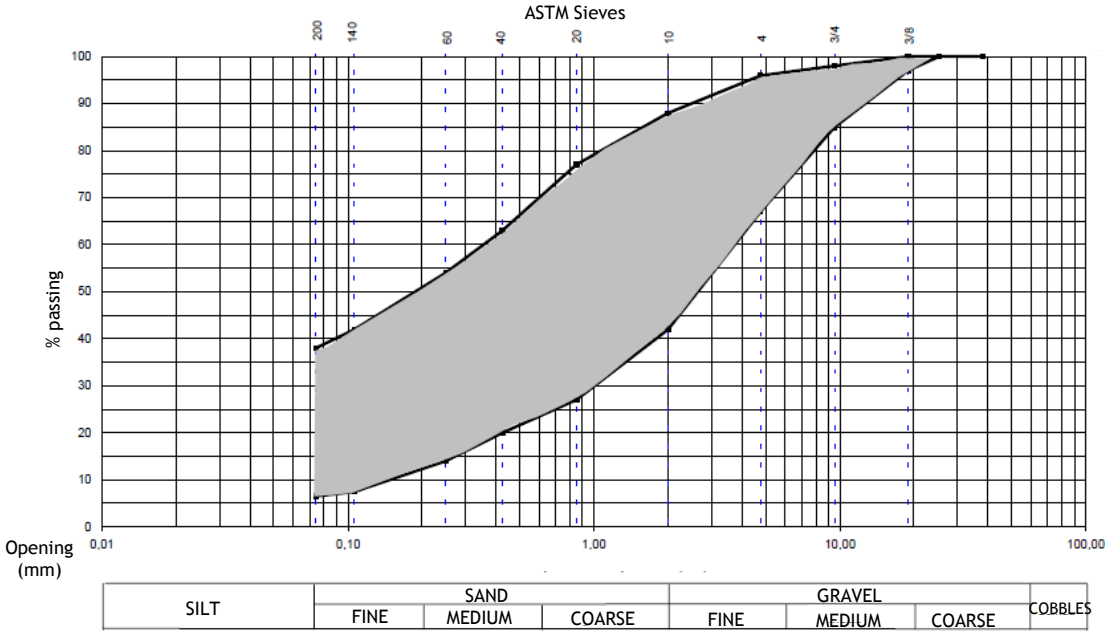

Figure 47. Grading envelope of the granitic residual soils of the Covilhã region - the hatched area corresponds to circa 80 curves, adapted from Cavaleiro, 2001.

These are well-graded materials, with various particle sizes from silt to gravel, although with sands as their predominant fraction. The predominant clay minerals have been assessed to be kaolinite and illite (Cavaleiro, 2001), which result from the alteration of muscovite and feldspar present in the original parent rock (Begonha, 2001).

Given the low percentage of fines and the fact that its constituent minerals exhibit low plasticity, this residual soil is generally classified as non-plastic. However, when assessing the Atterberg limits on the clayey matrix of the soils, Plasticity Indexes of less than 20% have been reported (Cavaleiro, 2001).

Curiously, and although they present a broad range of grain sizes, their spatial arrangement is not uniform, as would be expectable in a sedimentary soil with similar grading profile. This is thought to be the result of relic bonds, inherited from the parent rock, and that have not yet been destroyed by weathering. This structure of cemented or bonded particles might help explain the reduced deformability of these materials when compared to sedimentary soils of similar grading (Fernandes, 2011).

In conclusion, although the representativity of the grading curves of these materials may be questionable, it is clear that the predominant fraction is typically sand, which is originated

from the quartz of the parent rock. Additionally, the clay fraction is often reduced and its minerals present low activity, which explains the non-plasticity of these soils. As a result, their behaviour can be better approximated to a granular than to a cohesive soil.

The granitic residual soil analysed in this thesis has been mostly characterised through laboratory testing. No sampling was undertaken during the course of this study as the characterisation of the granitic residual soils in analysis had been completed by other PhD students at UBI.

Grading tests from circa 15 samples have shown this soil to be classified as a well-graded silty very gravelly fine to coarse sand, with a low fines content (less than 20%). The range of obtained PSD curves is shown below in Figure 48.

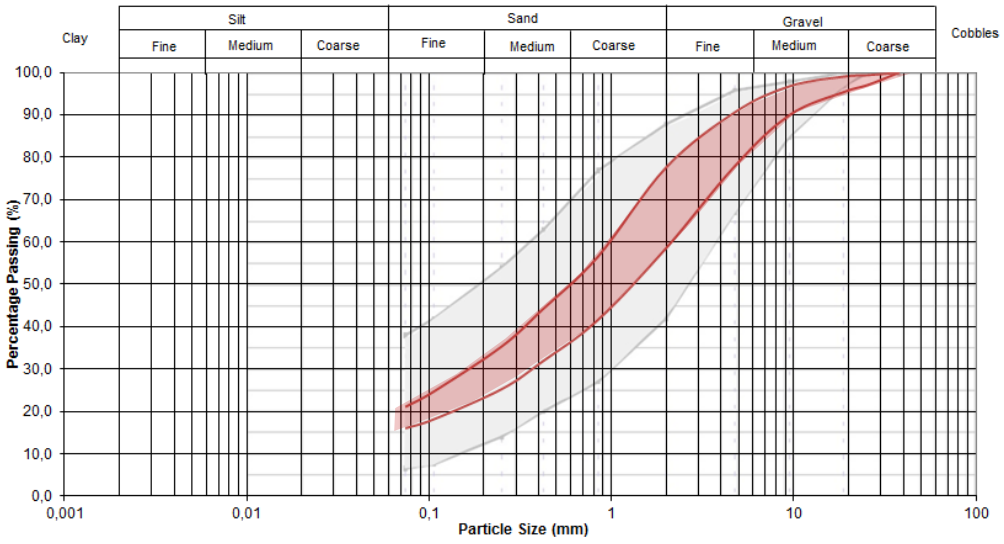

Notes:

1. The hatched area corresponds to the grading envelope of the soil in analysis.

2. The PSD curves have been ploted against the grading results shown previously in Figure 47 for comparison purposes.

Figure 48. Particle size curves of the granitic residual soil in analysis.

The grading results are in agreement with the typical grading curves for the granitic residual soils of the region as described by Cavaleiro (2001), which also classify the soil as well-graded. The soil in analysis has a similar content of sand and gravel when compared to the samples in Cavaleiro (2001), although with a slightly higher percentage of coarser material.

The well-graded classification has been based on the ASTM (2011) requirements in terms of the coefficients of uniformity (C_u, Equation 10) and of curvature (C_c, Equation 11):

- $C_u > 6$ and $C_c = 1 - 3$ (sandy soil);
- $C_u > 4$ and $C_c = 1 - 3$ (gravelly soil).

$$C_u = \frac{D_{60}}{D_{10}} \quad (10)$$

$$C_c = \frac{D_{30}^2}{D_{10} D_{60}} \quad (11)$$

where D_{10}, D_{30} and D_{60} are the grain sizes that correspond to 10%, 30% and 60% of passing material respectively, and that can be read off the PSD curves.

A well-graded soil, by definition, contains a wide range of grain sizes that fill up the voids very effectively and form a rather dense set. It should be noted this assessment has estimated values for D_{10} as no sedimentation tests were undertaken. Moreover, and in spite of the percentage of fines exceeding 12% on these soils, the assessment of C_u and C_c has been undertaken on the basis that these materials behave similarly to a granular soil.

Drained and undrained consolidated triaxial tests have also been undertaken on remoulded samples. These have been used to assess their drained and undrained tangent ($E_t{}'$ and E_{u_t}) and secant ($E_s{}'$ and E_{u_s}) deformability moduli, as well as the peak and residual angles of shearing resistance. The results are summarised in Table 5 below, along with the correspondent values for both dry and saturated unit weights.

Table 5. Geotechnical parameters assessed form the triaxial test campaign.

E_{u_s} (MPa)	E_{u_t} (MPa)	$E_s{}'$ (MPa)	$E_t{}'$ (MPa)	γ_d (kN/m^3)	γ_{sat} (kN/m^3)	φ'_{peak} (°)	$\varphi'_{critical}$ (°)
16.6 – 23.3 (18.5)	25.2 – 37.0 (29.4)	12.0 – 34.5 (25.8)	21.8 – 46.0 (34.3)	19.3 – 19.8 (19.5)	21.0-21.9 (21.5)	37.5 – 43.6 (40.6)	35.3 – 36.9 (36.1)

Note: Values in brackets correspond to average values, obtained for approximately 15 different samples.

The values above exceed the ones obtained through a wider triaxial test campaign conducted on granitic soils of the region in Cavaleiro (2001), which reported angles of shearing resistance between 26.9° and 37.7°. However, these were established considering effective cohesion values of up to circa 20kPa, while the values in Table 5 have been derived for null cohesion. When applying the same principle to the historical results, angles of shearing resistances between 31.3° and 42.5° are obtained, which in turn agree well with the values reported in Table 5.

Direct shear tests conducted on undisturbed samples of the same materials in Cavaleiro (2001) are summarised in Figure 49 below. Cohesion values from 4kPa to 42kPa and angles of shearing resistance between 35° and 45° were reported.

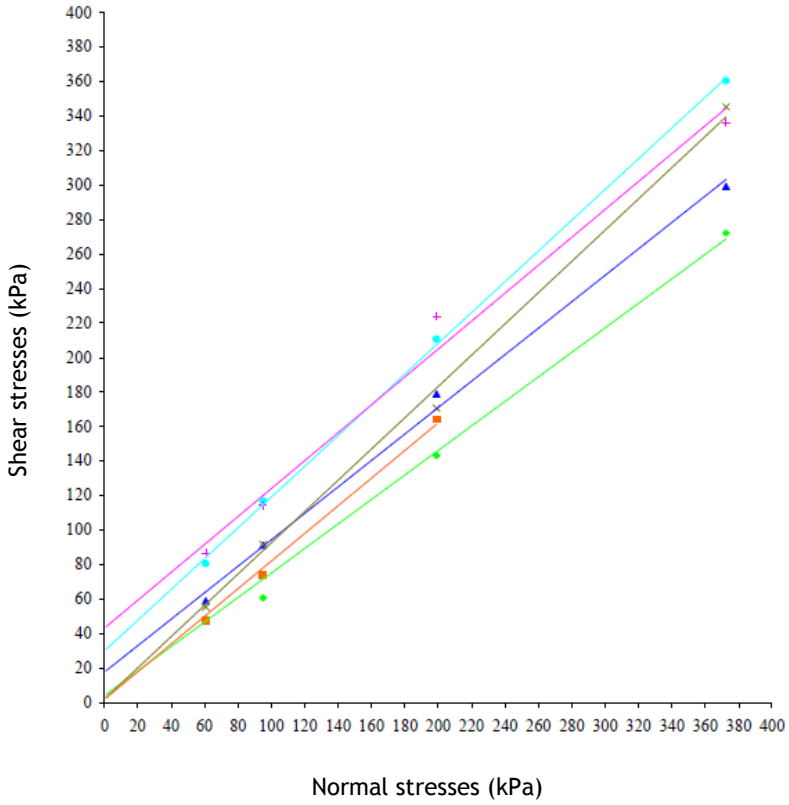

Figure 49. Direct shear test results, adapted from Cavaleiro (2001).

The same source also classified all samples as non-plastic according to their Atterberg limits.

As mentioned in Section 1.2, an experimental embankment was constructed using granitic residual soils from the Covilhã area. This was supervised by other UBI's PhD students to assist in the study of the geotechnical properties of this soil. The controlled embankment was built with a 16.0m footprint and a 20.0m development (Figure 50) and completed in November 2010.

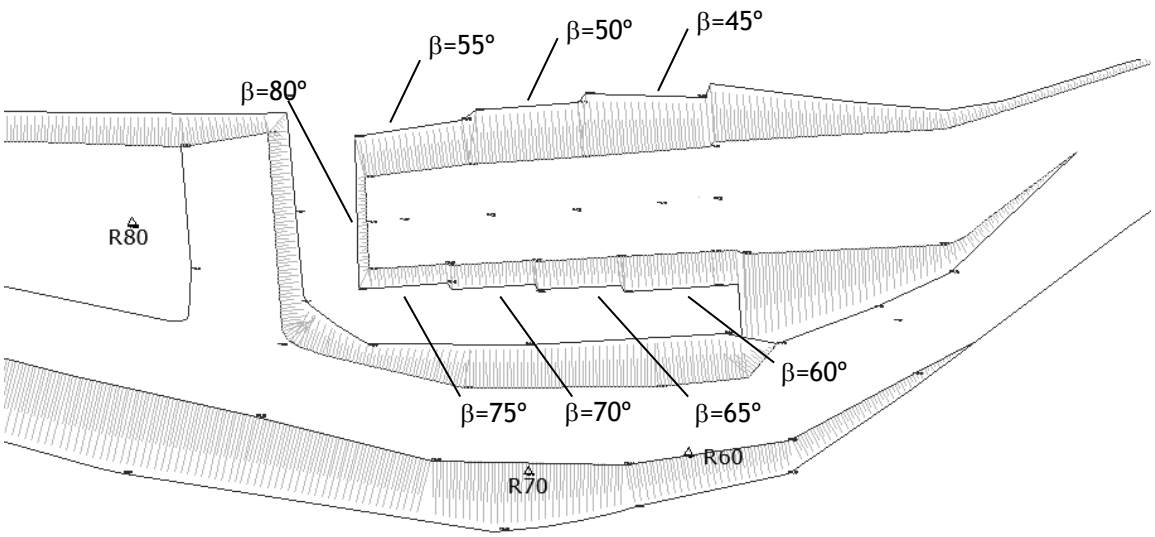

PLAN

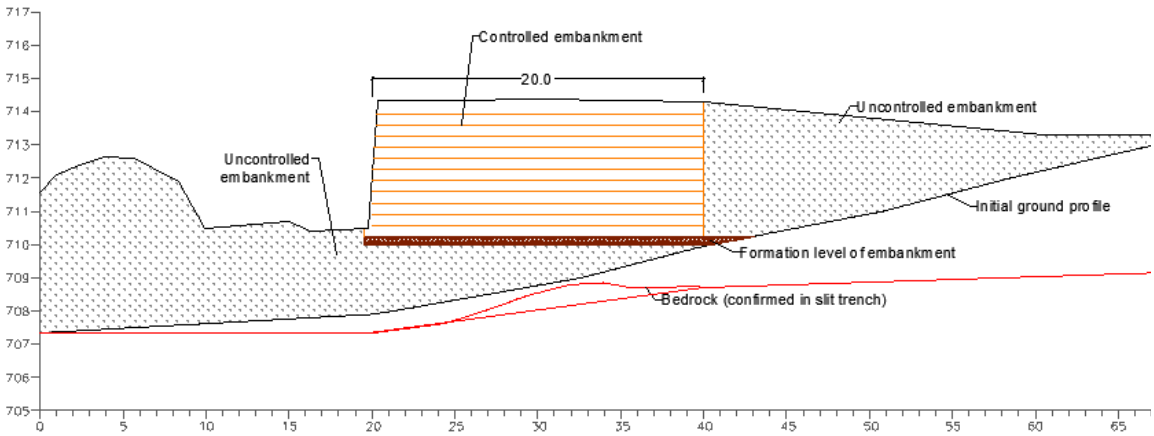

SIDE ELEVATION

Figure 50. Plan and elevation of the controlled embankment, presented with permission of Filipe Nunes (PhD student D716 at UBI).

The embankment height (4.0m) was kept constant across its full extent and its shoulders were built with varying gradients, so as to try to experimentally establish what would be the steepest stable configuration. The side slopes gradients varied between 45º and 80º with the horizontal, in 5º increments (refer to Figure 50 for the location of each of these faces in plan).

Additionally, a surcharge of 10kPa was applied at the top of the embankment, in August 2011 and near its steepest face. Circa 4 years after its application there are still no signs of instability in the slopes. The embankment was initially protected from weathering effects by

means of a plastic film, which has deteriorated with time, leaving the embankment unprotected against the erosive effects of rain and wind (Figures 51 and 52).

Figure 51. Side view of the embankment shortly after construction.

Figure 52. View of the embankment at its current stage.

4. Slope stability analysis

4.1 Introduction

As mentioned earlier in Chapter 3, the engineering properties of residual soils are generally considered as good for geotechnical purposes, in particular those derived from the weathering of igneous and volcanic rocks (Law, Shen, & Lee, 1998). This is apparent from the direct observation of natural slopes formed within residual soils; as these tend to remain stable at substantially steeper configurations than most sedimentary soil slopes.

Assessing the stability of natural slopes never is a purely analytical exercise, as there are always limitations on the extent which analytical methods can be applied to them. This assessment should also reflect the past history and the nature of the slope, i.e. its geology, topography and evidence of previous failures. After all, the models in which slope stability is assessed are based on very few variables, often assumed uniform across the whole slope or within a given stratum, which contrasts with the inherent heterogeneity of soils.

As such, non-analytical methods are always an essential part of the stability assessment of an existing slope and usually include the following:

- Visual inspection of the slope;
- Analysis of aerial photos;
- Observation of existing slopes in similar ground conditions to the slope in question.

A careful visual inspection of residual soil slopes, combined with some geological knowledge, can provide a good indication as to whether a particular slope is stable or not. Slopes with smooth contours usually indicate that they have primarily been formed by surface erosion processes without signs of instability. On the other hand, irregular surfaces suggest that some form of slip movement may have occurred at some point in the past (Figure 53).

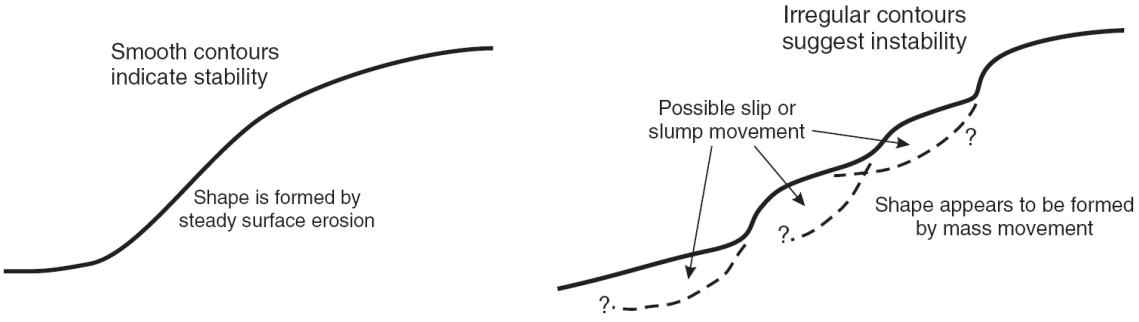

Figure 53. Clues to assess the stability of a residual soil slope based on surface features (Wesley, 2010).

The mechanism by which failure of a slope occurs is strongly dependent on the existing ground conditions. As mentioned earlier in Chapter 2, when dealing with soil slopes the most common mechanisms are translational and rotational slips. In both cases failure occurs, theoretically, once the driving shear forces due to the self-weight of the moving soil and additional surcharges become equal to, if not larger than, the resisting intrinsic shear forces within the soil.

In stress terms, if the shear stress mobilised by the failing soil mass at the failure plane is τ_{mob} and the available shear strength of the soil is referred to as τ_f, then the lump FoS against shear failure is defined by Equation 12.

$$FoS = \frac{\tau_f}{\tau_{mob}} \quad (12)$$

This suggests that failure is likely to occur when FoS $\leq$ 1.0, although as mentioned in Chapter 2 instability can occur for FoS above unity. This is not only related to any uncertainties in soil parameters but also with the rate of movement of the unstable soil block as shown in Figure 54 (Cartier, 1986). This demonstrates that the shear strength along a given failure plane depends on its displacement rate. The quicker the movement of the unstable mass the smaller is the percentage of the maximum shear resistance that gets mobilised along the slip plane.

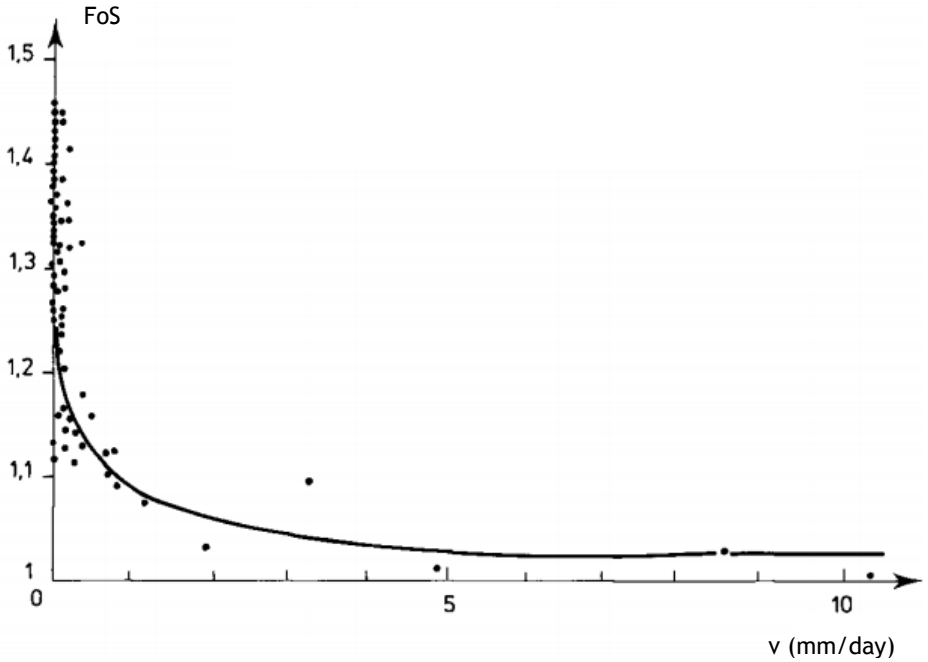

Figure 54. Critical FoS vs. rate of movement, adapted from Cartier (1986).

The outcome of any design method relies heavily on the soil parameters used. As a result, these must be carefully assessed in order to obtain a reliable design. Otherwise, the concept of FoS is irrelevant, using overestimated shear strength values may prompt failure to occur with a FoS significantly above unity.

As stated earlier in Chapter 2, slips and landslides are often triggered by periods of prolonged or intense rainfall, which can result in a temporary peak in porewater pressures values. Therefore, any groundwater measurements within slopes are only valid at the time they are made and cannot be assumed to be relevant in long-term stability assessments. For these, and in accordance with EC7 the "design values [of groundwater pressures] shall represent the most unfavourable values that could occur during the design lifetime of the structure" (NP EN 1997-1:2010, 2010).

A significant number of slopes in residual soils remain stable at steep angles due to typically deep phreatic surfaces, which may result in suction effects on the soils above them. In this zone of porewater tension the effective normal stress across any potential failure surface is increased, resulting in greater shear strength and overall FoS values. The influence of intense rainfall on this zone is to increase the pore pressure from its negative value toward zero (i.e., to reduce or nullify the suction effects above the water table), or possibly turn it into a positive value if the phreatic surface rises. Consequently, a change in the existing negative pore pressure, even without variations in the groundwater table, may trigger a failure.

In the following subsections a brief review of the most relevant soil mechanics principles related to slope stability is made, along with an overview of the most common LEM and FEM approaches to this problem. Finally, the EC7 formulation and design implications on slope stability are presented along with a few considerations on how to introduce them in numerical analysis.

4.2 Soil mechanics principles for slope analysis

The majority of stability assessments are based on both the shear stresses required for static equilibrium of the potential sliding mass and the available shear strength. The ratio between the two provides a FoS against failure of the slope (Equation 12).

This procedure incorporates which conditions the analysis is supposed to be undertaken in (drained or undrained) and groundwater levels along the slope.

4.2.1 Concept of total and effective stresses

A soil's response to changes in its stress state depends on the interaction between its different phases. To simplify the problem, and although a soil is comprised of discrete particles, it is commonly addressed as a continuous medium.

This methodology allows for an expedite application of the effective stress principle, which is particularly useful in situations where the shear strength of the soil needs to be estimated. The effective stress (σ') is the average stress supported by the soil particles and corresponds to the difference between the total stress (σ) and the pore water pressure (u), as shown in Equation 13.

$$\sigma' = \sigma - u \quad (13)$$

Variations in effective stress are usually accompanied by volumetric changes. However, since the solid phase is considered to be undeformable, these changes are assumed to be the result of fluctuations in void volume. Therefore, in saturated soils (voids completely filled with water) the volumetric variations will correspond to the volume of water which is expelled (percolation). Naturally, this is conditioned by both the soil's boundary conditions and its permeability.

A load increment (total stress increase $\Delta\sigma$) is initially transferred into additional porewater pressures (Δu). However, as changes in volume are only dependent on changes in effective stress, this will only take place as water is expelled. Depending on the permeability, a certain amount of time will be required for the water to percolate and give rise to a change in volume. This is the basis for short and long term stability analysis.

4.2.2 Drained and undrained conditions

In general terms, drained and undrained conditions are related to the ability or inability of water to drain from or into a soil when equilibrium stress conditions are altered. This distinction is based not only on the percolation rate but also on the rate at which the loading is applied. More specifically, two drainage conditions may occur:

1. *Drained conditions* – During the length of time in which the soil is undergoing changes in stresses, the water is able to freely move in and out of the pores such that there is essentially no change in porewater pressures.
2. *Undrained conditions* – There is no flow of water in or out of the pores during the length of time in which the soil is subjected to changes in stresses. Since water is incompressible, the changes in soil stresses will cause porewater pressures to vary.

To better illustrate these two scenarios Figures 55 and 56 help clarify the main differences, respectively between a drained and an undrained loading, in terms of the evolution of total stress (σ), volume (V), porewater pressure (u) and effective stress (σ').

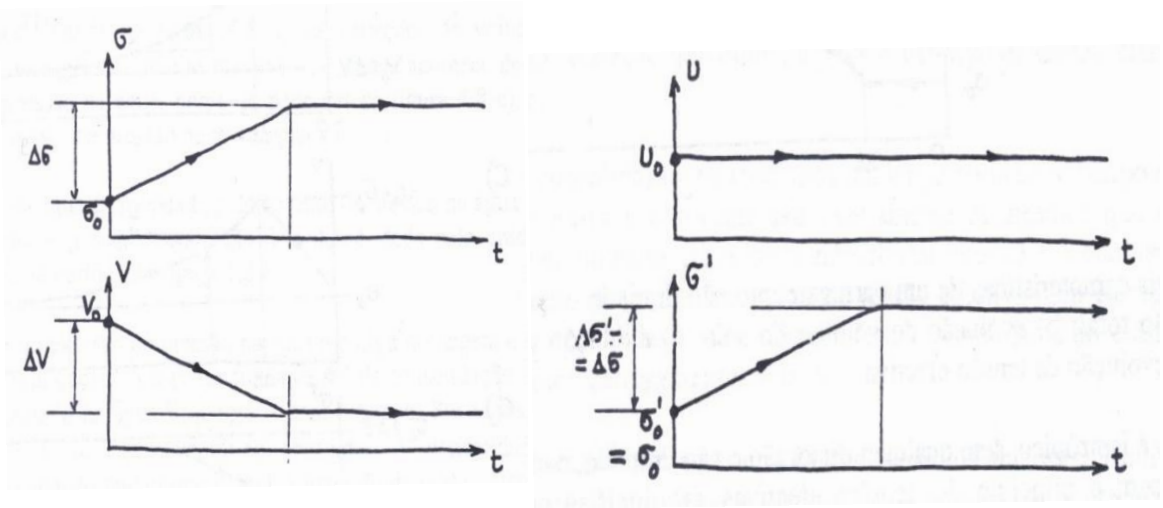

Figure 55. Drained conditions, adapted from Neves (2003).

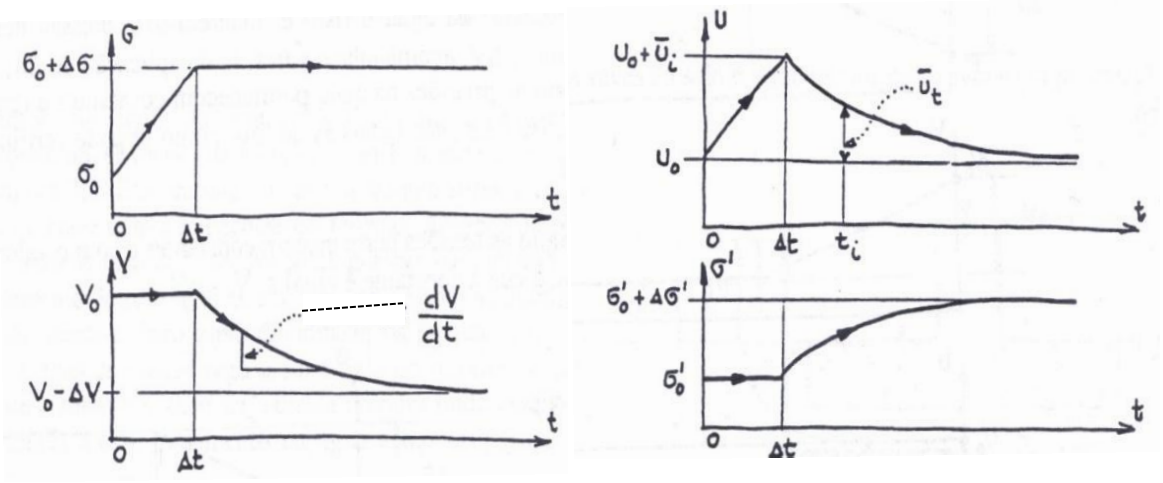

Figure 56. Undrained conditions, adapted from Neves (2003).

The designation “drained loading” implies that all drainage takes place during the application of the load and that pore pressure is kept constant at all times (Figure 55). In contrast, an “undrained loading” occurs in such a short period of time that it does not allow the soil to drain, remaining with constant volume (Figure 56).

In the latter case and as the time elapses, the stress increment ($\Delta\sigma$) is gradually dissipated from porewater pressure ($u_0 + \Delta\sigma$) into effective stress as water percolates and volume changes. However, the rate at which this process takes place is not constant over time, slowing down as the porewater pressure nears the initial value (prior to loading). This phenomenon is known as consolidation and it ends when, after a given period of time, the total and effective stresses and volume are exactly the same as those resulting from a drained loading. The excess porewater pressure dissipates entirely by the end of consolidation.

In short, the distinction between a drained and an undrained loading depends, above all, of the relationship between the loading and percolation rates. Hence the importance of analysing the drainage conditions on a site.

Since failure is governed by effective stress, all stability assessments for both drained and undrained conditions should be carried out using it. However, this would require the estimation or actual *in situ* measurements of the excess porewater pressure, a task which is often difficult and/or yields inaccurate results. Therefore, from a practical point of view, it is more convenient to use a total stress analysis approach under undrained conditions (short term analysis), often referred to as the "end of construction" stage.

4.2.3 Shear stress

The shear strength of a soil is one of its most important geotechnical properties, as it plays a crucial role in slope stability. However, its determination after a failure event, i.e. its residual shear strength, is often difficult to assess, given the collapse of the original soil structure and the challenge in obtaining undisturbed soil samples.

As mentioned earlier, soil shear strength is derived from two distinct components, friction and cohesion. However, in purely granular soils, i.e. where a null cohesion value in the Mohr-Coulomb failure criterion is considered, and ignoring the effects of the soil's dilatancy, the shear strength is a purely frictional phenomenon. According to Salih (2012), some researchers defend that albeit the saturation of a soil reduces its c' value due to a loss in suction effects, the frictional component remains unaffected.

Regardless of the drainage conditions, the shear strength of a soil is governed by its effective stress and its shear strength is given by the Mohr-Coulomb failure criterion (as previously stated in Equation 9):

$$\tau = c' + \sigma' tg\varphi' \quad (9)$$

where τ is the shear stress along the slip plane at failure, σ' is the effective normal stress along the slip plane at failure, c' is the effective cohesion, and φ' the effective angle of shearing resistance. The latter is often the subject of some debate as its value will depend on whether failure is predicted to occur along an old slip surface or within a soil mass that has never experienced a failure event in the past. On the second case it might be more appropriate to select the peak angle of shearing resistance in conjunction with overconsolidated or dense soils, or the critical angle if the soil is normally consolidated or loose. Often the latter is adopted for conservatism (Equation 14).

$$\tau_f = c' + \sigma' tg\varphi'_f \quad (14)$$

If failure occurs along a pre-exiting failure plane, the residual angle of shearing resistance may be most appropriate for the design (Equation 15).

$$\tau_f = c' + \sigma' tg\varphi'_r \quad (15)$$

When dealing with slow draining soils (mainly clays), the excess porewater pressure generated at the onset of loading may create conditions whereby failure can take place in the short term (that is before the occurrence of any significant dissipation of excess porewater pressure). In which case, the undrained shear strength (c_u) must be used (Equation 16).

$$\tau_f = c_u \quad (16)$$

The use of effective stresses and the Mohr-Coulomb failure criterion has proven to be adequate for engineering practice in saturated soils. This suggests that the equations mentioned above for drained conditions are in fact only valid for saturated soils (Pais & Gomes, Mechanical behaviour of unsaturated decomposed granitic residual soil, 2010). In general, unsaturated soils have a shear strength that can be expressed as a linear combination of the net normal stress $(\sigma_n - u_a)$ and of the matric suction $(u_a - u_w)$, as shown in Equation 17 (Fredlund & Rahardjo, 1993):

$$\tau = c' + (u_a - u_w) tg\phi^b + (\sigma_n - u_a)\, tg\varphi' \quad (17)$$

where c' is the same as for the saturated soil, φ' is the angle of shearing resistance related to variations in $(\sigma_n - u_a)$ as the term $(u_a - u_w)$ remains constant, and ϕ^b is the angle of shearing resistance introduced to relate the shear strength contribution from the matric suction stress state variable. Research suggests that ϕ^b is always smaller than or equal to the internal angle of shearing resistance φ' (Fredlund & Rahardjo, 1993).

However, the study of the effect of matric suction on the stability of residual soil slopes and the means of quantifying it are outwith the scope of this thesis. As such, and given that the effect of matric suction can be equated to an increase in the cohesion of soil, the Mohr-Coulomb failure criterion expressed in Equation 9 has been deemed as appropriate to be used throughout this thesis. Regardless, a brief explanation of how to account for matric suction in the cohesion of soils is presented below for completeness.

Equation 17 proposes the use of two independent stress state variables for assessing the shear strength of a soil as depicted graphically in Figure 57.

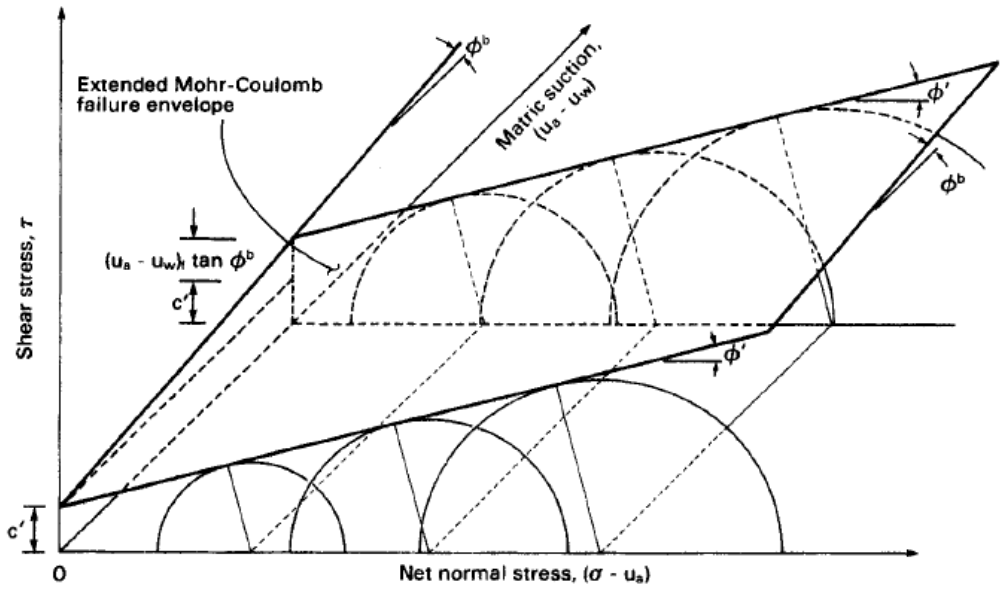

Figure 57. Extended Mohr-Coulomb failure envelope for unsaturated soils (Fredlund & Rahardjo, 1993).

In order to simplify this expression, and so that it becomes similar to the expression used in saturated soil mechanics, it is possible to include the contribution of matric suction in the definition of the cohesion intercept of the Mohr-Coulomb failure envelope, as expressed by Equation 18.

$$c = c' + (u_a - u_w) tg\phi^b \quad (18)$$

However, this does not mean that matric suction is a cohesion component of shear strength, it is merely lumped with effective cohesion for the purpose of translating the three-dimensional failure envelope onto a two-dimensional representative plot. The suction component of shear strength is referred to as total cohesion (Taylor, Fundamentals of Soil Mechanics, 1948). The cohesion intercept becomes the effective cohesion (c') when the matric suction reduces to zero and the shear strength expression can be re-written as Equation 19.

$$\tau = c + (\sigma_n - u_a)\, tg\varphi' \quad (19)$$

The difficulties associated with the measurement of negative pore-water pressures and their incorporation in slope stability analysis are the primary reason why they are usually ignored. This is a reasonable assumption when the major portion of the slip surface is below groundwater, although in cases where groundwater table is deep, or in shallower failure surfaces, this effect should not be disregarded (Rahardjo & Fredlund, 1991).

4.3 EC7's approach to slope stability

According to the current European standard for Geotechnical Design, the EC7, the design of a slope must ensure that "all possible limit states for the particular ground shall be considered in order to fulfil the fundamental requirements of stability, limited deformations, durability and limitations in movements of nearby structures or services" (NP EN 1997-1:2010, 2010).

These limit states naturally include the overall stability of the geotechnical structure itself as well as the assessment of ground movements which may compromise the structure's operation.

The overall stability of slopes (ultimate limit state) is to be analysed with the design values of actions, soil parameters and resistances specified either within the norm itself or in its national annexes. The design values to be used can be obtained through Equations 20 and 21.

- Design value of actions

$$F_d = \gamma_f . F_k \quad (20)$$

- Design values of geotechnical parameters

$$X_d = X_k / \gamma_m \quad (21)$$

In the previous expressions γ_f and γ_m are the partial factors for an action and a soil parameters, and can be found in Annex A of the EC7 (NP EN 1997-1:2010, 2010). F_k and X_k represent the characteristic values of the actions and of the soil geotechnical parameters respectively.

The EC7 prescribes three different Design Approaches for slope stability (DA 1, DA 2 and DA 3). The choice is left to national determination (Figure 58), i.e. each country can state in its National Annex the Design Approach(es) to be used for design.

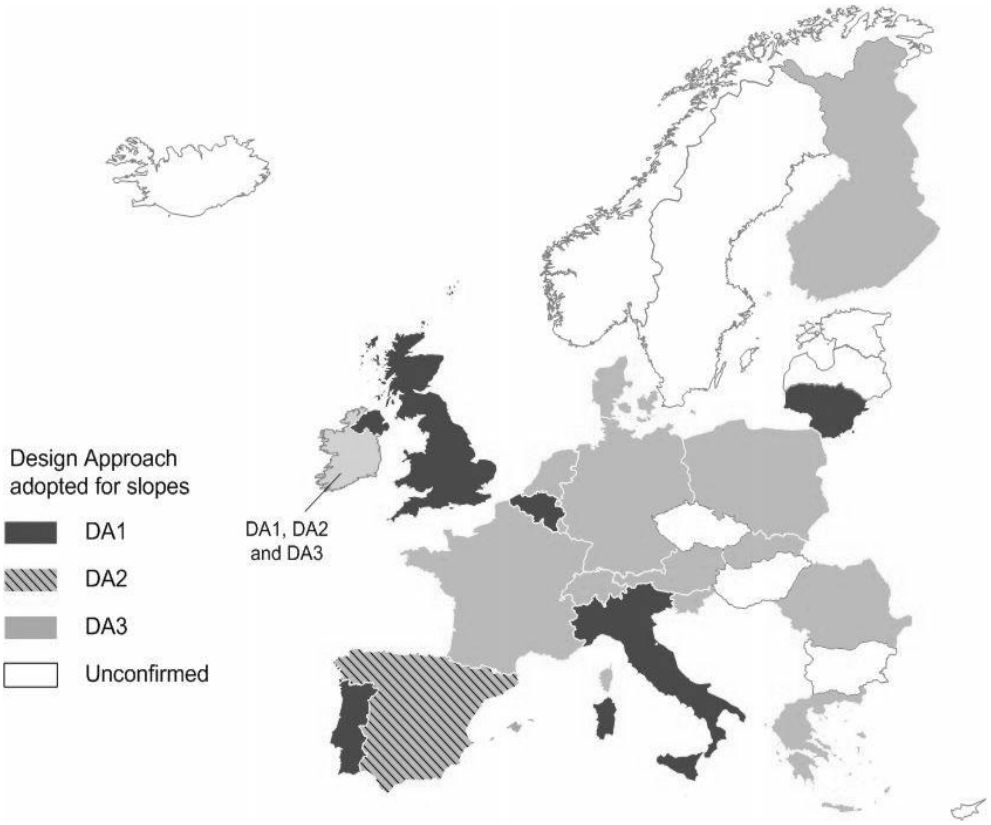

Figure 58. National choice of Design Approach for slopes (Bond & Harris, 2008).

The Design Approach chosen in the Portuguese Annex of EC7 is Design Approach 1 since this is, in essence, a problem in which the strength of soil is responsible for a significant part of the total resistance.

Within this Design Approach two sets of combinations must be verified (Combinations 1 and 2):

- Combination 1: A1 "+" M1 "+" R1;
- Combination 2: A2 "+" M2 "+" R1.

Where "+" implies "to be combined with" and A1, M1 and R1 correspond to different sets of partial factors to be applied to actions, soil parameters and resistances, respectively. In Combination 1, partial factors in excess of unity are applied to unfavourable actions or the effects of actions whereas in Combination 2, the inverse of partial factors exceeding unity are applied to the soil parameters. Therefore, these procedures result in increasing the effect of actions in Combination 1 and reducing the ground strength in Combination 2.

Given their "specific purpose", Combination 1 is especially relevant when the loading applied along the slope (other than the soil mass) controls the failure mechanism rather than the ground strength parameters. Also, when using Combination 1 the partial factor for permanent unfavourable actions should be applied to the weight density of the soil, which results in the following:

- In an effective stress analysis, the effect of the partial factor is to increase the destabilising action. However, it simultaneously increases the shearing resistance of the soil, thus partially cancelling out this effect;
- In a total stress analysis, the increase in weight density increases the destabilising action without increasing the shearing resistance of the soil. However, a higher partial factor is applied to the undrained shear strength in Combination 2 than to the permanent destabilising action in Combination 1.

In both cases, Combination 1 tends to be less critical than Combination 2 in almost all design situations. Regardless of the Design Approach used, the same fundamental inequality needs to be met, already expressed in Equation 1, which can be rewritten as Equation 22 (NP EN 1997-1:2010, 2010).

$$E_{d,dts} \leq E_{d,stb} \quad (1)$$

$$E_d = \gamma_f . F_k \leq R_d = \{X_k/\gamma_m\}/\gamma_R \quad (22)$$

The partial factor γ_f for the verification of structural (STR) and geotechnical (GEO) limit states, sets A1 and A2 respectively, depends not only on the duration of the action but also on its favourable or unfavourable effects, as summarised in Table 6. The values presented are the ones currently enforced by the Portuguese versions of the standard and may vary to the ones used elsewhere.

Table 6. Partial factors on actions (γ_f) (NP EN 1997-1:2010, 2010).

Action		Symbol	Set	
			A1	A2
Permanent	Unfavourable	γ_G	1.35	1.00
	Favourable		1.00	1.00
Variable	Unfavourable	γ_Q	1.50	1.30
	Favourable		0	0

In Design Approach 1, for combinations STR and GEO the γ_m values presented in Table 7 (sets M1 and M2) are to be applied to the following soil proprieties:

- $\gamma_{\varphi'}$ on the tangent of the angle of shearing resistance;
- $\gamma_{c'}$ on effective cohesion;
- γ_{cu} on undrained shear strength;
- γ_{qu} on unconfined strength;
- γ_{γ} on weight density.

Table 7. Partial factors for soil parameters (γ_m) (NP EN 1997-1:2010, 2010).

Soil parameter	Symbol	Set	
		M1	M2
Angle of shearing resistance*	$\gamma_{\varphi'}$	1.00	1.25
Effective cohesion	$\gamma_{c'}$	1.00	1.25
Undrained shear strength	γ_{cu}	1.00	1.40
Unconfined strength	γ_{qu}	1.00	1.40
Weight density	γ_{γ}	1.00	1.00

(*) = This factor is applied to tan φ'

In slope stability the ground resistance partial factors of safety (γ_r) to be applied to both Combinations are the same and are presented below in Table 8.

Table 8. Partial resistance factors (γ_R) for slopes and overall stability (NP EN 1997-1:2010, 2010).

Resistance	Symbol	Set		
		R1	R2	R3
Earth resistance	γ_R	1.00	1.10	1.00

Besides taking into account all of these partial factors of safety, depending on the choice of Design Approach and Combination, care should be given to the selection of the appropriate calculation method so as to reflect the following (NP EN 1997-1:2010, 2010):

- soil layering;
- occurrence and inclination of discontinuities;
- seepage and pore-water pressure distribution;

- short and long-term stability;
- type of failure (circular or non-circular surface; toppling; flow).

The standard also specifies that the soil mass should normally be regarded as a rigid body or as several rigid bodies moving simultaneously and that the failure surfaces will occur between these rigid bodies. Also, and although a variety of slip failure shapes may occur within a slope, when analysing a typical cutting slope or embankment, where ground conditions are relatively homogeneous and isotropic, circular failure surfaces should normally be assumed. An exception to this are slopes with relic failure planes, which can potentially be reactivated and may result in non-circular failures.

When accessing the stability of natural slopes, EC7 also recommends that any uncertainties regarding the weight density of the ground should be taken into account by considering upper and lower characteristic values to this parameter.

In terms of serviceability limit states, EC7 prescribes that the design must show that the slope's deformation will not affect the operability of any structures, roads or services sited on, in or near it and that special attention should be paid to time dependent settlements (consolidation and secondary consolidation effects).

When considering a cutting slope, as the current analytical and numerical methods of analysis do not provide reliable predictions, the serviceability limit can be avoided by limiting the mobilised shear strength considered in the analysis and by monitoring the movements *in situ* whilst specifying actions to reduce or stop them, if necessary.

4.4 Classical methods

Limit equilibrium methods assess the stability of a potentially unstable soil mass by comparing the forces tending towards movement along a given surface with the forces resisting it. They indicate whether or not a slope is stable based on the following:

- Selection of a potential failure surface through the slope;
- The Mohr-Coulomb failure criterion.

Regardless of the selected analysis method, arriving at an answer requires a series of initial assumptions, which differ with the approach used. Nevertheless, the following criteria must always be met:

- Sliding must be cinematically feasible (Michalowski, 1995);
- The distribution of forces acting on the failure surface can be obtained using known data (unit weight of the material, water pressure, etc.);
- Strength is mobilized simultaneously along the whole failure surface.

By complying with the above a balance between sliding and resisting forces can be obtained, thus estimating a FoS/MoS. Once the FoS/MoS of an hypothetical failure surface has been estimated, other cinematically feasible failure surfaces must be analysed until the one with the smallest FoS/MoS is found.

There are however two distinct approaches to limit equilibrium, one focuses on the entire unstable mass whereas the second divides it into vertical slices which are analysed separately. The former is valid for homogeneous materials, and the forces involved are calculated and compared at only one point on the failure surface. The method of slices can be used to analyse both homogenous and non-homogenous materials, and its different methods include particular assumptions or hypotheses regarding location, position and distribution of forces acting on the slices. Forces acting on each slice are assessed individually and all the results are then combined to arrive at a global stability assessment. The most common slice methods are the Fellenius', Bishop's and Janbu's simplified methods, with only the latter being suited for non-circular (polygonal) slip surfaces.

4.4.1 Stability of slopes with a circular failure surface

The commonly used hypothesis of a circular failure surface requires a significant iterative process as it is not usually clearly defined from the start. The stability assessment mainly consists of finding the most unfavourable slip circle, to which corresponds to the minimum FoS/MoS. Therefore, this type of analysis is generally undertaken numerically.

These failures can take place both in drained and undrained situations and should be analysed separately for each of these. For the purpose of this thesis only drained conditions have been considered given the predominantly granular nature of the soils in study.

4.4.1.1 Drained conditions (long term analysis)

When considering the long term stability of a slope, i.e. by the time the excess porewater pressure is presumed to have completely dissipated, an effective stress analysis should be used. This implies that the porewater pressure distribution must be assessed along the slip plane, in order to obtain the corresponding effective normal stress. This has led to the development of slice methods, in which the unstable soil mass is divided into a series of vertical slices where limiting equilibrium conditions are individually assessed.

Following that, the contributions from all slices are combined to determine the total applied and available shear strength along the failure surface. This discretisation enables non homogeneous soils, with spatial variations in terms of proprieties, to be easily analysed.

Therefore, assessing the FoS/MoS involves analysing force and moment equilibrium of an *n* number of slices. Figure 59 exemplifies the forces acting within a typical slice, where the location of the normal force (N) is assumed to be acting in the middle of its base.

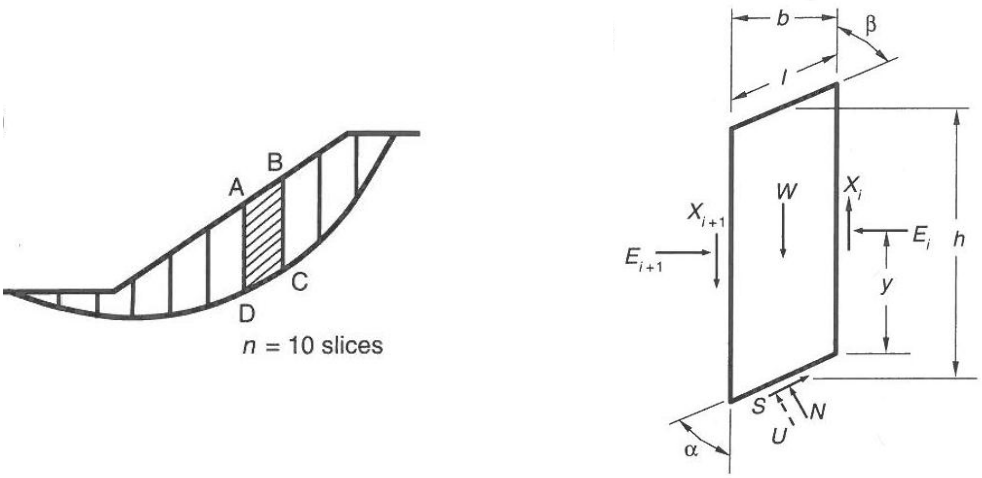

Figure 59. Free body diagram of a typical slice within a slope (Barnes, 2010).

Since the number of unknown variables and of equations results in a statically indeterminate system, different methods resort to different sets of assumptions (Table 9) to work out the FoS/MoS of a slope. These only allow the different methods to partially fulfil the static equilibrium.

Table 9. Slice methods assumptions, adapted from (Das, 2011).

Method	Assumptions	Equilibrium Conditions Satisfied		
		$\Sigma F_x = 0$	$\Sigma F_y = 0$	$\Sigma M = 0$
Ordinary method of slices (Fellenius)	• Circular slip surfaces only • Interslice forces are zero	No	No	Yes
Bishop's simplified method	• Circular slip surfaces only • Interslice shear forces are zero	No	Yes*	Yes
Janbu's simplified method	• Slip surfaces of any shape • Interslice forces are parallel with unknown inclination	Yes	Yes	No

* Used only to derive the effective vertical stress at the bottom of each slice.

The ordinary method is considered the simplest of the methods of slices since it is the only procedure that results in a linear equation for obtaining the FoS. It assumes that the interslice forces can be neglected because they are parallel to the base of each slice (Fellenius, 1936).

The indiscriminate change in direction of the resultant intersliceforce, from one slice to the next, results in factor/margins of safety errors that may be as much as 60% (Whitman & Bailey, 1967). The factor/margin of safety is derived from the sum of all moments about a common point (i.e. the centre of rotation of the entire mass), which leads to the following expression (Equation 23).

$$FoS/MoS = \frac{\sum M_{resisting}}{\sum M_{driving}} = \frac{\sum R\times(c'l_i + W_i \cos\alpha_i \tan\varphi_i')}{\sum W_i \, sen\, \alpha_i} \quad (23)$$

However, from the list presented in Table 9, and when it comes to analysing circular slip surfaces, the most common slice method is the Bishop's simplified method (Figure 60), in which the unknown tangential forces are ignored as the equilibrium would not be significantly affected by them. As such, the equilibrium of forces in the vertical direction can be expressed by Equation 24.

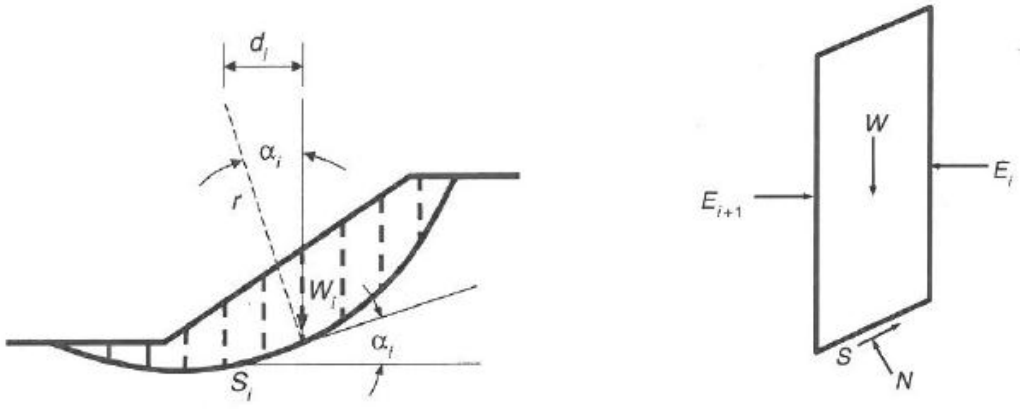

Figure 60. Free body diagram for Bishop's simplified method (Barnes, 2010).

$$\sum F_V = 0 \Leftrightarrow N_i \cos\alpha_i + \tau_{mob_i} sen\, \alpha_i = W_i \quad (24)$$

Given the number of unknowns, a second equation related to the equilibrium of moments for all slices also needs to be used (Equation 25).

$$\sum M_{Stabilizing\ Forces} = \sum M_{Instabilizing\ Forces} \Leftrightarrow$$

$$\Leftrightarrow \sum \tau_{mob_i} l_i + (N_i - u_i l_i) \times tan\ \varphi_i' = \sum W_i sen\ \alpha_i \quad (25)$$

Since the mobilized shear strength (τ_{mob}) results from the ratio between the shear strength of the soil (τ_f) by the existing FoS/MoS (refer to Equation 12), by combining the previous expressions a formulation for the FoS/MoS can be derived (Equations 26 and 27).

$$FoS/MoS = \frac{\sum [c_i' l_i\ cos\ \alpha_i + (W_i - u_i l_i\ cos\ \alpha_i)\ tan\ \varphi_i'] \left(1/m_{\alpha_i}\right)}{\sum W_i\ sen\ \alpha_i} \quad (26)$$

$$\text{with } m_{\alpha_i} = cos\ \alpha_i + \frac{1}{FoS} sen\ \alpha_i\ tan\ \varphi_i' \quad (27)$$

The adaptability of this method made it into one of the most reliable and widely used in engineering practice, although its need for trial-and-error procedures until convergence is met, is usually numerically undertaken.

4.4.2 Stability of slopes with a noncircular failure surface

When more complex and noncircular slip surfaces need to be analysed, the method of analysis needs to differ. As such, from the three overall equilibrium expressions, it is essential to focus on the satisfying the force equilibrium in both the horizontal and vertical directions, as opposed to moment equilibrium.

From the existing methods of solving this type of problems, the Janbu's simplified method is one of the most popular. In this case, the interslice forces are assumed to be horizontal and no interslice shear forces are considered. However, this assumption may lead to an underestimation of the FoS/MoS (Equations 28 and 29). As a result, a correction factor should be applied to the derived value.

$$FoS_0/MoS_0 = \frac{\sum [c_i' l_i\ cos\ \alpha_i + (W_i - u_i l_i\ cos\ \alpha_i)\ tan\ \varphi_i'] \left(m_{\alpha_i}\right)}{\sum W_i\ tan\ \alpha_i} \quad (28)$$

$$\text{with } m_{\alpha_i} = \frac{sec\ \alpha_i{}^2}{1 + \frac{tan\ \alpha_i\ tan\ \varphi_i'}{FoS}} \quad (29)$$

The final FoS/MoS is then given by Equation 30, where the correction factor (f_0) depends on both the depth of the slip surface and the type of soil (Figure 61).

$$FoS/MoS = FoS_0/\mathrm{MoS}_0 \times f_0 \quad (30)$$

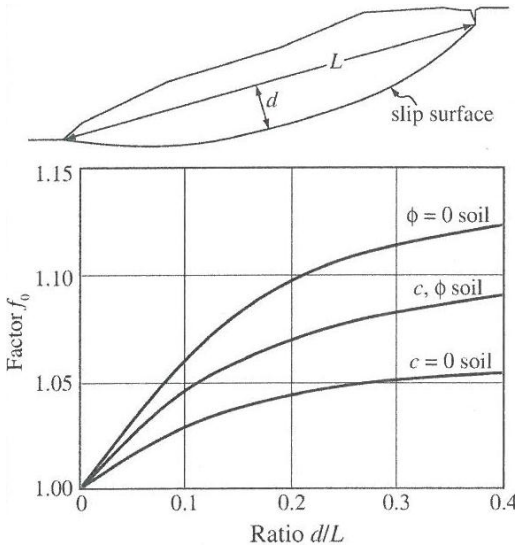

Figure 61. Correction factor f_0 (Barnes, 2010).

4.4.3 Location of the critical failure surface

Correctly choosing the location of the critical slip surface is of great importance, as otherwise an overestimated FoS/MoS may be arrived at. Consequently, slope stability calculations are almost exclusively undertaken numerically, so that thousands of failure surfaces can be assessed, until the one with the lowest factor of safety is located.

4.4.3.1 Circular failure surfaces

The process of finding the most critical failure plane can be optimised by concentrating the calculations on a specific area within which the critical slip is likely to be located. One possible approximation can be done using the empirical method suggested by Whitlow (1995), presented in Figure 62 below, in which the position of the centre of rotation can be estimated in relation to the slope's angle (β) and height (H).

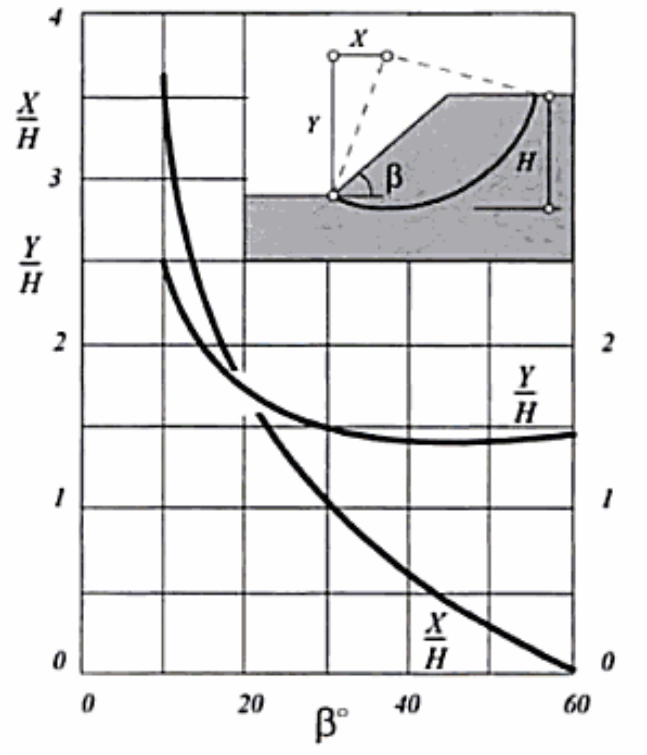

Figure 62. Initial location of the critical slip circle (Whitlow, 1995).

Nevertheless, after choosing the most probable area where the centre point might be located, there are still three common methods of searching for the critical slip surface (U.S. Army Corps of Engineers, 2003), as illustrated in Figure 63:

a) *Constant radius method* – The radius R is held constant while the location of the centre is varied until the minimum factor of safety is obtained;
b) *Common point method* – All circles are passed through a common point such as the toe of the slope, while both the centres and radii are varied until the minimum factor of safety is obtained;
c) *Fixed tangent method* – All circles are made tangent to a fixed line, while both the centres and the radii are varied until the minimum factor of safety is obtained.

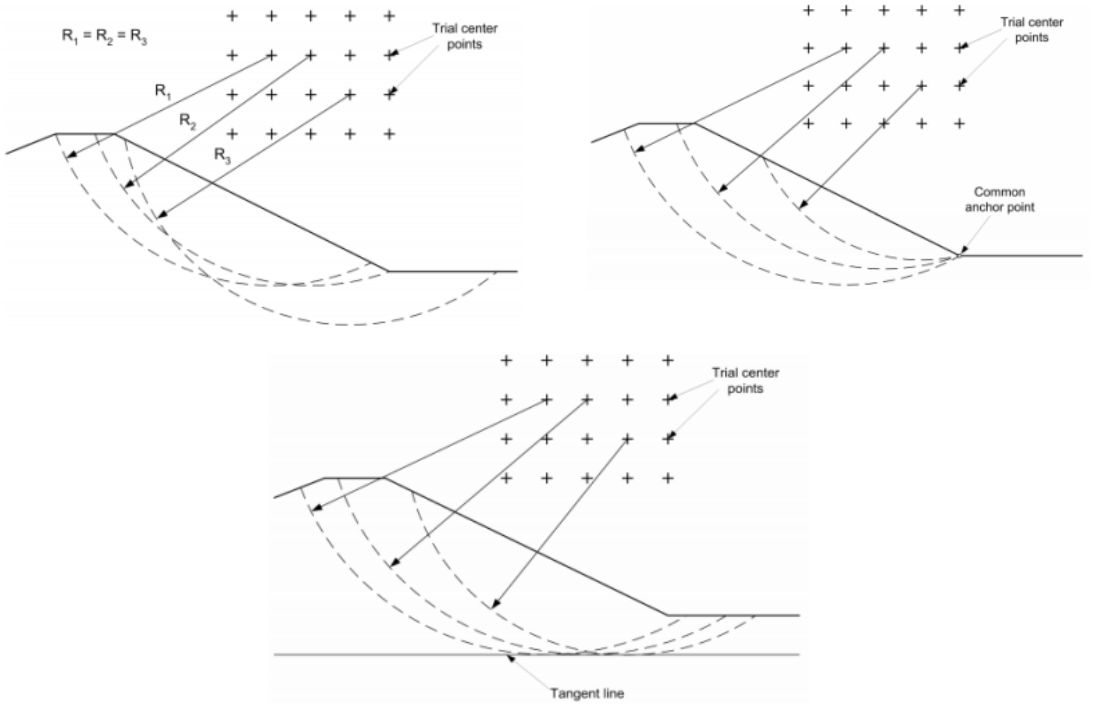

Figure 63. Search methods for circular slip surfaces (U.S. Army Corps of Engineers, 2003).

4.4.3.2 Noncircular failure surfaces

A number of techniques have also been proposed to help locate the geometry of the most critical noncircular slip surface. Figure 64 illustrates one of the most useful procedures, proposed by Celestino & Duncan (1981), in which an initial slip surface is assumed and represented by a series of points that are connected by straight lines.

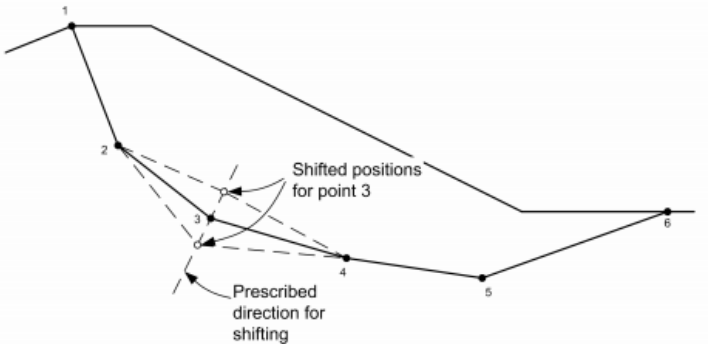

Figure 64. Search method for noncircular slip surfaces (U.S. Army Corps of Engineers, 2003).

Using the initial slip surface a first FoS/MoS is assessed. Next, all points except one are held fixed, and the "floating" point is moved slightly in both horizontal and vertical directions, above or below the slip surface. A new FoS/MoS is then calculated for each shifted position and the process is repeated for each of the points on the slip surface. As any point moves, all other remain at their original location. Only after all points have been shifted in both

directions, and the FoS/MoS has been computed for each shift, a new location for the slip surface, based on the findings, is proposed.

At this stage, the slip surface is moved to this new location and the process of shifting points is repeated. This process continues until either no further reduction in the FoS/MoS is noted or when the distance that the shear surface is moved on successive approximations becomes minimal.

4.4.3.3 Solutions using slope stability charts

The use of slope stability charts provides usually a quick and efficient way to determine a first and preliminary estimate of the FoS/MoS before engaging in more detailed numerical simulations. They were firstly introduced by Taylor (1937, 1948), and although very practical, chart solutions have some important limitations, as they were developed for homogeneous soils and assuming circular slip surfaces. Therefore, it is always necessary to approximate the real conditions in the slope with a fictitious equivalent slope that has homogeneous properties. These are outwith the scope of this thesis and therefore have not been developed.

4.5 Numerical analysis

There is probably no analysis conducted by geotechnical engineers which has received more programming attention than the limit equilibrium methods of slices. This is due to the fact these methods tend to require iterative procedures, which are usually numerically undertaken. The available commercial software which assesses slope stability, with both circular and non-circular slip surfaces, has the advantage of enabling a large number of calculations to be carried out in a very short period of time. Additionally, they have the advantage of providing a graphical output, which shows the geometry of all of the analysed slip surfaces and their correspondent FoS/MoS.

However, LEM methods consider forces acting on one or several discrete points along the slip plane, whilst assuming that failure occurs instantaneously and that the available shear strength is mobilised along the whole slip plane at the same time. As an alternative, stress-strain methods can be used to overcome these limitations. By considering the stress-strain relationship of the materials during deformation and failure, software can output the type and magnitude of the displacements in the slope which are consistent with its state of equilibrium. They can also provide the slope's FoS/MoS, which may be different from the one obtained with limit equilibrium analyses, as no specific failure surface is defined (Matthews, Farook et al, 2014).

For the purpose of this thesis, both LEM and FEM numerical analyses have been undertaken. Furthermore, in order to validate the outputs from the LEM software's, a hand calculations check has been performed. As mentioned earlier, the commercial software used throughout this thesis is SLOPE/W, specifically designed for dealing with LEM slope stability problems, and PLAXIS 2D, a finite element code for soil and rock analyses. The formulation of SLOPE/W allows slope stability to be assessed using the Fellenius', Bishop's simplified and Janbu's simplified methods.

4.5.1 EC7 Design implications

The design of cutting slopes and embankments using both LEM and FEM analyses is not as direct as it would first appear using the partial factors approach. This results from the fact that EC7 requires different partial factors to be applied to unfavourable and favourable actions, which is not possible with typical slope stability calculations, since they cannot easily separate favourable and unfavourable actions.

Therefore, since Design Approach 1 requires permanent actions to be factored, the solution is to factor the soil's unit weight, which leads to treating the favourable and unfavourable effects in the same way, as they result from the same source. This is often known as the single source principle.

As a result, in Design Approach 1 Combination 1 (DA1-1), partial factors $\gamma_G = 1.35$ and $\gamma_Q = 1.5$ are applied to permanent and variable unfavourable actions, respectively. Partial factors on material properties and resistances are unitary. In slope stability software, this can be achieved by factoring the soils' weight densities by 1.35 and any applied surcharges by 1.5. A search is then made for the critical slip circle with a "target" factor of safety of 1.0.

In Design Approach 1 Combination 2 (DA1-2), partial factors $\gamma_G = 1.0$ and $\gamma_Q = 1.3$ are applied to permanent and variable unfavourable actions, respectively. Partial factors on resistances are unitary and partial factors on soil properties are $\gamma_{\varphi'} = \gamma_{c'} = 1.25$ and $\gamma_{cu} = 1.40$. This results in factoring the soils' effective drained strengths down by 1.25 (in the case of the angle of shearing resistance ϕ', the partial safety factor is applied to $tan\,\varphi'$), the soil's undrained strengths by 1.40 and any applied surcharges up by 1.3. A search is then made for the critical slip circle with the minimum MoS.

The concept of MoS arises in the Eurocodes as a means of ensuring an adequate reliability and ensuring a reduction in the overall cost of construction. It is based on a semi-probabilistic approach and makes use of a thorough definition of both loading and resistances. In simple terms, it replaces the concept of overall FoS by making use of characteristic and representative values for both actions and reactions and partial safety coefficients to ensure an acceptable probability of failure is obtained.

Throughout the remaining sections of this document only the concept of MoS will be used in the analyses, as defined in NP EN 1997-1:2010 (2010).

4.5.2 Numerical difficulties associated with the limit equilbrium method of slices

Limit equilibrium methods of slices require a limited amount of input information but can quickly perform an extensive trial and error search for the critical slip surface. However, they commonly make use of saturated effective shear strength parameters and ignore the shear strength contribution from the negative pore-water pressures above the groundwater table (Rahardjo & Fredlund, 1991).

As a result, and since some of the available software is exclusively focused on saturated soil mechanics, the contribution of any matric suction to shear strength has to be incorporated as part of the cohesion of the soil. In other words, this approach has the advantage of retaining the shear strength equation conventional form. To account for the effect of matric suction, the soil in the negative porewater pressure region has to be subdivided into several discrete layers, each with a different constant cohesion (that must be manually defined). This is known as the "total cohesion" method (Fredlund & Rahardjo, 1993).

An example of this application is provided below in Figure 65, where the effective cohesion varies as the matric suction effect on the soil increases. The proportional relationship between the two is expressed Figure 66.

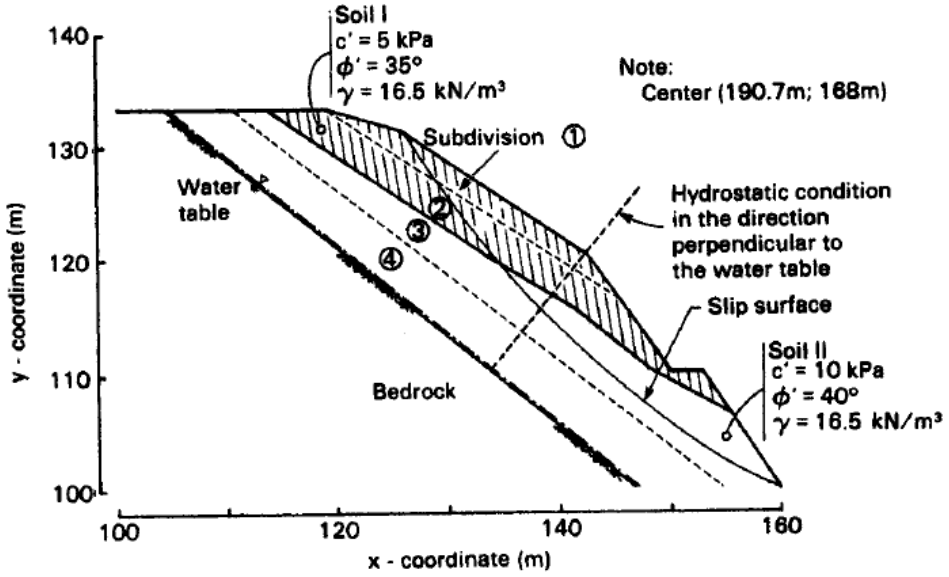

Figure 65. Example of "Total Cohesion" method (Rahardjo & Fredlund, 1991).

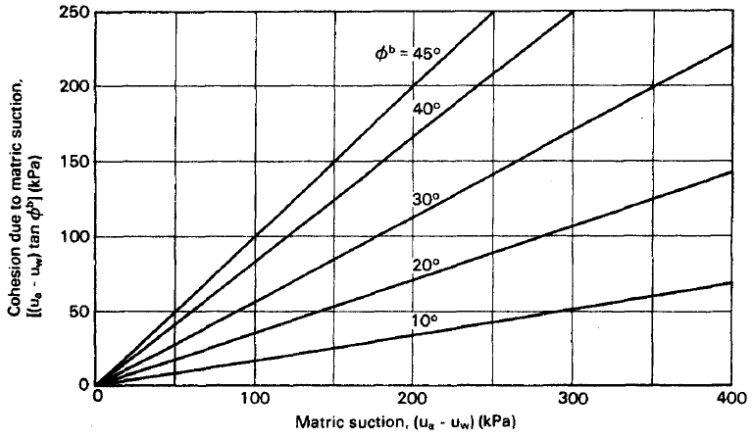

Figure 66. The component of cohesion due to matric suction for various ϕ^b angles (Fredlund & Rahardjo, 1993).

In the previous example the matric suction in each subdivision was assessed based on the porewater pressure at the centre of the subdivision and by assuming an atmospheric pore air pressure condition, i.e. $u_a = 0$.

The models used in this thesis have not addressed the quantification of the effect of matric suction. This is mainly due to the fact that, although its contribution to the overall resistance can be "converted" into cohesion, it typically requires a much finer discretisation of the ground models, with different soil layers being attributed distinct cohesion values (as per the example in Figure 65). However, if considering an average cohesion value across the slope is deemed as acceptable, then the stability assessments undertaken in this thesis may still be considered valid and be used in future problems where this phenomenon needs to be addressed.

4.5.3 Finite element method

The FEM software used in this thesis contains several FEM models from which the Hardening Soil model (HSM) has been adopted. This is widely used for modelling granular materials and it has been deemed as the most suited to simulate the behaviour of dense sands (Brinkgreve, 2002). The HSM simulates triaxial test results more accurately by considering the stress dependency of the soil stiffness modulus.

The non-linear shear-stress strain behaviour in loading is represented by a hyperbolic function, with average secant modulus (E_{50}), while a stiffer linear response occurs during the unloading stage, as described by the parameter, E_{ur} (Figure 67) The shear strength is characterized by conventional Mohr-Coulomb parameters (c', φ').

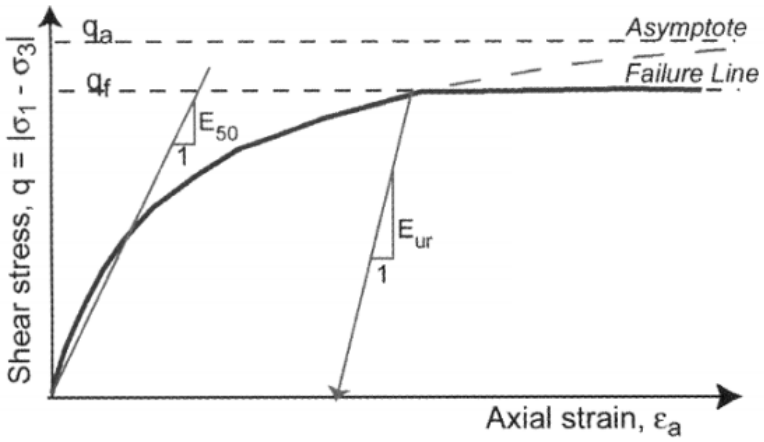

Figure 67. Shear stress-strain behaviour of the Hardening Soil model (Schanz, Vermeer, & Bonnier, 1999).

To estimate the MoS of the FEM models, the commercial software has a built-in 'c', φ' reduction' procedure which works by successively reducing the soil strength parameters c' and tan φ' until a fully developed failure mechanism occurs (Farshidfar & Nayeri, 2015). This allows the software to compute the MoS as the ratio between the available shear strength and the strength at failure.

The biggest limitation of this type of analyses is its inability of computing stability problem with a low MoS, i.e., significantly below unity.

5. Calculation analysis and discussion

Since the main objective of this thesis relies on the completion of numerous slope stability analysis, with a total of over 3000 different models, a solely hand calculation procedure would not be feasible. Therefore, numerical analyses have been undertaken using the commercial software SLOPE/W and PLAXIS 2D. However, before initiating the calculation procedure, a hand calculation check has been performed, which covered the three most common methods of slices that were previously mentioned in Table 9 (p. 63):

- Ordinary method of slices (Fellenius);
- Bishop's simplified method;
- Janbu's simplified method.

As pointed out previously, the ultimate goal has been to draft a design chart that would allow an expedite stability assessment of a granitic residual soil slope. Therefore, to begin the analysis procedure an envelope of ground conditions and soil parameters had to be established. The inputs which have been considered are:

- Slope geometry;
- Effective angle of shearing resistance;
- Effective cohesion (resulting from 'real' cohesion, dilatancy and/or matric suction);
- Groundwater conditions;
- Applied surcharge at the crest of the slope.

For each of the previous items a range of values has been established, which has been deemed to cover for the most common situations. As for the soil parameters, these have been based on the on-going and past research conducted at UBI to characterise the granitic residual soils of the region.

The sets of parameters that have been used in the analysis are presented in Table 10 below.

Table 10. Envelope of parameters analysed in LEM models.

Parameters		Range of values			
Geometry	Angle	1(V):2(H)	1(V):1.5(H)	1(V):1(H)	2(V):1(H)
	Height	2.0m – 8.0m, with 1.0m intervals			
Characteristic effective angle of shearing resistance		35°, 36°, 37° and 38°			
Characteristic effective cohesion		0kPa, 5kPa and 10kPa			
Groundwater		Dry Low groundwater level High groundwater level			
Surcharge		0kPa, 5kPa and 10kPa			

The soil bulk unit weight has been taken as 21kN/m^3 which has been considered appropriate given the results of the laboratory campaign and existing bibliography on the subject.

Having completed the LEM runs, and in order to compare their findings with FEM analyses, the following models have also been analysed in PLAXIS 2D (Table 11). These have been deemed as a sufficient pool of results to try to establish a comparison between FoS using both approaches.

Table 11. Envelope of parameters analysed in FEM models.

Parameters		Range of values		
Geometry	Angle	1(V):2(H)	1(V):1.5(H)	1(V):1(H)
	Height	5.0m and 8.0m		
Characteristic effective angle of shearing resistance		35°		
Characteristic effective cohesion		0kPa, 5kPa and 10kPa		
Groundwater		Dry Low groundwater level High groundwater level		
Surcharge		0kPa, 5kPa and 10kPa		

The models with the steepest gradient, 2(V):1(H), presented FoS significantly below unity and therefore had to be excluded from the FEM analyses. Furthermore, for a 1(V):1(H) slope it has only been possible to compute models where the soils had an effective cohesion of 10kPa. As for the remaining cases, only using the highest characteristic cohesion value has it been possible to assess slope stability when a high groundwater level is considered.

Finally, six of the above ground models have been selected to help estimate the benefit of each of the different remedial measures that have been analysed. These will be presented in detail in Chapter 6.

5.1 LEM Validation

The validation of the LEM software has been undertaken by assessing the stability of the ground model presented in Figure 68. A 1(V):2(H) slope has been modelled in SLOPE/W with the soil parameters and groundwater table presented below. The failure plane was geometrically defined within the model and intersecting the water table, so as to include porewater pressures within the slices. Worth pointing out that as the cohesion of the granitic soil has been identified as one of the soil parameters to vary through the analyses, the validation ground model also incorporated that feature.

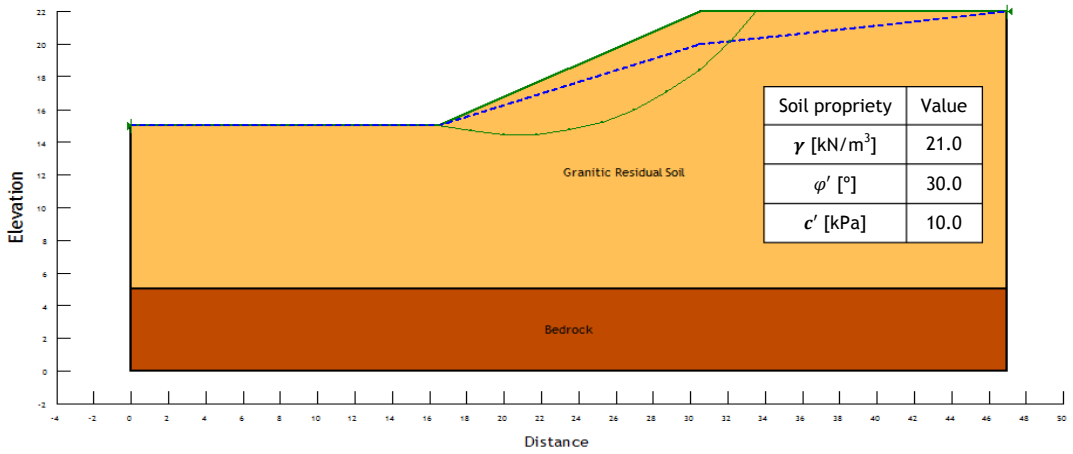

Figure 68. SLOPE/W Validation model.

The pre-defined slip surface has been divided into a fixed number of slices (10 in total) on both SLOPE/W and the hand calculations. The MoS obtained for each of the three models by both approaches are presented below in Table 12.

Table 12. Comparison between MoS attained using SLOPE/W and in hand calculations.

Method of slices	Margins of safety		
	SLOPE/W	Hand calculations	Difference
Bishop	1.598	1.605	+0,4%
Fellenius	1.551	1.549	-0,1%
Janbu	1.490	1.483	-0,5%

The differences reported above have been considered insignificant and likely to be the result of rounding dimensions. As such, the software has been considered validated. The SLOPE/W outputs can be found in Appendix A, along with the Excel validation sheets.

Table 12 suggests that from the three different methods, the Janbu's appears to be significantly more conservative than the remaining two. However, and as explained in Section 4.4.2, the obtained MoS should be adjusted by a correction factor (f_0 - Equation 30) to arrive at the final MoS. Table 13 presents the final MoS for all three validation models after the adjustment in the Janbu's MoS.

Table 13. Final MoS for the SLOPE/W validation models.

Method of slices	Margins of safety	
	SLOPE/W (Final)	Percentage difference between FoS and Bishop's FoS
Bishop	1.598	-
Fellenius	1.551	-2,9%
Janbu	1.594	-0,3%

Table 13 reveals a much better correlation between all MoS, particularly between the Janbu's and Bishop's simplified methods.

5.2 Methodology and ground models

As mentioned earlier, the stability assessments undertaken in this thesis have selected a few key parameters, internal and external, which have been deemed to most influence the stability of slopes in the granitic residual soil in analysis.

Additionally, and in order to create a design chart that is compliant with current standards, the EC7's requirements had to be considered. As such, both design actions and resistances have been factored in accordance to the partial factors of safety listed in Tables 6 to 8. The factored soil parameters used throughout the analyses are presented in Table 14 below. Note that these refer exclusively to Design Approach 1 Combination 2, as this is typically the most critical combination for slope stability.

Table 14. Characteristic and factored (as per EC7) soil parameters.

Soil Parameter / Action	Units	Characteristic value	Factored value
γ_m	kN/m^3	21	21
φ'	deg (°)	35.0; 36.0; 37.0 and 38.0	29.3; 30.2; 21.1 and 32.0
c'	kPa	0; 5 and 10	0; 4 and 8

With regard to groundwater, and as briefly described in Table 10, three different scenarios have been analysed. Firstly, the different models have been run without the presence of a

water table, which then served as baselines to analyse the influence of increasingly higher groundwater levels on the stability of the slope.

A second set of runs has considered the water table to coincide with the toe of the slope, and raising moderately behind the slope's face. A final set of calculations has been considered with the water table passing again through the toe of the slope but rising sharply behind its face, reaching only one metre below ground level at the crest. It should be noted the highest groundwater table is deemed as very conservative and highly unlikely to occur. Therefore, this is considered as an upper limit to the rises in groundwater levels. Figure 69 helps illustrate these three distinct scenarios.

Scenario 1

No groundwater

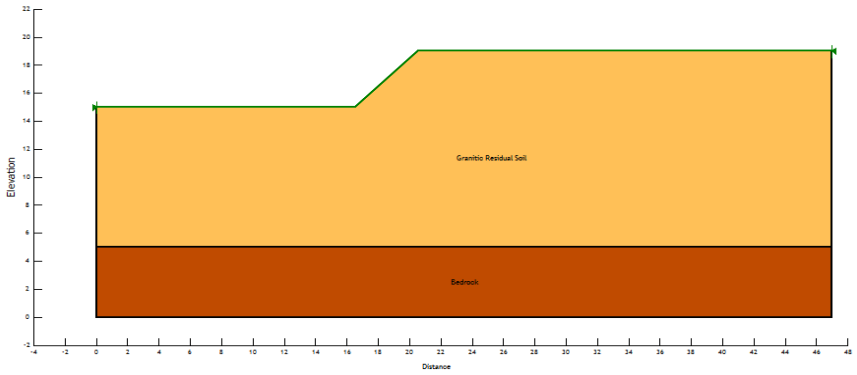

Scenario 2

Low groundwater table

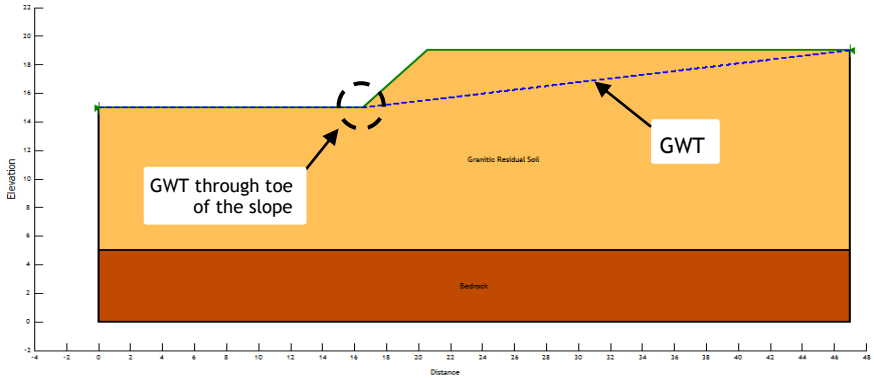

Scenario 3

High groundwater table

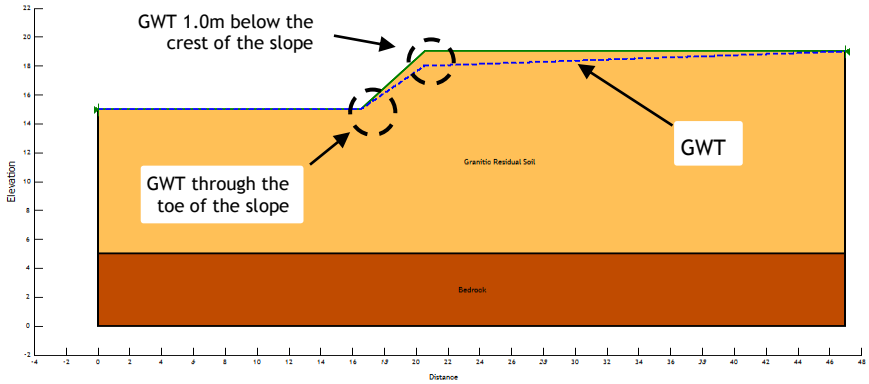

Figure 69. Groundwater scenarios model.

As for the surcharges applied on the top of the slope, they have also been factored according to the EC7 using the partial factors of safety presented in Table 6. As such, surcharges of 0kPa, 6.5kPa and 13kPa have been applied in the models.

All of the analysis have considered a minimum depth of 0.50m for the slip surfaces, as a failure shallower than that is as thought of not endangering the overall stability of the slope. The critical slip surface for each model has been assessed with a manually defined grid and radius search method, with both of them carefully positioned on the model to ensure the critical slip surface was located.

The different scenarios have been all analysed using the three different limit equilibrium methods and ignoring the formation of tension cracks.

5.3 Overview of the LEM results

To enable an overview of the results, these have been grouped by groundwater conditions and then subdivided by the cohesion of the soil and the applied surcharge at the crest. To facilitate its analysis plots for each individual set of conditions have been produced similar to the ones presented below in Figures 70 to 72.

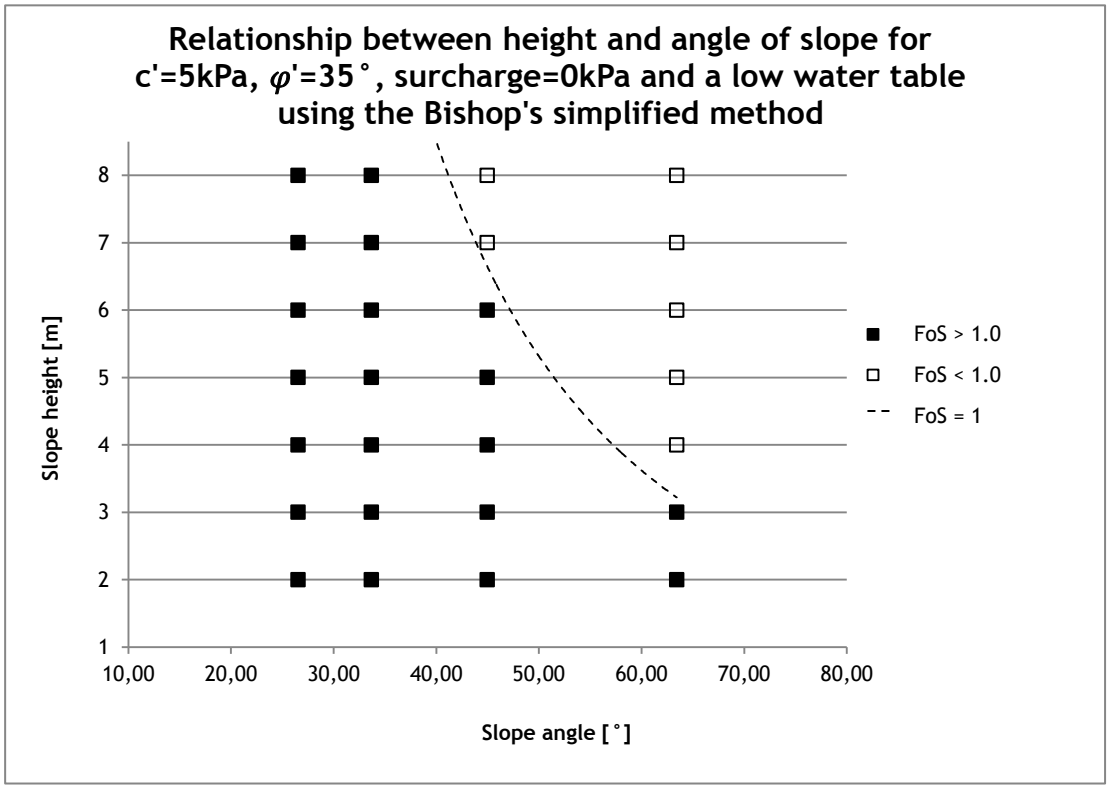

Figure 70. Example of slope height vs. slope angle plot using the Bishop's simplified method.

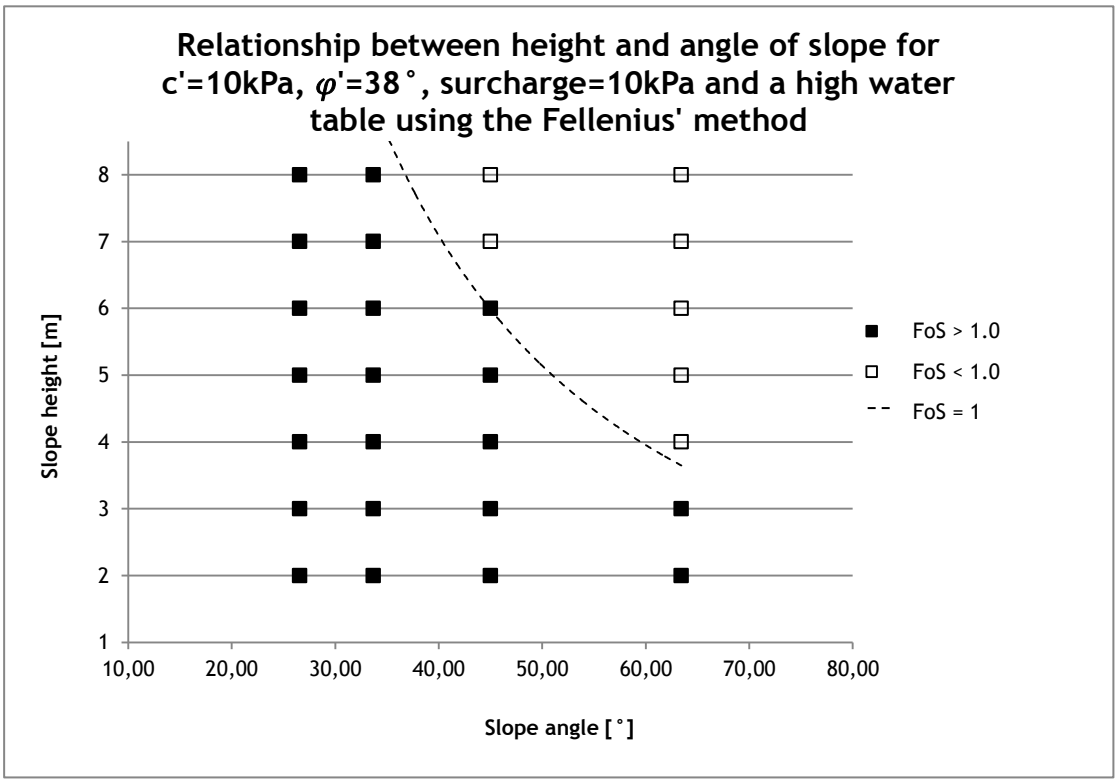

Figure 71. Example of slope height vs. slope angle plot using the Fellenius' method.

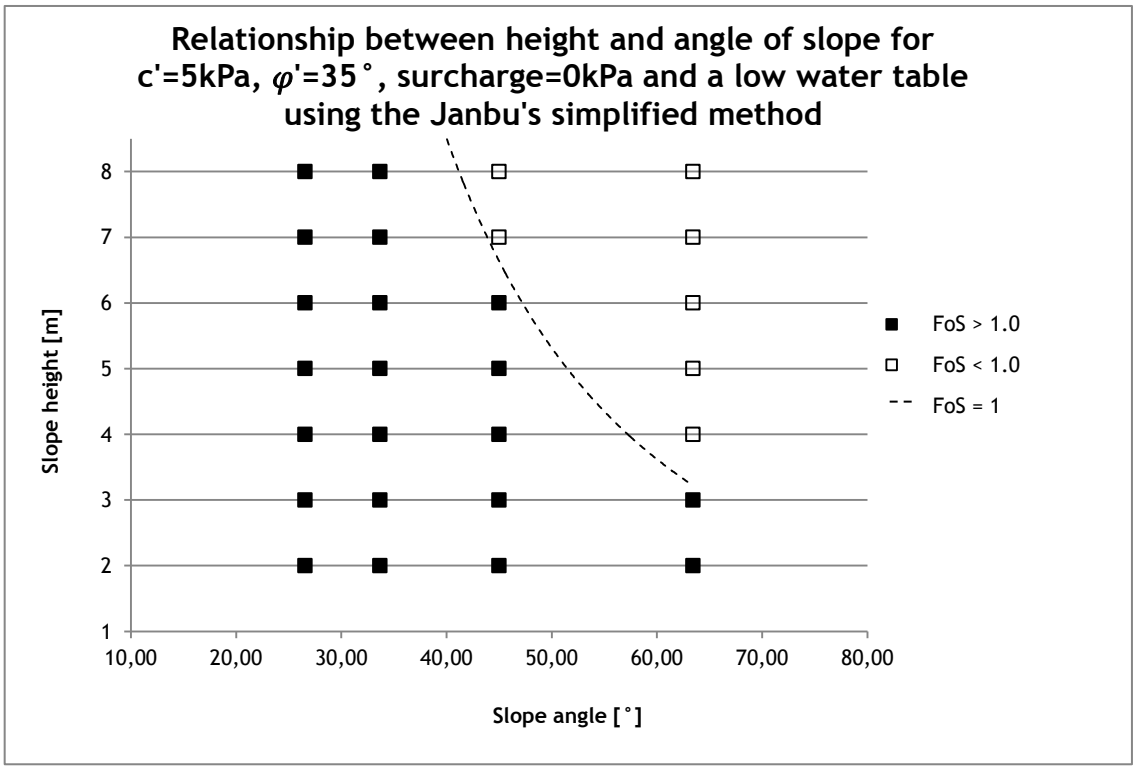

Figure 72. Example of slope height vs. slope angle plot using the Janbu's simplified method.

With all of the plots it was possible to assess, for each set of conditions, what would be the minimum characteristic angle of shearing resistance (from the range in analysis, 35° to 38°) that ensured compliance with current standards.

5.3.1 Proposed charts for stability assessment

By interpreting all of the LEM results, the following design charts are proposed for use when assessing the minimum required φ'_k to achieve a MoS equal to or above unity according to EC7 requirements. As such, a design chart per LEM method is presented below.

Given that the analyses have shown the MoS not to change significantly when the slope is taken as fully dry or with a low groundwater table, these results have been grouped and in the sporadic circumstances where both analyses required a different φ'_k to comply with EC7, the most critical is presented. These are marked within the charts.

The results presented in red correspond to the design requirements for a slope with a high groundwater table, always equal to or higher than the values in black, which correspond to a dry/low groundwater level situation.

Where boxes have been left empty, it should be interpreted that even the upper limit of the values for the angle of shearing resistance (φ'_k of 38º) is insufficient to comply with EC7 requirements.

BISHOP'S METHOD OF SLICES

Minimum characteristic φ' to achieve a FoS ≥ 1.0 according to EC7

Slope height (m)	Effective cohesion = 0kPa								Effective cohesion = 5kPa								Effective cohesion = 10kPa								Slope height (m)
	Slope angle								Slope angle								Slope angle								
	1.0(V):2.0(H)		1.0(V):1.5(H)		1.0(V):1.0(H)		2.0(V):1.0(H)		1.0(V):2.0(H)		1.0(V):1.5(H)		1.0(V):1.0(H)		2.0(V):1.0(H)		1.0(V):2.0(H)		1.0(V):1.5(H)		1.0(V):1.0(H)		2.0(V):1.0(H)		
Applied surcharge = 0kPa																									
2	35	35	36	38					35	35	35	35	35	35	35	35	35	35	35	35	35	35	35	35	2
3		36	38												38										3
4		38												38											4
5													35				35	35	35	35	35				5
6												37											37		6
7													36												7
8													37												8
Applied surcharge = 5kPa																									
2	35	35	37						35	35	35	35	35	35	35	36	35	35	35	35	35	35	35	35	2
3		36	38																						3
4		38	38									35	35									35			4
5																							36*		5
6												37													6
7													37												7
8													38												8
Applied surcharge = 10kPa																									
2	35	35	38						35	35	35	35	35	35	38		35	35	35	35	35	35	35	35	2
3		37												36										36	3
4													35									35			4
5												36								35			38		5
6												38	36												6
7													38												7
8										36										36					8

Notes:

- Values in black correspond to a dry/low groundwater table slope;
- Values in red correspond to a high groundwater table slope;
- * denotes that for a dry slope scenario a lesser φ'_k is required to achieve a FoS ≥ 1.0 as per EC7 requirements.

FELLENIUS' METHOD OF SLICES

Minimum characteristic φ' to achieve a FoS ≥ 1.0 according to EC7

Slope height (m)	Effective cohesion = 0kPa				Effective cohesion = 5kPa				Effective cohesion = 10kPa				Slope height (m)
	Slope angle				Slope angle				Slope angle				
	1.0(V):2.0(H)	1.0(V):1.5(H)	1.0(V):1.0(H)	2.0(V):1.0(H)	1.0(V):2.0(H)	1.0(V):1.5(H)	1.0(V):1.0(H)	2.0(V):1.0(H)	1.0(V):2.0(H)	1.0(V):1.5(H)	1.0(V):1.0(H)	2.0(V):1.0(H)	
Applied surcharge = 0kPa													
2	35	35 / 38			35	35	35	35 / 35	35	35	35	35 / 35	2
3		37						35				35	3
4								35				36	4
5							35	35			35	35	5
6						35	36			35	35	38	6
7						38	38			35			7
8													8
Applied surcharge = 5kPa													
2	35	35 / 38			35	35	35	35 / 36	35	35	35	35 / 35	2
3		38						35				35	3
4								35				35	4
5							35	35			35	37	5
6						35	36			35	35	37	6
7						36	37			35			7
8													8
Applied surcharge = 10kPa													
2	35	36			35	35	35	38	35	35	35	35 / 35	2
3		38						38				35	3
4												35	4
5							35	35			35	35	5
6						35	37			35	35	38	6
7						36	37			35			7
8													8

Notes:

- Values in black correspond to a dry/low groundwater table slope;
- Values in red correspond to a high groundwater table slope.

JANBU'S METHOD OF SLICES

Minimum characteristic φ' to achieve a FoS ≥ 1.0 according to EC7

Slope height (m)	Effective cohesion = 0kPa				Effective cohesion = 5kPa				Effective cohesion = 10kPa				Slope height (m)
	Slope angle				Slope angle				Slope angle				
	1.0(V):2.0(H)	1.0(V):1.5(H)	1.0(V):1.0(H)	2.0(V):1.0(H)	1.0(V):2.0(H)	1.0(V):1.5(H)	1.0(V):1.0(H)	2.0(V):1.0(H)	1.0(V):2.0(H)	1.0(V):1.5(H)	1.0(V):1.0(H)	2.0(V):1.0(H)	
Applied surcharge = 0kPa													
2	35	35 / 37			35	35	35 / 35	35 / 35	35	35	35 / 35	35 / 35	2
3		38 / 38				35 / 35	35 / 36			35 / 35	35 / 35		3
4							35 / 35				35 / 35		4
5						35 / 37				35 / 35		35	5
6							35 / 36				35 / 35		6
7							36 / 37					38 / 38	7
8												36 / 37	8
Applied surcharge = 5kPa													
2	35	35 / 37			35	35	35 / 35	35 / 35	35	35	35 / 35	35 / 35	2
3		37 / 38				35 / 36	35 / 37			35 / 35	35 / 35		3
4							35 / 38				35 / 35		4
5						35 / 38				35 / 35		35	5
6							35 / 37				35 / 35		6
7							37 / 38					37 / 38	7
8												37 / 38	8
Applied surcharge = 10kPa													
2	35	35 /			35	35	35 / 35	35 / 37*	35	35	35 / 35	35 / 35	2
3		38 /				35 / 35	35 / 35			35 / 35	35 / 35		3
4							35 / 35				35 / 35		4
5						35 / 38				35 / 35		35 / 36	5
6							36 / 36				35 / 35		6
7							36 / 38					35 / 38	7
8												38 / 38	8

Notes:

- Values in black correspond to a dry/low groundwater table slope;
- Values in red correspond to a high groundwater table slope;
- * denotes that for a dry slope scenario a lesser φ'_k is required to achieve a FoS ≥ 1.0 as per EC7 requirements.

5.3.2 Comparative analysis of the LEM results

However, the charts presented above only allow for a qualitative interpretation of the different LEM results for each set of pre-established parameters and conditions. Although useful, from a design point of view, as they indicate the minimum φ_k' required to achieve a MoS equal to or above unity according to EC7, these do not help portrait the variations in MoS depending on the method used or when conditions are changed. As such, a more thorough analysis has been undertaken and its outcomes can be found in Appendix B. Examples of the SLOPES/W models used in the analyses are illustrated in Appendix C.

To help interpret the results from the numerical trials these have been split to individually cover the following:

- The effect of an increase in surcharge on the crest;
- The effects of a rise in groundwater levels;
- A direct comparison between the outcomes of all three methods for all sets of conditions.

5.3.2.1 Interpretation of the LEM results

Through the application of the three LEM methods the following conclusions have been drawn. It should be noted at this point that although the analyses have been undertaken numerically for the Janbu's method, the correction factor applied to the attained MoS has been assessed manually for each individual case, in accordance with Figure 61.

Effects of surcharge increases on the slope's crest

It has been observed that, in non-cohesive soils, increases in surcharge to 5kPa and 10kPa typically result in maximum reductions in the MoS of circa 5% and 10%, respectively. Also, these changes are quite often negligible. Furthermore, these results are fairly consistent throughout all slope gradients and independent of groundwater conditions. It appears that the critical slip surfaces tend to mostly develop at a shallow depth along the slope's face and therefore are not considerably affected by surcharge variations at the crest.

When an effective cohesion of 5kPa is considered, the repercussions of a surcharge increase are more critical. If groundwater is absent, the reduction in MoS is up to 15%, for a surcharge of 5kPa, and 20% (Bishop) to 25% (Fellenius and Janbu) for a surcharge of 10kPa. However, these extreme values only occur in slopes with heights of 2 to 3m. When ignoring the latter the differences in MoS are reduced to a maximum of circa 5% and 10% for 5kPa and 10kPa surcharges. The conclusions are similar for the remaining groundwater conditions. As opposed to the previous set of conditions (non-cohesive soil) the differences in MoS are noticeable

over the full range of heights, whereas before from a height of 5m to 6m the differences were negligible.

If an effective cohesion of 10kPa is considered, and ignoring groundwater, the reduction in MoS is up to 15%, for a surcharge of 5kPa, and 25% for a surcharge of 10kPa. Again, these extreme values occur for small heights (2m to 3m high). When ignoring the latter, the differences in MoS are confined to maximums of circa 10% and 15%, respectively for 5kPa and 10kPa surcharges. The conclusions are similar for the remaining groundwater conditions.

For all LEM methods used in this thesis, increases in surcharge at the crest have been ascertained as more detrimental to the overall stability within cohesive materials, than in purely granular soils. In the latter case, for slopes above 3.0m high the differences are quite often negligible. Lastly, and even though the conclusions are similar regardless of the position of the water table, i.e. reductions in MoS of the same magnitude, having a higher water table leads to a slightly more penalising effect from surcharge increases.

Effect of groundwater level rises

When solely varying groundwater levels in the models, the differences in MoS are far more expressive. For purely granular soils, the consideration of a low groundwater table does not seem to affect the MoS obtained when groundwater is absent. However, rising these levels to what has been defined has a high groundwater table, leads to reductions in the MoS of over 50%.

Nevertheless, and with both high and low water levels, the reductions in MoS appear to be independent from the surcharge applied at the crest, although strongly linked to the slope angle.

For the Bishop's and Janbu's methods, the slopes modelled with the two slacker gradients, 1(V):2(H) and 1(V):1.5(H), have a similar response to groundwater level changes. A greater effect is reported in steeper slopes, particular in a 2(V):1(H) gradient. Sharp drops in the MoS are obtained for slopes over 3m high, when using the Bishop's method, or over 2m to 3m high for the Janbu's method.

A different trend emerges when analysing the results of the Fellenius' method. Here, the reductions in MoS seem to be more expressive for slacker slopes, diminishing as the slope angle is increased. The maximum reductions are reported under 35%.

Similar conclusions can be drawn from the SLOPE-W runs on slopes in soils with a 5kPa and 10kPa effective cohesion. The only exception to this is that in these cases and when considering slacker slopes, 1(V):2(H) and 1(V):1.5(H), differences of up to 15% are reported between models where groundwater is absent and having a low water table. This is more noticeable as height increases. This might be explained by the fact that as these materials have a certain cohesion value, they drive the critical slip surfaces deeper. As a result, in

slacker slopes they will more easily intersect what has been defined as a low groundwater table.

In addition, the reductions in MoS by rising groundwater seem to be inversely proportional to the cohesion of the intersected materials, i.e. greater reductions are reported for lower or null effective cohesion values.

Comparison between LEM methods

The comparison between methods has been undertaken considering the Bishop's method as a reference. As such, all the conclusions below refer to comparisons between the latter and the remaining two methods.

In non-cohesive materials the MoS seems to converge for slacker slopes and for greater heights. Also, and in line with the results of the sensitivity analysis to groundwater changes, results show that for steeper slopes, 1(V):1(H) and 2(V):1(H), the Fellenius' method gives MoS significantly higher than the Bishop's method (up to circa 70%) for high groundwater levels. This is in agreement with the findings of (Whitman & Bailey, 1967), which reported the Fellenius method to result in errors as much as 60%.

This contrasts with the findings of the Janbu's methods which report a significant reduction in the MoS for the same models by up to 25% when compared to the Bishop's. Again this may be the result of the lesser aptitude/inadequacy of this method to circular slips in non-cohesive soils. According to Figure 61 these are also the cases where a smaller correction factor is applied.

Overall, for slacker slopes, 1(V):2(H) and 1(V):1.5(H), a good correlation is achieved between all methods, with maximum differences of 10% and frequently under 5%.

Different conclusions are drawn for slopes in cohesive materials, with the exception of the Fellenius' method. This still reports significantly higher MoS than the Bishop's method for high groundwater tables within the steepest slopes. On all remaining models the Fellenius's method reveals lesser MoS than the Bishops' but only up to circa 10%.

When comparing the outcome of the Janbu's method, it is clear that overall these results are closer to the Bishop's than those obtained with the Fellenius's method. However, greater divergences are noted for high groundwater levels and in steeper slopes, 1(V):1(H) and 2(V):1(H).

Nevertheless, when groundwater is absent or at a low level, this method generally reports greater MoS than the Bishop's method, albeit marginally.

5.4 Overview of the FEM results.

As listed earlier in Table 11, fewer scenarios have been considered for the FEM modelling. Similarly to the LEM procedure, these outputs have also been grouped by groundwater conditions and then subdivided by the cohesion of the soil and the applied surcharge at the crest. Given the smaller pool of results all the obtained MoS are presented below in Table 15. Note that only a $\varphi_k{}'$ of 35° has been used. The cells left blank correspond to scenarios where the FEM modelling could not be undertaken due to numerical error.

Table 15. MoS for FEM analyses ($\phi'_k = 35°$).

Slope height (m)	Effective cohesion = 0kPa			Effective cohesion = 5kPa			Effective cohesion = 10kPa		
	Slope angle			Slope angle			Slope angle		
	1(V):2(H)	1(V):1.5(H)	1(V):1(H)	1(V):2(H)	1(V):1.5(H)	1(V):1(H)	1(V):2(H)	1(V):1.5(H)	1(V):1(H)
Applied surcharge = 0kPa							**No groundwater**		
5	1.099	-	-	1.672	1.347	-	2.066	1.705	1.326
8	1.038	-	-	1.489	1.175	-	1.775	1.428	1.067
Applied surcharge = 0kPa							**Low water table**		
5	1.058	-	-	1.557	1.328	-	1.897	1.649	1.328
8	0.979	-	-	1.306	1.127	-	1.514	1.347	1.066
Applied surcharge = 0kPa							**High water table**		
5	-	-	-	1.161	-	-	1.465	1.207	-
8	-	-	-	-	-	-	1.144	-	-
Applied surcharge = 5kPa							**No groundwater**		
5	0.880	-	-	1.630	1.325	-	2.010	1.659	1.295
8	0.906	-	-	1.479	1.166	-	1.739	1.411	1.056
Applied surcharge = 5kPa							**Low water table**		
5	0.877	-	-	1.534	1.311	-	1.857	1.614	1.295
8	0.905	-	-	1.276	1.095	-	1.499	1.334	1.066
Applied surcharge = 5kPa							**High water table**		
5	-	-	-	1.147	-	-	1.437	1.212	-
8	-	-	-	-	-	-	1.124	-	-
Applied surcharge = 10kPa							**No groundwater**		
5	0.745	-	-	1.579	1.284	-	1.938	1.598	1.264
8	0.754	-	-	1.444	1.144	-	1.710	1.402	1.050
Applied surcharge = 10kPa							**Low water table**		
5	0.749	-	-	1.481	1.289	-	1.778	1.565	1.262
8	0.755	-	-	1.254	1.104	-	1.462	1.299	1.037
Applied surcharge = 10kPa							**High water table**		
5	-	-	-	1.115	-	-	1.406	1.151	-
8	-	-	-	-	-	-	1.110	-	-

5.4.1 Comparative analysis of the FEM results

A similar procedure to process the outputs of the FEM analyses has been undertaken and can be found in Appendix D. To help in the interpretation of the results, they have been organised to cover the following:

- The effect of an increase in surcharge on the slope's crest;
- The effects of a rise in groundwater levels; and
- A comparison between the LEM and FEM approaches on all the common sets of conditions.

5.4.1.1 Interpretation of the FEM results

By using the HSM available within the PLAXIS 2D software it has been possible to arrive at the following conclusions.

Effects of surcharge increases on the slope's crest

When considering a purely granular soil, significant reductions in the MoS have been obtained by increasing the surcharge to 5kPa and 10kPa, respectively up to circa 20% and 30%. Greater reductions are reported for the 5.0m models than for the 8.0m ones and surcharge increases appear to be less critical for higher water levels.

When an effective cohesion is considered, the repercussions of a surcharge increase are overall less critical (as opposed to the LEM analyses), with reductions generally under 5% and up to a maximum of 6.3%. The effect of the surcharge increase appears to be similar when groundwater is absent and in slopes with a low water table. A lesser effect is noted when groundwater rises to high levels.

These changes report lesser reductions to the MoS as the slope gradient increases, although the pool of results is not sufficiently large to arrive at a definite conclusion.

Effect of groundwater level rises

As opposed to the above, changes in groundwater levels appear to be more critical for cohesive than non-cohesive materials. However, it should be noted that only two non-cohesive models were used and that on these it has not been numerically possible to assess their stability for a high water table.

For cohesive materials no significant differences are reported for effective cohesions of 5kPa or 10kPa. Also, negligible reductions occur for the steepest configuration 1(V):1(H). 1(V):2(H)

and 1(V):1.5(H) models show reductions in the MoS of circa 30% and 35% for a high groundwater table, respectively for 5.0m and 8.0m heights.

When considering a low groundwater table reductions are up to 10% and 15%, respectively for 5.0m and 8.0m heights in 1(V):2(H) slope. For a slightly steeper slope, 1(V):1.5(H), these values are reduced to up 5% and 10%, respectively for 5.0m and 8.0m heights.

There is no significant variation with the increase in surcharge, which leads to the conclusion that variations in groundwater levels are substantially more critical than increases in surcharge.

Comparison between LEM and FEM approaches

The comparison between FEM and LEM methods has revealed there is a significant divergence in the obtained MoS for purely granular materials. All LEM methods appear to overestimate the safety of the slope by up to circa 40%. These differences are more expressive as the height and the applied surcharge at the crest increase.

In soils with apparent cohesion the results of the Bishop's simplified method are between circa 5% and 10% higher than the FEM outcomes. The differences appear to increase with the gradient of the slope, with rising groundwater level and the slope's height. No noticeable differences are reported for surcharge increase.

The Fellenius' method presents MoS values both over and under the FEM ones, with differences generally under circa 5% but with values between 5% and 10%. No tendency is apparent for changes in groundwater levels or applied surcharges.

The majority of the MoS values obtained with the Janbu's simplified method present the best correlation with the FEM approach (for soils with apparent cohesion), with differences reported predominantly under 5%. The best correlation occurs for greater applied surcharges and slacker slope gradients

6. Remedial measures

6.1 Purpose and limits of remedial work

The ultimate purpose of installing stabilising elements and/or providing additional support is to increase the forces resisting slope failure. This can be achieved by increasing the shear strength of the *in situ* materials, changing the geometry of the slope or providing additional shear resistance along a potential failure surface.

Remedial measures, as their name suggest, are those carried out after a slope failure event or when excessive deformation is reported which may trigger instability. As such, their design requires an estimate of the relevant soil parameters, a prediction of the geometry of the failure surface and especially an assessment of the factors causing the instability.

This is usually the outcome of back analyses, which allow for the estimate of the "real" geotechnical soil parameters (Tomlinson, 2001). These include cohesion, angles of shearing resistance, deformability moduli and an understanding of the hydrological conditions. If there is a likelihood of seismic activity in the area, this should also be taken into account in the analysis.

In addition, other factors such as the financial, plant/labour and material resources available, the scale and dimension of the problem and, above all, the urgency in the undertaking of corrective measures are likely to strongly influence the proposed design.

Intuitively, the most effective remedial measures, and often also the least onerous ones, are those that act directly on the factors triggering instability.

In general term, the MoS of a slope can be improved by either reducing the destabilising forces or increasing the stabilising ones. This is commonly achieved by either one or a combination of the following options (Figure 73):

- Modifying slope geometry;
- Installing/improving drainage;
- Installing resisting elements on the slope;
- Setting up retaining walls/elements at the toe.

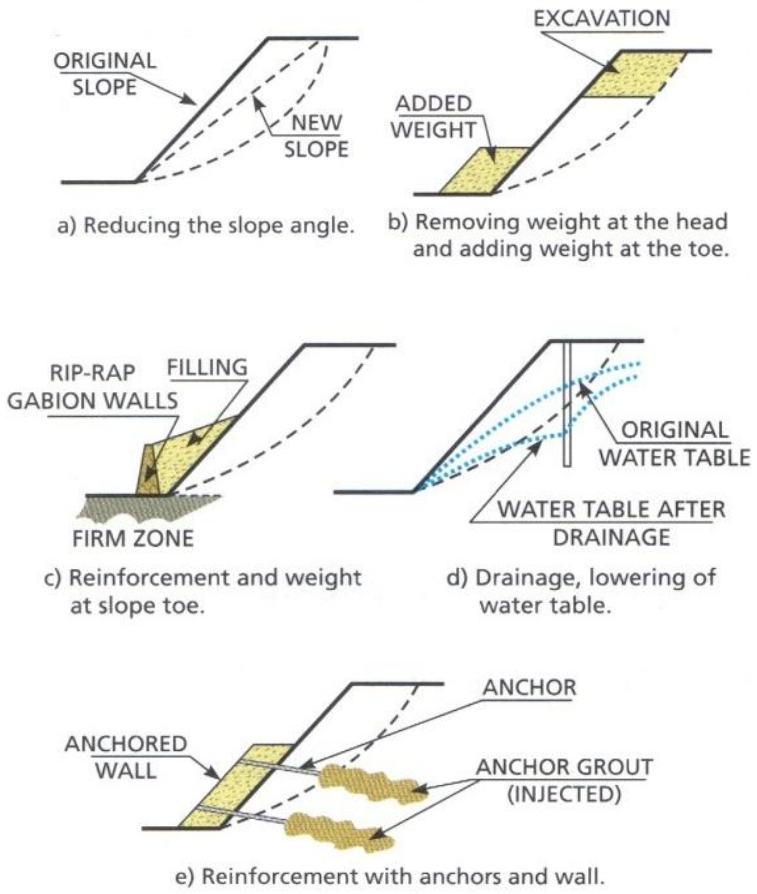

Figure 73. Most common stabilising techniques of slopes (Vallejo, Ferrer et al., 2004).

When a slope becomes unstable, it is very useful to perform a back analysis, to allow an estimation of the "real" geotechnical parameters found on site.

6.2 Monitoring

When remedial measures are proposed, and given all of the uncertainties in the back analysis process, it is good practice to set up a monitoring plan to investigate any slope movement before, during and after the remedial works are undertaken. Such results are often used to prove the adequacy of the proposed solution and may help to anticipate any failure re-activation. However, these must be taken at an adequate frequency and processed in due time to be an effective tool. Typically, a monitoring plan should target the following:

- The location of the failure surface or surfaces;
- The profile of movement along the slope, including its rate;
- The location of the water table and existing pore pressures.

Monitoring is also useful prior to a failure event to help detect any signs of instability, e.g. tension cracks, small failures near the crest or signs of uplift at its toe. Unfortunately, this is generally limited to cases where the consequences of failure are very significant, affecting buildings and/or infrastructure, due to its cost.

The most common monitoring apparatus for investigating movement and its rate are displacement targets and inclinometers, whilst standpipes and piezometers measure the piezometric head at the locations they are installed at, thus providing an indication of the porewater pressure. The control of earth pressures on retaining walls and on ground anchors is usually carried out using load cells.

It should be noted that the monitoring requirements and frequency will vary depending on the set of circumstances in which failure has occurred. Simultaneously, alert and alarm values should be defined by the Designer, prior to commencement of Construction, and which will enable a pro-active response to any signs of instability. The results may even suggest changes in the monitoring frequency.

6.3 Reprofiling

Altering the geometry of a slope results in the redistribution of the acting weight forces. A new and more stable configuration is usually achieved by (Figure 74):

- Reducing the slope angle;
- Removing weight at the head of the slope;
- Increasing weight at the slope toe.

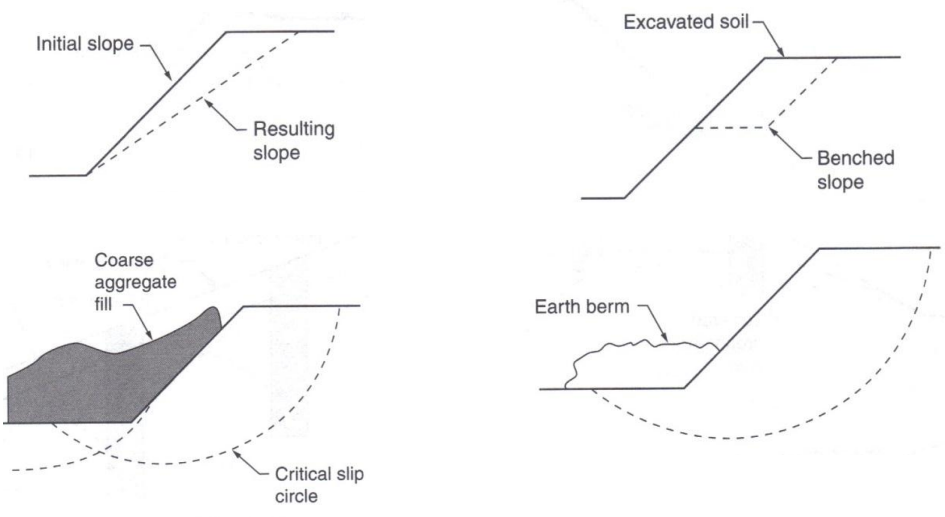

Figure 74. Earthwork construction techniques to reduce shear stresses or to increase resistive forces, adapted from Cashman & Preene (2001).

However, the measures listed above are often impossible to materialise on site. This is due to geometry restrictions on either the upper or bottom part of the slope or the presence of infrastructure. Therefore, geometry changes are usually considered either as an emergency solution, to prevent an imminent failure, or associated with the construction of retaining elements. In the latter case, this will correspond to the backfill to a new retaining wall, typically comprising free-draining material so as to add extra weight to the toe area whilst allowing any water ingress to drain out of the slope.

Alternatively, it is possible to help stabilise a slope by creating benches and berms that will cut into potential superficial failure surfaces. This will prevent them from affecting the overall stability of the slope. Furthermore, these measures may also be related with debris retention or to allow maintenance works to be undertaken.

6.4 Drainage

The aim of drainage is to eliminate or reduce the amount of water within a slope, thus decreasing pore pressures in any failure planes. Since water is often the main trigger to slope instability (generating pore pressures, softening the ground or inducing erosion around the toe), drainage is often considered the most effective corrective measure.

A reduction in groundwater level and piezometric head allows for a progressive improvement in soil strength as effective stress is increased in the dewatered soil. Drainage measures can involve a multitude of solutions although typically four main methods can be used:

- Stopping surface run off from reaching the slope's face by means of cut-off ditches, low walls and embankments;
- Collecting water along the slope and subsequently pumping it or channelling it using drainage ditches and French or Herringbone drains;
- Lowering groundwater using a deep drainage system such as wellpoints, deep wells or ranking drains;
- Stopping groundwater from reaching the slope by means of a cut-off wall, such as cement-bentonite slurry wall.

Figure 75 shows a wide range of available techniques, which fall broadly into the categories mentioned earlier. The most common ones will be discussed in further detail over the next subsections.

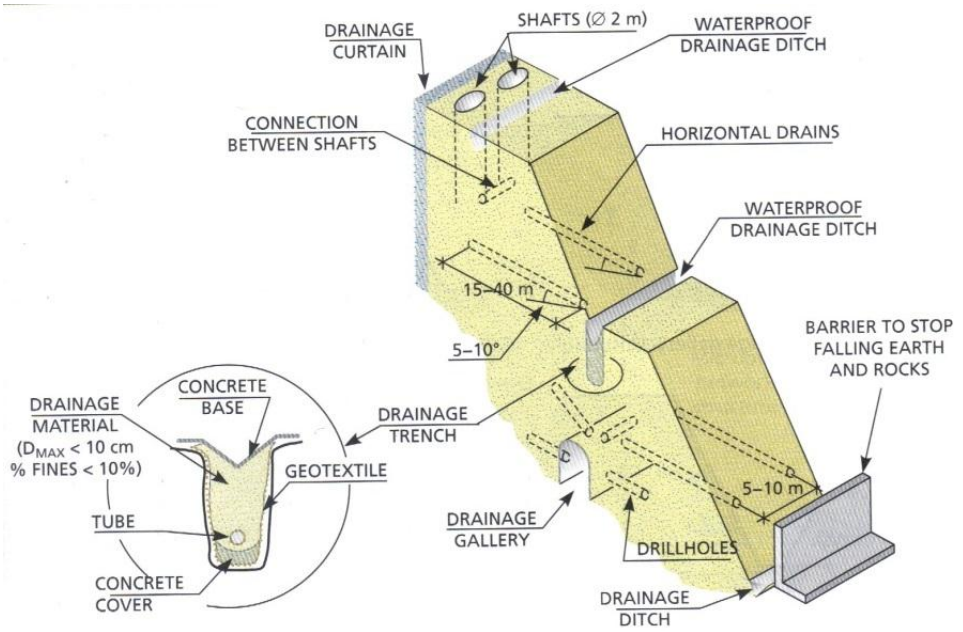

Figure 75. Measures for slope drainage and protection (Vallejo, Ferrer et al., 2004).

In extreme cases, where either the slope face is too steep or the hydraulic gradient within it is too high, significant seepage can occur which may even daylight and potentiate local erosion (Figure 76). If left unattended, this can even result in overall failure.

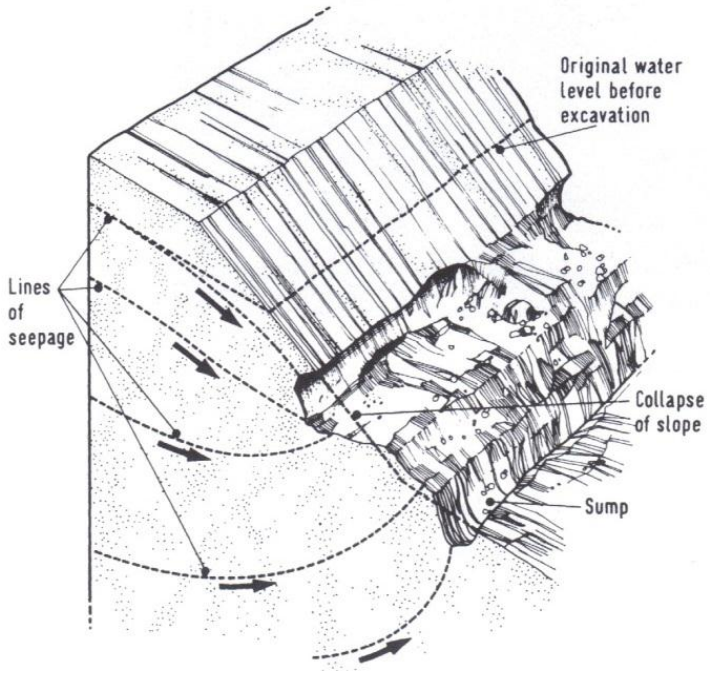

Figure 76. Effects of seepage on an excavated slope (Cashman & Preene, 2001).

To prevent piping from occurring, sufficient resistance must be provided against internal soil erosion in the areas where water outflow may occur. As such, preferential seepage paths should be considered when determining the hydraulic conditions within a slope. Also, these seepage paths should be controlled using suitably permeable materials and carefully designed and constructed filter drainage systems.

When possible/practical, drainage design should aim at preventing water from reaching and/or accumulating along the slope. The critical areas for this will be the crest and any flat areas where water ponding may occur after rainy periods.

The water collected by the drainage system is typically led to concentration points, usually by gravity, from where it is pumped or discharged into an existing water line or connected to an existing drainage service. In the latter case, the Designer should ensure the additional drainage does not exceed the capacity of the existing system.

Despite the beneficial effect of drainage in slope stability, EC7 specifically specifies that "unless the adequacy of the drainage system can be demonstrated and its maintenance ensured, the design groundwater table should be taken as the maximum possible level, which may be the ground surface." Furthermore, "if the safety and serviceability of the designed structure depends on the successful performance of a drainage system, the consequences of its failure shall be considered".

Therefore, to take full advantage of any dewatering system the Designer must demonstrate the reliability of the proposed drainage system and specify a maintenance programme (within the Geotechnical Design Report). Alternatively, the drainage system must be able to operate adequately without maintenance.

The more reliable groundwater lowering systems need to be flexible and robust in nature and able to cope with ground conditions slightly different from those anticipated with few or minor modifications. To be in line with EC7, such systems should also be easy to modify and upgrade if ground conditions are substantially different from those expected.

6.4.1 Superficial drainage

The basic rule of good practice is to collect and control the surface water run-off before or as soon as it enters the site. The most common way to achieve this is to establish ground level drainage by means of drainage ditches and trenches taken to a pre-established depth, typically ranging between 0.5m and 3.0m. When up to depths of circa 1.0m these elements can be excavated by hand, which makes them ideal for remote area or zones where plant access is difficult.

To deal with rainwater and surface or subsurface run-off it is common to resort to Herringbone drains. These consist of a number of main drains into which smaller drains (known as subsidiary) discharge from both sides (Figure 77). The subsidiaries run parallel to each other at an angle to the main drain and typically do not exceed 30 metres in length. The spacing of these subsidiaries will depend upon on the ground conditions.

Figure 77. Example of Herringbone drains on a railway cutting (Construction Marine Ltd., 2012)

Both subsidiary and main drains consist of typically shallow trenches, filled with granular draining material and often wrapped around a geotextile separator. They can also be partially lined with an impermeable membrane at the bottom so as to ensure that the water collected does not infiltrate back into the slope.

Given the shallow depth of these drains they may or may not have a pipe at the bottom and usually discharge the water collected into ditches or trench drains.

When the intent is to lower a superficial groundwater level to a maximum depth of circa 3.0m below ground level, further to the Herringbone drains, deeper trench drains are usually used (Figure 78). These are extended to deeper depths and usually require excavation plant and the use of trench boxes. Their effect on the hydrological regime of the slope will depend on both the nature of the confining soils and on the distance between drains. In fine grained materials the water level may still rise significantly between drains.

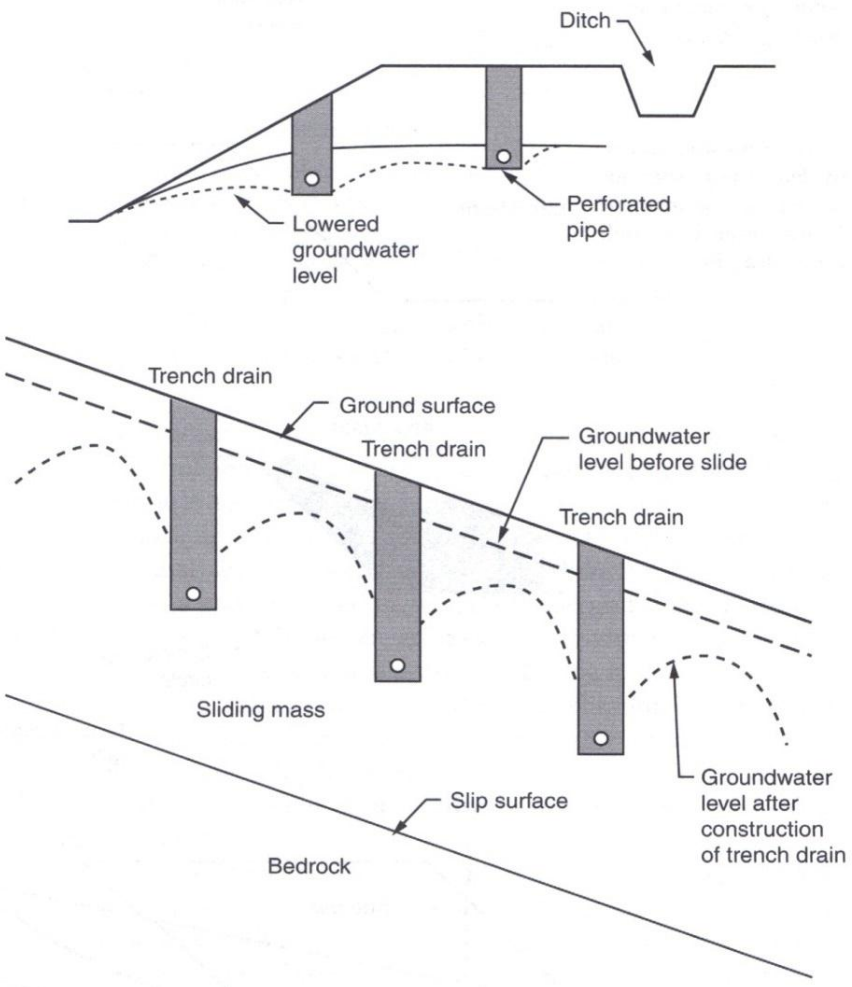

Figure 78. Ground level drainage control measures, adapted from Das (2011).

Trench drains, also known as filter drains, consist of trenches were the existing material is replaced by suitably compacted granular fill and in which a pipe is placed at the bottom to collect any groundwater. There is no fixed diameter for the pipes, although their size usually depends on the trench width, and they can either be perforated around their whole perimeter or only in half.

The grading and compaction level of the granular fill may differ from below the pipe's invert or above its crown. A geotextile separator should be used to avoid any fines from the existing soils to reduce the granular fill's permeability. The base and the downslope face of the trench may be lined with an impermeable membrane to ensure that any water collected does not seep back into the slope.

Towards the toe of the slope, where typically the hydraulic gradients are higher, additional measures should be considered to foment drainage whilst simultaneous ensuring additional protection against piping (Figure 79).

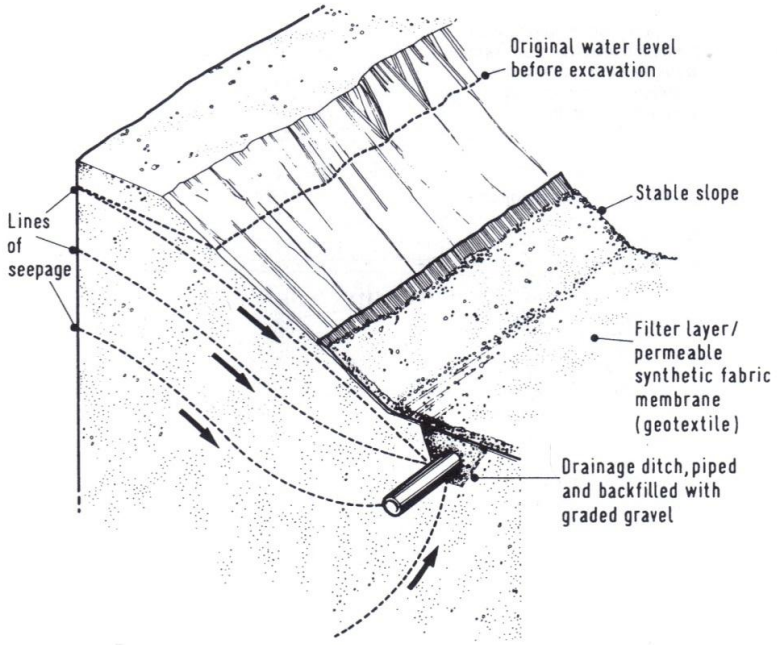

Figure 79. Stable excavated slope resulting from flat gradient and provision of drainage trench (Cashman & Preene, 2001).

These can be materialised by placing rockfill mattresses (gabion type structures) along the slope at that level, once again separated by a geotextile to ensure the voids in the rockfill do not become progressively filled with fines. This should be complemented with an effective drainage collection at the toe of the slope. If additional drainage is required, rockfilll counterforts/buttresses can be used to enhance drainage and potentially enhance the weight and stabilising forces on the slope (Figure 80).

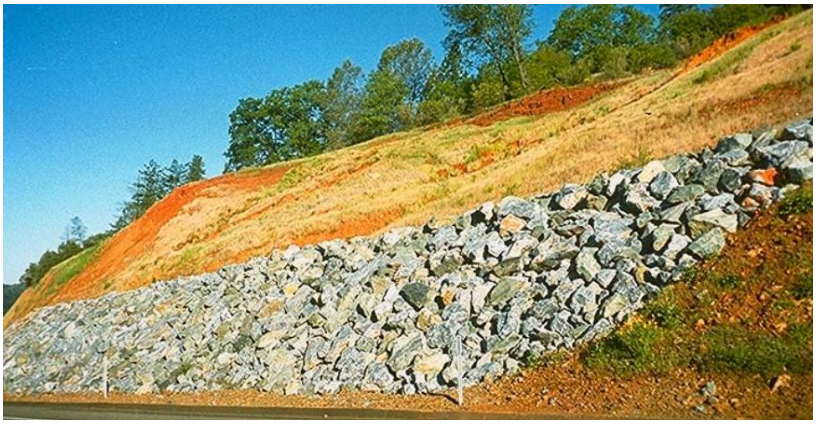

Figure 80. Rockfill buttress at the toe of a cutting.

Irrespectively of the surface drainage measures adopted, all drains should be cleaned out regularly, especially before the beginning of the rainy season. It is also advisable to prescribe inspection chambers every 20m to 30m along the drains to facilitate their maintenance.

As for the ditches, they should be sufficiently wide to allow a water velocity low enough to prevent erosion. This may be achieved by constructing check weirs at intervals along the ditch.

These procedures, often designated as preventive rather than stabilising, also help to minimise superficial erosion and are aligned with EC7 recommendations.

6.4.2 Deep drainage

Deep drainage is generally used to lower the water table and extract water from within the slope (Figure 81) rather than just collecting any superficial or sub-superficial run-off and impeding it from infiltrating into the materials below.

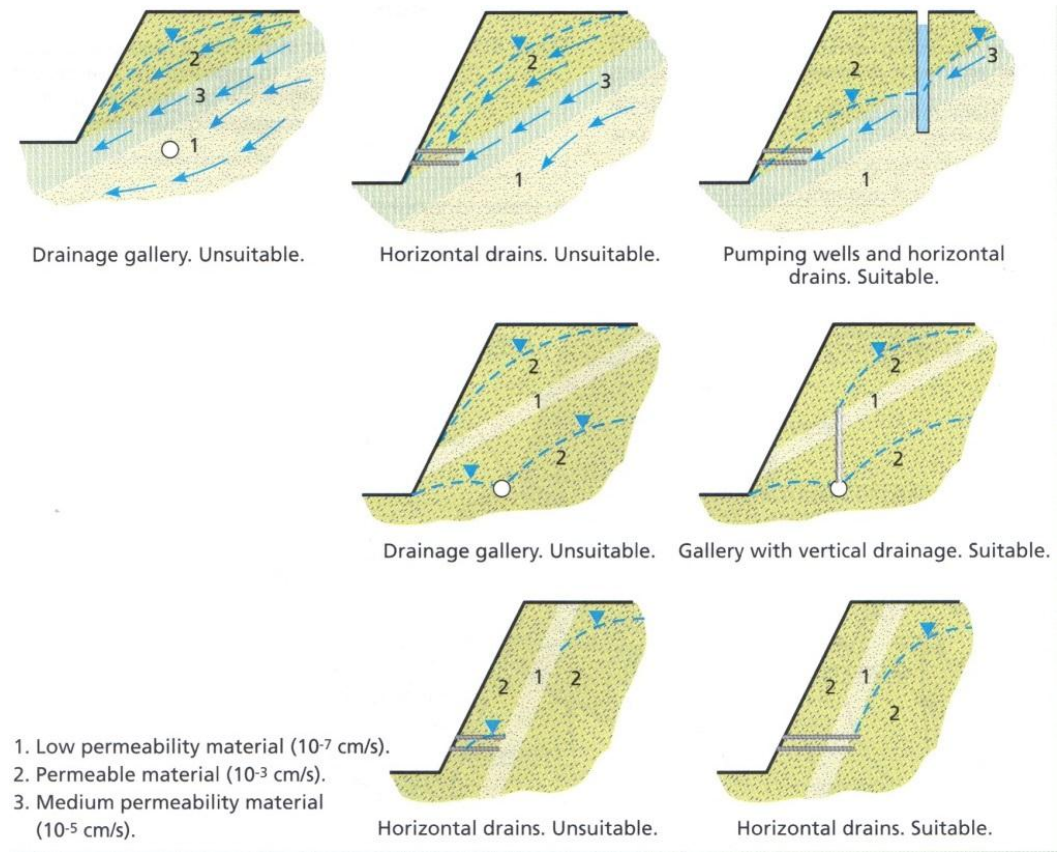

Figure 81. Examples of distribution and efficiency of drainage systems in a slope (Vallejo, Ferrer et al., 2004).

Several key aspects should be considered when designing such a system, from which the following stand out:

- The permeability of the soils to drain and the effectiveness/radius of drainage of the proposed elements;
- The required drilling depth to reach water level in order to achieve the envisaged groundwater profile. A minimum depth should always be specified based on the hydrogeological conditions of the site. On occasion, and especially when artesian water is a concern, maximum drilling depths may also be applicable;
- As per the comments on surface drainage, the durability of the drainage system should be addressed, as well as its susceptibility to damage with slope movement. The latter is especially relevant in situations where a creeping slope is intended to be stabilised by lowering its water table, as some movement is to be expected before ceasing. Thus, if the deep drainage system cannot tolerate such a movement it may lead to the exact opposite effect than the one intended.

The most common form of deep drainage is the use of horizontal or sub-horizontal ranking drains. These are boreholes drilled through a slope's face, typically ranging from 100mm to 150mm in diameter, and a maximum length of 30m to 40m (Figure 82). They are usually fitted with a 25mm to 50mm diameter slotted pipe and are quite common at the toe of the slopes, although they can be installed at different heights along the slope if needed. The drainage pipe may not be installed in the complete hole, although it is advisable to do so as to minimize the potential for blockage due to hole collapse. Furthermore, a system of two pipes can be used, an outer one which will be fixed to the hole and an inner one which can be removed/replaced for maintenance purposes.

Figure 82. Horizontal drain construction (Read & Stacey, 2009).

These devices are often installed with a surface (collar) casing, as illustrated in Figure 83, to minimize the risk of water seeping from the drain into the soil behind the slope's surface.

Drains are also usually drilled slightly upwards, in order to reduce the effects of collapse and blockage (Read & Stacey, 2009). However, when working in slopes with a shallow gradient, 1(V):2.5(H) or lesser, these are usually undertaken horizontally from a constructability point of view.

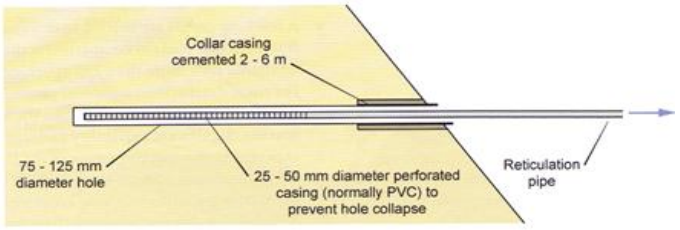

Figure 83. Horizontal drain design, adapted from Read & Stacey (2009).

The use of raking drains has its limitations, since its efficiency decreases as the water table is lowered and further superficial drainage is required to collect all of the drained water. Additionally, they can be cut and lost during slope movement, which may cause them to feed additional water into the existing slope. The use of a dual pipe system minimises this risk.

Other usual deep drainage elements are vertical wells. These typically start with diameters of 200mm and are used either to discharge the water by internal pumps, actioned when water in the well reaches a certain height, or using a passive system and making use of raking drains to lead the collected water out of the slope.

It is also possible to combine the use of vertical wells with vertical drains. This is especially relevant when dealing with a slope that has a horizontal low permeability stratum which allows the formation of a perched water table to occur, as presented in Figure 84.

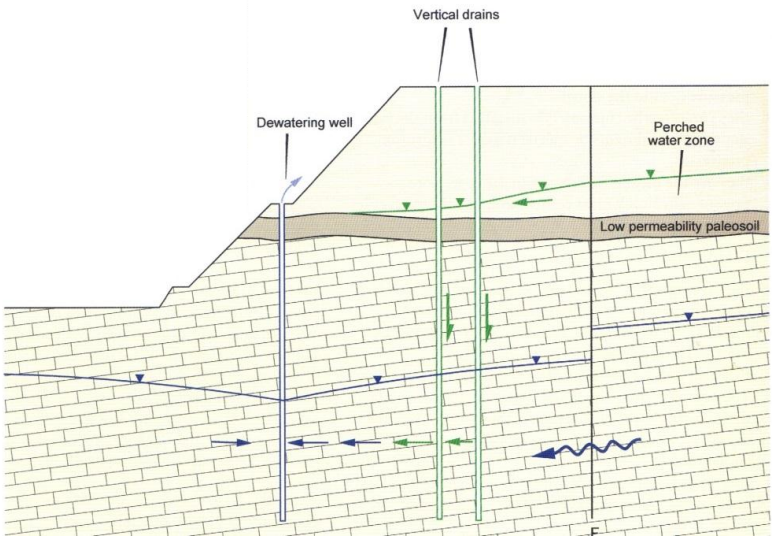

Figure 84. Example of combined use of vertical drains and wells (Read & Stacey, 2009).

The vertical drains can also be used on their own as relief drains, usually related to confined artesian water. In these cases, the head of water can be reduced by intersecting the phreatic surface with vertical drains and allowing the excess pressure to be drained. In such cases, a complementary drainage system may be required to deal with any water that might infiltrate the superficials.

When designing a drainage system that resorts to pumping equipment, careful consideration should be given in its selection. As a general rule of thumb, it is advisable to use a well larger than those needed to accommodate the pump(s), as surface water is likely to transport fines which should be allowed to settle in the bottom of the well. This also means that the pump should be suspended above the bottom of the drain to allow for some build-up of sediments (Figure 85). The choice of the pumping capacity is also a key factor in this type of solutions, since a greater capacity is needed to initially dewater a slope than is required to maintain the water level in its finally lowered position.

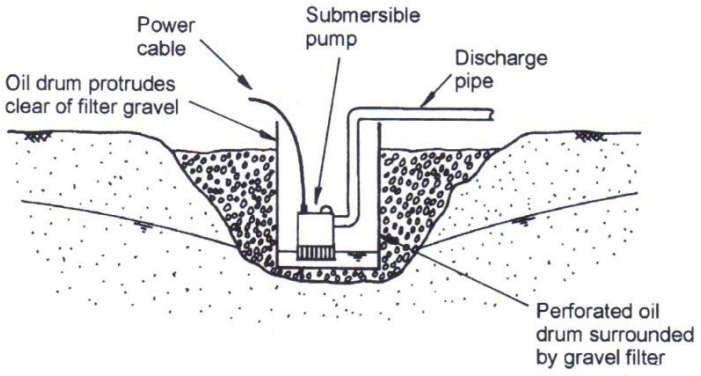

Figure 85. Typical form of well construction (Cashman & Preene, 2001).

6.5 Resistant structural elements

Alternatively, or in addition, to the methods discussed above, the resisting forces acting against failure in a slope can be improved by installing structural elements within it. These can either be unsheared elements which will intersect the critical slip surface, e.g. piles or sheet piles, or elements that increase the normal force applied to the slip plane, such as bolts and ground anchors, or a combination of both.

6.5.1 (Micro)piles and sheet piles

Pile walls consist of alignments of piles, arranged at suitable intervals to form a continuous structure which crosses the sliding mass and is embedded in stable ground. Their offset, length and detailing should be the result of a detailed analysis and will vary from case to

case. They are often installed with a capping beam at their top, which connects all elements and ensures these are mobilised as one. Their diameter typically varies from 0.6m to 2.0m.

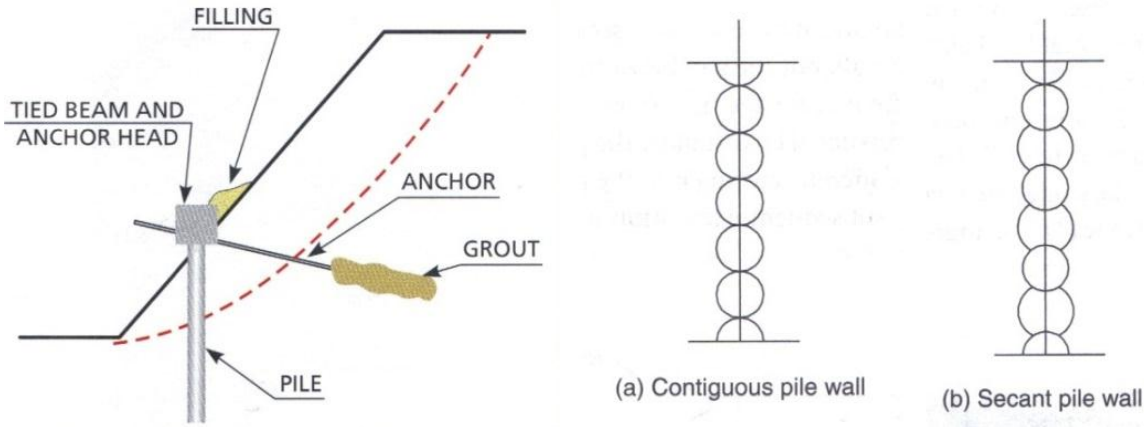

Figure 86. Example of a pile wall, adapted from Vallejo, Ferrer et al. (2004) and Das (2011).

The inappropriate use of rigid piles can however fail to fully address the stability problem of a slope. As shown in Figure 87, the nature of the pile-soil interaction and a comprehensive analysis of existing ground conditions on a slope, particularly when there is the potential for a planar failure, must be taken into account during the design of any remedial measures.

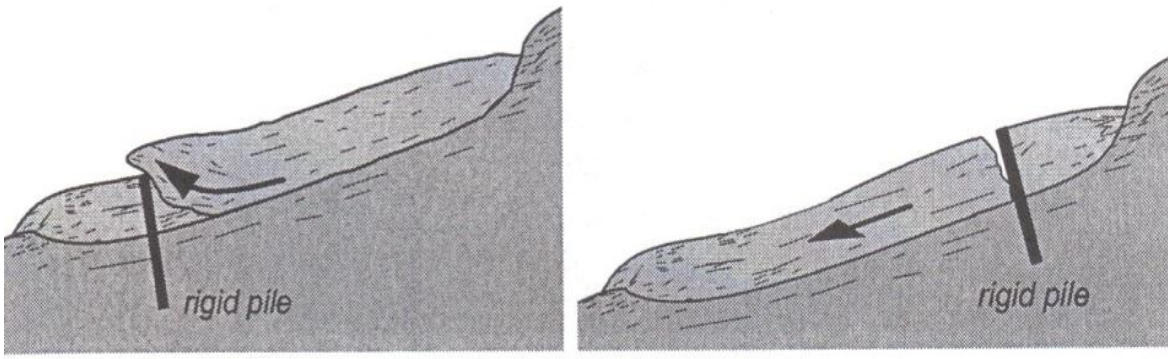

Figure 87. Potential problems related to the use of rigid piles for slope stability (Azizi, 2007).

A similar reinforcement can be achieved by the use of micropiles (Figure 88). This technique is especially advantageous when rock needs to be penetrated, due the smaller diameters used, typically ranging from 100mm to 200mm. The drawback of these elements, when compared to concrete piles, is their flexibility which may require additional works or stabilising measures to be undertaken.

Figure 88. Anchored micropile wall (Vallejo, Ferrer et al., 2004).

Given their size and the size of plant required to install them, micropiles can also be placed normal to the slip surface or slope's face. Similarly to any other reinforcement technique, their length needs to be assessed to ensure that not only the existing slip surface has its FoS increased but also that no other deep slip surface beneath them can occur, as shown in Figure 89.

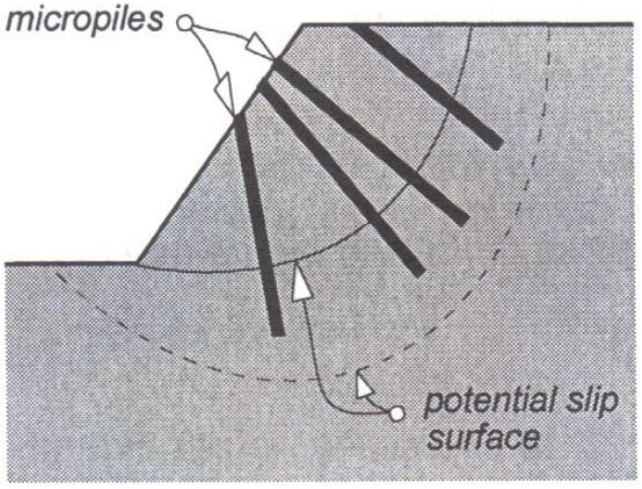

Figure 89. Potential problems related to the use of micropiles in conjunction with circular slip surfaces (Azizi, 2007).

Another common structural reinforcement in slopes is the use of sheet piles. These elements are suited for most ground conditions, apart from rock or boulderly soils, and can be quickly installed in their proposed location without the use of heavy plant. However, care should be taken about their length, as driving long piles can be a very difficult task.

The section of the sheet piles to be used will depend on the requirements of flexural and/or shear strength and the strength to resist the driving stresses. Where obstructions seriously impede progress, pre-boring may be needed. When hard driving through obstructions occurs there is a risk of torn clutches, which may lead to inadequate groundwater cut-off and severe reduction in pile strength.

Sheet piles (Figure 90) can then be used with a dual purpose, acting not only as a structural reinforcement, but also as a drainage curtain. Where soil and groundwater conditions impose high loads on these elements it may be necessary to supplement them with additional horizontal support.

Figure 90. Example of a sheet pile wall reinforced with soil nails (Nadgouda, 2006).

6.5.2 Anchors and soil nails

Soil nailing or anchoring consists of strengthening the existing ground by introducing steel reinforcements into the exposed face. These are usually installed in a top-downwards operation.

Anchors are steel cables or bars (Figure 91), anchored in stable areas of the soil mass, that work by traction and exert a normal force on slope's face. This is aimed at incrementing the normal stress on any failure surface.

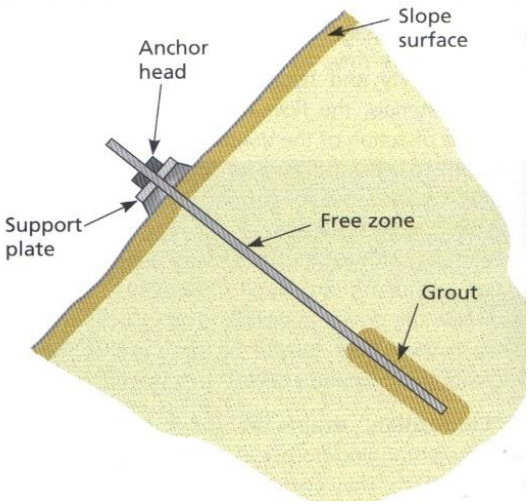

Figure 91. Diagram of anchor parts (Vallejo, Ferrer et al., 2004).

Depending on their function, they are classified as passive (the anchor is actioned when movement takes place), active (the anchor is stressed after installation until the allowable load is reached) or mixed (the anchor is stresses with a load less than its allowable load). They are frequently used in jointed rock slopes as a very effective measure of stabilising sliding masses or blocks.

The anchor heads are often joined to each other at the surface by means of capping beams so that they work together, distributing the stabilising forces more evenly throughout the slope (Figure 92).

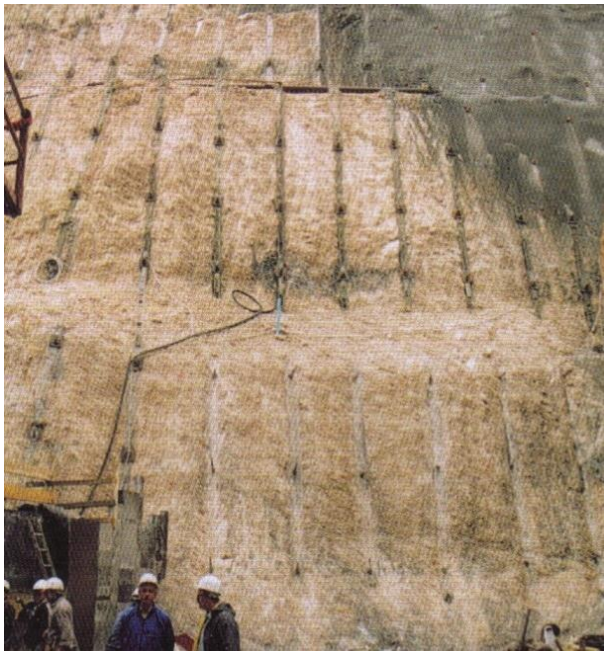

Figure 92. Excavation of a large slope stabilized with tied anchors (Vallejo, Ferrer et al., 2004).

Soil nails consist of high yield steel threadbars, with nominal diameters ranging from 15mm to 63.5mm and which, as opposed to ground anchors, are only typically passively loaded. Naturally, their length is dependent on the slope geometry and ground conditions. The latter also influences the way these elements are installed, which typically consist of one of the following methodologies, as illustrated in Figure 93:

- An open hole can be drilled first, to the required depth, then followed by the insertion of the threadbar and grouting of the hole. Applicable in cohesive soils and unweathered rocks;
- A self-drilling hollow core bar with a continuous rolled thread is typically used in conjunction with non-cohesive soils and highly weathered rocks. As the drilling advances, grout is applied through grouting ports. A percussion or high-energy firing device can also be used to install these type of elements if only a shorter length is required.

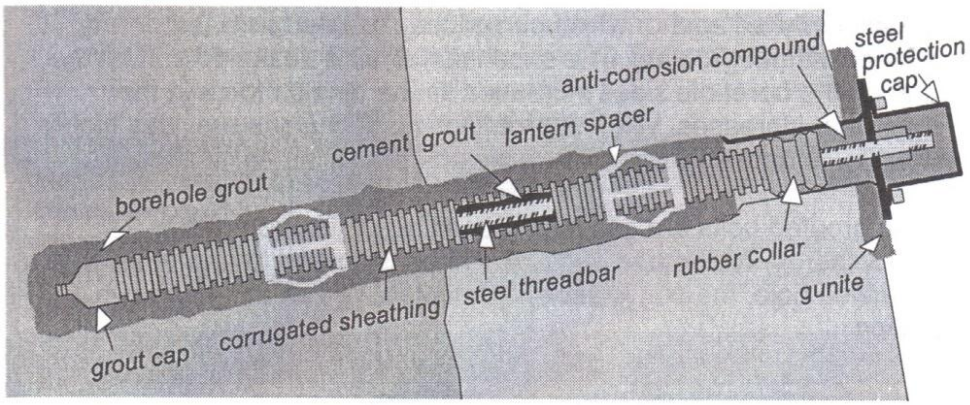

Permanent soil nail with corrosion protection

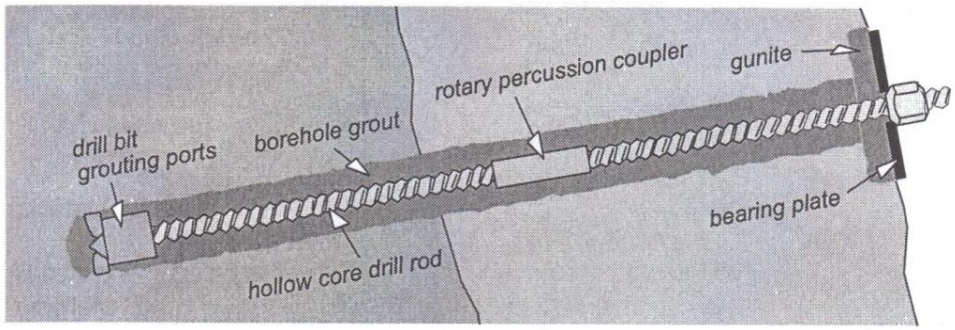

Self-drilling hollow core nail

Figure 93. Permanent soil nail with corrosion protection and self-drilling hollow core nail (Azizi, 2007).

Once the grout has set, the threadbars can then be tensioned and secured through the use of hexagonal nuts and bearing plates. In some circumstances, permanent nails with double corrosion protection, consisting of cement grout and corrugated sheathing, complete with an anti-corrosion compound around the steel protection cap.

Complementary to both these options, the surface of the slope can also be treated with shotcrete or fibrecrete. A shotcrete lining provides support and can lock key blocks into place, while protecting the slope from weathering. It is usually applied continuously and reinforced with a wire mesh. Alternatively, the reinforcement may come from discontinuous discrete fibres (steel or synthetic), which are incorporated in the shotcrete to improve its crack resistance, ductility, energy absorption and impact resistance characteristics, thus designed fibrecrete (Read & Stacey, 2009).

There are a few mechanisms of failure (Figure 94) of these surface treatments which should be addresses during the design stage, such as the loss of adhesion between the shotcrete and the slope surface or structural failure (flexural, shear, punching). Typically, if adhesion is lost the shotcrete tends to fail in flexure.

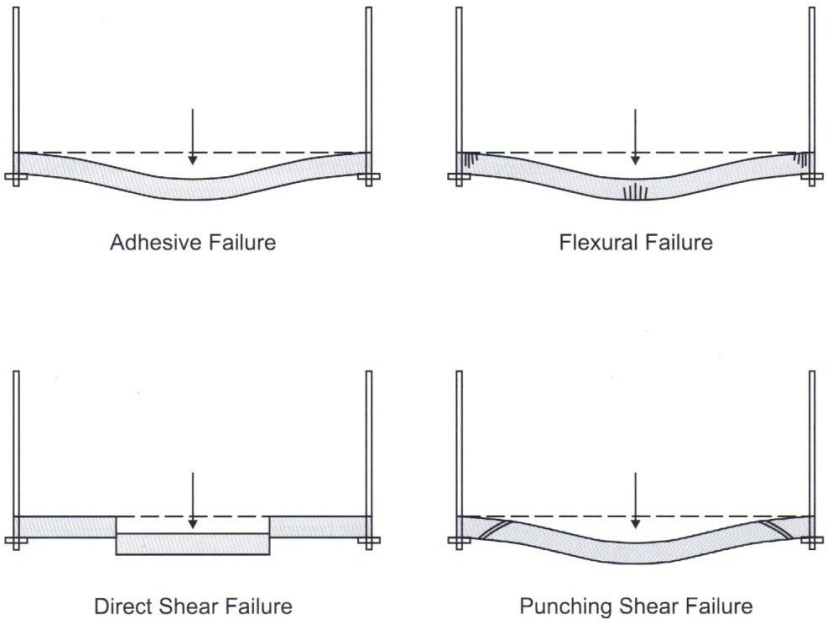

Figure 94. Possible failure modes for shotcrete (Read & Stacey, 2009).

Alternatively, the area between soil nails can be reinforced with geosynthetic mattresses, in order to prevent surface erosion and promote vegetation growth. The latter will, in the long term, act as a shield to the slope as briefly described in Section 2.1.2.3.

6.5.3 Walls and retaining elements

Walls are generally built at the toe of a slope to reinforce it and to prevent deterioration in this area, which is critical to prevent undermining. These elements are usually constructed either by excavating the toe of the slope by segments, so as not to cause (further) instability, or built in front of the slope. The latter requires the wedge between the new wall and the existing slope to be backfilled.

There are different types of walls which can be used in slope stabilisation, depending on whether a more flexible or more rigid system is required. Gabion walls are a traditional and effective way of quickly assembling a gravity retaining wall. They comprise rock fragments, or riprap, enclosed in a steel mesh, can assume different geometries and may be stepped towards or away from the slope (Figure 95). Given its constituents, the gabions offer a perfect drainage medium for any water flowing from the slope at its toe whilst preventing any toe erosion form occurring.

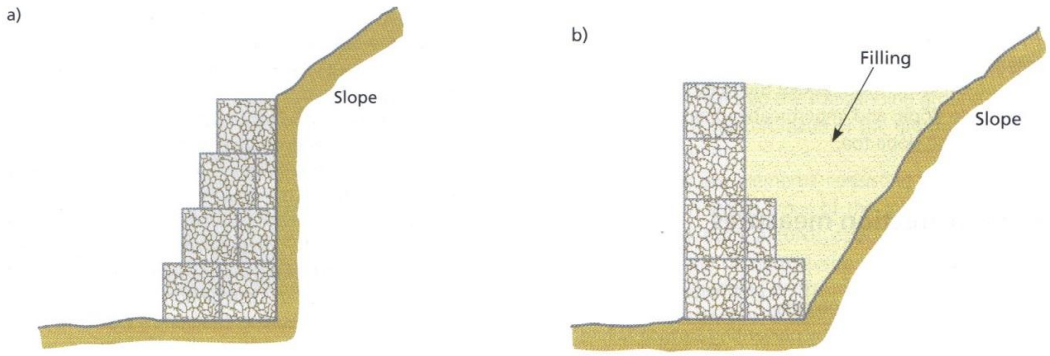

Figure 95. Gabion walls with a stepped external face (a) or internal face (b) with filling between the wall and the slope (Vallejo, Ferrer et al., 2004).

As a simpler and cheaper alternative to gabions, especially when an emergency response is required, concrete modular walls or even stacked tyres (to heights of 1m to 2m, Figure 96) can be used.

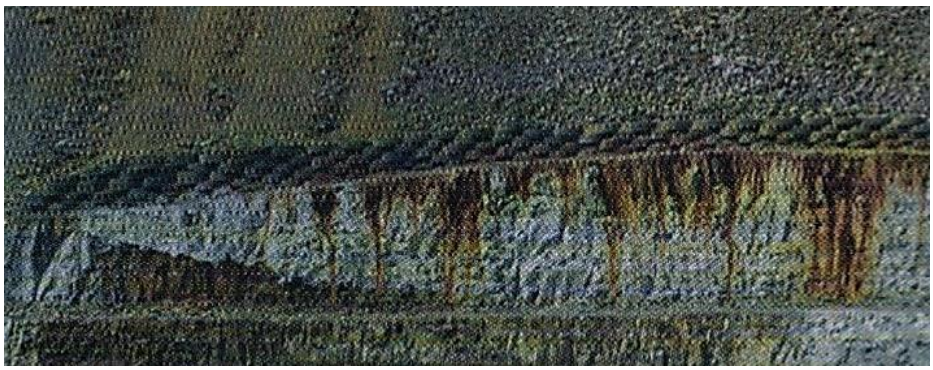

Figure 96. Stacked tyre retaining wall (Read & Stacey, 2009).

The use of reinforced earth retaining walls, although quite common in earthworks design, is discounted for remedial measures given their usual construction time.

If a more rigid retaining structure is required, a reinforced concrete cantilevered retaining wall is often the most cost-effective option. These are usually shaped as an L or an inverted T, using less material than a traditional gravity wall and, if necessary, can be reinforced by buttresses (Figure 97). As an alternative, tied-back walls may be used, comprising a concrete wall reinforced with anchors or bolts and that can be constructed progressively.

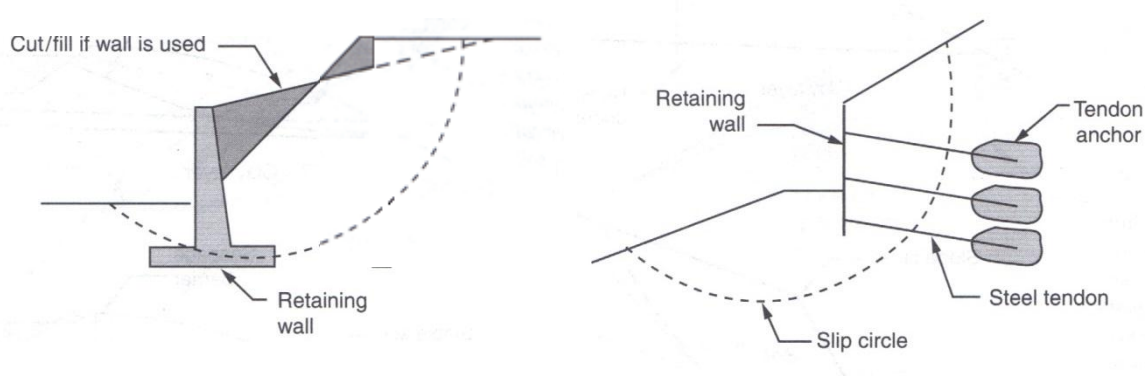

Figure 97. Examples of cantilevered wall and tieback anchor wall (Das, 2011).

When it is necessary to intersect a deeper slip surface, and as alternative to the use of (sheet) pile walls, diaphragm walls may be used (Figure 98). The latter are usually an alternative for when steel sheet-piles becomes either uneconomical or impractical, being able to reach depths in excess of 50m.

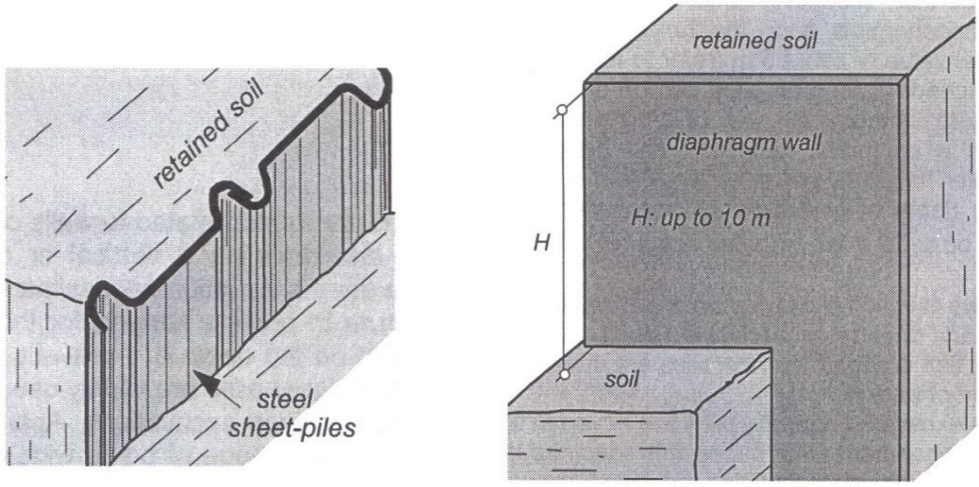

Figure 98. Examples of sheet-pile wall and diaphragm wall (Azizi, 2007).

Independently of the choice of retaining element, it is critical to address the effects of drainage on its performance.

6.6 LEM and FEM analysis of remedial measures

As demonstrated by the numerical modelling undertaken in Chapter 5, there is a significant dependency between MoS and slope gradient or groundwater level. As such, the merits of pursuing either one of these options can be derived from the results obtained earlier.

However, in order to also quantify the benefits of installing structural elements in the slope, further analyses are required. To achieve this, six distinct ground models have been selected (Table 16) in order to provide a better insight on the most appropriate remedial measure for each set of conditions.

Table 16. Sets of conditions to analyse the benefits of the different remedial measures.

Ground model		1	2	3	4	5	6
Parameters		Range of values					
Geometry	Angle	1(V):1(H)	1(V):1.5(H)	1(V):1.5(H)	1(V):2(H)	1(V):2(H)	1(V):2(H)
	Height	8.0m	5.0m	5.0m	5.0m	8.0m	8.0m
Characteristic effective angle of shearing resistance		35°					
Characteristic effective cohesion		10kPa	5kPa	10kPa	0kPa	0kPa	10kPa
Groundwater		Low groundwater level	Low groundwater level	High groundwater level	Dry	Dry	High groundwater level
Surcharge		0kPa, 5kPa and 10kPa					

For each of the models presented above the installation of the following structural elements has been analysed on both LEM and FEM approaches:

- Sheet piles (Figure 99);
- Soil nails (Figure 100);
- Gabion wall (Figure 101).

From the options above it should be noted that the use of sheet piles is essentially deemed as an academic exercise for granitic residual soils. Nevertheless, this option has been considered with the intended of broadening the range of application of these results. Furthermore, its

modelling, with the exception of the flexural rigidity in the FEM analyses, is equivalent to the use of vertical micropiles.

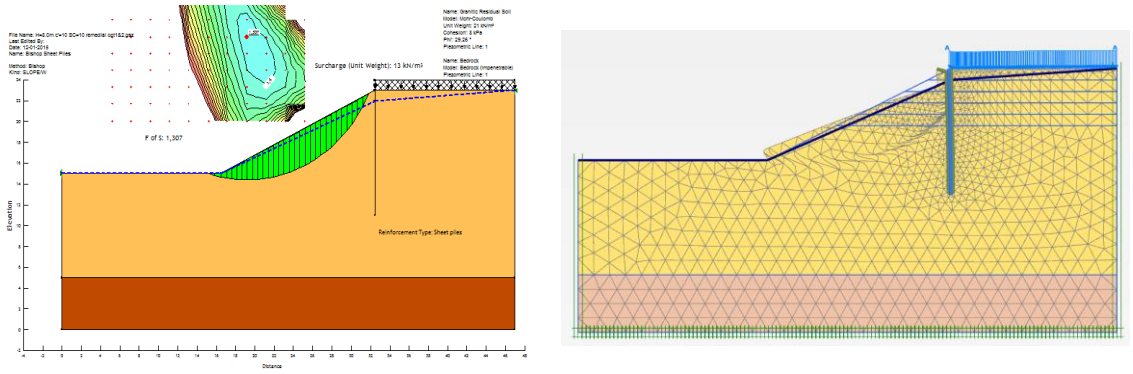

Figure 99 Example of sheet pile wall modelling in LEM and FEM and the associated failure mechanisms

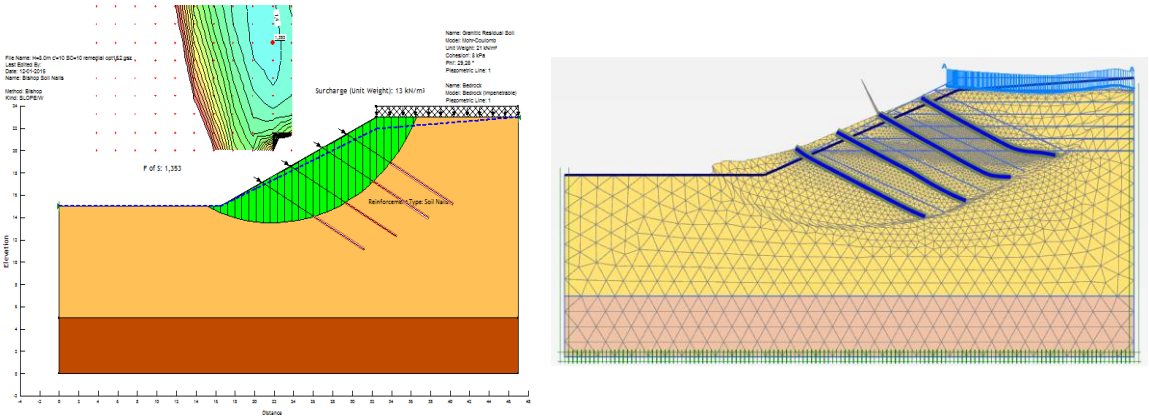

Figure 100 Example of soil nails modelling in LEM and FEM and the associated failure mechanisms

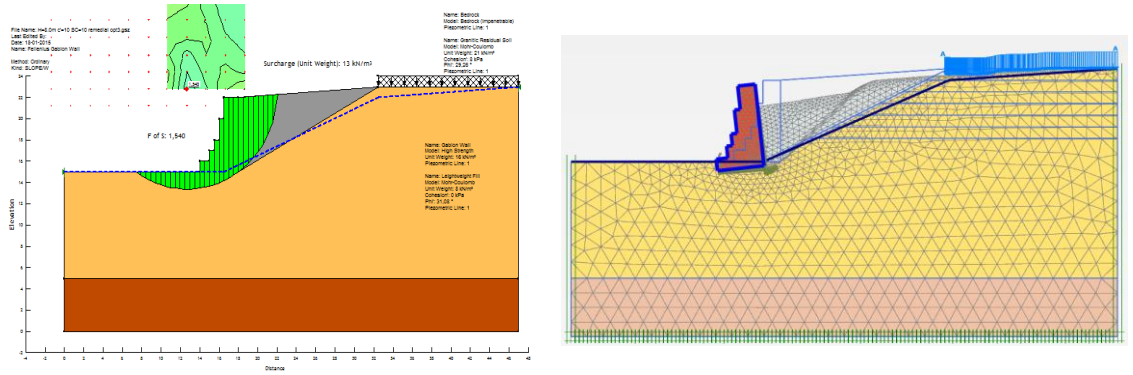

Figure 101 Example of gabion wall modelling in LEM and FEM and the associated failure mechanisms.

It should be noted that the procedure to assess the MoS within the FEM software (PLAXIS 2D) requires the outcome of that routine to be inspected in order to verify that a realistic failure mechanism occurred. This check has revealed the software to not deal adequately with purely granular slopes.

For the purpose of the calculations the following assumptions have been made:

- Sheet piles with a PU18-1 cross section and a S355GP steel grade, installed at the crest of the slope and extending to 3.0m beyond its toe (although from a constructability point of view, the drivability of the sheet piles in granitic residual soils may be an issue);
- 12m long and 25mm diameter soil nails have been considered in the models, installed in 100mm diameter grouted holes, and with a 1.5m horizontal spacing. 3 and 4 rows have been considered for the 5.0m and 8.0m high slopes, respectively;
- The geometry of the gabion baskets has been obtained from the Maccaferri Gabions Design Manual (Maccaferri Ltd., 1995), considering a ratio of H/B≥2. A unit weight of 16kN/m³ has been deemed appropriate for the wall. As for the backfill between the gabion wall and the existing slope, a lightweight aggregate has been assumed with a characteristic unit weight of 8kN/m³ and a φ'_k of 37°.

For the ground models listed above, the merits of reducing groundwater level and slacking an existing slope have only been derived from the LEM results. With regards to water pressures, this has been carried out by comparing the MoS of identical scenarios but with lower water tables, i.e. low vs. high water table and dry slope vs. a low water table. As for the change in geometry the comparison was been made using the closest slacker gradient.

6.6.1 Comparative analysis of remedial solutions

To help in the assessment of the most suited remedial option for each of the scenarios listed above, the gains in MoS for both LEM and FEM approaches are summarised in Table 17 below.

Table 17. Gain in MoS (percentage) of the different remedial measures.

Remedial Option	Effective cohesion = 0kPa	Effective cohesion = 5kPa	Effective cohesion = 10kPa
Sheet piles	Minor	5 - 10% (LEM) <5% (FEM)	10 - 20% (LEM) 5 - 10% (FEM)
Soil Nails	5 - 20% (LEM)	20 - 30% (LEM) 25% (FEM)	5 - 30% (LEM) 40 - 45% (FME)
Gabion Wall	30 - >50% (LEM) 15 - 35% (FEM)	30% (LEM) 20% (FEM)	25 - >40% (LEM) 25 - 40% (FEM)
Reducing groundwater level [(1)]	Not assessed	Not assessed	20 - >30% (LEM)
Slacking slope	Not assessed	15% (LEM)	15 - 25% (LEM)

[(1)] Only valid when reducing ground water level from high to low. Differences in MoS between a low water table and a fully dry slope are insignificant, as detailed in Section 5.3.2.

By analysing the outcome of the different analyses the following points have been inferred. Driving sheet piles from the crest of the slope does not appear to result in a significant improvement in the MoS. However, having these elements in place forces the critical slip plane to be shallower and purely along the slope's face. As such, and although the overall safety is not increased substantially, if the priority was to just ensure the safety of the crest of the slope, and accepting that a failure may occur below it, there would be great benefit in this option. FEM modelling also reveals that the overall maximum displacements along the face of the slope are not greatly reduced by adopting this remedial option.

The use of soil nails along the slope appears to be a more effective mean of enhancing its stability, particularly in cohesive soils, than the use of a sheet pile wall. However, the effectiveness of this remedial option is strongly dependent on their length and spacing (both vertical and horizontal).

In terms of displacements this option has proven to reduce the anticipated maximum total displacements along the slope's face between circa 30% and 50%. The FEM approach in these cases has provided a noticeable higher MoS than the LEM approach. This is likely explained by the abrupt change in the failure mechanism, with the resultant critical slip surface being significantly deeper in the PLAXIS 2D models than within the SLOPE/W runs.

The option to construct a retaining wall, for the purpose of this study only a gabion wall has been considered, has proven to have a similar effect across all options and to result in the greatest increases in terms of MoS. In fact, the failure mechanism after the wall is in place appears to be very much dependent on the properties of the backfill rather than the existing slope's materials.

Further analyses have confirmed that, apart from when lightweight aggregate is used as a backfill to the new wall, the merits of this option are left in between the use of sheet piles and soil nails. However, it should be noted that the above has not taken into account the bearing capacity assessment of the gabion wall foundation.

The benefits of changes in groundwater levels and slope angles have only been assessed through the use of LEM analyses on the 6 ground models presented above. Changes in the water table are only particular relevant for high water levels and can equate to gains of 20% to 30% in the MoS. As for the slope angle, slacking the slope can result in increases of 15% to 25% in the overall stability of the slope.

7. Conclusions

The majority of slope stability analyses performed in practice still use traditional limit equilibrium (LEM) approaches involving methods of slices that have remained essentially unchanged for decades. However, one important limitation of the conventional LEM method is that it requires an arbitrary selection of the search areas and shape of the potential failure surfaces prior to analysis. Accordingly, critical areas of the slope or critical shaped failure surfaces may be overlooked if the search areas and failure surface shapes are not well selected.

Nevertheless, the user-friendliness, simplicity and proven good record of LEM methods are enough to still make them a valuable tool against the use of formulations based on finite element (FEM) principles. The latter however, can help predict stress concentration problems and forecast deformations/displacements within the slope, which have been experienced problematic in LEM analysis and are often crucial in evaluating the performance and acceptability of some slopes which are sensitive to movement. As such, there is a tendency of nowadays resorting to FEM methods as a verification/validation of traditional LEM methods.

Also, LEM methods are especially useful when assessing the stability of a slope with a MoS below unity. On such cases, when remedial/strengthening measures are to be installed, it is then possible to quantify their merits in the overall stability of the slope using this approach. FEM methods, on the other hand, can rarely be used to compute a stability problem with a MoS significantly below unity.

Consequently, it is quite common to undertake LEM back analyses when prescribing remedial measures whilst assessing the factors leading to the instability. These analyses usually try to establish the 'real' strength parameters of the soil (φ' and c') when little information is available and usually by considering the soil as a homogenous material for simplicity.

The scope of this study has been to compare various stability assessment methods and conduct a parametric sensitivity analysis of the more relevant geotechnical inputs to slope stability problems in the residual granitic soils of the Covilhã region. This has incorporated variations in the applied surcharges and in groundwater levels, both deemed to be the most likely triggers of failure. The Fellenius's and simplified Janbu's and Bishops's methods have been used in the LEM approach to the problem whilst the Hardening Soil Model has been adopted in the FEM formulation. The following conclusions have been based on the undertaken 2D slope stability analyses.

1. Increments in the applied surcharge at the crest have been assessed as detrimental to slope stability, reducing the MoS in LEM approaches by up to 25%, but generally in the

order of 5% to 10% in non-cohesive materials and in soils with a c' of 5kPa, for surcharges of 5kPa and 10kPa respectively. The effects appear to be slightly more critical when considering a c' of 10kPa, which results in reductions between 10% and 15%, for surcharges of 5kPa and 10kPa respectively;

2. Point 1 has been concluded regardless of the groundwater table profile (reductions in MoS of the same magnitude) and adopted LEM method;
3. Using the FEM approach and looking at purely granular soils in the first instance, the reductions in MoS have been assessed between circa 20% and 30%, respectively for surcharges of 5kPa and 10kPa. When an effective cohesion is considered, surcharge variations appear less critical, with reductions generally under 5% (significantly lower than in the LEM analyses). Results also show that, albeit both approaches reveal the MoS to be more sensitive to groundwater level than to the applied surcharge at the crest, the latter appears to have a more critical effect on LEM analyses;
4. The variation in MoS from rises in groundwater levels has generally been established as more detrimental to slope stability than the increase in surcharge loads, with reductions up to 50% and strongly linked to the slope angle. This has been corroborated in both LEM and FEM approaches;
5. The exceptions to Point 4 occur when comparing LEM and FEM models when groundwater table in absent and when it has been defined as low. This is noticeable on slacker slopes (with 1(V):2(H) and 1(V):1.5(H) gradients) and whilst considering a given c' value in the soils. Variations of the same magnitude have been registered in both approaches with maximum values of circa 15%;
6. The Bishop's and Janbu's methods appear to be more severe when groundwater levels rises in steeper slopes, particular in a 2(V):1(H) gradient, whereas the Fellenius' method returns greater reductions in the MoS in slacker slopes;
7. LEM analyses suggest the reductions in MoS due to rises in groundwater levels appear to be inversely proportional to the cohesion of the intersected materials, i.e., the greater the c' of the soil the lesser the consequences of groundwater rises;
8. In non-cohesive materials, MoS from all three LEM methods seem to converge for slacker slopes and for greater heights, with maximum differences of 10%. However, for steeper slopes (with 1(V):1(H) and 2(V):1(H) gradients) the Fellenius' method reports a significantly higher MoS than the Bishop's method (up to circa 70%) for high groundwater levels;
9. In soils with effective cohesion, the Janbu's method appears to offer a better correlation with the Bishop's method although diverging from it for a high groundwater table and steeper slopes (1(V):1(H) and 2(V):1(H)). On these circumstances, the Fellenius' method reveals significantly higher MoS than the Bishop's method;

10. When groundwater is absent or at a low level, the Janbu's method appears to be generally less critical than the Bishop's method, which becomes more noticeable as the effective cohesion of the soil is increased;
11. The comparison between FEM and LEM methods has revealed there is a significant divergence in the obtained MoS for purely granular materials, with all LEM methods overestimating the slope's MoS by up to circa 40%. In cohesive materials these differences are predominantly kept between 5% and 10%;
12. The majority of MoS obtained with the Janbu's simplified method present the best correlation with the FEM results (for cohesive soils). Differences are predominantly registered below 5% and the greater the applied surcharge and the slacker the slope the better is the correlation between this LEM method and the FEM results.

It should be noted that the conclusions listed above are based exclusively on circular slip surface analyses for the LEM methods. Composite slip surface analyses have been occasionally undertaken in SLOPE/W using the Janbu's simplified method but have reported higher FoS and, as such, have been discarded from the analyses.

The stability charts provided within this thesis are only to be perceived as indicative and shall only be used as a preliminary tool to help corroborate site observations. A detailed design will necessarily require further analysis to be undertaken. However, attention is drawn to the findings of Chowdhury & Xu (1995) which demonstrate how the use of LEM methods requires engineering judgement to ensure all critical slip surfaces are detected.

Further to the parametric study of soil parameters and groundwater and surcharge conditions, this thesis has also attempted to capture the suitability and effectiveness of some of the discussed slope remedial options. As such, the following observations may help to contribute to a better insight on the most appropriate remedial measure for each set of conditions, and have been based on both FEM and LEM approaches to the problem:

13. The use of soil nails along the slope, and according to the FEM approach, appears to be the most effective way of enhancing its MoS, especially when in cohesive materials, registering gains of up to 45%. However, using LEM models these gains fall to circa 30% and 10%, respectively for 5.0m and 8.0m high slopes, and which renders this option not as interesting as some of the alternatives for higher slopes;
14. Opting for a retaining wall at the base of the slope has also showed significant improvements in the stability of the slope (gains up to 40%), and with the advantage of offering a somehow similar gain for both cohesive and non-cohesive slopes. Nevertheless, it should be noted that the gain is intrinsically linked to the properties of the backfill material to be used;

15. When dealing with high groundwater levels, reducing the water pressures within the slope has proven to increase its safety by around 30%, whereas slacking its geometry can enhance stability by up to 25%;
16. Finally, sheet piles appear to be the reinforcement option which contributes the least to the stability of the slope with gains of less than 20%. Contrary to the modelling of the soil nails, the FEM approach reveals smaller gains in safety for this option, reporting marginal increases of between 5% and 10%.

The remedial options discussed and analysed are to be perceived as concept ideas as their gains in terms of MoS will vary on a case to case basis. Furthermore, the feasible geometry and existing restraints at a site often leads the designer to opt between a limited number of feasible choices. Also, the list above has no consideration on the ease of installation/set up of any of the options and has excluded the possibility of combining the effects of more than one remedial option.

Finally, in certain situations it is not the stability of the slope itself which may be the priority but rather the safety of any infrastructure or civil works located within it or near it, which may require a different approach to the problem.

7.1 Further research and recommended works

All stability calculations have been based on the principles of saturated soils. However, this approach is only exact for slopes where the majority of the critical slip surface falls within the saturated zone. However, for situations where a failure occurs above the groundwater table, thus within the partially saturated zone, slope stability would have been better evaluated using an assumption of unsaturated soil, which could have been more cost effective, although requiring an advanced understanding of matric suction contribution to slope stability.

As such, the analysis undertaken within this thesis could benefit from a way of quantifying the matric suction within the specific granitic residual soils of the Covilhã region, as briefly discussed in Section 4.2.3, and the establishment of a way of incorporating such beneficial effect in the Mohr-Coulomb failure criterion.

Furthermore, the results presented in this thesis can be extended and/or developed by the following:

1. The different groundwater levels considered in the analyses have proven not to be the best suited to assess the repercussion of groundwater rise in slope stability as the results obtained for a low groundwater level are identical to the ones reported in a

fully dry slope. Therefore, consideration of an intermediate groundwater table, between what has been defined as a low and a high levels may provide an enhanced insight of the sensitivity of slope stability to changes in this variable;

2. The pre-established range of surcharges applied on top of the slope has proven to be significantly less detrimental to slope stability than the rises in groundwater. As such, consideration should be given to a more broader range of surcharges (15kPa and 20kPa) and their influence in the obtained MoS;
3. The narrow range of φ' values used in this thesis has been derived from the laboratorial test results undertaken in samples from granitic residual soil of the Covilhã region. However, in order to enlarge the spectrum of application of these results, a broader interval of φ' values should be analysed. Also, as the range of parameters is expanded, the pool of possible FEM ground models should also be increased to help corroborate or prove wrong the points raised between LEM and FEM approaches;
4. The validation of the conclusions reached within this thesis with examples/case studies where monitoring has been undertaken, even if retro analysed, would increase the degree in confidence in the values obtained and help assess which of the LEM methods is better suited for stability analyses in granitic residual soils;
5. The study of the benefits of different remedial measures than those analysed in this study would also be beneficial, so as to better inform on the best practices for each possible scenario;
6. Additionally, it would be advantageous to try to quantify the beneficial effects of combining different remedial measures to allow some guidance to designers on which is the most effective approach for each given set of conditions;
7. Lastly, a direct comparison between the obtained MoS following EC7 and the correspondent lump FoS would offer a better understanding between these two distinct approaches and their consequences in terms of design.

8. Bibliography

ASTM D2487 - 11. (2011). *Standard Practice for Classification of Soils for Engineering Purposes (Unified Soil Classification System)*. USA: ASTM Internationa.

Aung, A. M., & Leong, E. C. (2011). Stiffness profiles of residual soil sites using continuous surface wave method. Pattaya, Thailand: Kasetsart University.

Azizi, F. (2007). *Engineering Design in Geotechnics*. Plymouth, UK: University of Plymouth.

Barnes, G. (2010). *Soil mechanics: principle and practice* (3rd ed.). Basingtoke, UK: Palgrave Macmillan.

Begonha, A. (2001). Meteorização do granito e deterioração da pedra em monumentos . *Colecção Monografias*. Porto: FEUP.

Bobrowsky, P., & Highland, L. (2008). *The Landslide Handbook - A Guide to Understanding Landslides*. Reston, Virginia: U.S. Geological Survey.

Bond, A., & Harris, A. (2008). *Decoding Eurocode 7*. New York, USA: Taylor & Francis.

Brinkgreve, R. (2002). *PLAXIS Finite Element Code for Soil and Rock Analyses, 2D-Version*. Rotterdam: Balkema.

BS 5930:1999+A1:2007. (2007). Code of practice for site investigations. UK: BSI.

BS 6031:2009. (2009). Code of practice for earthworks. UK: BSI.

BS EN 12063:1999. (1999). Execution of special geotechnical work. Sheet pile walls. UK: BSI.

BS EN 14199:2015. (2015). Execution of special geotechnical works. Micropiles. UK: BSI.

BS EN 14475:2006. (2006). Execution of special geotechnical works. Reinforced fill. UK: BSI.

BS EN 14490:2010. (2010). Execution of special geotechnical works. Soil nailing. UK: BSI.

BS EN 1536:2010+A1:2015. (2010). Execution of special geotechnical work. Bored piles. UK: BSI.

BS EN 1537:2013. (2013). Execution of special geotechnical works. Ground anchors. UK: BSI.

BS EN 1538:2010+A1:2015. (2010). Execution of special geotechnical works. Diaphragm walls. UK: BSI.

Cartier, G. (1986). La stabilisation des pentes instables par clouage. *Bulletin de Liaison des Laboratoires des Ponts et Chaussées, 141*.

Cashman, P., & Preene, M. (2001). *Groundwater Lowering in Construction - A Practical Guide*. New York, USA: Spon Press.

Cavaleiro, V. M. (2001). *Condicionantes geotécnicas à expansão do núcleo urbano da cidade da Covilhã - PhD Thesis*. Covilhã, Portugal: Universidade da Beira Interior.

Celestino, T. B., & Duncan, J. M. (1981). Simplified Search for Non-Circular Slip Surfaces. *Tenth International Conference on Soil Mechanics and Foundation Engineering*, pp. pp. 391-394.

Chowdhury, R. N., & Xu, D. W. (1995). Geotechnical system. *Reliability Engineering and System*, pp. 141-151.

Clayton, C. R., Mathews, M. C., & Simons, N. E. (1995). *Site Investigation* (Second Edition ed.). Cambridge: Wiley-Blackwell.

Construction Marine Ltd. (2012). *Clay Cross Cutting Stabilisation*. (CML) Retrieved 10 05, 2014, from Specialist Civil Engineering Contractor Construction Marine Ltd. (CML) Website: http://www.cml-civil-engineering.co.uk/clay-cross.html

Cruden, D. M., & Varnes, D. J. (1996). *Landslide types and processes. In: Turner A.K.; Shuster R.L. (eds) Landslides: Investigation and Mitigation.* US National Research Council, Transportation Research Board. Washington: National Academy Press.

Das, B. (2011). *Geotechnical Engineering Handbook*. USA: J. Ross Publishing, Inc.

Dawson, R. F., Morgenstern, N. R., & Stokes, A. W. (1998). Liquefaction flowslides in Rocky Mountain coal mine waste dumps. *Canadian Geotechnical Journal, 35*, pp. 328-343.

Duncan, J. M. (1996). State of the Art: Limit Equilibrium and Finite-Element Analysis of Slopes. *Journal of Geotechnical Engineering*(No 7), pp. 577-596.

Europa Turismo. (n.d.). *Geographic Guide*. (Europa Turismo) Retrieved 03 10, 2015, from http://mapa.europa-turismo.net/fotos/mapa-portugal.gif

Farshidfar, N., & Nayeri, A. (2015). Slope Stability Analysis by Shear Strength Reduction Method. *Journal of Civil Engineering and Urbanism, 5*, 35-37.

Fellenius, W. (1936). *Calculation of the stability of earth dams* (Vol. 4). Proceedings of the Second Congress on Large Dams.

Fernandes, M. M. (2011). *Mecânica dos Solos - Conceitos e Princípios Fundamentais* (2th Edition ed.). Porto: FEUP.

FHWA-NHI-10-024. (2009). Geotechnical Engineering Circular No.11. *Design and Construction of Mechanically Stabilized Earth Walls and Reinforced Soil Slopes, I*. USA: U. S. Department of Transportation - Federal Highway Administration.

FHWA-SA-97-075. (1997). Geotechnical Engineering Circular No.3. *Earthquake Engineering for Highways, Design Principles, I & II*. USA: U. S. Department of Transportation - Federal Highway Administration.

FHWA-SA-97-076. (1997). Geotechnical Engineering Circular No.3. *Earthquake Engineering for Highways, Design Principles, II*. USA: U. S. Department of Transportation - Federal Highway Administration.

Fonseca, A. V. (1996). *Geomecânica dos Solos Residuais do Granito do Porto. Critérios para Dimensionamento de Fundações Directas - Tese de doutoramento*. Porto, Portugal: Faculdade de Engenharia da Universidade do Porto.

Fox, Liam; ABC News. (2012, January 25). *Website for ABC News*. (ABC News) Retrieved September 19, 2012, from http://www.abc.net.au/news/2012-01-24/fears-for-missing-after-landslide-in-png-highlands/3790914

Fredlund, D. G., & Rahardjo, H. (1993). *Soil Mechanics for Unsaturated Soils*. Jonh Wiley & Sons, Inc.

Gerscovich, D. M. (2010). *Resistência ao Cisalhamento - Notes for the class on Soil and Rock Mechanics*. Rio de Janeiro, Brasil: Universidade do Estado do Rio de Janeiro.

Guerra, N. M. (2008). *Análise de estruturas geotécnicas*. Lisboa, Portugal: IST.

Guidicini, G., & Nieble, C. (1984). *Estabilidade de Taludes Naturais e de Escavação*. São Paulo, Brasil: EDGARD BLÜCHER LTDA.

Huat, B. B. (2012). *A Handbook of Tropical Residual Soil Engineering*. London, UK: CRC Press/Balkema.

IAEG. (1979). Rock and Soil Description and Classification for Engineering Geological Mapping. *Bulletin IAEG, 19*, pp. 364-371.

IAEG. (1990). A suggested method for reporting a landslide. *Bulletin IAEG, 41*, pp. 5-12.

Law, K., Shen, J., & Lee, C. (1998). Strength of loose remoulded granite soil. *Slope Engineering in Hong Kong*, pp. 169-176.

LCPC. (2003). Practical anual for the use of soils and rocky materials in embankment construction. Paris, France: LCPC.

Maccaferri Ltd. (1995). *Maccaferri Gabions - Retaining structures*. Bologna, Italy: Maccaferri Ltd.

Matthews, C., Farook, Z., & Helm, P. (2014, May). Slope stability analysis - limit equilibrium or the finite element method? *Ground Engineering*, 22-28.

McRoberts, E. D., & Sladen, J. A. (1985). *Observations on static and earthquake liquefaction methodologies* (Vol. 1). Quebec City, Canada: Canadian Geotechnical Society.

Mencl, V., & Záruba, Q. (1982). *Landslides and Their Control*. Prague: ACADEMIA, Publishing House of the Czechoslovak Academy of Sciences.

Michalowski, R. L. (1995). Slope stability analysis: a kinematical approach. *Géotechnique, 45*, 283-293.

Mikhail, K. (1998, July 17). *Website of the Trans-Siberian Photogallery*. Retrieved September 19, 2012, from Trans-Siberian Web Encyclopedia: http://www.transsib.ru/Gallery/index.php?LNG=EN&CATEG=14BREA

Nadgouda, K. (2006, June 23). *Geotechnical ENgineering 101 and more...* Retrieved 10 03, 2014

Nagy, L., Tábacks, A., Huszák, T., Mahler, A., & Varga, G. (2013). Comparison of permeability testing methods. *Proceedings of the 18th International Conference on Soil Mechanics and Geotechnical Engineering*, pp. 399-402.

Neves, E. (2003). *Mecânica dos Solos - Notes for the class on Soil and Rock Mechanics*. Lisboa: Instituto Superior Técnico.

NF P 11-300:1992. (1992). Classification des matériaux utilisables dans la construction des remblais et des couches de forme d´infrastructures routières. Paris, France: AFNOR.

NF P 94-290. (to be published). Earth structures. Paris, France: AFNOR.

NP EN 1990:2009. (2009). *Eurocódigo - Bases para o projecto de estruturas*. Caparica, Portugal: Instituto Português da Qualidade.

NP EN 1991-1-1:2009. (2009). Eurocódigo 1 - Acções em estruturas; Parte 1-1: Acções gerais; Pesos volúmicos, pesos próprios, sobrecargas em edifícios. Caparica, Portugal: IPQ.

NP EN 1997-1:2010. (2010). *Eurocódigo 7 - Projecto geotécnico Parte 1: Regras gerais*. Caparica, Portugal: Instituto Português da Qualidade.

Pais, L. A. (2007). *Comportamento mecânico do solo residual granítico da Covilhã com efeito de contaminantes - Dissertação para obtenção do grau de doutor em engenharia civil*. Covilhã, Portugal: Universidade da Beira Interior.

Pais, L. A., & Gomes, L. F. (2010). *Mechanical behaviour of unsaturated decomposed granitic residual soil*. Adelaide: CI-Premier Pte Ltd.

Petley, D. (2008, December 11). *The Landslide Blog*. Retrieved September 19, 2012, from http://www.landslideblog.org/2008/12/vaiont-vajont-landslide-of-1963.html

Petley, D. (2010, September 26). *The Landslide Blog*. Retrieved September 19, 2012, from http://www.landslideblog.org/2010/09/images-of-yesterdays-landslide-induced.html

Rahardjo, H., & Fredlund, D. G. (1991). Calculation procedures for slope stability analyses involving negative pore-water pressures. *Slope stability engineering: developments and applications*, pp. 43-49.

Rathje, E., Jibson, R., Kelson, K., Bay, J., & Pack, R. (2004, November 17). *Website for the Field Reconnaissance of the Landslides east of Yamakoshi Village*. (GEER Beyond Reconnaissance Team) Retrieved September 17, 2012, from http://www.geerassociation.org/GEER_Post%20EQ%20Reports/Niigata-ken_2004/17%20Nov%202004%20Yamakoshi%20Landslides%20East.htm

Read, J., & Stacey, P. (2009). *Guidelines for Open Pit Slope Design*. Leiden, The Netherlands: CRC Press.

Rogers, J.; Missouri S&T. (2008). *Website for the Missouri University of Science and Technology Courses*. (Missouri S&T) Retrieved September 19, 2012, from Website with GE 342 - Military Geology: http://web.mst.edu/~rogersda/umrcourses/ge342/

Salih, A. G. (2012). Review on Granitic Residual Soils Geotechnical Properties. *The Electronic Journal of Geotechnical Enginering (EJGE)*, pp. 2645-2658.

Sassa, K., Fukuoka, H., Wang, F., & Wang, G. (2007). *Progress in Landslide Science*. Berlin: Springer-Verlag.

Sassa, K., Fukuoka, H., Wang, F., & Wang, G. (2007). *Progress in Landslide Science*. Berlin, Germany: Springer-Verlag.

Schanz, T., Vermeer, P. A., & Bonnier, P. G. (1999). The hardening model: Formulation and verification. *PLAXIS Symp. Beyond 2000 in Computational Geotechnics*, pp. 281-296.

Schuster , R. L., & Highland, L. M. (2001). *U.S. Geological Survey*. Retrieved March 05, 2015, from http://pubs.usgs.gov/of/2001/ofr-01-0276/

Smith, G. N. (1990). *Elements of Soil Mechanics* (6th Edition ed.). Edinburgh: BSP Professional Books.

Taylor, D. W. (1937). Stability of Earth Slopes. *Journal of the Boston Society of Civil Engineers, 24*, pp. 197-246.

Taylor, D. W. (1948). *Fundamentals of Soil Mechanics*. New York, USA: John Wiley & Sons.

Terzaghi, K., & Peck, R. B. (1948). *Soil mechanics in engineering practice*. New York: Jonh Wiley & Sons, Inc.

The Government of the Hong Kong Special Administrative Region. (2000). *Guide to Site Investigation*. Hong Kong, China: Government Publications Centre.

Tomlinson, M. (2001). *Foundation Design and Construction* (7th Edition ed.). Harlow, UK: Pearson Education Ltd.

U.S. Army Corps of Engineers. (2003). *Engineering and Design Slope Stability*. Washington, USA: Headquarters USACE.

Vallejo, L., Ferrer, M., Ortuño, L., & Oteo, C. (2004). *Ingeniería Geológica*. Madrid, Spain: Isabel Capella.

Wattie, R. (2008). *Sidi Bou Said*. Retrieved March 05, 2013, from http://www.snaphappyross.co.uk/middleeast/tunisia/sidibousaid.shtml

Wesley, L. D. (2010). *Geotechnical Engineering in Residual Soils*. Hoboken, New Jersey: John Wiley & Sons, Inc.

Whitlow, R. (1995). *Basic Soil Mechanics* (3rd Edition ed.). Edinburgh: Addison Wesley Longman Ltd.

Whitman, R., & Bailey, W. A. (1967). Use of computer for slope stability analysis. *ASCE Journal of the SoilMechanics and Foundation Division, 93*.

Wilson, Mark A.; The College of Wooster. (2009, September 21). *Wikipedia*. Retrieved September 20, 2012, from http://en.wikipedia.org/wiki/File:TalusConesIsfjorden.jpg

Wooten, Rick; NCGS. (n.d.). *Geologic hazards in North Carolina — Landslides*. (NCGS) Retrieved September 20, 2012, from Web Site of the North Carolina Geological Survey: http://www.geology.enr.state.nc.us/Landslide_Info/Landslides_background.htm

Appendices

List of Appendices:

- Appendix A – SLOPE/W hand validation
- Appendix B – Comparative analysis of LEM results
- Appendix C – Examples of SLOPE/W runs outputs
- Appendix D - Comparative analysis of FEM results

Appendix A – SLOPE/W hand validation

A.1 Bishop's simplified method

SLOPE\W Output

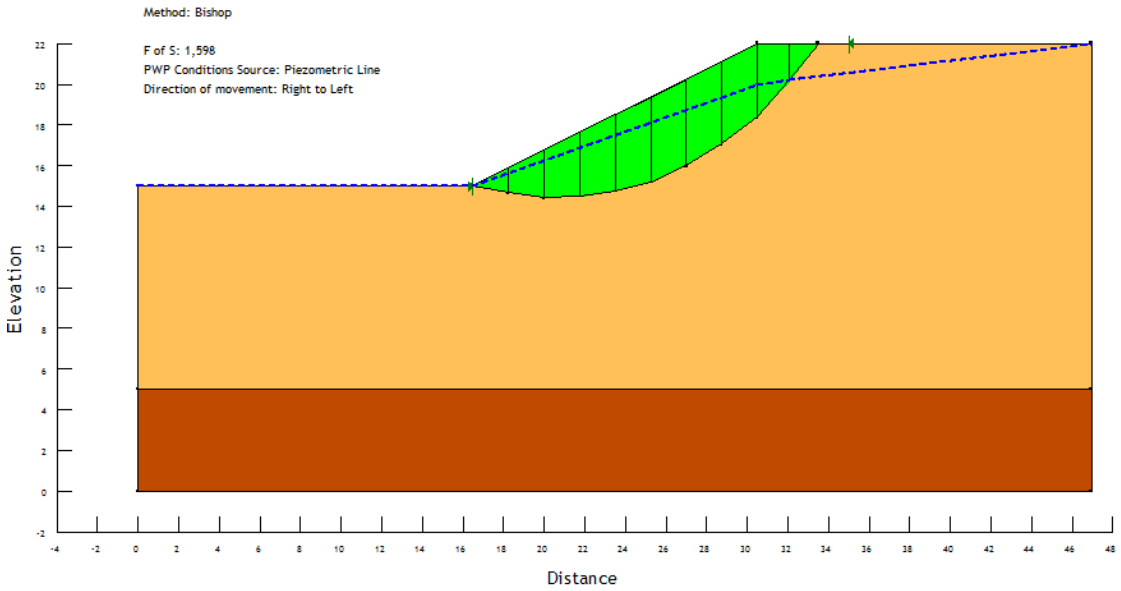

Hand validation

Slope Stability Check Using Bishop Simplified Method

Input Values

Unit Weight of Soil	21	kN/m3
Unit Weight of Water	10	kN/m3
Friction Angle of Soil	30	Deg
Cohesion of Soil	10	kPa
Trial Factor of Safety	1.000	Initial FoS
Slope Angle	26.57	Deg
Slope Height	7	m

Slice	Slice Width (m)	Slice Height (m)	Water Height (m)	Weight (kN/m)	Max H Slice-1 (m)	li (m)	Base Angle ai Deg	Wi x sena (kN/m)	Friction and cohesion Term (kN/m)	Bishop Term Trial FoS Value	DL	Bishop Term New FoS Value	DL	Bishop Term New FS Value	DL	Bishop Term New FS Value	DL	Bishop Term New FS Value	DL	Bishop Term New FS Value	DL
1	1.75	0.60	0.48	22	-	1.75	-11	-4	25	0.9	29	0.9	28.0	0.9	28	0.9	28	0.9	28	0.9	28
2	1.75	1.76	1.38	65	1.20743	1.76	-7	-8	41	0.9	44	0.9	43.2	0.9	43	0.9	43	0.9	43	0.9	43
3	1.75	2.73	2.10	100	2.30343	1.75	0	2	54	1.0	54	1.0	53.8	1.0	54	1.0	54	1.0	54	1.0	54
4	1.75	3.44	2.56	126	3.15060	1.77	10	21	65	1.1	60	1.1	61.5	1.0	62	1.0	62	1.0	62	1.0	62
5	1.75	3.96	2.83	145	3.72890	1.80	13	34	73	1.1	66	1.1	66.6	1.1	69	1.1	69	1.1	69	1.1	69
6	1.75	4.23	2.85	155	4.19880	1.92	24	64	76	1.1	68	1.1	73.2	1.1	74	1.1	74	1.1	74	1.1	74
7	1.75	4.15	2.52	153	4.28550	2.07	32	81	80	1.2	66	1.1	76.1	1.0	77	1.0	77	1.0	77	1.0	77
8	1.75	3.82	1.91	140	4.04160	2.19	37	85	78	1.1	69	1.0	76.9	1.0	78	1.0	78	1.0	78	1.0	78
9	1.60	2.69	0.79	91	3.59220	2.41	48	68	61	1.1	56	1.0	63.0	0.9	66	0.9	66	0.9	66	0.9	66
10	1.40	0.90	0.00	28	1.79700	2.28	52	21	29	1.1	27	0.9	31.6	0.9	32	0.9	33	0.9	33	0.9	33
							Sum	363		Sum	542		577.0		583		582		583		583
										New FS	1,495	New FS	1,590	New FS	1,603	New FS	1,605	New FS	1,605	New FS	1,605

A.2 Fellenius' (Ordinary) method

SLOPE\W Output

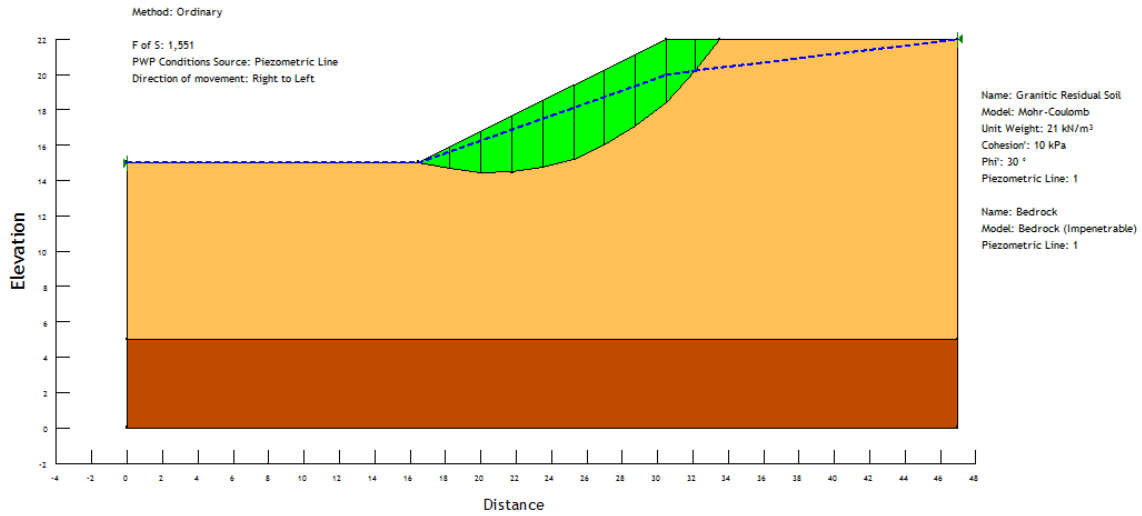

Hand validation

Slope Stability Check Using Fellenius Method
Table to Compute Factor of Safety
Input the following Values

Unit Weight of Soil	***21***	kN/m3
Unit Weight of Water	***10***	kN/m3
Friction Angle of Soil	***30***	Deg
Cohesion of Soil	***10***	kPa
Trial Factor of Safety	***1,000***	Inicial FoS
Slope Angle	***26,57***	Deg
Slope Height	***7***	m

Slice	Width (m)	Height (m)	Water (m)	Area (m2)	Weight (kN/m)	Max H Slice-1 (m)	li (m)	Base Angle Deg		Times Sin Base Angle (kN/m)	Times Cos Slice Angle (kN/m)
1	***1,75***	***0,60***	***0,48***	1,06	22	-	1,78	***-11***	***-11***	-4	26
2	***1,75***	***1,76***	***1,38***	3,07	65	1,20740	1,76	***-7***	***-7***	-8	41
3	***1,75***	***2,73***	***2,10***	4,77	100	2,30340	1,75	***1***	***1***	2	54
4	***1,75***	***3,44***	***2,56***	6,02	126	3,15060	1,77	***10***	***10***	21	64
5	***1,75***	***3,96***	***2,83***	6,93	145	3,72880	1,80	***13***	***13***	34	72
6	***1,75***	***4,23***	***2,85***	7,40	155	4,18660	1,92	***24***	***24***	64	75
7	***1,75***	***4,15***	***2,53***	7,27	153	4,26500	2,07	***32***	***32***	81	74
8	***1,75***	***3,82***	***1,91***	6,68	140	4,04160	2,19	***37***	***37***	85	71
9	***1,60***	***2,69***	***0,79***	4,31	91	3,59220	2,41	***48***	***48***	68	54
10	***1,40***	***0,90***	***0,00***	1,26	26	1,79700	2,28	***52***	***52***	21	32
								Sum		383	662
										FS	**1,549**

A.3 Janbu's simplified method

SLOPE\W Output

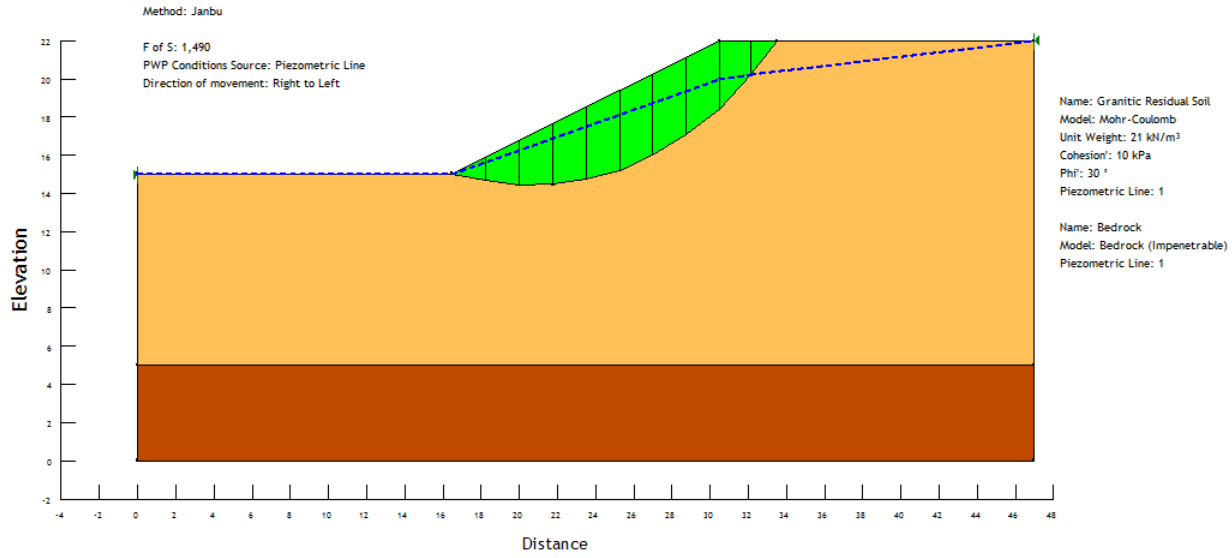

Hand validation

Slope Stability Check Using Janbu Simplified Method
Table to Compute Factor of Safety
Input the following Values

Unit Weight of Soil	***21***	kN/m3
Unit Weight of Soil	***10***	kN/m3
Friction Angle of Soil	***30***	Deg
Cohesion of Soil	***10***	kPa
Trial Factor of Safety	***1,000***	Inicial FoS
Slope Angle	***26,57***	Deg
Slope Height	***7***	m

Slice	Width (m)	Height (m)	Water (m)	Area (m2)	Weight (kN/m)	Max H Slice-1 (m)	li (m)	Base Angle Deg	Times Sin Base Angle (kN/m)	Times Tan Friction Angle (kN/m)	Janbu Term Trial FoS Value DL	DL	Janbu Term New FoS Value DL	DL	Janbu Term New FS Value DL	DL	Janbu Term New FS Value DL	DL	Janbu Term New FS Value DL	DL
1	***1,75***	***0,60***	***0,48***	1,06	22	-	1,78	***-11***	-4	25	1,2	30	1,1	29	1,1	29	1,1	29	1,1	29
2	***1,75***	***1,76***	***1,38***	3,07	65	1,20740	1,76	***-7***	-8	41	1,1	45	1,1	44	1,1	44	1,1	44	1,1	44
3	***1,75***	***2,73***	***2,10***	4,77	100	2,30340	1,75	***1***	2	54	1,0	54	1,0	54	1,0	54	1,0	54	1,0	54
4	***1,75***	***3,44***	***2,56***	6,02	126	3,15060	1,77	***10***	21	65	0,9	61	1,0	62	1,0	62	1,0	62	1,0	62
5	***1,75***	***3,96***	***2,83***	6,93	145	3,72880	1,80	***13***	35	73	0,9	68	1,0	70	1,0	70	1,0	70	1,0	70
6	***1,75***	***4,23***	***2,85***	7,40	155	4,18660	1,92	***24***	71	78	1,0	75	1,0	79	1,0	80	1,0	80	1,0	80
7	***1,75***	***4,15***	***2,53***	7,27	153	4,26500	2,07	***32***	96	80	1,0	82	1,1	88	1,1	90	1,1	90	1,1	90
8	***1,75***	***3,82***	***1,91***	6,68	140	4,04160	2,19	***37***	106	79	1,1	87	1,2	95	1,2	96	1,2	96	1,2	96
9	***1,60***	***2,69***	***0,79***	4,31	91	3,59220	2,41	***48***	102	61	1,4	84	1,5	94	1,6	96	1,6	96	1,6	96
10	***1,40***	***0,90***	***0,00***	1,26	26	1,79700	2,28	***52***	34	29	1,5	45	1,7	50	1,8	51	1,8	52	1,8	52
								Sum	454		Sum	628		665,3		671		672		672
											New FS	**1,384**	**New FS**	**1,467**	**New FS**	**1,480**	**New FS**	**1,482**	**New FS**	**1,483**

Appendix B – Comparative analysis of LEM results

B.1 Effect of surcharge on slope's crest

B.1.1 Purely granular soil

Table B1 below illustrates the variation in MoS with the applied surcharge on the slope's crest when considering the residual soil as a purely granular material. The baseline for these results is the outcome of the null surcharge simulations.

Table B1. Reduction in MoS for changes in applied surcharge for a non-cohesive residual soil.

Reduction in MoS for changes in surcharge for a non-cohesive residual soil												
Slope height (m)	Bishop's method				Fellenius' method				Janbu's method			
	Slope angle				Slope angle				Slope angle			
	1(V):2(H)	1(V):1.5(H)	1(V):1(H)	2(V):1(H)	1(V):2(H)	1(V):1.5(H)	1(V):1(H)	2(V):1(H)	1(V):2(H)	1(V):1.5(H)	1(V):1(H)	2(V):1(H)
Cohesion = 0kPa					Applied surcharge = 5kPa					No groundwater		
2	4.9%	4.9%	5.0%	3.2%	4.7%	0.0%	5.0%	4.9%	0.0%	2.9%	0.4%	3.4%
3	1.5%	2.0%	2.2%	0.6%	1.7%	2.3%	4.5%	4.6%	0.9%	1.6%	0.3%	4.1%
4	1.1%	2.3%	1.4%	2.2%	0.9%	1.1%	1.3%	3.6%	0.2%	0.7%	0.9%	1.4%
5	0.0%	0.5%	1.4%	0.5%	0.0%	0.5%	0.4%	2.3%	0.1%	0.0%	-0.1%	1.1%
6	0.6%	0.3%	0.4%	1.3%	0.3%	0.2%	0.4%	1.0%	0.4%	0.2%	0.4%	0.3%
7	0.4%	0.1%	0.1%	0.9%	-0.4%	0.1%	0.3%	-2.0%	0.0%	0.0%	-0.5%	0.5%
8	0.2%	0.2%	0.3%	0.6%	0.2%	0.2%	0.2%	0.3%	-0.5%	-0.3%	-0.3%	0.5%
Cohesion = 0kPa					Applied surcharge = 10kPa					No groundwater		
2	8.8%	9.1%	8.8%	7.2%	12.3%	5.6%	10.0%	8.6%	7.8%	6.9%	1.9%	5.7%
3	3.4%	3.9%	4.2%	2.9%	9.8%	5.0%	8.3%	8.3%	3.2%	3.7%	1.6%	7.7%
4	2.5%	4.1%	2.9%	4.2%	4.7%	3.1%	2.5%	6.9%	4.4%	1.1%	0.7%	2.2%
5	0.1%	1.3%	2.6%	2.4%	0.0%	1.3%	1.6%	4.6%	2.9%	-1.1%	-0.9%	0.8%
6	1.2%	0.8%	0.8%	3.1%	1.3%	0.7%	1.0%	2.4%	2.5%	-0.7%	-0.7%	-0.4%
7	0.9%	0.4%	0.2%	2.3%	0.0%	0.5%	0.6%	-2.3%	1.0%	0.8%	-0.1%	2.3%
8	0.6%	0.4%	0.7%	1.4%	0.5%	0.4%	0.5%	1.0%	0.0%	0.4%	0.6%	1.9%

Reduction in MoS for changes in surcharge for a non-cohesive residual soil												
Slope height (m)	Bishop's method				Fellenius' method				Janbu's method			
	Slope angle				Slope angle				Slope angle			
	1(V):2(H)	1(V):1.5(H)	1(V):1(H)	2(V):1(H)	1(V):2(H)	1(V):1.5(H)	1(V):1(H)	2(V):1(H)	1(V):2(H)	1(V):1.5(H)	1(V):1(H)	2(V):1(H)
Cohesion = 0kPa					Applied surcharge = 5kPa					Low water table		
2	4.9%	5.4%	5.0%	3.0%	3.1%	0.2%	5.0%	4.9%	0.4%	3.6%	0.4%	4.6%
3	1.4%	-1.2%	2.2%	0.6%	1.7%	2.3%	4.5%	4.6%	1.3%	1.8%	3.8%	4.5%
4	1.2%	1.9%	1.4%	2.2%	0.8%	1.1%	1.2%	3.6%	0.2%	0.9%	0.8%	1.4%
5	0.0%	-0.6%	1.3%	0.5%	0.0%	0.5%	0.4%	2.6%	0.5%	0.6%	0.3%	1.6%
6	0.5%	0.4%	0.4%	1.5%	0.3%	0.3%	0.5%	1.0%	0.4%	0.2%	0.4%	0.3%
7	0.4%	0.2%	0.2%	0.9%	0.3%	0.1%	0.3%	1.3%	-0.1%	-0.4%	-0.3%	0.5%
8	0.2%	0.2%	0.2%	0.9%	0.2%	0.1%	0.1%	0.3%	0.0%	0.1%	0.1%	1.0%
Cohesion = 0kPa					Applied surcharge = 10kPa					Low water table		
2	8.9%	9.5%	8.8%	7.0%	10.5%	5.4%	9.9%	8.6%	9.6%	8.4%	2.9%	8.1%
3	3.4%	1.2%	4.1%	2.9%	10.3%	4.8%	8.3%	8.3%	2.8%	3.4%	4.6%	7.7%
4	2.5%	3.6%	2.9%	4.2%	8.3%	3.0%	2.4%	6.9%	5.7%	-0.5%	-0.8%	0.7%
5	0.1%	0.4%	2.6%	2.4%	0.0%	2.2%	1.6%	5.1%	2.2%	0.3%	-1.5%	0.3%
6	1.2%	0.9%	0.8%	2.8%	0.9%	0.7%	1.0%	2.4%	2.6%	-1.2%	-1.2%	-0.9%
7	0.9%	0.4%	0.6%	2.3%	0.7%	0.5%	0.5%	2.5%	1.0%	0.5%	0.5%	2.3%
8	0.6%	0.4%	0.6%	1.4%	0.5%	0.4%	0.5%	1.0%	-0.5%	-0.1%	-0.1%	1.5%

Reduction in MoS for changes in surcharge for a non-cohesive residual soil												
Slope height (m)	Bishop's method				Fellenius' method				Janbu's method			
	Slope angle				Slope angle				Slope angle			
	1(V):2(H)	1(V):1.5(H)	1(V):1(H)	2(V):1(H)	1(V):2(H)	1(V):1.5(H)	1(V):1(H)	2(V):1(H)	1(V):2(H)	1(V):1.5(H)	1(V):1(H)	2(V):1(H)
Cohesion = 0kPa					Applied surcharge = 5kPa				High water table			
2	1.9%	3.4%	3.6%	3.0%	3.3%	3.5%	3.9%	4.9%	3.6%	2.1%	5.1%	4.3%
3	1.0%	1.1%	1.3%	0.0%	1.3%	1.2%	1.2%	4.3%	0.9%	1.2%	3.0%	2.5%
4	0.3%	0.0%	1.4%	0.0%	0.8%	0.8%	0.0%	3.0%	0.8%	0.6%	0.0%	0.0%
5	0.2%	0.6%	0.0%	1.7%	0.7%	0.7%	1.1%	2.8%	0.6%	1.0%	0.5%	0.5%
6	0.0%	0.0%	0.3%	1.4%	0.6%	0.0%	0.0%	1.6%	0.0%	-0.1%	0.0%	-0.3%
7	0.6%	0.0%	0.0%	0.0%	0.0%	0.6%	0.5%	0.0%	0.4%	0.0%	0.0%	1.0%
8	0.0%	0.0%	0.1%	0.7%	0.1%	0.2%	0.0%	0.9%	0.5%	1.0%	0.8%	-0.5%
Cohesion = 0kPa					Applied surcharge = 5kPa				High water table			
2	5.4%	6.6%	6.6%	7.0%	7.1%	8.9%	8.7%	8.6%	7.4%	7.4%	9.0%	6.9%
3	2.4%	3.2%	3.5%	0.3%	4.1%	4.3%	4.6%	7.7%	2.1%	1.9%	4.8%	4.2%
4	1.0%	1.4%	2.6%	0.0%	2.3%	2.8%	0.0%	5.6%	2.4%	1.2%	0.6%	0.0%
5	0.6%	1.2%	0.0%	0.0%	2.0%	1.9%	2.1%	2.5%	1.7%	1.9%	0.5%	0.5%
6	0.0%	0.0%	0.6%	1.4%	1.2%	0.6%	0.0%	2.0%	0.3%	0.4%	0.0%	0.6%
7	0.9%	0.0%	0.0%	0.0%	0.0%	1.1%	0.9%	-0.4%	1.4%	0.5%	0.5%	-0.5%
8	0.0%	0.2%	0.3%	0.7%	0.4%	0.8%	0.0%	0.9%	0.5%	1.6%	1.3%	-0.5%

B.1.2 Soil with an effective cohesion of 5kPa

Table B2 below illustrates the variation in MoS with the applied surcharge on the slope's crest when considering the residual soil as having an effective cohesion of 5kPa. The baseline for these results is the outcome of the null surcharge simulations.

Table B2. Reduction in MoS for changes in applied surcharge for a c'=5kPa residual soil.

Reduction in MoS for changes in surcharge for a c'=5kPa residual soil												
Slope height (m)	Bishop's method				Fellenius' method				Janbu's method			
	Slope angle				Slope angle				Slope angle			
	1(V):2(H)	1(V):1.5(H)	1(V):1(H)	2(V):1(H)	1(V):2(H)	1(V):1.5(H)	1(V):1(H)	2(V):1(H)	1(V):2(H)	1(V):1.5(H)	1(V):1(H)	2(V):1(H)
Cohesion = 5kPa					**Applied surcharge = 5kPa**						**No groundwater**	
2	7.6%	10.5%	9.6%	11.5%	8.6%	9.8%	11.6%	13.2%	9.8%	11.2%	13.3%	14.6%
3	4.8%	5.1%	5.6%	6.7%	5.5%	6.4%	6.8%	7.5%	5.7%	6.1%	5.3%	8.9%
4	3.8%	3.7%	4.8%	4.4%	3.3%	4.3%	5.3%	5.7%	3.9%	4.0%	5.0%	6.8%
5	2.6%	2.0%	3.6%	4.0%	3.0%	4.0%	3.9%	4.8%	2.4%	3.9%	3.2%	4.2%
6	1.8%	2.6%	2.7%	3.0%	1.7%	1.5%	2.8%	4.2%	1.4%	2.0%	3.2%	3.9%
7	1.3%	3.1%	2.2%	2.1%	1.4%	1.7%	2.4%	7.4%	1.8%	2.2%	3.1%	3.5%
8	1.6%	1.3%	1.7%	1.7%	1.2%	1.2%	1.9%	2.8%	0.4%	0.1%	0.8%	1.5%
Cohesion = 5kPa					**Applied surcharge = 10kPa**						**No groundwater**	
2	15.5%	17.6%	16.9%	19.7%	16.7%	18.2%	20.1%	22.1%	17.3%	19.1%	21.8%	22.5%
3	9.6%	10.2%	10.4%	12.2%	10.5%	12.1%	12.5%	13.6%	10.5%	11.3%	10.7%	15.0%
4	7.1%	7.5%	8.9%	8.5%	6.9%	8.0%	9.9%	10.6%	7.7%	8.2%	9.8%	12.5%
5	5.4%	5.0%	6.8%	7.4%	5.8%	6.8%	7.3%	8.8%	5.1%	7.1%	6.9%	8.9%
6	3.7%	5.0%	5.1%	5.1%	4.0%	3.9%	5.6%	7.8%	4.2%	5.3%	6.8%	8.0%
7	2.6%	5.2%	4.1%	4.6%	3.4%	3.5%	4.6%	9.6%	4.3%	4.3%	5.6%	7.0%
8	3.1%	2.6%	3.3%	2.2%	2.8%	3.2%	4.1%	5.2%	2.1%	2.1%	3.1%	4.1%

Reduction in MoS for changes in surcharge for a c'=5kPa residual soil												
Slope height (m)	Bishop's method				Fellenius' method				Janbu's method			
	Slope angle				Slope angle				Slope angle			
	1(V):2(H)	1(V):1.5(H)	1(V):1(H)	2(V):1(H)	1(V):2(H)	1(V):1.5(H)	1(V):1(H)	2(V):1(H)	1(V):2(H)	1(V):1.5(H)	1(V):1(H)	2(V):1(H)
Cohesion = 5kPa					Applied surcharge = 5kPa				Low water table			
2	7.7%	7.8%	9.6%	10.1%	8.9%	9.0%	11.6%	13.2%	8.3%	9.5%	12.9%	14.0%
3	4.0%	4.6%	5.6%	6.7%	4.5%	5.5%	6.8%	7.5%	4.9%	5.8%	4.8%	8.4%
4	2.6%	3.5%	4.8%	4.4%	3.2%	3.7%	5.3%	5.7%	3.7%	5.1%	5.5%	7.2%
5	2.0%	2.2%	3.7%	4.0%	2.1%	2.6%	3.8%	4.8%	2.7%	3.9%	4.5%	5.5%
6	1.4%	2.7%	2.7%	3.2%	1.9%	2.0%	2.8%	4.2%	1.0%	1.3%	2.7%	3.4%
7	1.5%	0.7%	2.1%	1.6%	0.6%	1.8%	2.4%	4.6%	2.7%	2.1%	3.2%	3.5%
8	0.7%	0.9%	1.7%	0.5%	1.2%	1.4%	2.0%	2.8%	1.6%	2.1%	2.5%	2.2%
Cohesion = 5kPa					Applied surcharge = 10kPa				Low water table			
2	14.5%	14.7%	16.9%	19.2%	16.5%	17.0%	20.1%	22.1%	15.5%	17.4%	21.8%	23.1%
3	8.3%	9.8%	10.4%	12.2%	9.4%	10.8%	12.5%	13.6%	10.1%	11.6%	11.1%	15.4%
4	6.0%	7.4%	8.9%	8.5%	6.5%	7.7%	9.9%	10.6%	7.2%	9.0%	10.2%	12.9%
5	4.4%	4.3%	6.9%	7.4%	4.5%	5.4%	7.3%	8.8%	5.2%	6.9%	8.1%	10.2%
6	3.1%	5.0%	5.1%	6.1%	3.8%	4.2%	5.6%	7.8%	3.9%	4.0%	6.3%	7.5%
7	2.8%	2.2%	4.1%	4.2%	2.7%	3.4%	4.6%	7.1%	3.9%	4.1%	5.2%	9.7%
8	1.8%	1.8%	3.3%	3.1%	2.5%	2.9%	4.2%	5.2%	4.6%	5.4%	6.5%	6.6%

Reduction in MoS for changes in surcharge for a c'=5kPa residual soil												
Slope height (m)	Bishop's method				Fellenius' method				Janbu's method			
	Slope angle				Slope angle				Slope angle			
	1(V):2(H)	1(V):1.5(H)	1(V):1(H)	2(V):1(H)	1(V):2(H)	1(V):1.5(H)	1(V):1(H)	2(V):1(H)	1(V):2(H)	1(V):1.5(H)	1(V):1(H)	2(V):1(H)
Cohesion = 5kPa					Applied surcharge = 5kPa				High water table			
2	7.6%	7.9%	9.3%	9.0%	8.4%	9.5%	11.3%	13.1%	8.4%	9.0%	12.6%	13.7%
3	4.4%	4.9%	5.1%	5.0%	4.7%	5.3%	6.5%	7.1%	4.5%	5.6%	5.1%	7.6%
4	3.0%	3.1%	3.6%	3.1%	3.2%	3.9%	4.8%	5.3%	2.6%	3.1%	3.6%	3.9%
5	1.7%	1.8%	1.3%	1.9%	2.6%	3.1%	3.7%	3.1%	2.3%	2.5%	3.1%	5.4%
6	1.5%	1.9%	1.4%	1.3%	1.9%	2.3%	2.8%	5.0%	1.7%	1.6%	1.9%	2.7%
7	1.1%	1.5%	1.1%	1.0%	1.3%	1.6%	2.0%	5.6%	-0.7%	0.0%	0.2%	2.6%
8	1.1%	0.7%	0.9%	0.4%	1.1%	1.1%	1.9%	2.7%	0.0%	0.0%	0.5%	2.0%
Cohesion = 5kPa					Applied surcharge = 10kPa				High water table			
2	14.3%	15.2%	16.2%	18.0%	15.5%	17.7%	19.5%	21.8%	15.7%	16.9%	21.7%	22.9%
3	8.4%	9.1%	9.4%	12.7%	9.3%	10.7%	11.9%	12.9%	9.1%	10.5%	10.5%	12.6%
4	5.7%	5.9%	7.0%	5.8%	6.7%	7.5%	9.0%	9.8%	5.7%	6.3%	7.2%	7.2%
5	3.8%	3.8%	2.6%	3.6%	5.0%	5.9%	6.9%	7.0%	3.4%	3.9%	5.0%	6.7%
6	3.0%	3.6%	2.7%	4.4%	4.0%	4.6%	5.4%	5.2%	2.5%	2.4%	2.7%	4.5%
7	2.1%	2.8%	2.2%	1.6%	2.8%	3.2%	4.0%	5.0%	1.7%	2.7%	2.8%	9.8%
8	1.8%	1.3%	1.8%	0.7%	2.6%	2.8%	3.7%	4.4%	1.9%	1.7%	2.7%	2.4%

B.1.3 Soil with an effective cohesion of 10kPa

Table B3 below illustrates the variation in MoS with the applied surcharge on the slope's crest when considering the residual soil as having an effective cohesion of 10kPa. The baseline for these results is the outcome of the null surcharge simulations.

Table B3. Reduction in MoS for changes in applied surcharge for a c'=10kPa residual soil.

Reduction in MoS for changes in surcharge for a c'=10kPa residual soil												
Slope height (m)	**Bishop's method**				**Fellenius' method**				**Janbu's method**			
	Slope angle				**Slope angle**				**Slope angle**			
	1(V):2(H)	**1(V):1.5(H)**	**1(V):1(H)**	**2(V):1(H)**	**1(V):2(H)**	**1(V):1.5(H)**	**1(V):1(H)**	**2(V):1(H)**	**1(V):2(H)**	**1(V):1.5(H)**	**1(V):1(H)**	**2(V):1(H)**
Cohesion = 10kPa					**Applied surcharge = 5kPa**						**No groundwater**	
2	9.2%	10.2%	11.2%	14.7%	11.3%	11.8%	12.8%	14.7%	8.4%	10.6%	13.9%	11.5%
3	5.9%	6.4%	6.6%	10.5%	6.7%	6.9%	7.4%	9.3%	6.3%	7.9%	9.0%	10.0%
4	4.6%	5.3%	5.6%	6.1%	5.0%	5.4%	5.9%	7.1%	4.3%	5.0%	6.7%	7.8%
5	3.5%	3.3%	3.7%	4.5%	3.3%	4.2%	4.9%	5.7%	3.7%	4.4%	5.0%	6.0%
6	2.2%	2.8%	3.3%	3.5%	2.6%	2.9%	3.4%	3.3%	2.0%	2.9%	3.7%	4.8%
7	1.8%	2.5%	2.5%	1.1%	1.5%	3.2%	2.9%	3.8%	2.1%	2.7%	3.2%	2.9%
8	1.6%	2.0%	2.2%	2.4%	1.7%	2.2%	2.8%	3.4%	1.7%	2.4%	2.3%	5.8%
Cohesion = 10kPa					**Applied surcharge = 10kPa**						**No groundwater**	
2	17.9%	19.3%	19.4%	22.8%	20.4%	21.0%	22.4%	24.9%	18.8%	21.7%	25.5%	24.5%
3	12.2%	12.7%	12.2%	17.3%	13.2%	13.6%	13.6%	16.7%	12.5%	14.6%	21.7%	18.0%
4	8.8%	9.4%	10.4%	11.2%	9.5%	10.3%	11.0%	12.9%	8.8%	9.8%	12.1%	14.4%
5	6.8%	6.5%	7.6%	8.0%	6.5%	8.0%	9.2%	10.5%	7.0%	8.2%	9.3%	10.9%
6	4.5%	5.6%	6.3%	6.7%	5.2%	5.6%	6.6%	6.9%	5.5%	6.0%	7.3%	9.7%
7	3.8%	4.7%	4.8%	4.6%	4.2%	5.6%	5.9%	7.4%	3.2%	4.5%	6.0%	7.7%
8	3.1%	3.9%	4.5%	5.2%	3.5%	3.8%	5.4%	5.8%	4.3%	4.6%	4.9%	7.4%

Reduction in MoS for changes in surcharge for a c'=10kPa residual soil												
Slope height (m)	Bishop's method				Fellenius' method				Janbu's method			
	Slope angle				Slope angle				Slope angle			
	1(V):2(H)	1(V):1.5(H)	1(V):1(H)	2(V):1(H)	1(V):2(H)	1(V):1.5(H)	1(V):1(H)	2(V):1(H)	1(V):2(H)	1(V):1.5(H)	1(V):1(H)	2(V):1(H)
Cohesion = 10kPa					**Applied surcharge = 5kPa**						**Low water table**	
2	8.7%	11.0%	11.2%	13.0%	10.5%	10.7%	12.8%	14.7%	11.9%	11.0%	14.3%	15.2%
3	5.6%	6.4%	7.2%	6.5%	7.2%	6.6%	8.3%	9.3%	7.7%	7.9%	9.1%	10.4%
4	3.9%	3.9%	5.6%	6.1%	4.5%	5.0%	5.9%	7.1%	4.7%	5.8%	7.1%	8.3%
5	2.4%	3.3%	3.7%	4.5%	2.9%	3.6%	4.9%	5.7%	3.5%	4.4%	5.0%	6.0%
6	2.0%	2.8%	3.4%	3.8%	2.6%	2.6%	3.4%	5.0%	3.8%	2.2%	3.7%	4.8%
7	1.6%	2.2%	2.5%	2.5%	1.7%	2.2%	2.9%	3.8%	2.5%	2.2%	3.2%	3.4%
8	1.4%	1.6%	2.2%	2.4%	1.2%	2.0%	2.6%	2.9%	1.4%	2.1%	2.3%	3.4%
Cohesion = 10kPa					**Applied surcharge = 10kPa**						**Low water table**	
2	17.1%	19.3%	19.4%	21.9%	18.8%	19.5%	22.2%	24.9%	21.7%	21.8%	25.8%	27.0%
3	10.8%	12.2%	13.1%	14.5%	13.0%	12.9%	15.1%	16.7%	13.2%	14.2%	16.1%	18.4%
4	7.7%	7.4%	10.3%	11.2%	8.7%	9.4%	10.9%	12.9%	8.8%	10.3%	12.6%	14.8%
5	5.3%	6.8%	7.4%	8.0%	6.4%	7.2%	9.2%	10.6%	6.9%	8.2%	9.3%	10.9%
6	4.1%	5.4%	6.4%	7.2%	5.0%	5.3%	6.6%	8.8%	6.7%	5.7%	7.8%	9.6%
7	3.4%	4.3%	4.8%	4.9%	3.8%	4.3%	5.9%	7.4%	4.6%	4.9%	6.4%	9.0%
8	2.9%	3.2%	4.4%	4.3%	2.7%	3.9%	5.2%	5.9%	3.1%	4.3%	4.5%	6.5%

Reduction in MoS for changes in surcharge for a c'=10kPa residual soil												
Slope height (m)	Bishop's method				Fellenius' method				Janbu's method			
	Slope angle				Slope angle				Slope angle			
	1(V):2(H)	1(V):1.5(H)	1(V):1(H)	2(V):1(H)	1(V):2(H)	1(V):1.5(H)	1(V):1(H)	2(V):1(H)	1(V):2(H)	1(V):1.5(H)	1(V):1(H)	2(V):1(H)
Cohesion = 10kPa					Applied surcharge = 5kPa				High water table			
2	8.8%	10.2%	10.8%	11.8%	9.7%	10.8%	12.3%	14.4%	8.4%	10.8%	11.2%	12.3%
3	5.3%	5.8%	7.0%	2.4%	6.4%	6.9%	8.0%	8.5%	7.6%	7.1%	7.9%	8.6%
4	3.7%	3.5%	3.1%	4.9%	4.3%	4.7%	5.5%	6.1%	4.2%	4.4%	5.7%	5.7%
5	2.5%	3.1%	3.0%	3.3%	3.0%	3.6%	4.2%	4.7%	4.5%	3.2%	3.8%	4.1%
6	2.2%	1.6%	1.8%	3.0%	2.8%	2.9%	3.3%	4.0%	2.7%	2.0%	2.0%	5.9%
7	2.3%	1.8%	1.5%	1.0%	3.2%	2.5%	2.5%	3.4%	2.6%	2.3%	3.2%	4.3%
8	1.5%	1.6%	1.0%	0.5%	1.7%	2.0%	2.1%	2.5%	1.8%	1.3%	1.3%	2.5%
Cohesion = 10kPa					Applied surcharge = 10kPa				High water table			
2	17.0%	18.4%	18.7%	22.1%	18.4%	19.3%	22.4%	23.8%	19.1%	21.2%	22.8%	22.6%
3	10.5%	11.1%	12.8%	10.9%	12.4%	13.0%	14.4%	15.5%	12.8%	12.7%	14.1%	15.9%
4	7.4%	6.7%	6.6%	9.1%	8.5%	9.3%	10.3%	11.1%	8.4%	8.9%	10.8%	10.4%
5	5.2%	5.9%	5.7%	6.0%	6.1%	7.2%	8.1%	8.7%	7.5%	6.6%	7.5%	8.0%
6	4.4%	3.6%	3.4%	4.6%	5.2%	5.6%	6.3%	6.7%	5.3%	4.6%	4.2%	7.4%
7	3.9%	3.5%	3.0%	3.3%	5.2%	4.8%	4.8%	6.9%	3.8%	3.8%	4.8%	6.5%
8	2.7%	3.0%	1.9%	1.0%	3.3%	4.1%	4.0%	5.0%	4.7%	4.5%	4.3%	4.2%

B.2 Effect of groundwater level

B.2.1 Purely granular soil

Table B4 below illustrates the variation in MoS with raising groundwater levels when considering the residual soil as a purely granular material. The baseline for these results is the outcome of the simulations without porewater pressures.

Table B4. Reduction in MoS for changes in groundwater levels for a non-cohesive residual soil.

Reduction in MoS for changes in groundwater levels for a non-cohesive residual soil												
Slope height (m)	Bishop's method				Fellenius' method				Janbu's method			
	Slope angle				Slope angle				Slope angle			
	1(V):2(H)	1(V):1.5(H)	1(V):1(H)	2(V):1(H)	1(V):2(H)	1(V):1.5(H)	1(V):1(H)	2(V):1(H)	1(V):2(H)	1(V):1.5(H)	1(V):1(H)	2(V):1(H)
Cohesion = 0kPa					Applied surcharge = 0kPa						Low water table	
2	0.0%	-0.6%	0.0%	1.1%	1.7%	0.1%	0.0%	0.0%	0.0%	-0.8%	0.0%	-1.6%
3	0.0%	0.2%	0.0%	0.0%	0.0%	0.0%	0.0%	0.0%	0.0%	0.3%	3.4%	0.0%
4	0.0%	0.3%	0.0%	0.0%	0.0%	0.2%	0.1%	0.0%	0.0%	0.2%	0.0%	0.0%
5	0.0%	0.0%	0.1%	0.0%	0.0%	0.0%	0.0%	-1.2%	0.0%	0.0%	0.0%	0.0%
6	0.0%	0.0%	0.0%	0.5%	0.0%	0.0%	-0.1%	0.0%	0.1%	0.0%	0.0%	0.0%
7	0,0%	0,0%	-0,1%	0,0%	-0,7%	0,0%	0,1%	-5,0%	0,0%	0,4%	-0,1%	0,0%
8	0.0%	0.0%	0.1%	0.0%	0.0%	0.0%	0.0%	0.0%	0.0%	0.0%	0.0%	0.0%
Cohesion = 0kPa					Applied surcharge = 0kPa						High water table	
2	10.1%	6.8%	-0.1%	1.1%	14.0%	7.5%	0.9%	0.0%	10.7%	6.7%	0.0%	3.1%
3	16.0%	12.0%	6.4%	14.7%	19.0%	16.2%	15.0%	13.1%	19.5%	19.0%	18.2%	39.2%
4	22.8%	23.7%	22.0%	54.1%	23.0%	21.3%	16.1%	17.3%	24.4%	25.7%	26.3%	47.1%
5	25.9%	24.8%	34.7%	53.3%	25.5%	22.5%	18.3%	17.6%	29.6%	29.6%	34.1%	65.6%
6	32,4%	32,7%	39,0%	60,1%	29,7%	26,6%	22,6%	23,6%	35,4%	36,9%	44,7%	66,5%
7	32.4%	32.7%	39.0%	60.1%	31.4%	31.0%	22.6%	22.2%	31.8%	31.1%	44.7%	70.2%
8	34.3%	35.3%	43.1%	59.6%	31.3%	28.1%	25.6%	24.1%	35.8%	38.0%	48.6%	66.5%

Reduction in MoS for changes in groundwater levels for a non-cohesive residual soil												
Slope height (m)	Bishop's method				Fellenius' method				Janbu's method			
	Slope angle				Slope angle				Slope angle			
	1(V):2(H)	1(V):1.5(H)	1(V):1(H)	2(V):1(H)	1(V):2(H)	1(V):1.5(H)	1(V):1(H)	2(V):1(H)	1(V):2(H)	1(V):1.5(H)	1(V):1(H)	2(V):1(H)
Cohesion = 0kPa					Applied surcharge = 5kPa				Low water table			
2	0.0%	-0.1%	0.0%	0.8%	0.0%	0.3%	0.0%	0.0%	0.3%	-0.1%	0.0%	-0.4%
3	0.0%	-3.1%	0.0%	0.0%	0.0%	0.0%	0.0%	0.0%	0.4%	0.5%	1.4%	0.5%
4	0.0%	-0.1%	0.0%	0.0%	-0.1%	0.1%	0.0%	0.0%	0.0%	0.4%	0.0%	0.0%
5	0.0%	-1.1%	0.0%	0.0%	0.0%	0.0%	0.0%	-0.9%	0.5%	0.6%	0.5%	0.5%
6	0.0%	0.1%	0.0%	0.8%	0.0%	0.0%	0.0%	0.0%	0.0%	0.0%	0.0%	0.0%
7	0,0%	0,0%	0,1%	0,0%	0,0%	0,0%	0,1%	0,3%	-0,1%	0,0%	0,2%	0,0%
8	0.0%	0.0%	0.0%	0.3%	0.0%	0.0%	0.0%	0.0%	0.5%	0.5%	0.3%	0.5%
Cohesion = 0kPa					Applied surcharge = 5kPa				High water table			
2	7.3%	5.3%	-1.6%	0.8%	12.8%	10.8%	-0.2%	0.0%	13.9%	5.9%	2.7%	7.2%
3	15.5%	11.2%	5.5%	14.2%	18.7%	15.3%	12.0%	12.9%	19.6%	18.7%	17.2%	38.3%
4	22.1%	21.9%	21.9%	53.0%	23.0%	21.1%	15.0%	16.8%	24.9%	25.7%	25.6%	46.3%
5	26.0%	24.8%	33.8%	53.9%	26.0%	22.6%	18.9%	18.0%	30.0%	30.4%	34.5%	65.4%
6	29.8%	28.8%	34.5%	62.7%	28.3%	24.5%	20.1%	17.8%	33.2%	33.7%	40.5%	60.1%
7	32,6%	32,6%	39,0%	59,8%	30,0%	27,0%	22,8%	26,5%	35,7%	36,9%	45,0%	66,6%
8	34.1%	35.2%	43.0%	59.7%	31.2%	28.1%	25.5%	24.5%	36.4%	38.8%	49.2%	66.2%

Reduction in MoS for changes in groundwater levels for a non-cohesive residual soil												
Slope height (m)	Bishop's method				Fellenius' method				Janbu's method			
	Slope angle				Slope angle				Slope angle			
	1(V):2(H)	1(V):1.5(H)	1(V):1(H)	2(V):1(H)	1(V):2(H)	1(V):1.5(H)	1(V):1(H)	2(V):1(H)	1(V):2(H)	1(V):1.5(H)	1(V):1(H)	2(V):1(H)
Cohesion = 0kPa					Applied surcharge = 10kPa				Low water table			
2	0.1%	-0.3%	0.0%	0.9%	-0.3%	-0.2%	0.0%	0.0%	1.9%	0.9%	1.0%	1.0%
3	0.0%	-2.5%	0.0%	0.0%	0.5%	-0.2%	0.0%	0.0%	-0.4%	0.0%	0.0%	0.0%
4	0.0%	-0.1%	0.0%	0.0%	3.9%	0.1%	0.0%	0.0%	1.3%	-1.4%	-1.4%	-1.4%
5	0.0%	-0.9%	0.0%	0.0%	0.0%	0.9%	0.0%	-0.6%	-0.7%	1.4%	-0.5%	-0.5%
6	0.0%	0.0%	0.0%	0.3%	-0.4%	0.0%	0.0%	0.0%	0.2%	-0.5%	-0.5%	-0.5%
7	0,0%	0,0%	0,3%	0,0%	0,0%	0,0%	-0,1%	0,0%	0,0%	0,0%	0,5%	0,0%
8	0.0%	0.0%	0.0%	0.0%	0.0%	0.0%	0.0%	0.0%	-0.5%	-0.5%	-0.7%	-0.5%
Cohesion = 0kPa					Applied surcharge = 10kPa				High water table			
2	6.8%	4.2%	-2.5%	0.9%	9.0%	10.7%	-0.5%	0.0%	10.3%	7.1%	5.2%	7.5%
3	15.1%	11.5%	5.7%	12.5%	13.9%	15.6%	11.6%	12.6%	18.7%	17.4%	16.9%	36.9%
4	21.6%	21.6%	21.8%	52.1%	21.2%	21.1%	13.9%	16.2%	22.9%	25.8%	26.2%	45.9%
5	26.3%	24.7%	32.9%	52.2%	26.9%	23.0%	18.7%	15.8%	28.7%	31.7%	35.0%	65.5%
6	29.3%	28.4%	34.4%	62.0%	28.0%	24.6%	19.7%	17.0%	32.0%	34.6%	41.2%	60.7%
7	32,4%	32,4%	38,9%	59,2%	29,7%	27,1%	22,9%	25,0%	35,7%	36,7%	45,0%	65,5%
8	33.9%	35.2%	42.8%	59.3%	31.2%	28.4%	25.2%	24.0%	36.1%	38.7%	49.0%	65.7%

B.2.2 Soil with an effective cohesion of 5kPa

Table B5 below illustrates the variation in MoS with changes in groundwater levels when considering the residual soil as having an effective cohesion of 5kPa. The baseline for these results is the outcome of the simulations without porewater pressures.

Table B5 Reduction in MoS for changes in groundwater levels for a c'=5kPa residual soil.

Reduction in MoS for changes in groundwater levels for a c'=5kPa residual soil												
Slope height (m)	Bishop's method				Fellenius' method				Janbu's method			
	Slope angle				Slope angle				Slope angle			
	1(V):2(H)	1(V):1.5(H)	1(V):1(H)	2(V):1(H)	1(V):2(H)	1(V):1.5(H)	1(V):1(H)	2(V):1(H)	1(V):2(H)	1(V):1.5(H)	1(V):1(H)	2(V):1(H)
Cohesion = 5kPa					Applied surcharge = 0kPa						Low water table	
2	3.7%	3.2%	0.0%	0.8%	7.4%	2.3%	0.4%	0.0%	7.0%	3.1%	-0.5%	0.7%
3	4.1%	0.6%	0.0%	0.0%	8.4%	2.7%	0.0%	0.0%	6.4%	1.5%	-0.9%	-0.9%
4	5.3%	0.3%	0.0%	0.0%	9.0%	3.2%	0.0%	0.0%	8.4%	2.0%	-1.0%	-0.9%
5	6.1%	0.8%	0.0%	0.0%	10.3%	4.8%	0.0%	0.0%	8.9%	2.9%	-1.8%	-1.9%
6	7.0%	0.7%	0.0%	-1.7%	11.8%	4.4%	0.0%	0.0%	10.9%	3.8%	-0.4%	-0.5%
7	8,0%	4,0%	0,0%	0,4%	13,7%	5,4%	0,0%	2,7%	12,4%	4,7%	-1,0%	-0,9%
8	10.8%	2.9%	0.0%	0.0%	15.1%	3.7%	-0.1%	0.0%	13.1%	2.6%	-1.0%	-0.3%
Cohesion = 5kPa					Applied surcharge = 0kPa						High water table	
2	13.3%	11.0%	8.0%	8.4%	16.6%	10.8%	7.7%	2.4%	16.3%	12.6%	3.2%	4.8%
3	20.6%	18.1%	18.0%	18.1%	21.8%	18.4%	13.8%	11.7%	22.3%	20.4%	13.2%	19.0%
4	25.7%	24.5%	22.0%	31.6%	24.7%	22.0%	17.8%	15.3%	28.4%	27.5%	25.5%	31.2%
5	29.1%	27.9%	30.9%	38.5%	27.9%	25.0%	19.9%	18.8%	31.0%	32.2%	31.1%	42.9%
6	32,9%	35,1%	35,5%	54,4%	30,9%	28,2%	23,8%	23,1%	36,3%	36,7%	39,7%	57,3%
7	32.9%	35.1%	35.5%	54.4%	32.2%	35.1%	23.8%	25.4%	34.1%	34.8%	39.7%	51.8%
8	35.4%	36.1%	39.8%	57.1%	32.2%	30.1%	26.3%	22.9%	36.6%	38.6%	42.7%	67.0%

Reduction in MoS for changes in groundwater levels for a c'=5kPa residual soil												
Slope height (m)	Bishop's method				Fellenius' method				Janbu's method			
	Slope angle				Slope angle				Slope angle			
	1(V):2(H)	1(V):1.5(H)	1(V):1(H)	2(V):1(H)	1(V):2(H)	1(V):1.5(H)	1(V):1(H)	2(V):1(H)	1(V):2(H)	1(V):1.5(H)	1(V):1(H)	2(V):1(H)
Cohesion = 5kPa					Applied surcharge = 5kPa				Low water table			
2	3.9%	0.2%	0.0%	-0.8%	7.7%	1.5%	0.4%	0.0%	5.4%	1.2%	-0.9%	0.0%
3	3.2%	0.0%	0.0%	0.0%	7.3%	1.8%	0.0%	0.0%	5.6%	1.3%	-1.4%	-1.4%
4	4.2%	0.1%	0.0%	0.0%	8.8%	2.7%	0.0%	0.0%	8.2%	3.1%	-0.5%	-0.5%
5	5.5%	1.0%	0.0%	0.0%	10.2%	3.4%	0.0%	0.0%	9.1%	2.8%	-0.5%	-0.5%
6	6.6%	0.8%	0.0%	-1.4%	12.0%	4.9%	0.0%	0.0%	10.5%	3.1%	-0.9%	-0.9%
7	8,2%	1,6%	0,0%	0,0%	13,0%	5,5%	0,0%	-0,3%	13,2%	4,6%	-1,0%	-1,0%
8	10.0%	2.5%	0.0%	-1.3%	15.1%	6.9%	0.0%	0.0%	14.2%	7.0%	-1.3%	-1.4%
Cohesion = 5kPa					Applied surcharge = 5kPa				High water table			
2	13.3%	8.4%	7.6%	5.8%	16.4%	10.6%	7.4%	2.3%	15.0%	10.5%	2.5%	3.8%
3	20.3%	17.9%	17.5%	16.6%	21.1%	17.4%	13.5%	11.4%	21.3%	20.1%	13.1%	17.8%
4	25.0%	24.1%	21.1%	30.7%	24.6%	21.8%	17.4%	14.9%	27.5%	26.8%	24.5%	29.0%
5	28.4%	27.7%	29.2%	37.1%	27.6%	24.2%	19.7%	17.3%	30.9%	31.2%	31.0%	43.7%
6	31.0%	30.6%	31.9%	46.1%	29.3%	26.9%	22.2%	22.6%	34.5%	34.4%	38.4%	52.8%
7	32,8%	34,0%	34,8%	53,8%	30,9%	28,1%	23,5%	21,6%	34,7%	35,3%	37,8%	56,9%
8	35.0%	35.7%	39.4%	56.5%	32.1%	30.0%	26.3%	22.9%	36.3%	38.5%	42.6%	66.6%

Reduction in MoS for changes in groundwater levels for a c'=5kPa residual soil												
Slope height (m)	Bishop's method				Fellenius' method				Janbu's method			
	Slope angle				Slope angle				Slope angle			
	1(V):2(H)	1(V):1.5(H)	1(V):1(H)	2(V):1(H)	1(V):2(H)	1(V):1.5(H)	1(V):1(H)	2(V):1(H)	1(V):2(H)	1(V):1.5(H)	1(V):1(H)	2(V):1(H)
Cohesion = 5kPa					Applied surcharge = 10kPa						Low water table	
2	2.6%	-0.3%	0.0%	0.2%	7.2%	0.8%	0.4%	0.0%	5.0%	1.1%	-0.5%	1.5%
3	2.8%	0.1%	0.0%	0.0%	7.3%	1.3%	0.0%	0.0%	5.9%	1.8%	-0.5%	-0.5%
4	4.1%	0.2%	0.0%	0.0%	8.7%	2.9%	0.0%	0.0%	7.9%	2.9%	-0.5%	-0.5%
5	5.0%	0.1%	0.0%	0.0%	9.8%	3.4%	0.0%	0.0%	8.9%	2.7%	-0.5%	-0.5%
6	6.4%	0.6%	0.0%	-0.6%	11.6%	4.8%	0.0%	0.0%	10.6%	2.5%	-0.9%	-0.9%
7	8,2%	0,9%	0,0%	0,0%	13,2%	5,3%	0,0%	0,0%	12,0%	4,4%	-1,4%	1,9%
8	9.7%	2.1%	0.0%	1.0%	14.9%	6.4%	0.0%	0.0%	15.3%	8.4%	0.5%	0.5%
Cohesion = 5kPa					Applied surcharge = 10kPa						High water table	
2	12.1%	8.4%	7.3%	6.4%	15.4%	10.2%	7.1%	2.1%	14.8%	10.3%	3.2%	5.4%
3	19.6%	17.0%	17.0%	18.6%	20.7%	17.1%	13.2%	11.1%	21.1%	19.7%	13.0%	16.7%
4	24.5%	23.3%	20.4%	29.6%	24.6%	21.6%	17.0%	14.5%	26.9%	26.1%	23.4%	27.0%
5	27.9%	27.0%	27.7%	35.9%	27.3%	24.3%	19.5%	17.2%	29.7%	29.9%	29.7%	41.5%
6	30.7%	30.1%	31.1%	46.7%	29.2%	26.8%	22.0%	19.7%	33.1%	32.6%	36.6%	51.6%
7	32,6%	33,4%	34,2%	52,9%	30,5%	27,9%	23,2%	19,1%	34,6%	35,6%	37,9%	58,5%
8	34.5%	35.2%	38.9%	56.4%	32.1%	29.8%	26.0%	22.3%	36.4%	38.4%	42.5%	65.8%

B.2.3 Soil with an effective cohesion of 10kPa

Table B6 below illustrates the variation in MoS with changes in groundwater levels when considering the residual soil as having an effective cohesion of 10kPa. The baseline for these results is the outcome of the simulations without porewater pressures.

Table B6. Reduction in MoS for changes in groundwater levels for a c'=10kPa residual soil.

Reduction in MoS for changes in groundwater levels for a c'=10kPa residual soil												
Slope height (m)	Bishop's method				Fellenius' method				Janbu's method			
	Slope angle				Slope angle				Slope angle			
	1(V):2(H)	1(V):1.5(H)	1(V):1(H)	2(V):1(H)	1(V):2(H)	1(V):1.5(H)	1(V):1(H)	2(V):1(H)	1(V):2(H)	1(V):1.5(H)	1(V):1(H)	2(V):1(H)
Cohesion = 10kPa					**Applied surcharge = 0kPa**						**Low water table**	
2	4.7%	0.5%	0.0%	1.5%	8.2%	3.8%	0.3%	0.0%	3.1%	2.4%	-0.9%	-2.4%
3	6.2%	1.2%	0.2%	3.2%	8.2%	3.8%	-0.7%	0.0%	7.4%	2.9%	3.7%	-0.9%
4	6.3%	2.5%	0.0%	0.0%	10.4%	4.2%	0.0%	0.0%	8.9%	3.0%	-1.0%	-0.9%
5	7.8%	2.3%	0.2%	0.0%	10.5%	4.2%	0.0%	-0.2%	9.6%	2.6%	-1.4%	-1.4%
6	8.6%	2.2%	0.0%	-0.6%	11.8%	5.3%	0.0%	-0.7%	10.2%	4.9%	-1.0%	-0.9%
7	9,9%	3,2%	0,0%	-0,3%	13,6%	7,7%	0,0%	0,0%	12,3%	6,5%	-1,4%	-2,2%
8	11.1%	4.0%	0.0%	0.0%	15.8%	7.9%	0.2%	-0.1%	14.8%	6.6%	-0.8%	1.5%
Cohesion = 10kPa					**Applied surcharge = 0kPa**						**High water table**	
2	12.6%	9.8%	3.5%	6.8%	14.8%	10.7%	7.1%	4.1%	13.6%	10.7%	4.2%	5.5%
3	19.2%	17.0%	13.2%	20.8%	19.3%	16.1%	12.6%	9.5%	19.7%	18.7%	21.1%	14.2%
4	23.5%	22.2%	21.0%	23.8%	23.2%	20.0%	15.2%	14.5%	24.9%	23.4%	19.7%	23.3%
5	26.6%	25.4%	28.2%	32.0%	25.0%	22.2%	18.2%	16.2%	27.5%	27.3%	26.2%	31.6%
6	31,0%	30,6%	33,7%	45,2%	27,9%	26,4%	23,1%	20,8%	32,8%	33,4%	35,1%	45,9%
7	31.0%	30.6%	33.7%	45.2%	32.3%	34.5%	23.1%	21.6%	31.5%	33.0%	35.1%	44.1%
8	32.1%	32.2%	36.4%	49.9%	29.9%	26.9%	24.9%	21.3%	34.3%	34.6%	37.6%	51.2%

Reduction in MoS for changes in groundwater levels for a c'=10kPa residual soil												
Slope height (m)	Bishop's method				Fellenius' method				Janbu's method			
	Slope angle				Slope angle				Slope angle			
	1(V):2(H)	1(V):1.5(H)	1(V):1(H)	2(V):1(H)	1(V):2(H)	1(V):1.5(H)	1(V):1(H)	2(V):1(H)	1(V):2(H)	1(V):1.5(H)	1(V):1(H)	2(V):1(H)
Cohesion = 10kPa					Applied surcharge = 5kPa				Low water table			
2	4.2%	1.4%	0.0%	-0.5%	7.3%	2.6%	0.3%	0.0%	7.0%	2.8%	-0.5%	1.2%
3	5.9%	1.1%	0.8%	-1.1%	8.7%	3.5%	0.2%	0.0%	8.8%	2.9%	3.8%	-0.5%
4	5.6%	1.0%	0.0%	0.0%	9.9%	3.8%	0.0%	0.0%	8.9%	3.8%	-0.5%	-0.5%
5	6.8%	2.3%	0.2%	0.0%	10.2%	3.6%	0.0%	-0.2%	9.4%	2.6%	-1.4%	-1.4%
6	8.4%	2.2%	0.0%	-0.3%	11.8%	5.0%	0.0%	1.0%	11.8%	4.2%	-0.9%	-0.9%
7	9,7%	2,9%	0,0%	1,0%	13,7%	6,7%	0,0%	0,0%	12,6%	6,0%	-1,4%	-1,7%
8	10.9%	3.7%	0.0%	0.0%	15.3%	7.6%	0.0%	-0.6%	14.5%	6.3%	-0.9%	-0.9%
Cohesion = 10kPa					Applied surcharge = 5kPa				High water table			
2	12.2%	9.9%	3.0%	3.5%	13.3%	9.6%	6.5%	3.8%	13.5%	10.7%	1.7%	6.1%
3	18.7%	16.4%	13.5%	13.6%	19.0%	16.1%	13.1%	8.7%	20.8%	18.1%	20.1%	12.9%
4	22.8%	20.8%	18.9%	22.8%	22.6%	19.4%	14.9%	13.6%	24.5%	22.9%	18.8%	21.4%
5	25.9%	25.2%	27.7%	31.1%	24.8%	21.7%	17.6%	15.3%	28.1%	26.4%	25.2%	30.2%
6	29.1%	28.3%	30.4%	34.8%	27.2%	23.1%	20.7%	18.1%	30.5%	29.0%	31.5%	37.4%
7	31,3%	30,1%	33,1%	45,2%	29,2%	25,8%	22,7%	20,5%	33,1%	33,1%	35,0%	46,7%
8	32.0%	31.9%	35.6%	49.0%	29.9%	26.7%	24.3%	20.5%	34.3%	33.9%	36.9%	49.6%

Reduction in MoS for changes in groundwater levels for a c'=10kPa residual soil												
Slope height (m)	Bishop's method				Fellenius' method				Janbu's method			
	Slope angle				Slope angle				Slope angle			
	1(V):2(H)	1(V):1.5(H)	1(V):1(H)	2(V):1(H)	1(V):2(H)	1(V):1.5(H)	1(V):1(H)	2(V):1(H)	1(V):2(H)	1(V):1.5(H)	1(V):1(H)	2(V):1(H)
Cohesion = 10kPa					Applied surcharge = 10kPa						Low water table	
2	3.7%	0.5%	0.0%	0.4%	6.3%	2.0%	0.0%	0.0%	6.7%	2.5%	-0.5%	1.0%
3	4.7%	0.6%	1.3%	0.0%	8.0%	3.0%	0.9%	0.0%	8.1%	2.5%	-3.2%	-0.5%
4	5.2%	0.3%	0.0%	0.0%	9.6%	3.3%	0.0%	0.0%	8.9%	3.6%	-0.5%	-0.5%
5	6.3%	2.6%	0.0%	0.0%	10.4%	3.4%	0.0%	-0.1%	9.5%	2.6%	-1.4%	-1.4%
6	8.1%	2.0%	0.0%	-0.1%	11.6%	4.9%	0.0%	1.3%	11.4%	4.6%	-0.5%	-1.1%
7	9,5%	2,7%	0,0%	-0,1%	13,3%	6,5%	0,0%	0,0%	13,6%	6,8%	-0,9%	-0,8%
8	10.9%	3.4%	0.0%	-0.9%	15.0%	8.0%	0.0%	0.6%	13.7%	6.3%	-1.3%	0.5%
Cohesion = 10kPa					Applied surcharge = 10kPa						High water table	
2	11.6%	8.8%	2.6%	5.9%	12.7%	8.8%	7.1%	2.7%	14.0%	10.1%	0.9%	3.2%
3	17.7%	15.5%	13.8%	14.7%	18.6%	15.5%	13.4%	8.2%	19.9%	16.9%	13.4%	11.9%
4	22.3%	19.9%	17.7%	22.0%	22.4%	19.1%	14.6%	12.8%	24.5%	22.6%	18.4%	19.7%
5	25.3%	24.9%	26.7%	30.5%	24.6%	21.6%	17.3%	14.5%	27.9%	26.1%	24.7%	29.3%
6	28.9%	27.7%	29.4%	33.7%	27.1%	23.1%	20.6%	17.3%	29.9%	28.6%	30.5%	35.1%
7	31,1%	29,7%	32,5%	44,5%	28,7%	25,7%	22,2%	20,4%	33,2%	32,9%	34,2%	45,2%
8	31.8%	31.6%	34.8%	47.7%	29.8%	27.1%	23.7%	21.2%	34.5%	34.5%	37.1%	49.6%

B.3 Comparison between LEM methods

B.3.1 Purely granular soil

Table B7 below illustrates the variation in MoS between LEM methods for a purely granular material. The baseline for these comparisons is the obtained results for the Bishop's method.

Table B7. Reduction in MoS between LEM methods for a non-cohesive residual soil.

Reduction in MoS between LEM methods for a non-cohesive residual soil												
Slope height (m)	**Bishop's method**				**Fellenius' method**				**Janbu's method**			
	Slope angle				**Slope angle**				**Slope angle**			
	1(V):2(H)	**1(V):1.5(H)**	**1(V):1(H)**	**2(V):1(H)**	**1(V):2(H)**	**1(V):1.5(H)**	**1(V):1(H)**	**2(V):1(H)**	**1(V):2(H)**	**1(V):1.5(H)**	**1(V):1(H)**	**2(V):1(H)**
Cohesion = 0kPa					**Applied surcharge = 0kPa**						**No groundwater**	
2	N/A	N/A	N/A	N/A	3.4%	7.0%	1.8%	6.7%	3.4%	5.8%	7.1%	-38.8%
3	N/A	N/A	N/A	N/A	1.4%	0.2%	-8.2%	-7.5%	0.3%	-1.1%	-2.4%	-16.4%
4	N/A	N/A	N/A	N/A	2.8%	4.6%	4.7%	10.6%	1.7%	3.2%	3.5%	19.9%
5	N/A	N/A	N/A	N/A	1.5%	1.6%	10.6%	8.2%	-1.2%	-0.4%	10.0%	13.7%
6	N/A	N/A	N/A	N/A	5.5%	5.2%	2.9%	24.6%	2.7%	2.8%	0.5%	24.5%
7	N/A	N/A	N/A	N/A	2,0%	0,9%	2,1%	14,2%	-1,1%	-1,5%	0,3%	10,8%
8	N/A	N/A	N/A	N/A	0.8%	0.8%	2.6%	14.3%	0.1%	-0.2%	1.6%	10.6%
Cohesion = 0kPa					**Applied surcharge = 0kPa**						**Low water table**	
2	N/A	N/A	N/A	N/A	5.0%	7.7%	1.9%	5.7%	3.4%	5.6%	7.1%	-42.5%
3	N/A	N/A	N/A	N/A	1.4%	0.0%	-8.2%	-7.5%	0.3%	-1.1%	1.1%	-16.4%
4	N/A	N/A	N/A	N/A	2.8%	4.4%	4.8%	10.6%	1.7%	3.1%	3.5%	19.9%
5	N/A	N/A	N/A	N/A	1.5%	1.6%	10.5%	7.2%	-1.2%	-0.4%	10.0%	13.7%
6	N/A	N/A	N/A	N/A	1,4%	0,9%	2,2%	10,0%	-1,1%	-1,1%	0,3%	10,8%
7	N/A	N/A	N/A	N/A	0.1%	0.0%	2.2%	14.0%	-2.6%	-2.0%	0.3%	-0.5%

Reduction in MoS between LEM methods for a non-cohesive residual soil												
Slope height (m)	Bishop's method				Fellenius' method				Janbu's method			
	Slope angle				Slope angle				Slope angle			
	1(V):2(H)	1(V):1.5(H)	1(V):1(H)	2(V):1(H)	1(V):2(H)	1(V):1.5(H)	1(V):1(H)	2(V):1(H)	1(V):2(H)	1(V):1.5(H)	1(V):1(H)	2(V):1(H)
8	N/A	N/A	N/A	N/A	0.8%	0.8%	2.6%	14.3%	0.1%	-0.2%	1.5%	10.6%
Cohesion = 0kPa					**Applied surcharge = 0kPa**						**High water table**	
2	N/A	N/A	N/A	N/A	7.6%	7.7%	2.9%	5.7%	4.0%	5.6%	7.2%	-35.9%
3	N/A	N/A	N/A	N/A	5.0%	5.0%	1.7%	-9.5%	4.5%	6.9%	10.6%	17.1%
4	N/A	N/A	N/A	N/A	3.1%	1.7%	-2.5%	-61.0%	3.9%	5.8%	8.8%	7.8%
5	N/A	N/A	N/A	N/A	0.9%	-1.4%	-11.9%	-61.9%	3.8%	6.1%	9.2%	36.5%
6	N/A	N/A	N/A	N/A	2.6%	-0.6%	-18.1%	-67.1%	7.3%	9.4%	9.9%	19.8%
7	N/A	N/A	N/A	N/A	-2,0%	-8,1%	-24,3%	-64,3%	3,3%	4,8%	9,6%	25,0%
8	N/A	N/A	N/A	N/A	-3.7%	-10.2%	-27.4%	-61.0%	2.5%	4.0%	11.2%	25.9%
Cohesion = 0kPa					**Applied surcharge = 5kPa**						**No groundwater**	
2	N/A	N/A	N/A	N/A	3.2%	2.3%	1.9%	8.3%	-1.6%	3.8%	2.6%	-38.5%
3	N/A	N/A	N/A	N/A	1.6%	0.5%	-5.7%	-3.2%	-0.3%	-1.6%	-1.8%	-12.3%
4	N/A	N/A	N/A	N/A	2.5%	3.5%	4.6%	11.8%	0.9%	1.6%	2.9%	19.3%
5	N/A	N/A	N/A	N/A	1.5%	1.6%	9.7%	9.9%	-1.2%	-0.9%	8.6%	14.2%
6	N/A	N/A	N/A	N/A	5.3%	5.1%	2.9%	24.4%	2.5%	2.7%	0.4%	23.8%
7	N/A	N/A	N/A	N/A	1,3%	0,8%	2,3%	10,1%	-1,5%	-1,6%	-0,3%	10,5%
8	N/A	N/A	N/A	N/A	0.8%	0.8%	2.5%	14.1%	-0.6%	-0.7%	1.1%	10.5%

Reduction in MoS between LEM methods for a non-cohesive residual soil												
Slope height (m)	Bishop's method				Fellenius' method				Janbu's method			
	Slope angle				Slope angle				Slope angle			
	1(V):2(H)	1(V):1.5(H)	1(V):1(H)	2(V):1(H)	1(V):2(H)	1(V):1.5(H)	1(V):1(H)	2(V):1(H)	1(V):2(H)	1(V):1.5(H)	1(V):1(H)	2(V):1(H)
Cohesion = 0kPa					Applied surcharge = 5kPa				Low water table			
2	N/A	N/A	N/A	N/A	3.2%	2.7%	1.9%	7.5%	-1.2%	3.8%	2.6%	-40.2%
3	N/A	N/A	N/A	N/A	1.6%	3.5%	-5.7%	-3.2%	0.2%	1.9%	-0.3%	-11.8%
4	N/A	N/A	N/A	N/A	2.4%	3.7%	4.6%	11.8%	0.8%	2.0%	2.9%	19.3%
5	N/A	N/A	N/A	N/A	1.6%	2.6%	9.7%	9.1%	-0.7%	0.8%	9.1%	14.6%
6	N/A	N/A	N/A	N/A	5.3%	5.1%	2.9%	23.8%	2.6%	2.7%	0.4%	23.2%
7	N/A	N/A	N/A	N/A	1,2%	0,8%	2,3%	10,3%	-1,6%	-1,6%	-0,1%	10,5%
8	N/A	N/A	N/A	N/A	0.8%	0.8%	2.5%	13.9%	0.0%	-0.2%	1.4%	10.7%
Cohesion = 0kPa					Applied surcharge = 5kPa				High water table			
2	N/A	N/A	N/A	N/A	8.9%	7.9%	3.3%	7.5%	5.6%	4.3%	6.7%	-29.5%
3	N/A	N/A	N/A	N/A	5.3%	5.1%	1.6%	-4.7%	4.5%	7.0%	10.9%	19.2%
4	N/A	N/A	N/A	N/A	3.7%	2.5%	-3.9%	-56.1%	4.4%	6.4%	7.5%	7.8%
5	N/A	N/A	N/A	N/A	1.4%	-1.3%	-10.7%	-60.1%	4.2%	6.5%	9.7%	35.7%
6	N/A	N/A	N/A	N/A	3.2%	-0.6%	-18.4%	-66.7%	7.3%	9.4%	9.6%	18.4%
7	N/A	N/A	N/A	N/A	-2,6%	-7,4%	-23,7%	-64,3%	3,1%	4,8%	9,6%	25,7%
8	N/A	N/A	N/A	N/A	-3.6%	-10.0%	-27.5%	-60.7%	3.0%	5.0%	11.8%	25.0%

Reduction in MoS between LEM methods for a non-cohesive residual soil												
Slope height (m)	Bishop's method				Fellenius' method				Janbu's method			
	Slope angle				Slope angle				Slope angle			
	1(V):2(H)	1(V):1.5(H)	1(V):1(H)	2(V):1(H)	1(V):2(H)	1(V):1.5(H)	1(V):1(H)	2(V):1(H)	1(V):2(H)	1(V):1.5(H)	1(V):1(H)	2(V):1(H)
Cohesion = 0kPa					Applied surcharge = 10kPa				No groundwater			
2	N/A	N/A	N/A	N/A	7.0%	3.5%	3.1%	8.1%	2.4%	3.5%	0.0%	-41.0%
3	N/A	N/A	N/A	N/A	7.9%	1.4%	-3.6%	-1.5%	0.1%	-1.3%	-1.5%	-10.6%
4	N/A	N/A	N/A	N/A	4.9%	3.6%	4.3%	13.1%	3.7%	0.3%	1.3%	18.3%
5	N/A	N/A	N/A	N/A	1.5%	1.6%	9.6%	10.3%	1.6%	-2.8%	6.7%	12.3%
6	N/A	N/A	N/A	N/A	5.6%	5.1%	3.0%	24.0%	3.9%	1.3%	-1.1%	21.8%
7	N/A	N/A	N/A	N/A	1,1%	0,9%	2,5%	10,2%	-1,0%	-1,1%	0,0%	10,8%
8	N/A	N/A	N/A	N/A	0.7%	0.8%	2.5%	14.0%	-0.5%	-0.2%	1.5%	11.0%
Cohesion = 0kPa					Applied surcharge = 10kPa				Low water table			
2	N/A	N/A	N/A	N/A	6.7%	3.5%	3.1%	7.3%	4.1%	4.5%	1.0%	-40.9%
3	N/A	N/A	N/A	N/A	8.4%	3.6%	-3.6%	-1.5%	-0.3%	1.2%	-1.5%	-10.6%
4	N/A	N/A	N/A	N/A	8.6%	3.9%	4.3%	13.1%	4.9%	-1.0%	-0.2%	17.1%
5	N/A	N/A	N/A	N/A	1.5%	3.3%	9.6%	9.8%	1.0%	-0.5%	6.3%	11.8%
6	N/A	N/A	N/A	N/A	5.2%	5.1%	3.0%	23.8%	4.1%	0.8%	-1.6%	21.2%
7	N/A	N/A	N/A	N/A	1,1%	0,9%	2,1%	10,2%	-1,0%	-1,1%	0,2%	10,8%
8	N/A	N/A	N/A	N/A	0.7%	0.8%	2.5%	14.0%	-1.0%	-0.7%	0.8%	10.6%

Reduction in MoS between LEM methods for a non-cohesive residual soil												
Slope height (m)	Bishop's method				Fellenius' method				Janbu's method			
	Slope angle				Slope angle				Slope angle			
	1(V):2(H)	1(V):1.5(H)	1(V):1(H)	2(V):1(H)	1(V):2(H)	1(V):1.5(H)	1(V):1(H)	2(V):1(H)	1(V):2(H)	1(V):1.5(H)	1(V):1(H)	2(V):1(H)
Cohesion = 0kPa					Applied surcharge = 10kPa				High water table			
2	N/A	N/A	N/A	N/A	9.2%	10.0%	5.0%	7.3%	6.1%	6.3%	7.6%	-31.5%
3	N/A	N/A	N/A	N/A	6.7%	6.0%	2.8%	-1.4%	4.3%	5.5%	10.5%	20.3%
4	N/A	N/A	N/A	N/A	4.4%	3.0%	-5.3%	-51.9%	5.2%	5.6%	6.9%	7.8%
5	N/A	N/A	N/A	N/A	2.4%	-0.6%	-9.5%	-58.0%	4.9%	6.8%	9.7%	36.8%
6	N/A	N/A	N/A	N/A	3.8%	0.1%	-18.8%	-66.0%	7.6%	9.9%	9.4%	19.1%
7	N/A	N/A	N/A	N/A	-2,9%	-6,8%	-23,1%	-65,0%	3,9%	5,3%	10,1%	24,6%
8	N/A	N/A	N/A	N/A	-3.3%	-9.6%	-27.7%	-60.7%	3.0%	5.3%	12.1%	25.0%

B.3.2 Soil with an effective cohesion of 5kPa

Table B8 below illustrates the variation in MoS between LEM methods when considering the residual soil as having an effective cohesion of 5kPa. The baseline for these comparisons is the obtained results for the Bishop's method.

Table B8 Reduction in MoS between LEM methods for a c'=5kPa residual soil.

Reduction in MoS between LEM methods for a c'=5kPa residual soil												
Slope height (m)	Bishop's method				Fellenius' method				Janbu's method			
	Slope angle				Slope angle				Slope angle			
	1(V):2(H)	1(V):1.5(H)	1(V):1(H)	2(V):1(H)	1(V):2(H)	1(V):1.5(H)	1(V):1(H)	2(V):1(H)	1(V):2(H)	1(V):1.5(H)	1(V):1(H)	2(V):1(H)
Cohesion = 5kPa					Applied surcharge = 0kPa					No groundwater		
2	N/A	N/A	N/A	N/A	5.1%	6.8%	-1.9%	0.8%	0.7%	1.8%	-6.8%	-7.5%
3	N/A	N/A	N/A	N/A	5.3%	4.7%	5.2%	2.5%	1.4%	0.3%	-0.9%	-5.2%
4	N/A	N/A	N/A	N/A	6.1%	5.5%	6.0%	1.8%	0.7%	0.3%	1.1%	-6.9%
5	N/A	N/A	N/A	N/A	5.0%	3.9%	5.6%	2.1%	0.7%	-0.8%	1.2%	-3.4%
6	N/A	N/A	N/A	N/A	7.6%	9.1%	3.8%	1.4%	2.7%	3.8%	-2.1%	-4.9%
7	N/A	N/A	N/A	N/A	4,0%	7,4%	5,5%	0,1%	-0,2%	2,9%	0,6%	-1,8%
8	N/A	N/A	N/A	N/A	4.6%	4.1%	4.2%	4.2%	0.8%	0.5%	-0.2%	-3.5%
Cohesion = 5kPa					Applied surcharge = 0kPa					Low water table		
2	N/A	N/A	N/A	N/A	8.7%	6.0%	-1.5%	0.1%	4.1%	1.8%	-7.3%	-7.5%
3	N/A	N/A	N/A	N/A	9.6%	6.7%	5.2%	2.5%	3.8%	1.3%	-1.9%	-6.2%
4	N/A	N/A	N/A	N/A	9.7%	8.2%	6.0%	1.8%	3.9%	2.0%	0.2%	-7.9%
5	N/A	N/A	N/A	N/A	9.2%	7.7%	5.7%	2.1%	3.6%	1.3%	-0.6%	-5.3%
6	N/A	N/A	N/A	N/A	12,4%	12,5%	3,8%	3,0%	6,7%	6,8%	-2,5%	-3,7%
7	N/A	N/A	N/A	N/A	10,0%	8,8%	5,5%	2,4%	4,6%	3,6%	-0,4%	-3,2%

Reduction in MoS between LEM methods for a c'=5kPa residual soil												
Slope height (m)	Bishop's method				Fellenius' method				Janbu's method			
	Slope angle				Slope angle				Slope angle			
	1(V):2(H)	1(V):1.5(H)	1(V):1(H)	2(V):1(H)	1(V):2(H)	1(V):1.5(H)	1(V):1(H)	2(V):1(H)	1(V):2(H)	1(V):1.5(H)	1(V):1(H)	2(V):1(H)
8	N/A	N/A	N/A	N/A	9.2%	4.9%	4.2%	4.2%	3.3%	0.3%	-1.1%	-3.8%
Cohesion = 5kPa					**Applied surcharge = 0kPa**						**High water table**	
2	N/A	N/A	N/A	N/A	8.7%	6.6%	-2.2%	-5.7%	4.2%	3.6%	-12.3%	-11.7%
3	N/A	N/A	N/A	N/A	6.7%	5.0%	0.4%	-5.1%	3.5%	3.2%	-6.7%	-4.1%
4	N/A	N/A	N/A	N/A	4.9%	2.3%	0.9%	-21.6%	4.4%	4.3%	5.5%	-7.6%
5	N/A	N/A	N/A	N/A	3.4%	0.0%	-9.3%	-29.2%	3.3%	5.3%	1.5%	4.1%
6	N/A	N/A	N/A	N/A	4.8%	2.7%	-11.3%	-45.5%	7.1%	8.7%	7.8%	7.6%
7	N/A	N/A	N/A	N/A	1,1%	-2,4%	-11,7%	-68,3%	4,8%	5,3%	7,0%	4,7%
8	N/A	N/A	N/A	N/A	-0.1%	-4.9%	-17.3%	-72.1%	2.6%	4.4%	4.6%	20.5%
Cohesion = 5kPa					**Applied surcharge = 5kPa**						**No groundwater**	
2	N/A	N/A	N/A	N/A	6.1%	6.0%	0.3%	2.8%	3.1%	2.5%	-2.5%	-3.6%
3	N/A	N/A	N/A	N/A	6.0%	5.9%	6.4%	3.3%	2.3%	1.3%	-1.3%	-2.7%
4	N/A	N/A	N/A	N/A	5.6%	6.0%	6.6%	3.1%	0.8%	0.7%	1.3%	-4.2%
5	N/A	N/A	N/A	N/A	5.4%	5.8%	5.9%	2.9%	0.4%	1.1%	0.8%	-3.2%
6	N/A	N/A	N/A	N/A	7.5%	8.0%	3.9%	2.6%	2.3%	3.2%	-1.5%	-4.0%
7	N/A	N/A	N/A	N/A	4,2%	6,1%	5,7%	5,6%	0,4%	2,0%	1,6%	-0,2%
8	N/A	N/A	N/A	N/A	4.2%	4.0%	4.5%	5.2%	-0.4%	-0.6%	-1.2%	-1.8%

Reduction in MoS between LEM methods for a c'=5kPa residual soil												
Slope height (m)	Bishop's method				Fellenius' method				Janbu's method			
	Slope angle				Slope angle				Slope angle			
	1(V):2(H)	1(V):1.5(H)	1(V):1(H)	2(V):1(H)	1(V):2(H)	1(V):1.5(H)	1(V):1(H)	2(V):1(H)	1(V):2(H)	1(V):1.5(H)	1(V):1(H)	2(V):1(H)
Cohesion = 5kPa					**Applied surcharge = 5kPa**						**Low water table**	
2	N/A	N/A	N/A	N/A	9.9%	7.2%	0.7%	3.5%	4.7%	3.5%	-3.5%	-2.9%
3	N/A	N/A	N/A	N/A	10.1%	7.6%	6.4%	3.3%	4.7%	2.6%	-2.8%	-4.1%
4	N/A	N/A	N/A	N/A	10.2%	8.5%	6.6%	3.1%	5.0%	3.7%	0.8%	-4.7%
5	N/A	N/A	N/A	N/A	10.0%	8.1%	5.9%	2.9%	4.2%	2.9%	0.3%	-3.7%
6	N/A	N/A	N/A	N/A	12.8%	11.9%	3.9%	3.9%	6.4%	5.5%	-2.5%	-3.5%
7	N/A	N/A	N/A	N/A	9,2%	9,8%	5,7%	5,3%	5,8%	5,0%	0,6%	-1,2%
8	N/A	N/A	N/A	N/A	9.7%	8.3%	4.5%	6.4%	4.2%	4.0%	-2.5%	-2.0%
Cohesion = 5kPa					**Applied surcharge = 5kPa**						**High water table**	
2	N/A	N/A	N/A	N/A	9.5%	8.2%	0.1%	-0.9%	5.1%	4.8%	-8.1%	-5.9%
3	N/A	N/A	N/A	N/A	7.1%	5.4%	1.9%	-2.7%	3.6%	3.9%	-6.7%	-1.2%
4	N/A	N/A	N/A	N/A	5.1%	3.2%	2.2%	-18.9%	4.0%	4.3%	5.5%	-6.7%
5	N/A	N/A	N/A	N/A	4.3%	1.3%	-6.8%	-27.6%	3.8%	5.9%	3.3%	7.6%
6	N/A	N/A	N/A	N/A	5.2%	3.1%	-9.7%	-40.0%	7.2%	8.5%	8.2%	8.9%
7	N/A	N/A	N/A	N/A	1,3%	-2,3%	-10,7%	-60,5%	3,1%	4,0%	6,2%	6,3%
8	N/A	N/A	N/A	N/A	-0.1%	-4.5%	-16.1%	-68.0%	1.6%	3.7%	4.2%	21.8%

Reduction in MoS between LEM methods for a c'=5kPa residual soil												
Slope height (m)	Bishop's method				Fellenius' method				Janbu's method			
	Slope angle				Slope angle				Slope angle			
	1(V):2(H)	1(V):1.5(H)	1(V):1(H)	2(V):1(H)	1(V):2(H)	1(V):1.5(H)	1(V):1(H)	2(V):1(H)	1(V):2(H)	1(V):1.5(H)	1(V):1(H)	2(V):1(H)
Cohesion = 5kPa					Applied surcharge = 10kPa				No groundwater			
2	N/A	N/A	N/A	N/A	6.4%	7.5%	2.0%	3.8%	2.8%	3.5%	-0.5%	-3.8%
3	N/A	N/A	N/A	N/A	6.3%	6.6%	7.5%	4.0%	2.4%	1.5%	-0.6%	-1.8%
4	N/A	N/A	N/A	N/A	5.8%	6.0%	7.1%	4.0%	1.3%	1.0%	2.0%	-2.1%
5	N/A	N/A	N/A	N/A	5.4%	5.6%	6.1%	3.5%	0.4%	1.4%	1.2%	-1.7%
6	N/A	N/A	N/A	N/A	7.9%	8.0%	4.3%	4.2%	3.2%	4.1%	-0.2%	-1.7%
7	N/A	N/A	N/A	N/A	4,7%	5,7%	6,0%	5,4%	1,5%	1,9%	2,1%	0,9%
8	N/A	N/A	N/A	N/A	4.3%	4.6%	5.0%	7.2%	-0.2%	-0.1%	-0.4%	0.4%
Cohesion = 5kPa					Applied surcharge = 10kPa				Low water table			
2	N/A	N/A	N/A	N/A	10.9%	8.5%	2.4%	3.6%	5.3%	4.9%	-1.0%	-2.4%
3	N/A	N/A	N/A	N/A	10.6%	7.8%	7.5%	4.0%	5.6%	3.2%	-1.1%	-2.3%
4	N/A	N/A	N/A	N/A	10.2%	8.5%	7.1%	4.0%	5.2%	3.7%	1.6%	-2.6%
5	N/A	N/A	N/A	N/A	10.2%	8.8%	6.1%	3.5%	4.5%	3.9%	0.8%	-2.2%
6	N/A	N/A	N/A	N/A	13.1%	11.8%	4.3%	4.8%	7.5%	5.9%	-1.1%	-2.1%
7	N/A	N/A	N/A	N/A	9,9%	9,9%	6,0%	5,4%	5,6%	5,4%	0,7%	2,8%
8	N/A	N/A	N/A	N/A	9.8%	8.9%	5.0%	6.3%	6.0%	6.4%	0.1%	-0.1%

Reduction in MoS between LEM methods for a c'=5kPa residual soil												
Slope height (m)	Bishop's method				Fellenius' method				Janbu's method			
	Slope angle				Slope angle				Slope angle			
	1(V):2(H)	1(V):1.5(H)	1(V):1(H)	2(V):1(H)	1(V):2(H)	1(V):1.5(H)	1(V):1(H)	2(V):1(H)	1(V):2(H)	1(V):1.5(H)	1(V):1(H)	2(V):1(H)
Cohesion = 5kPa					Applied surcharge = 10kPa				High water table			
2	N/A	N/A	N/A	N/A	10.0%	9.4%	1.8%	-0.7%	5.9%	5.5%	-4.9%	-4.9%
3	N/A	N/A	N/A	N/A	7.6%	6.7%	3.2%	-4.8%	4.2%	4.7%	-5.4%	-4.2%
4	N/A	N/A	N/A	N/A	5.9%	3.9%	3.0%	-16.5%	4.4%	4.6%	5.7%	-5.9%
5	N/A	N/A	N/A	N/A	4.5%	2.1%	-4.5%	-24.6%	2.9%	5.4%	3.9%	7.2%
6	N/A	N/A	N/A	N/A	5.9%	3.7%	-8.2%	-44.3%	6.6%	7.6%	7.8%	7.7%
7	N/A	N/A	N/A	N/A	1,8%	-2,1%	-9,6%	-62,5%	4,4%	5,2%	7,6%	12,7%
8	N/A	N/A	N/A	N/A	0.7%	-3.4%	-15.0%	-65.7%	2.7%	4.8%	5.5%	21.9%

B.3.3 Soil with an effective cohesion of 10kPa

Table B9 below illustrates the variation in MoS between LEM methods when considering the residual soil as having an effective cohesion of 10kPa. The baseline for these comparisons is the obtained results for the Bishop's method.

Table B9. Reduction in MoS between LEM methods for a c'=10kPa residual soil.

Reduction in MoS between LEM methods for a c'=10kPa residual soil												
Slope height (m)	Bishop's method				Fellenius' method				Janbu's method			
	Slope angle				Slope angle				Slope angle			
	1(V):2(H)	1(V):1.5(H)	1(V):1(H)	2(V):1(H)	1(V):2(H)	1(V):1.5(H)	1(V):1(H)	2(V):1(H)	1(V):2(H)	1(V):1.5(H)	1(V):1(H)	2(V):1(H)
Cohesion = 10kPa					Applied surcharge = 0kPa					No groundwater		
2	N/A	N/A	N/A	N/A	4.6%	4.3%	-3.8%	-0.2%	2.4%	0.3%	-9.9%	-7.6%
3	N/A	N/A	N/A	N/A	5.9%	4.9%	3.5%	1.7%	2.1%	0.1%	-10.1%	-4.5%
4	N/A	N/A	N/A	N/A	5.4%	5.3%	6.1%	-1.0%	1.9%	1.4%	0.4%	-7.4%
5	N/A	N/A	N/A	N/A	6.5%	5.5%	5.4%	0.6%	2.0%	1.6%	1.4%	-6.0%
6	N/A	N/A	N/A	N/A	8.1%	8.3%	5.0%	3.1%	4.1%	3.8%	-0.1%	-5.4%
7	N/A	N/A	N/A	N/A	5,4%	4,5%	4,2%	-0,2%	1,8%	1,1%	-1,2%	-4,8%
8	N/A	N/A	N/A	N/A	4.9%	5.0%	3.2%	1.9%	0.4%	0.6%	-0.4%	-6.6%
Cohesion = 10kPa					Applied surcharge = 0kPa					Low water table		
2	N/A	N/A	N/A	N/A	8.1%	7.5%	-3.5%	-1.7%	0.8%	2.2%	-10.9%	-11.8%
3	N/A	N/A	N/A	N/A	7.9%	7.4%	2.7%	-1.6%	3.3%	1.8%	-6.2%	-9.0%
4	N/A	N/A	N/A	N/A	9.4%	7.0%	6.1%	-1.0%	4.6%	2.0%	-0.6%	-8.4%
5	N/A	N/A	N/A	N/A	9.2%	7.4%	5.2%	0.4%	3.9%	1.9%	-0.1%	-7.5%
6	N/A	N/A	N/A	N/A	11.4%	11.2%	5.1%	3.0%	5.8%	6.5%	-1.0%	-5.7%
7	N/A	N/A	N/A	N/A	9,3%	8,9%	4,2%	0,1%	4,5%	4,5%	-2,7%	-6,8%
8	N/A	N/A	N/A	N/A	9.9%	8.8%	3.4%	1.8%	4.6%	3.2%	-1.2%	-5.0%

Reduction in MoS between LEM methods for a c'=10kPa residual soil												
Slope height (m)	Bishop's method				Fellenius' method				Janbu's method			
	Slope angle				Slope angle				Slope angle			
	1(V):2(H)	1(V):1.5(H)	1(V):1(H)	2(V):1(H)	1(V):2(H)	1(V):1.5(H)	1(V):1(H)	2(V):1(H)	1(V):2(H)	1(V):1.5(H)	1(V):1(H)	2(V):1(H)
Cohesion = 10kPa					Applied surcharge = 0kPa						High water table	
2	N/A	N/A	N/A	N/A	7.0%	5.2%	0.1%	-3.0%	3.4%	1.3%	-9.0%	-9.0%
3	N/A	N/A	N/A	N/A	6.0%	3.9%	2.9%	-12.2%	2.6%	2.2%	0.0%	-13.1%
4	N/A	N/A	N/A	N/A	5.0%	2.5%	-0.8%	-13.3%	3.7%	2.8%	-1.3%	-8.1%
5	N/A	N/A	N/A	N/A	4.4%	1.5%	-7.8%	-22.6%	3.2%	4.2%	-1.4%	-6.7%
6	N/A	N/A	N/A	N/A	5.5%	0.5%	-9.9%	-23.2%	5.4%	4.5%	1.7%	-2.9%
7	N/A	N/A	N/A	N/A	1,3%	-1,3%	-11,2%	-44,9%	4,4%	5,1%	0,9%	-3,5%
8	N/A	N/A	N/A	N/A	1.9%	-2.4%	-14.4%	-54.2%	3.6%	4.2%	1.4%	-3.9%
Cohesion = 10kPa					Applied surcharge = 5kPa						No groundwater	
2	N/A	N/A	N/A	N/A	6.8%	6.0%	-1.8%	-0.3%	3.3%	2.7%	-4.9%	-9.6%
3	N/A	N/A	N/A	N/A	6.7%	5.4%	4.4%	0.4%	2.4%	1.6%	-7.2%	-5.1%
4	N/A	N/A	N/A	N/A	5.8%	5.4%	6.4%	0.2%	2.0%	1.1%	1.5%	-5.3%
5	N/A	N/A	N/A	N/A	6.3%	6.4%	6.6%	1.8%	2.2%	2.7%	2.8%	-4.3%
6	N/A	N/A	N/A	N/A	8.6%	8.3%	5.1%	2.9%	3.9%	3.9%	0.3%	-4.0%
7	N/A	N/A	N/A	N/A	5,2%	5,3%	4,6%	2,5%	2,2%	1,4%	-0,4%	-3,0%
8	N/A	N/A	N/A	N/A	5.0%	5.2%	3.8%	3.0%	0.6%	1.0%	-0.3%	-3.0%

Reduction in MoS between LEM methods for a c'=10kPa residual soil												
Slope height (m)	Bishop's method				Fellenius' method				Janbu's method			
	Slope angle				Slope angle				Slope angle			
	1(V):2(H)	1(V):1.5(H)	1(V):1(H)	2(V):1(H)	1(V):2(H)	1(V):1.5(H)	1(V):1(H)	2(V):1(H)	1(V):2(H)	1(V):1.5(H)	1(V):1(H)	2(V):1(H)
Cohesion = 10kPa					Applied surcharge = 5kPa				Low water table			
2	N/A	N/A	N/A	N/A	9.9%	7.2%	-1.6%	0.3%	6.2%	4.1%	-5.4%	-7.7%
3	N/A	N/A	N/A	N/A	9.5%	7.7%	3.8%	1.5%	5.5%	3.4%	-4.1%	-4.4%
4	N/A	N/A	N/A	N/A	10.0%	8.0%	6.4%	0.2%	5.4%	3.9%	1.0%	-5.8%
5	N/A	N/A	N/A	N/A	9.6%	7.7%	6.4%	1.6%	4.9%	3.0%	1.2%	-5.8%
6	N/A	N/A	N/A	N/A	12.0%	10.9%	5.1%	4.2%	7.5%	5.8%	-0.6%	-4.7%
7	N/A	N/A	N/A	N/A	9,4%	9,0%	4,6%	1,5%	5,4%	4,5%	-1,8%	-5,8%
8	N/A	N/A	N/A	N/A	9.8%	9.1%	3.8%	2.3%	4.7%	3.7%	-1.1%	-3.9%
Cohesion = 10kPa					Applied surcharge = 5kPa				High water table			
2	N/A	N/A	N/A	N/A	7.9%	5.8%	1.7%	0.1%	4.7%	3.6%	-6.4%	-6.7%
3	N/A	N/A	N/A	N/A	7.0%	5.0%	4.0%	-5.3%	4.9%	3.6%	1.0%	-6.0%
4	N/A	N/A	N/A	N/A	5.7%	3.7%	1.8%	-11.8%	4.1%	3.7%	1.4%	-7.2%
5	N/A	N/A	N/A	N/A	4.9%	2.0%	-6.4%	-20.7%	5.2%	4.3%	-0.5%	-5.8%
6	N/A	N/A	N/A	N/A	6.2%	1.8%	-8.2%	-22.0%	5.9%	4.8%	1.9%	0.2%
7	N/A	N/A	N/A	N/A	2,2%	-0,6%	-10,1%	-41,4%	4,7%	5,5%	2,5%	0,0%
8	N/A	N/A	N/A	N/A	2.1%	-2.0%	-13.2%	-51.1%	3.9%	3.9%	1.7%	-1.8%

Reduction in MoS between LEM methods for a c'=10kPa residual soil												
Slope height (m)	Bishop's method				Fellenius' method				Janbu's method			
	Slope angle				Slope angle				Slope angle			
	1(V):2(H)	1(V):1.5(H)	1(V):1(H)	2(V):1(H)	1(V):2(H)	1(V):1.5(H)	1(V):1(H)	2(V):1(H)	1(V):2(H)	1(V):1.5(H)	1(V):1(H)	2(V):1(H)
Cohesion = 10kPa					**Applied surcharge = 10kPa**						**No groundwater**	
2	N/A	N/A	N/A	N/A	7.6%	6.3%	0.0%	2.6%	3.4%	3.3%	-1.7%	-5.3%
3	N/A	N/A	N/A	N/A	6.9%	5.9%	5.1%	1.0%	2.4%	2.2%	1.9%	-3.5%
4	N/A	N/A	N/A	N/A	6.1%	6.2%	6.7%	1.0%	2.0%	1.8%	2.4%	-3.5%
5	N/A	N/A	N/A	N/A	6.1%	7.0%	7.0%	3.2%	2.2%	3.4%	3.3%	-2.6%
6	N/A	N/A	N/A	N/A	8.7%	8.3%	5.2%	3.3%	5.0%	4.3%	1.0%	-2.0%
7	N/A	N/A	N/A	N/A	5,9%	5,3%	5,3%	2,6%	1,2%	0,9%	0,1%	-1,4%
8	N/A	N/A	N/A	N/A	5.3%	4.9%	4.2%	1.9%	1.8%	1.4%	0.1%	-4.1%
Cohesion = 10kPa					**Applied surcharge = 10kPa**						**Low water table**	
2	N/A	N/A	N/A	N/A	10.1%	7.7%	0.0%	2.2%	6.3%	5.2%	-2.1%	-4.6%
3	N/A	N/A	N/A	N/A	10.2%	8.2%	4.8%	1.0%	5.9%	4.1%	-2.5%	-4.0%
4	N/A	N/A	N/A	N/A	10.4%	9.0%	6.7%	1.0%	5.8%	5.0%	1.9%	-3.9%
5	N/A	N/A	N/A	N/A	10.2%	7.8%	7.0%	3.1%	5.6%	3.4%	1.9%	-4.0%
6	N/A	N/A	N/A	N/A	12.2%	11.0%	5.2%	4.6%	8.4%	6.7%	0.5%	-3.0%
7	N/A	N/A	N/A	N/A	9,8%	9,0%	5,3%	2,7%	5,7%	5,1%	-0,9%	-2,2%
8	N/A	N/A	N/A	N/A	9.7%	9.4%	4.2%	3.4%	4.9%	4.4%	-1.2%	-2.6%

Reduction in MoS between LEM methods for a c'=10kPa residual soil												
Slope height (m)	Bishop's method				Fellenius' method				Janbu's method			
	Slope angle				Slope angle				Slope angle			
	1(V):2(H)	1(V):1.5(H)	1(V):1(H)	2(V):1(H)	1(V):2(H)	1(V):1.5(H)	1(V):1(H)	2(V):1(H)	1(V):2(H)	1(V):1.5(H)	1(V):1(H)	2(V):1(H)
Cohesion = 10kPa					Applied surcharge = 10kPa				High water table			
2	N/A	N/A	N/A	N/A	8.7%	6.3%	4.6%	-0.8%	5.9%	4.7%	-3.5%	-8.3%
3	N/A	N/A	N/A	N/A	7.9%	6.0%	4.7%	-6.5%	5.1%	3.9%	1.4%	-6.8%
4	N/A	N/A	N/A	N/A	6.2%	5.2%	3.1%	-10.7%	4.7%	5.1%	3.2%	-6.5%
5	N/A	N/A	N/A	N/A	5.3%	2.9%	-5.0%	-19.0%	5.6%	4.9%	0.6%	-4.4%
6	N/A	N/A	N/A	N/A	6.4%	2.5%	-6.6%	-20.5%	6.3%	5.5%	2.5%	0.1%
7	N/A	N/A	N/A	N/A	2,6%	0,0%	-9,1%	-39,6%	4,2%	5,4%	2,7%	-0,1%
8	N/A	N/A	N/A	N/A	2.6%	-1.3%	-12.0%	-47.9%	5.6%	5.6%	3.7%	-0.5%

Appendix C – Examples of SLOPE/W runs outputs

C.1 1(V):2(H) slope with no surcharge and no effective cohesion

C.1.1 No groundwater

Slope height 5.0m

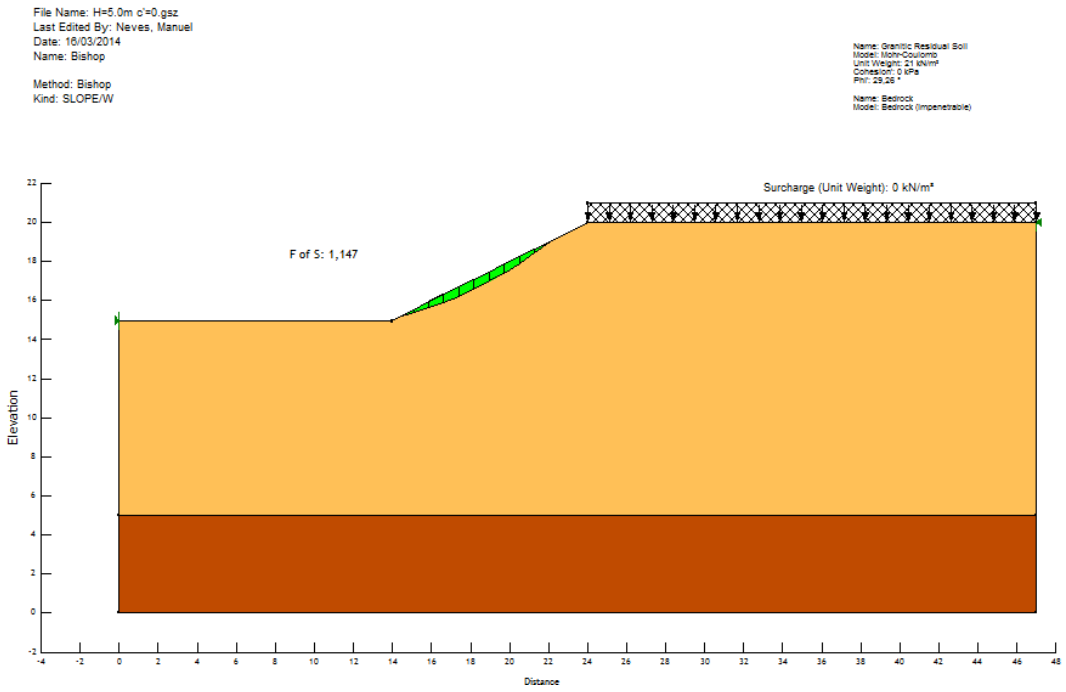

File Name: H=5.0m c'=0.gsz
Last Edited By: Neves, Manuel
Date: 16/03/2014
Name: Fellenius

Method: Ordinary
Kind: SLOPE/W

Name: Granitic Residual Soil
Model: Mohr-Coulomb
Unit Weight: 21 kN/m³
Cohesion: 0 kPa
Phi: 29,26 °

Name: Bedrock
Model: Bedrock (Impenetrable)

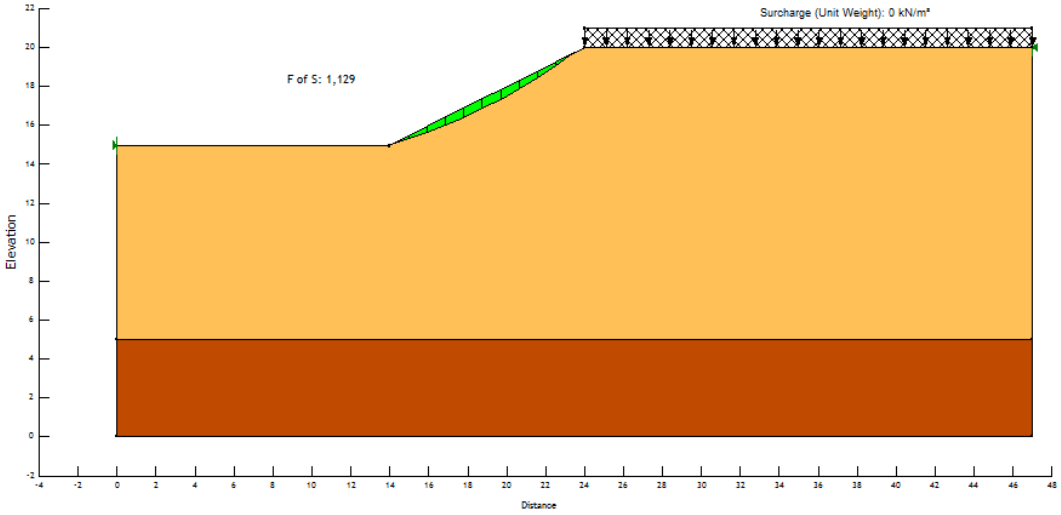

File Name: H=5.0m c'=0.gsz
Last Edited By: Neves, Manuel
Date: 16/03/2014
Name: Janbu

Method: Janbu
Kind: SLOPE/W

Name: Granitic Residual Soil
Model: Mohr-Coulomb
Unit Weight: 21 kN/m³
Cohesion: 0 kPa
Phi: 29,26 °

Name: Bedrock
Model: Bedrock (Impenetrable)

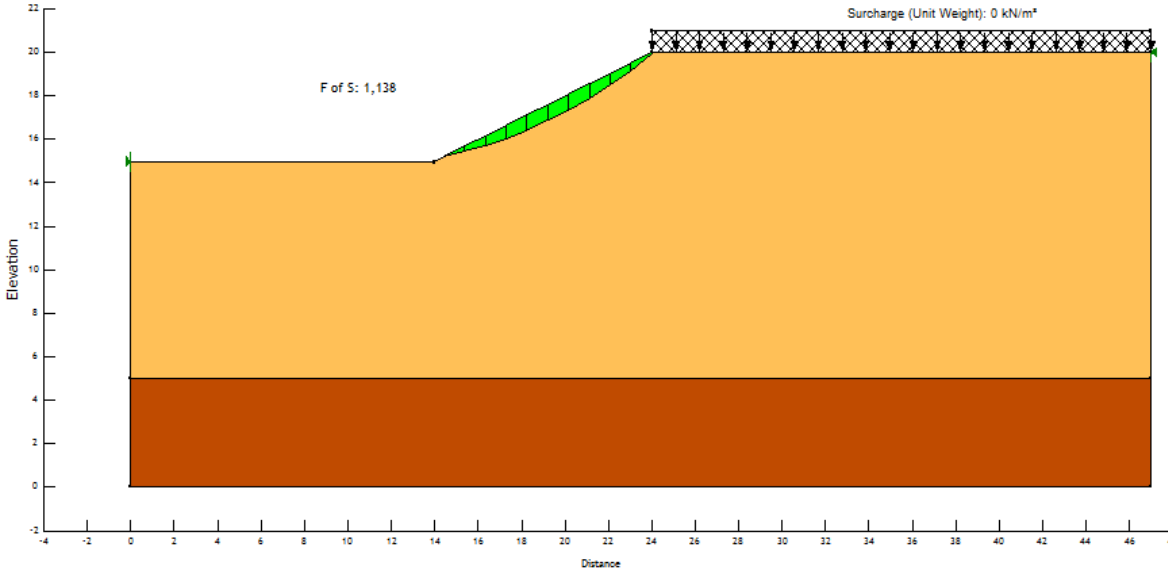

C.1.2 Low water table

Slope height 5.0m

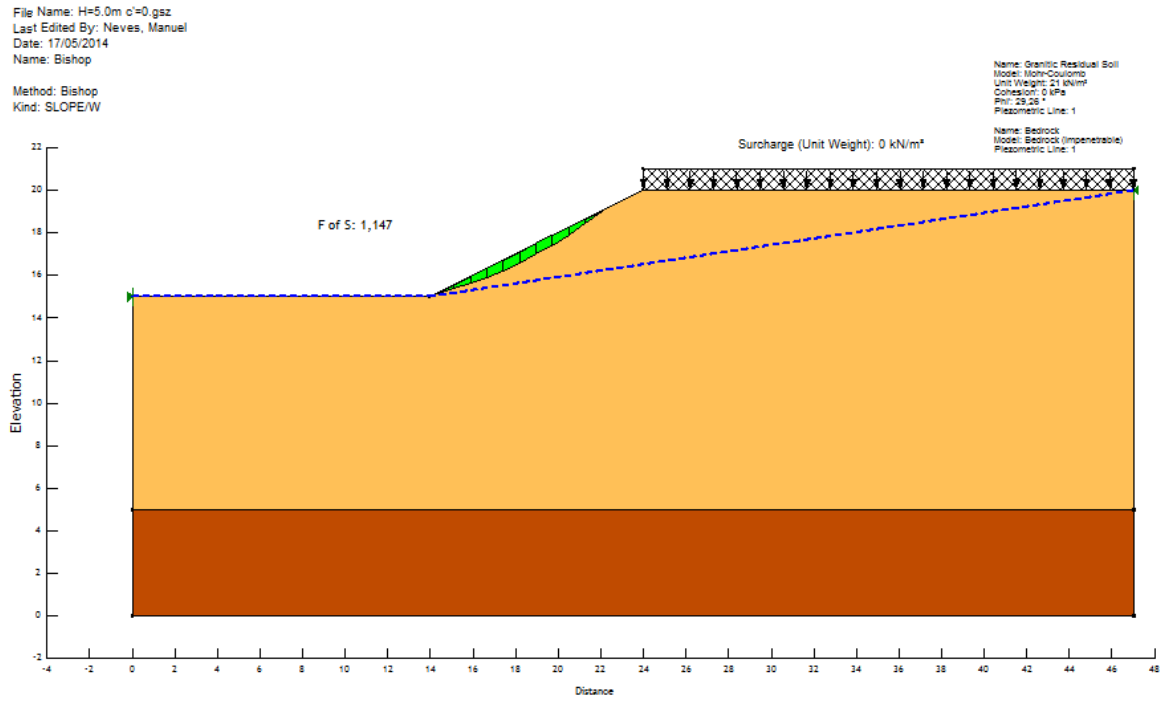

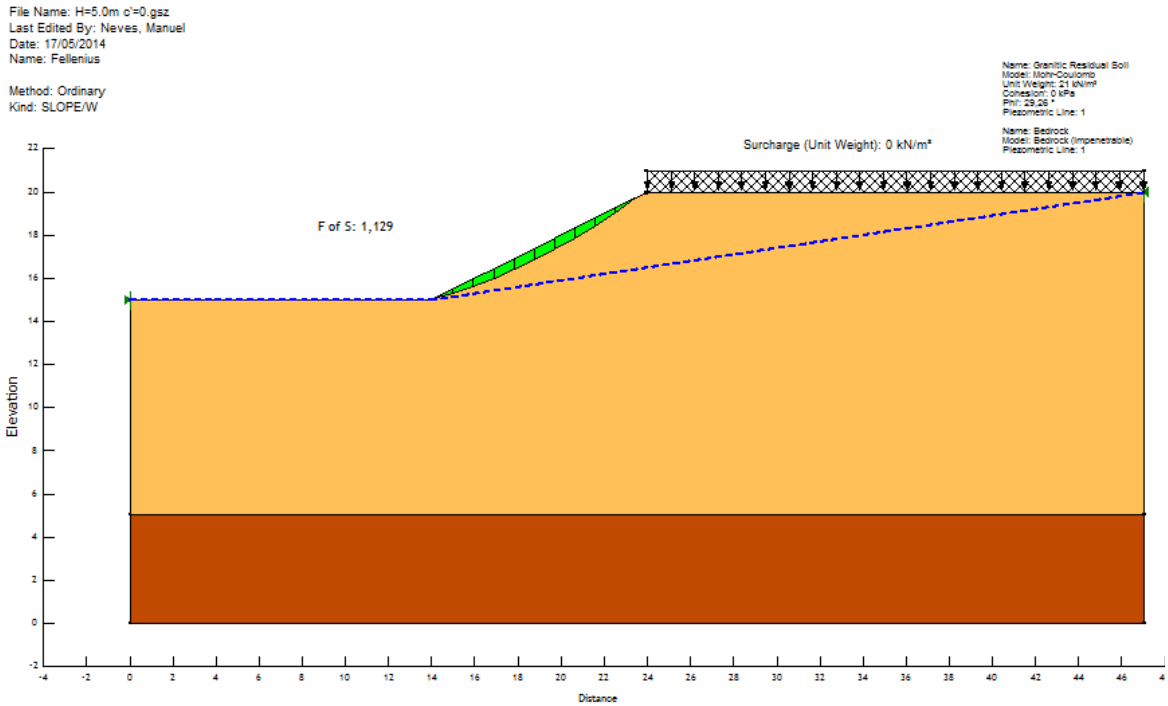

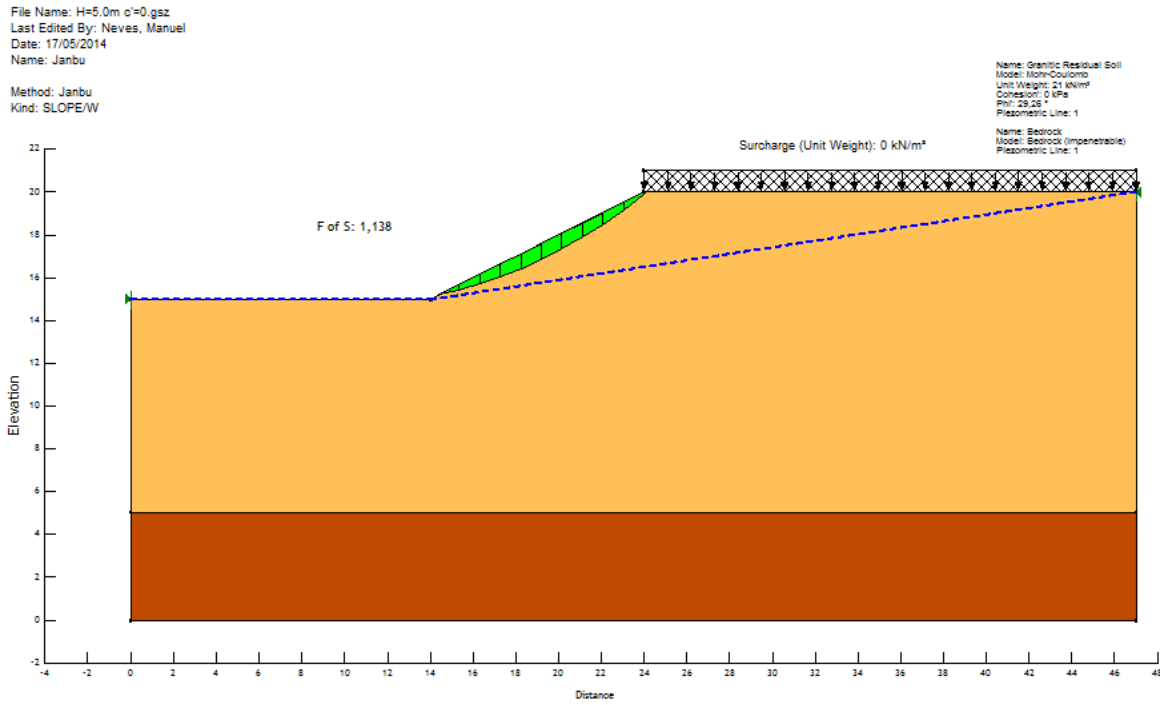

C.1.3 High water table

Slope height 5.0m

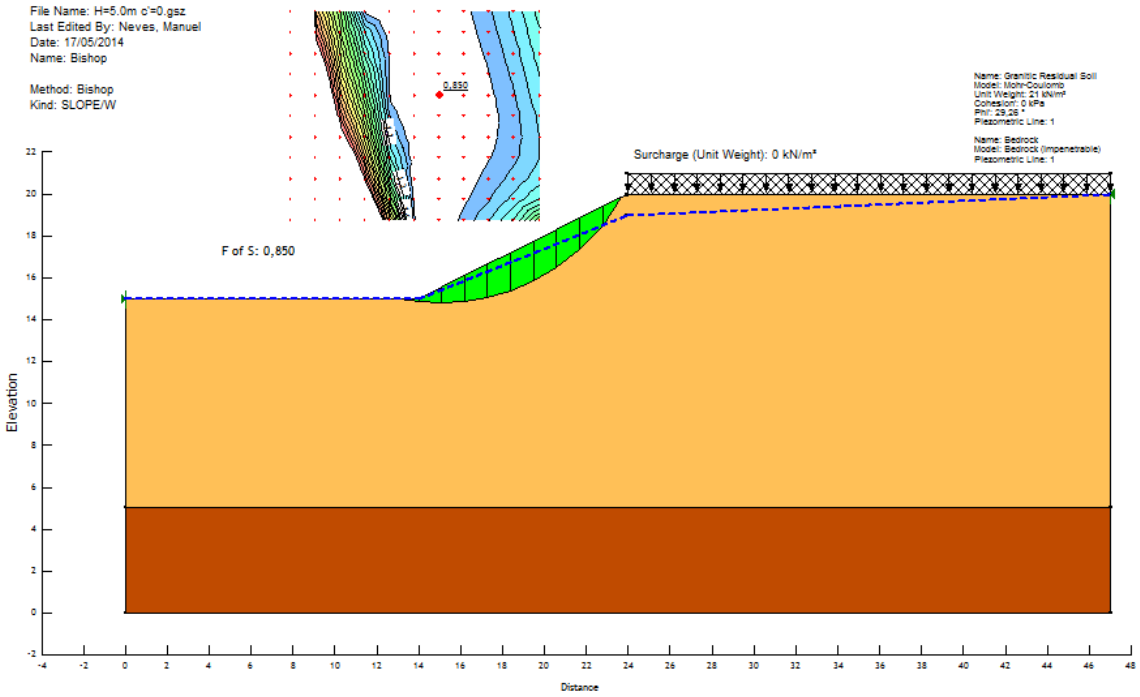

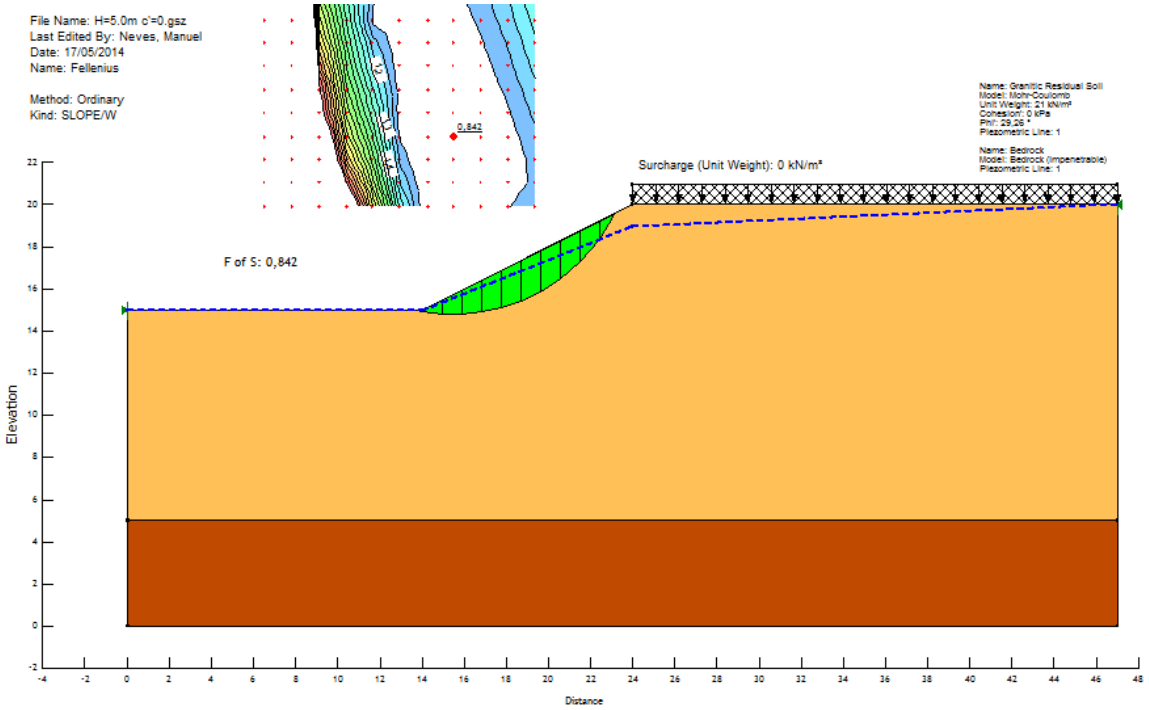
File Name: H=5.0m c'=0.gsz
Last Edited By: Neves, Manuel
Date: 17/05/2014
Name: Fellenius
Method: Ordinary
Kind: SLOPE/W
0,842
F of S: 0,842
Surcharge (Unit Weight): 0 kN/m²
Name: Granitic Residual Soil
Model: Mohr-Coulomb
Unit Weight: 21 kN/m³
Cohesion: 0 kPa
Phi': 29,26 °
Piezometric Line: 1
Name: Bedrock
Model: Bedrock (Impenetrable)
Piezometric Line: 1
Elevation
Distance

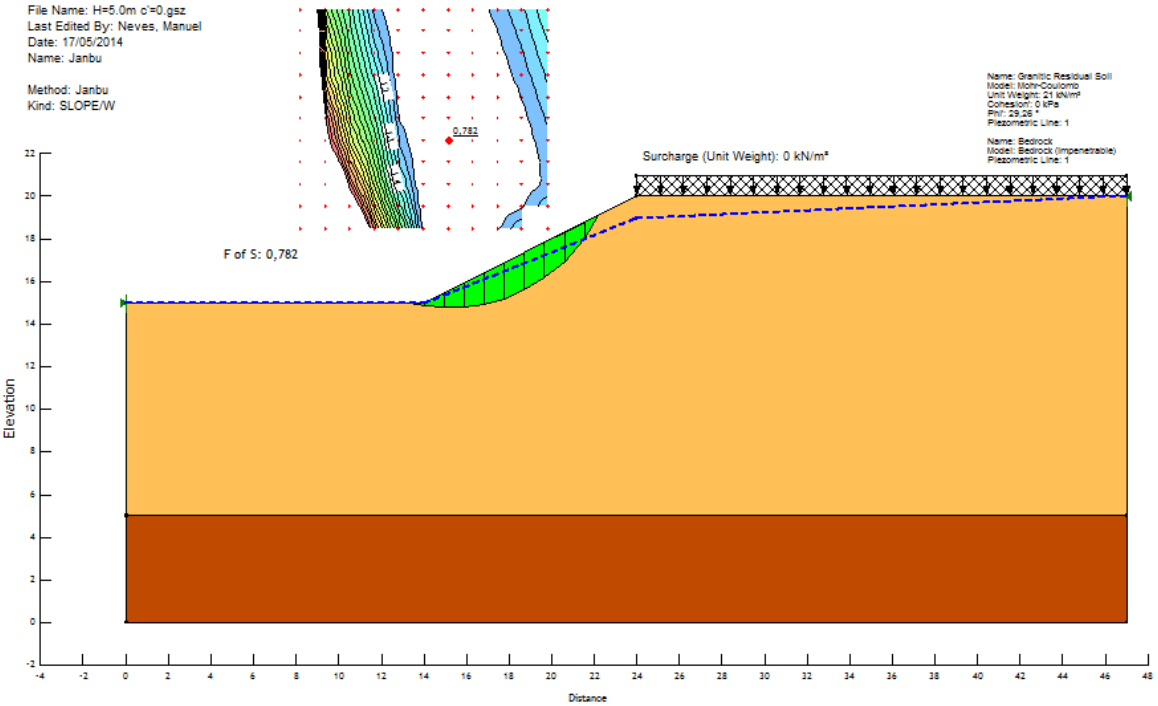
File Name: H=5.0m c'=0.gsz
Last Edited By: Neves, Manuel
Date: 17/05/2014
Name: Janbu
Method: Janbu
Kind: SLOPE/W
0,782
F of S: 0,782
Surcharge (Unit Weight): 0 kN/m²
Name: Granitic Residual Soil
Model: Mohr-Coulomb
Unit Weight: 21 kN/m³
Cohesion: 0 kPa
Phi': 29,26 °
Piezometric Line: 1
Name: Bedrock
Model: Bedrock (Impenetrable)
Piezometric Line: 1
Elevation
Distance

C.2 1(V):1.5(H) slope with a 10kPa surcharge and a 5kPa effective cohesion

C.2.1 No groundwater

Slope height 8.0m

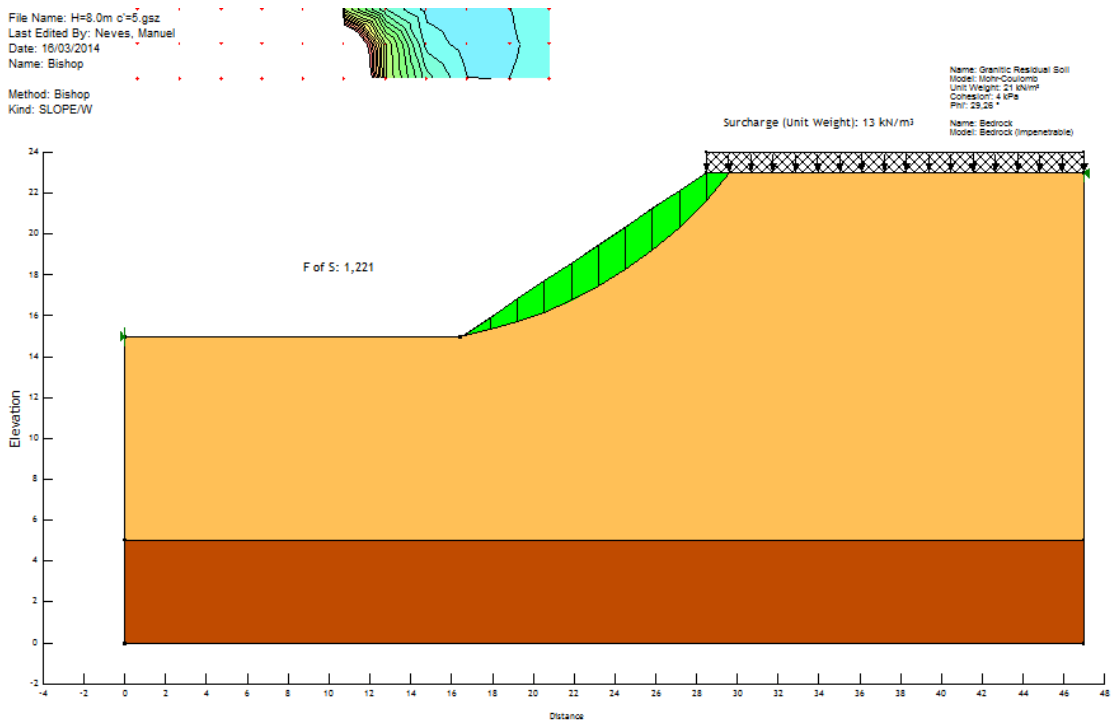

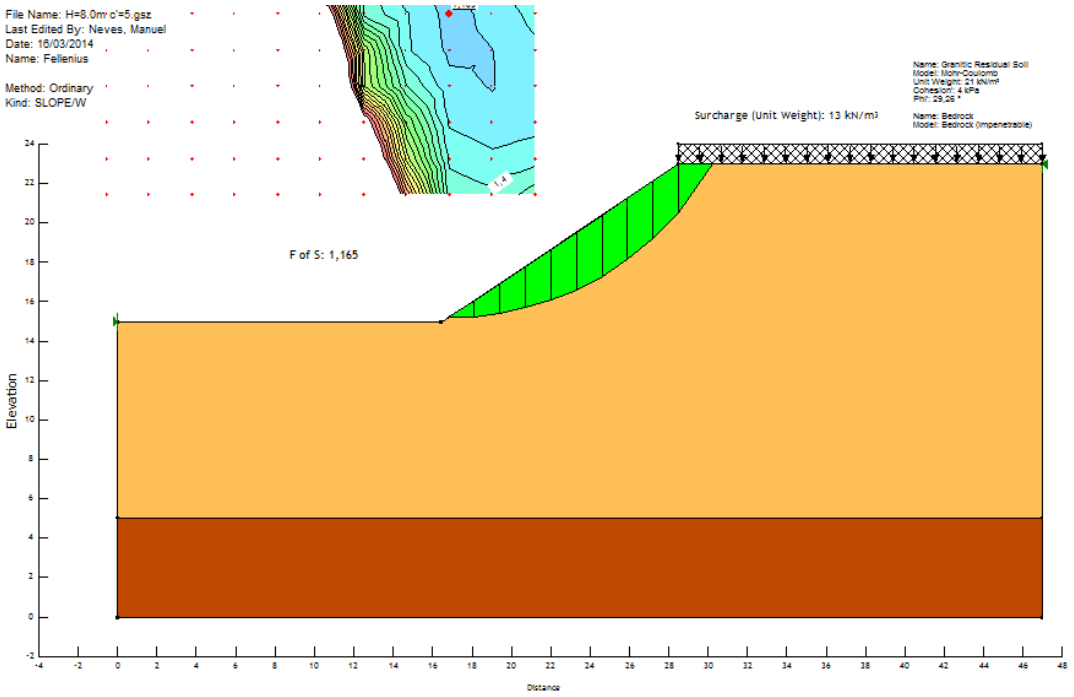
File Name: H=8.0m c'=5.gsz
Last Edited By: Neves, Manuel
Date: 16/03/2014
Name: Fellenius
Method: Ordinary
Kind: SLOPE/W
Surcharge (Unit Weight): 13 kN/m³
Name: Granitic Residual Soil
Model: Mohr-Coulomb
Unit Weight: 21 kN/m³
Cohesion: 4 kPa
Phi': 29,26 °
Name: Bedrock
Model: Bedrock (Impenetrable)
F of S: 1,165
Elevation
Distance

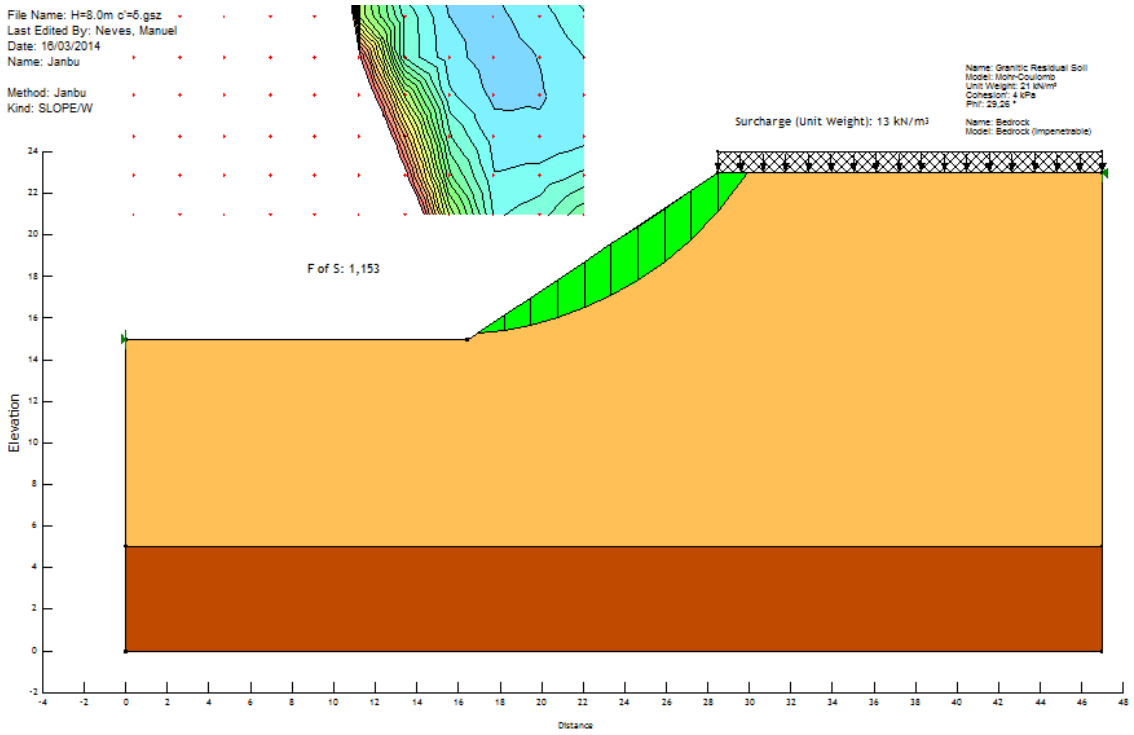
File Name: H=8.0m c'=5.gsz
Last Edited By: Neves, Manuel
Date: 16/03/2014
Name: Janbu
Method: Janbu
Kind: SLOPE/W
Surcharge (Unit Weight): 13 kN/m³
Name: Granitic Residual Soil
Model: Mohr-Coulomb
Unit Weight: 21 kN/m³
Cohesion: 4 kPa
Phi': 29,26 °
Name: Bedrock
Model: Bedrock (Impenetrable)
F of S: 1,153
Elevation
Distance

C.2.2 Low water table

Slope height 8.0m

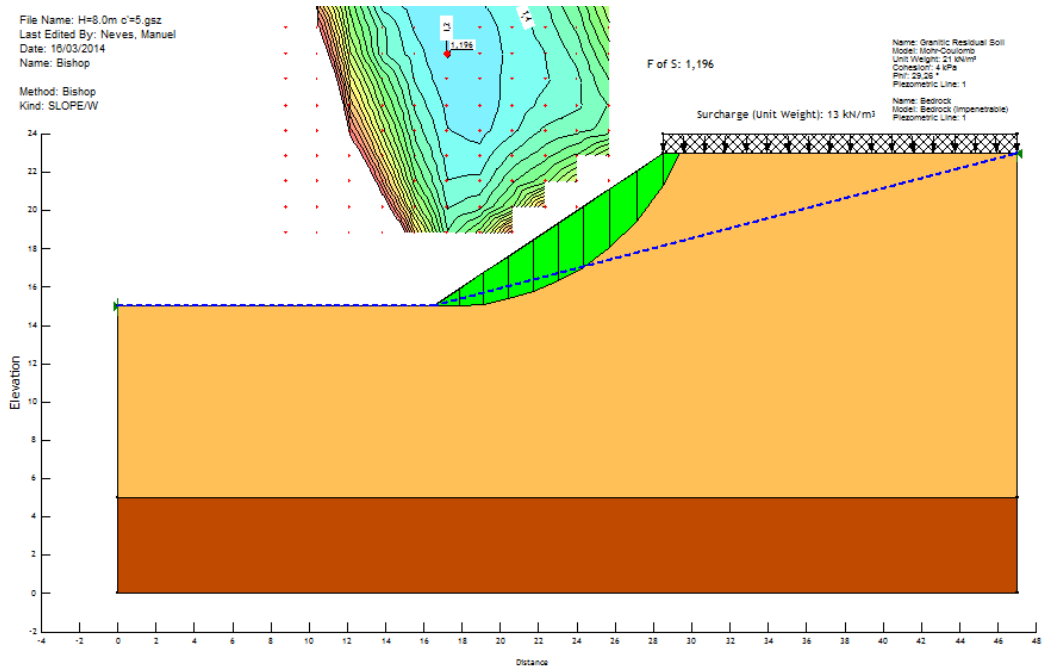

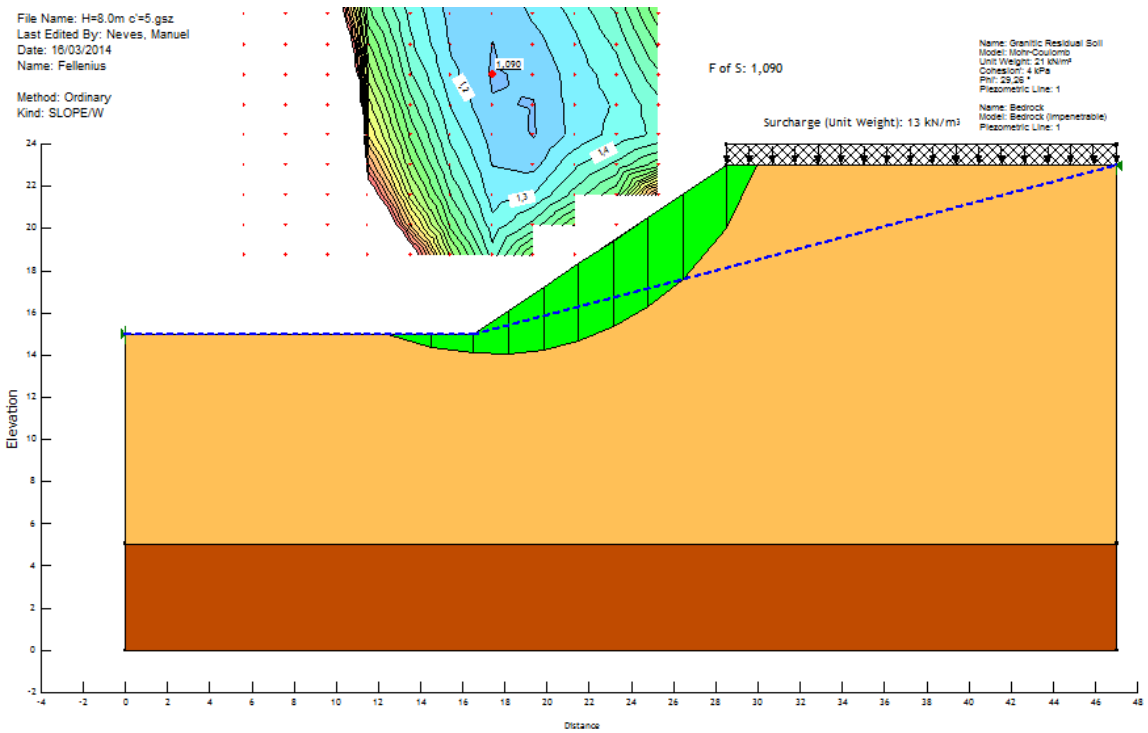

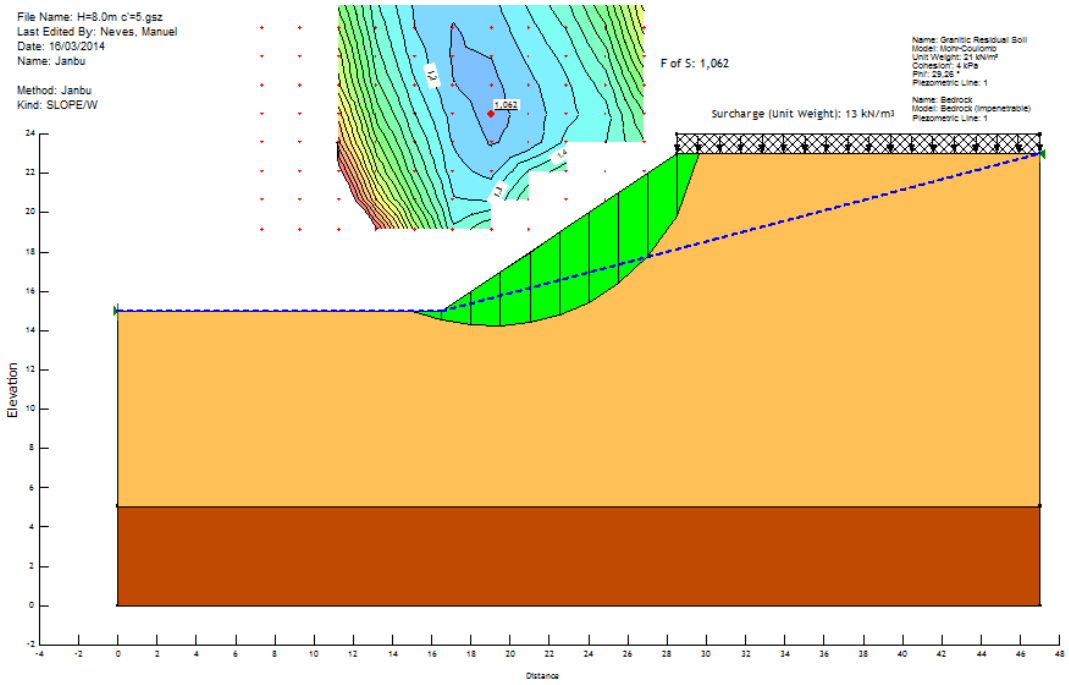

C.2.3 High water table

Slope height 8.0m

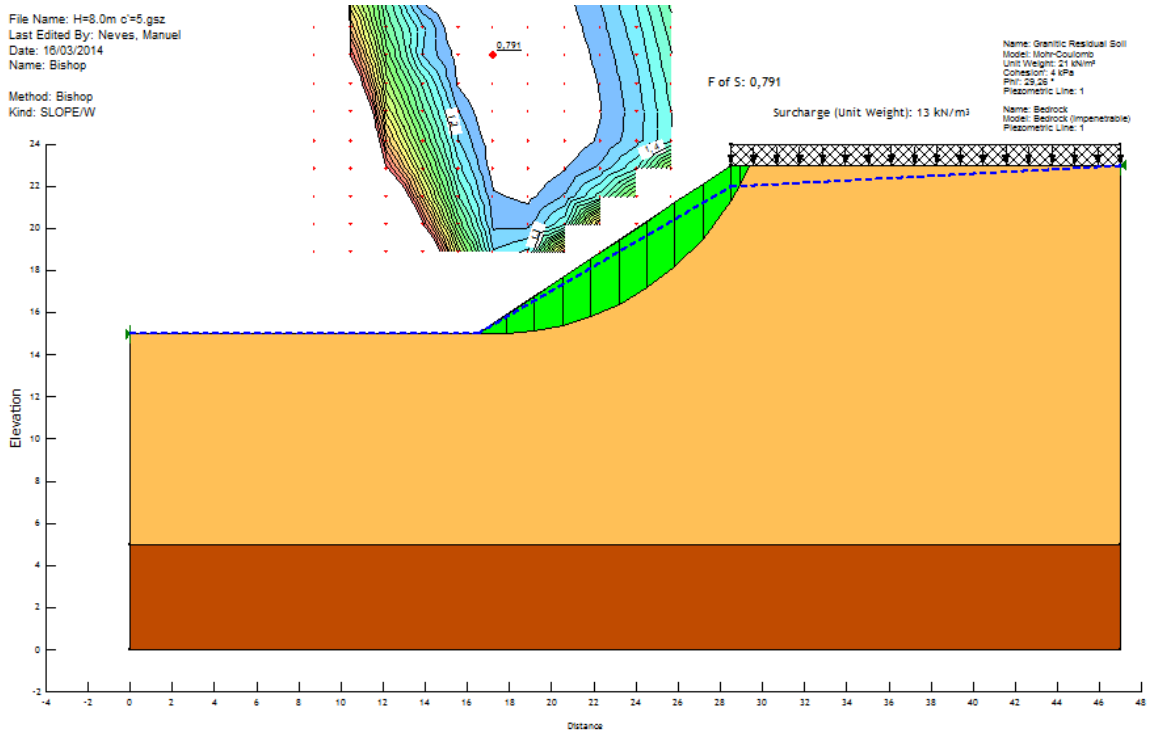

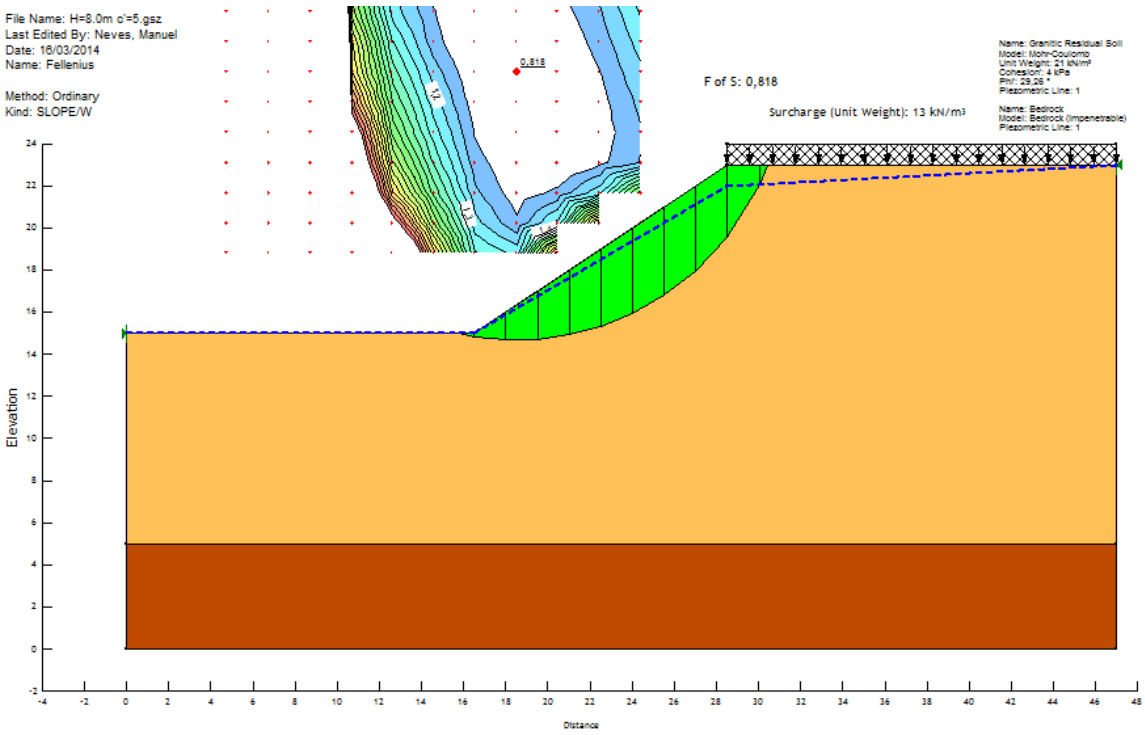
File Name: H=8.0m c'=5.gsz
Last Edited By: Neves, Manuel
Date: 16/03/2014
Name: Fellenius
Method: Ordinary
Kind: SLOPE/W
F of S: 0,818
Surcharge (Unit Weight): 13 kN/m³
Name: Granitic Residual Soil
Model: Mohr-Coulomb
Unit Weight: 21 kN/m³
Cohesion: 4 kPa
Phi': 29,26 °
Piezometric Line: 1
Name: Bedrock
Model: Bedrock (Impenetrable)
Piezometric Line: 1
Elevation
Distance

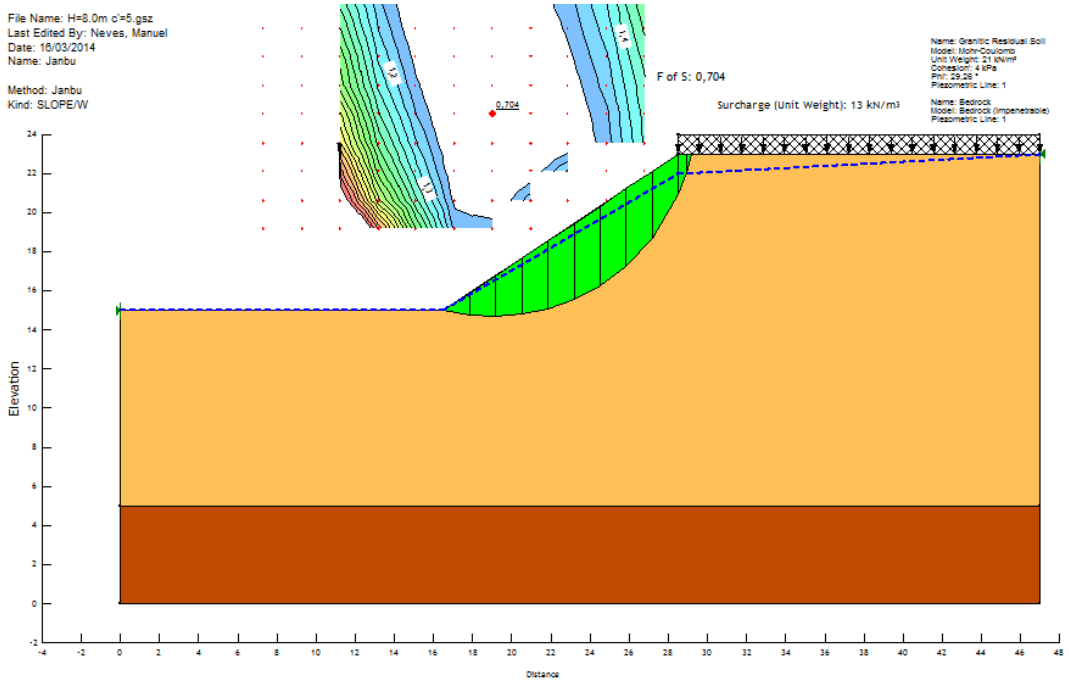
File Name: H=8.0m c'=5.gsz
Last Edited By: Neves, Manuel
Date: 16/03/2014
Name: Janbu
Method: Janbu
Kind: SLOPE/W
F of S: 0,704
Surcharge (Unit Weight): 13 kN/m³
Name: Granitic Residual Soil
Model: Mohr-Coulomb
Unit Weight: 21 kN/m³
Cohesion: 4 kPa
Phi': 29,26 °
Piezometric Line: 1
Name: Bedrock
Model: Bedrock (Impenetrable)
Piezometric Line: 1
Elevation
Distance

C.3 1(V):1(H) slope with a 5kPa surcharge and a 10kPa effective cohesion

C.3.1 No groundwater

Slope height 5.0m

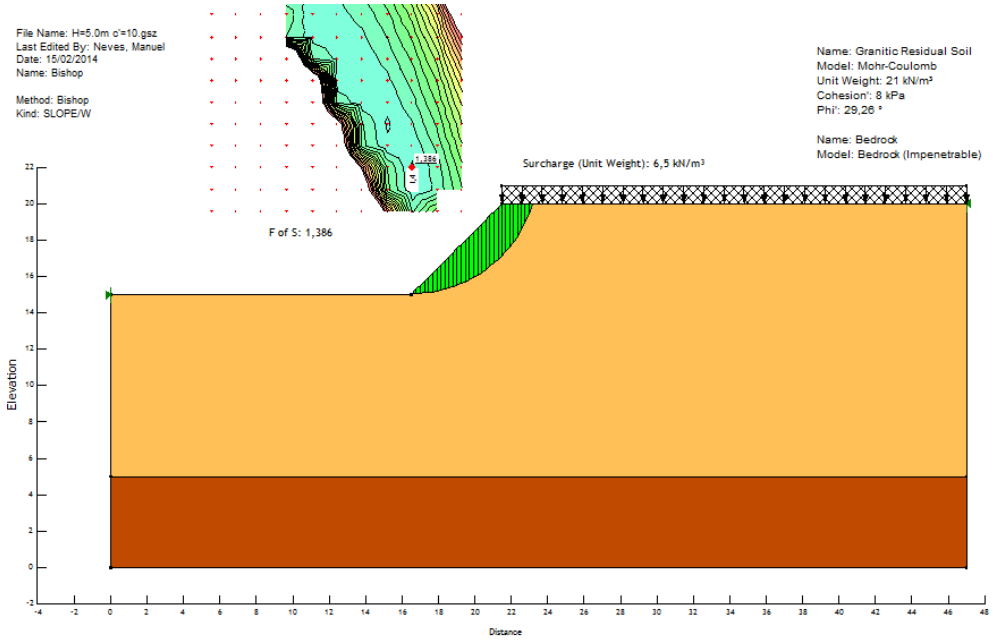

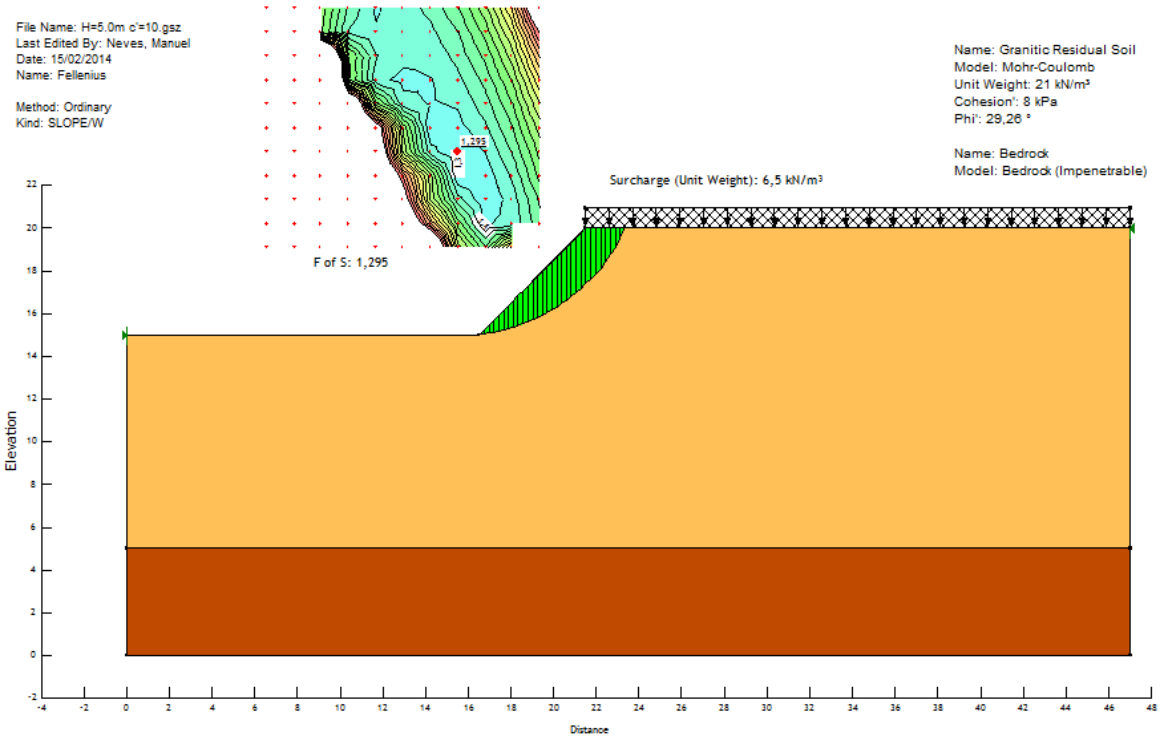
File Name: H=5.0m c'=10.gsz
Last Edited By: Neves, Manuel
Date: 15/02/2014
Name: Fellenius
Method: Ordinary
Kind: SLOPE/W
Name: Granitic Residual Soil
Model: Mohr-Coulomb
Unit Weight: 21 kN/m³
Cohesion': 8 kPa
Phi': 29,26 °
Name: Bedrock
Model: Bedrock (Impenetrable)
Surcharge (Unit Weight): 6,5 kN/m³
F of S: 1,295
Elevation
Distance

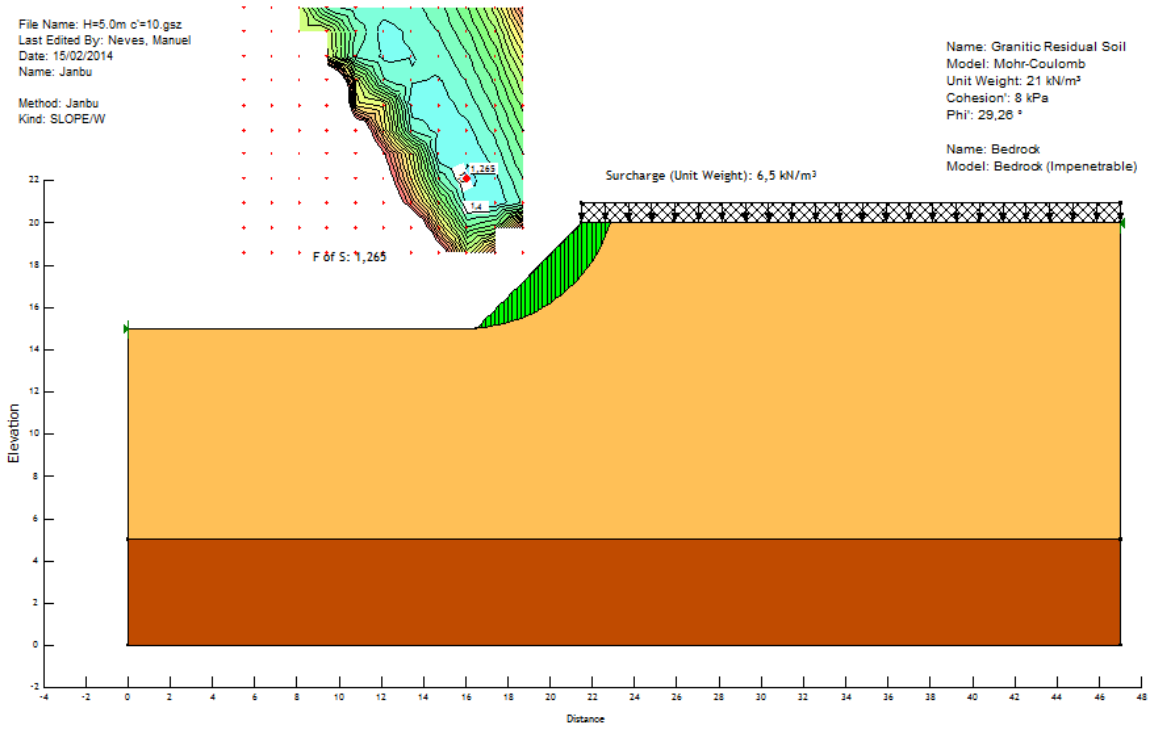
File Name: H=5.0m c'=10.gsz
Last Edited By: Neves, Manuel
Date: 15/02/2014
Name: Janbu
Method: Janbu
Kind: SLOPE/W
Name: Granitic Residual Soil
Model: Mohr-Coulomb
Unit Weight: 21 kN/m³
Cohesion': 8 kPa
Phi': 29,26 °
Name: Bedrock
Model: Bedrock (Impenetrable)
Surcharge (Unit Weight): 6,5 kN/m³
F of S: 1,265
Elevation
Distance

C.3.2 Low water table

Slope height 5.0m

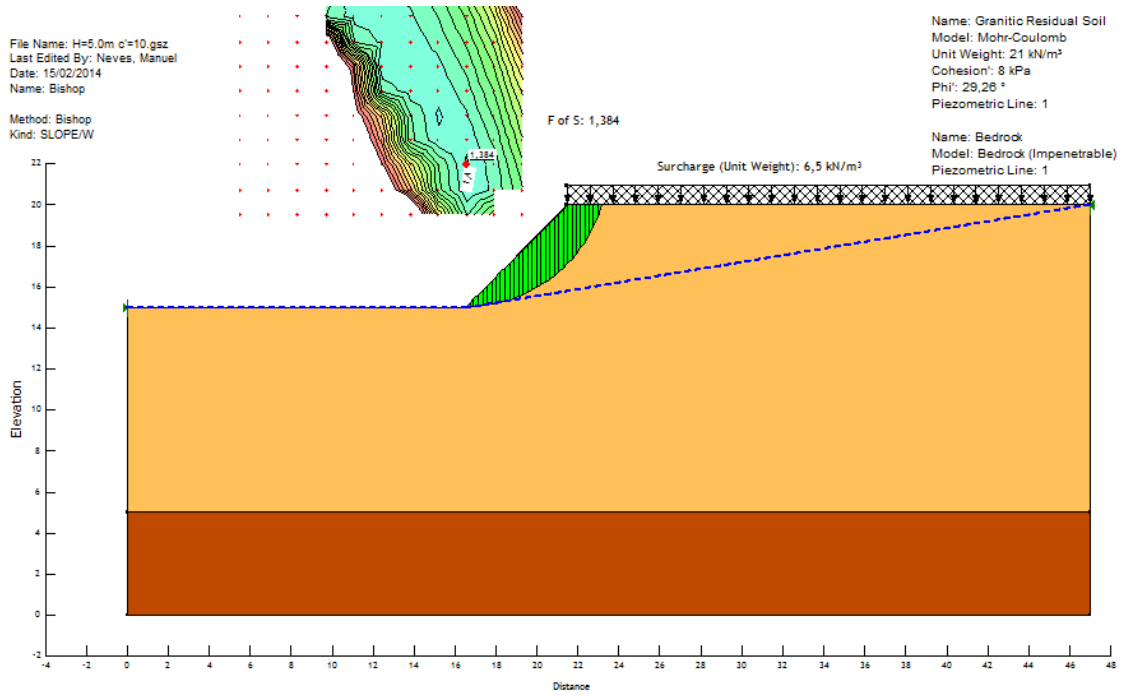

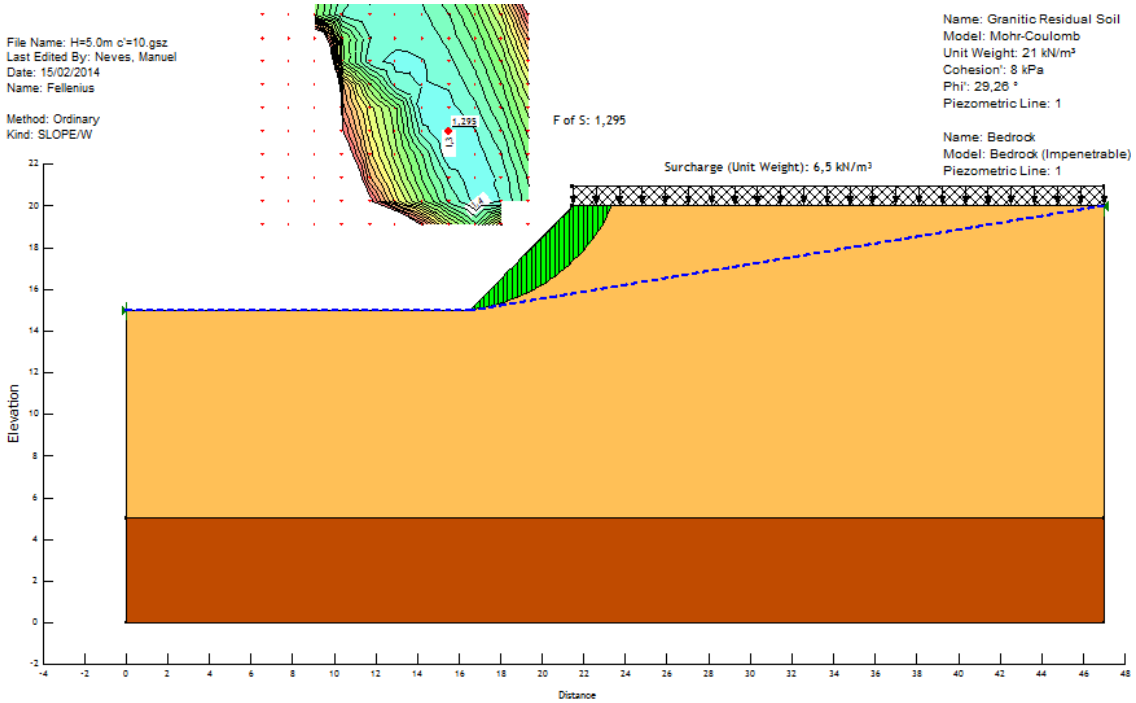

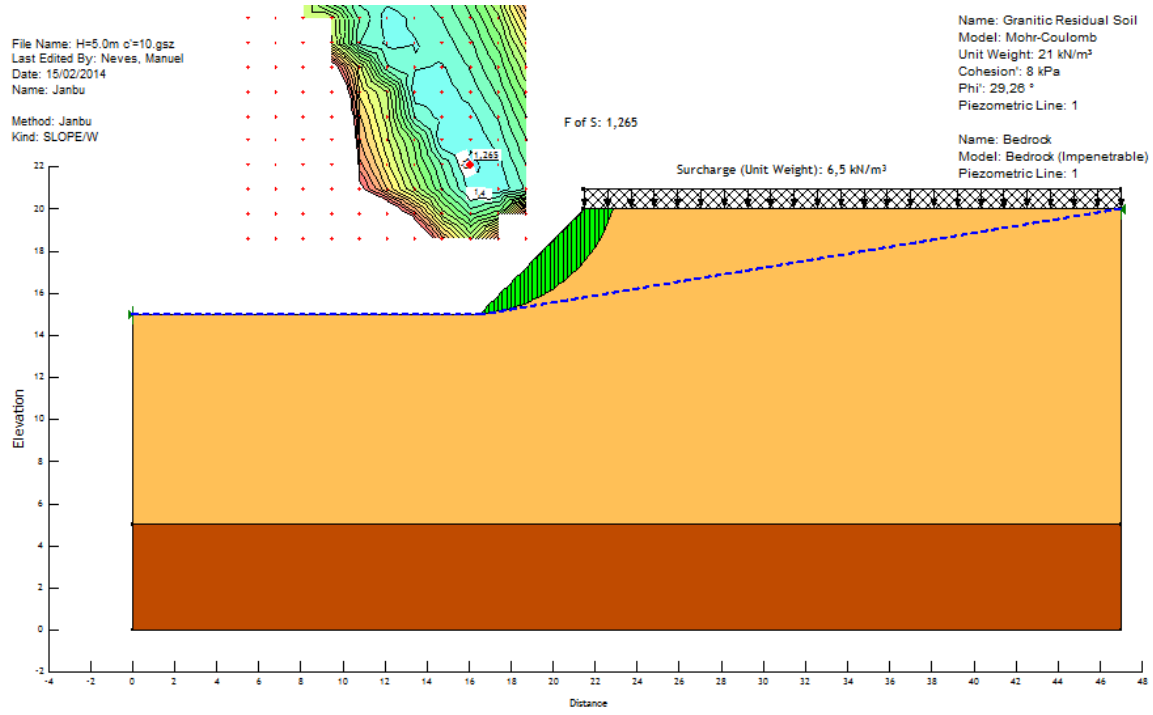

C.3.3 High water table

Slope height 5.0m

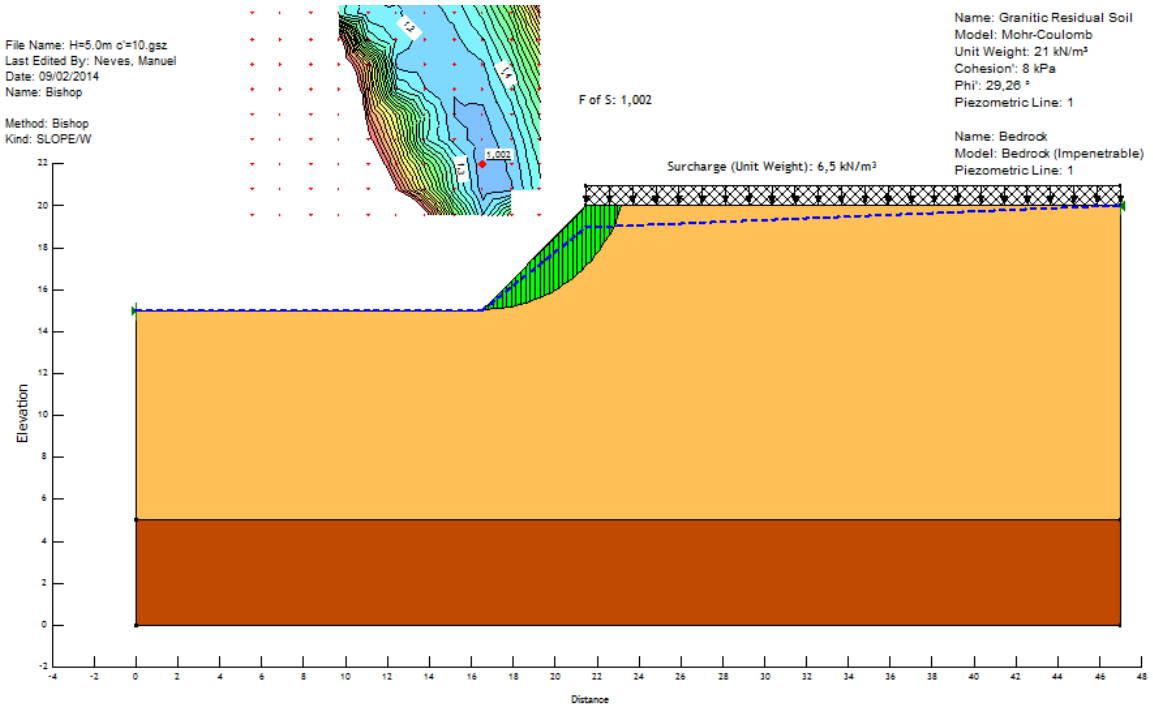

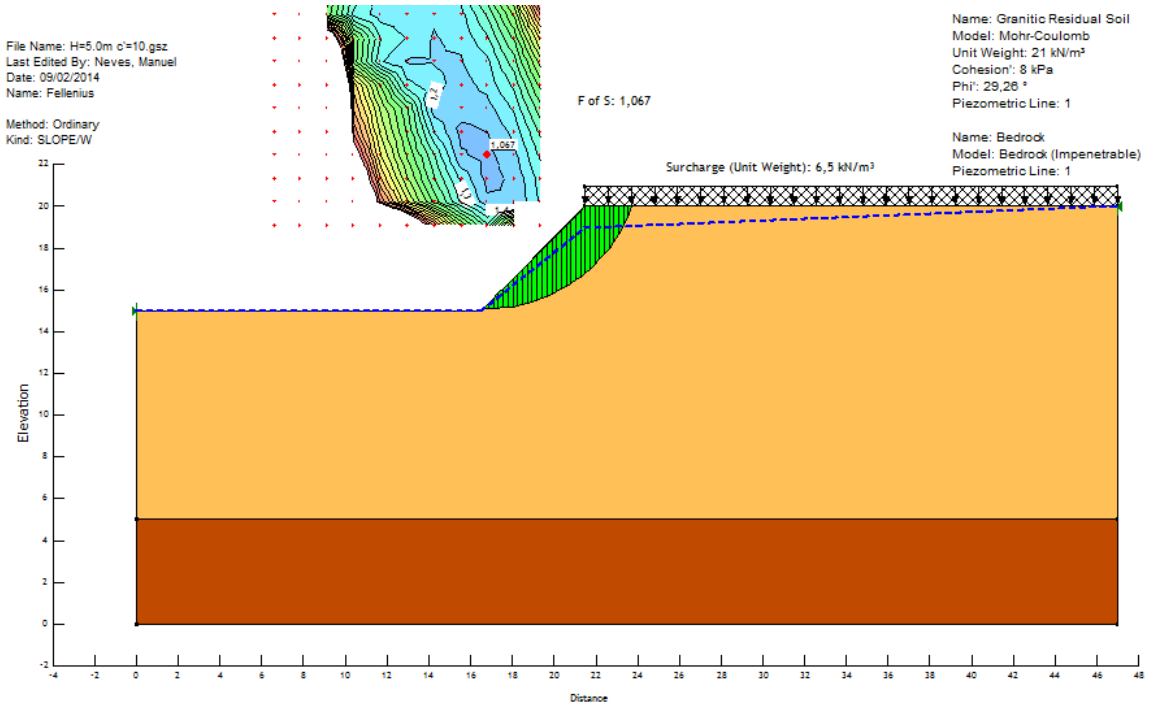
File Name: H=5.0m c'=10.gsz
Last Edited By: Neves, Manuel
Date: 09/02/2014
Name: Fellenius
Method: Ordinary
Kind: SLOPE/W
F of S: 1,067
Surcharge (Unit Weight): 6,5 kN/m³
Name: Granitic Residual Soil
Model: Mohr-Coulomb
Unit Weight: 21 kN/m³
Cohesion': 8 kPa
Phi': 29,26 °
Piezometric Line: 1
Name: Bedrock
Model: Bedrock (Impenetrable)
Piezometric Line: 1
Elevation
Distance

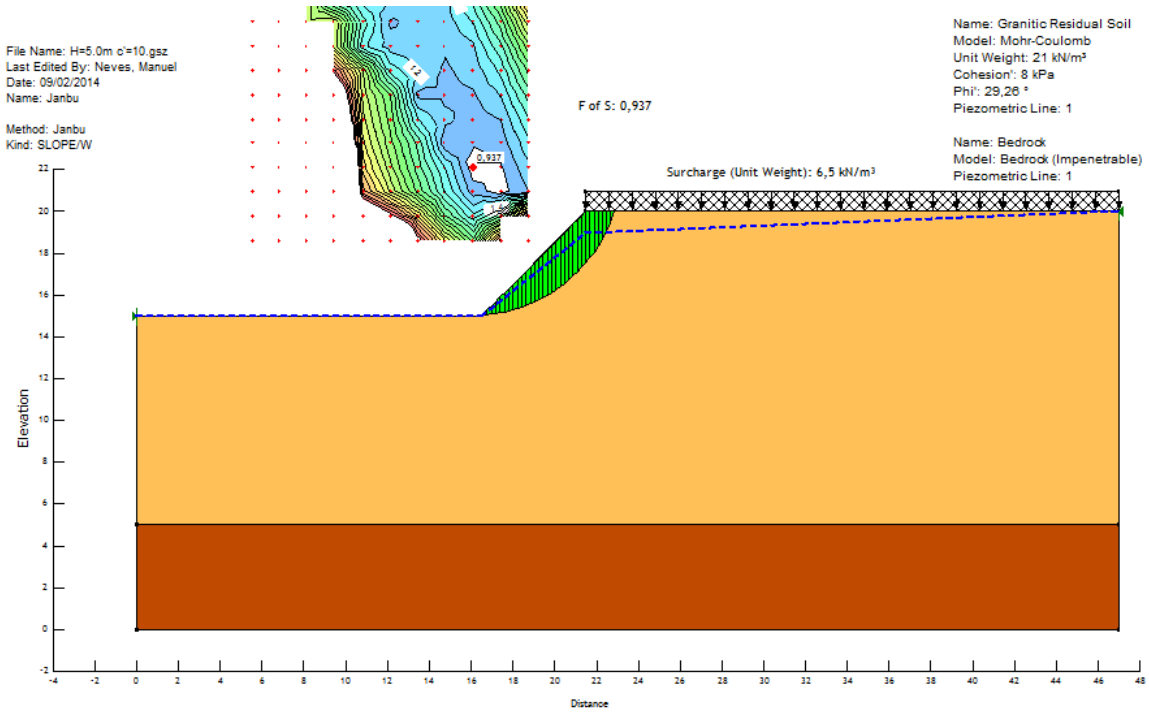
File Name: H=5.0m c'=10.gsz
Last Edited By: Neves, Manuel
Date: 09/02/2014
Name: Janbu
Method: Janbu
Kind: SLOPE/W
F of S: 0,937
Surcharge (Unit Weight): 6,5 kN/m³
Name: Granitic Residual Soil
Model: Mohr-Coulomb
Unit Weight: 21 kN/m³
Cohesion': 8 kPa
Phi': 29,26 °
Piezometric Line: 1
Name: Bedrock
Model: Bedrock (Impenetrable)
Piezometric Line: 1
Elevation
Distance

C.4 2(V):1(H) slope with a 10kPa surcharge and a 10kPa effective cohesion

C.4.1 No groundwater

Slope height 8.0m

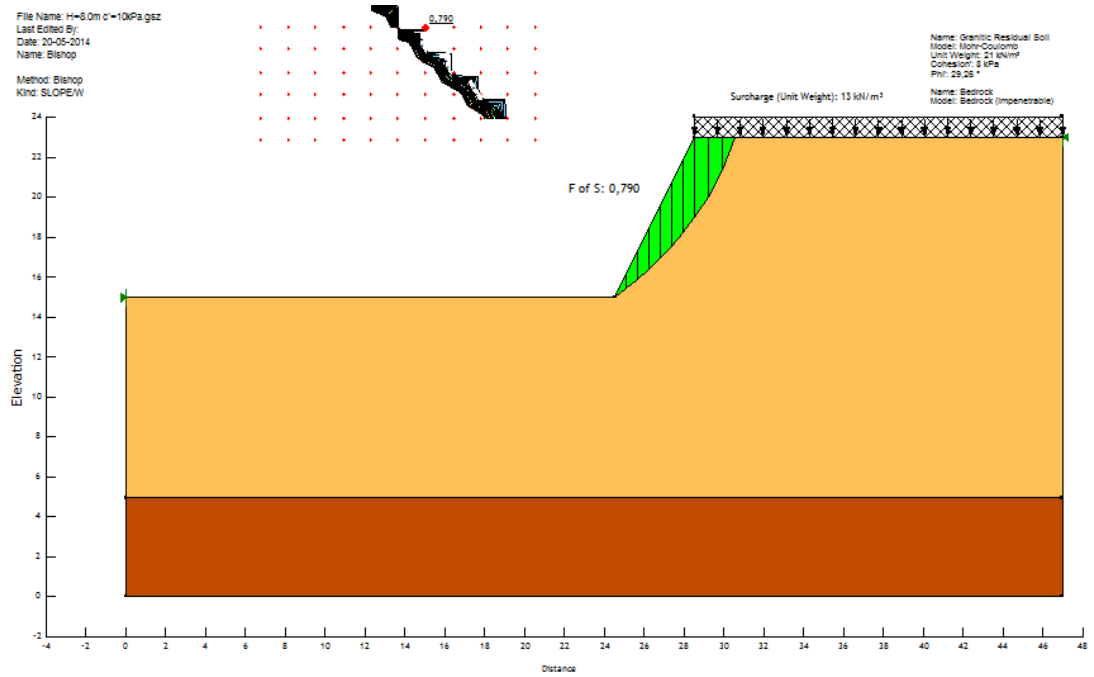

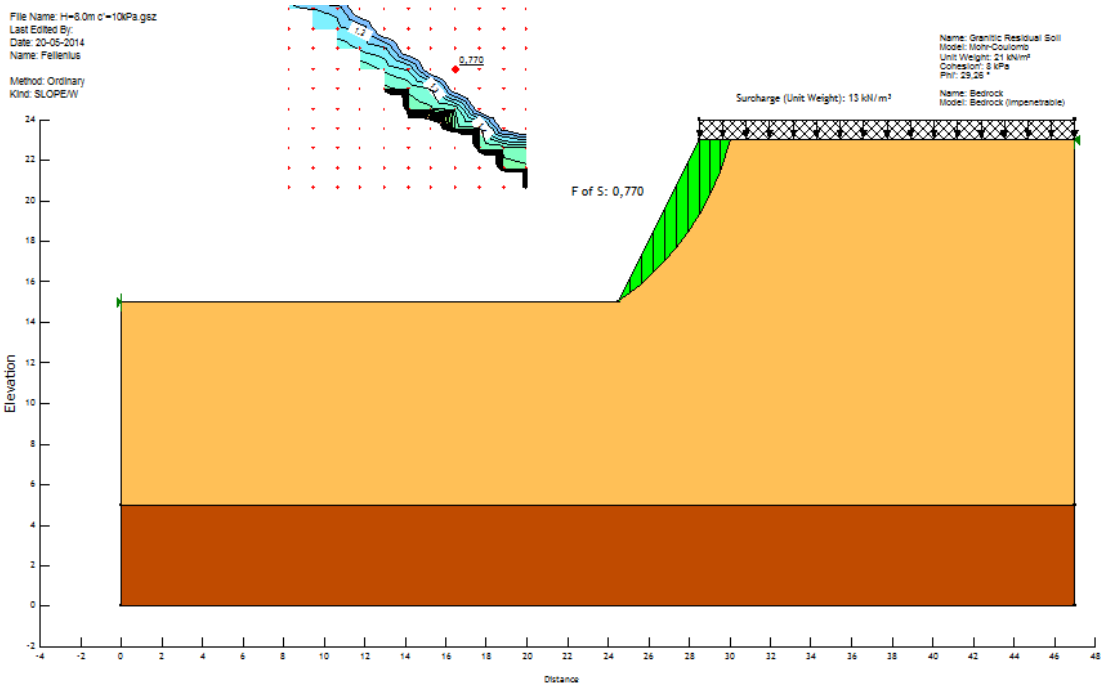

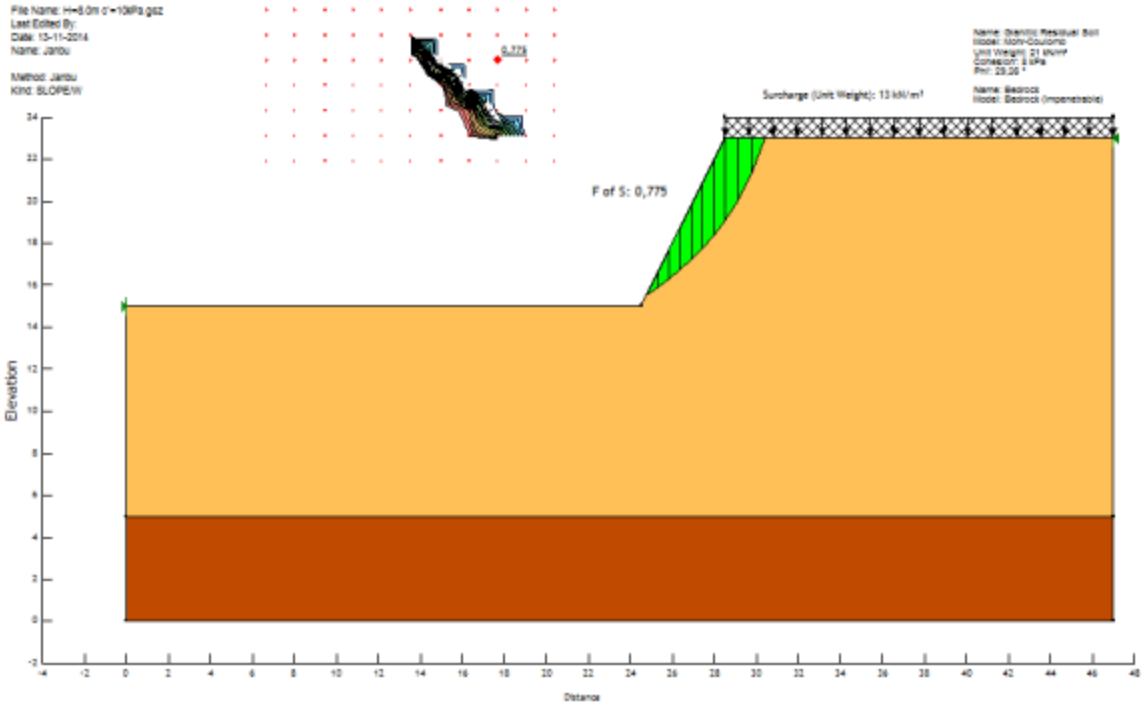

C.4.2 Low water table

Slope height 8.0m

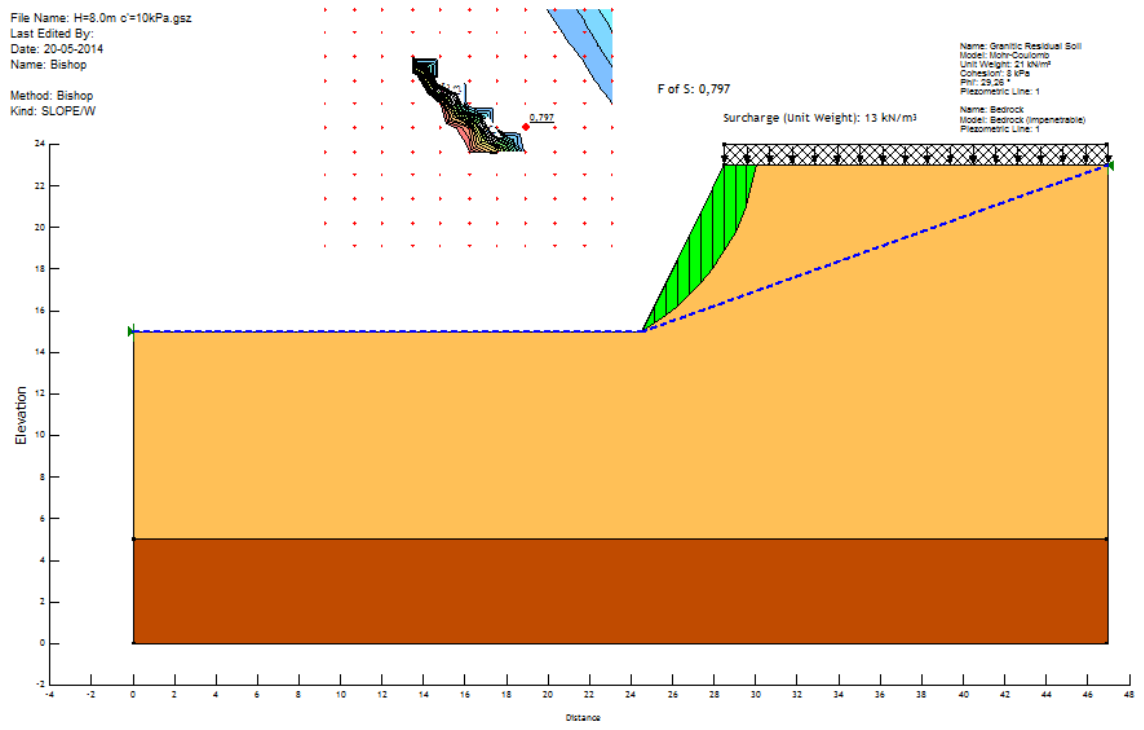

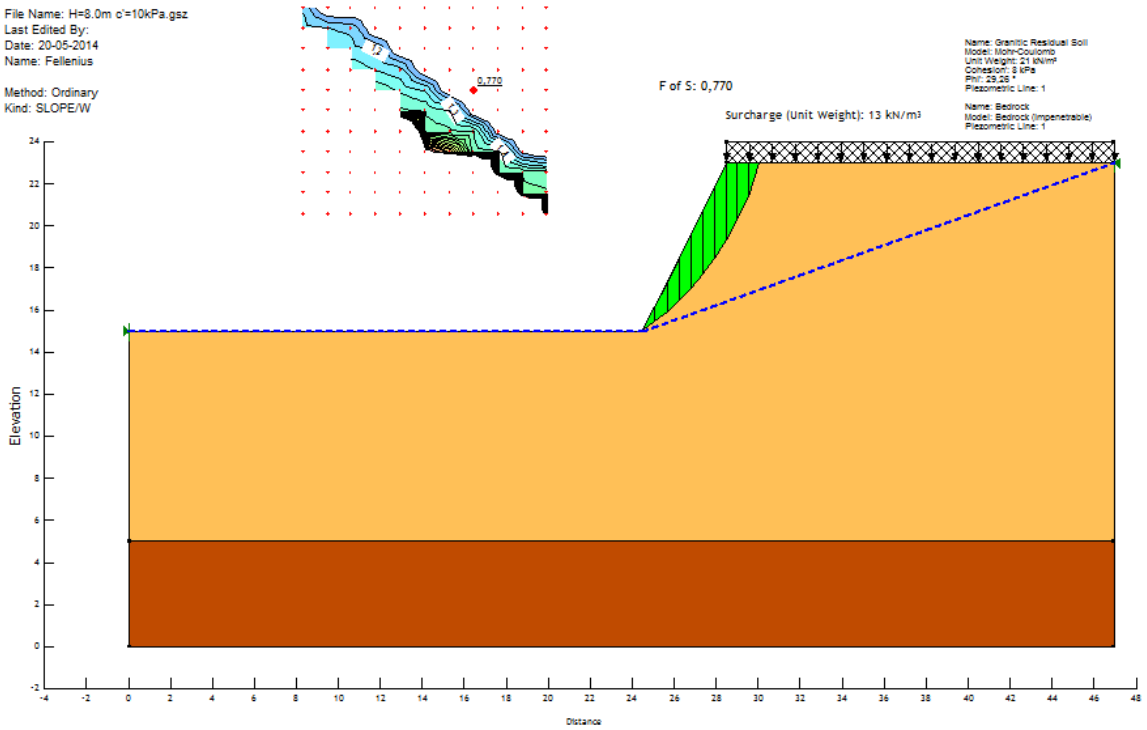
File Name: H=8.0m c'=10kPa.gsz
Last Edited By:
Date: 20-05-2014
Name: Fellenius
Method: Ordinary
Kind: SLOPE/W
0,770
F of S: 0,770
Surcharge (Unit Weight): 13 kN/m³
Name: Granitic Residual Soil
Model: Mohr-Coulomb
Unit Weight: 21 kN/m³
Cohesion: 8 kPa
Phi': 29,26 °
Piezometric Line: 1
Name: Bedrock
Model: Bedrock (Impenetrable)
Piezometric Line: 1
Elevation
Distance

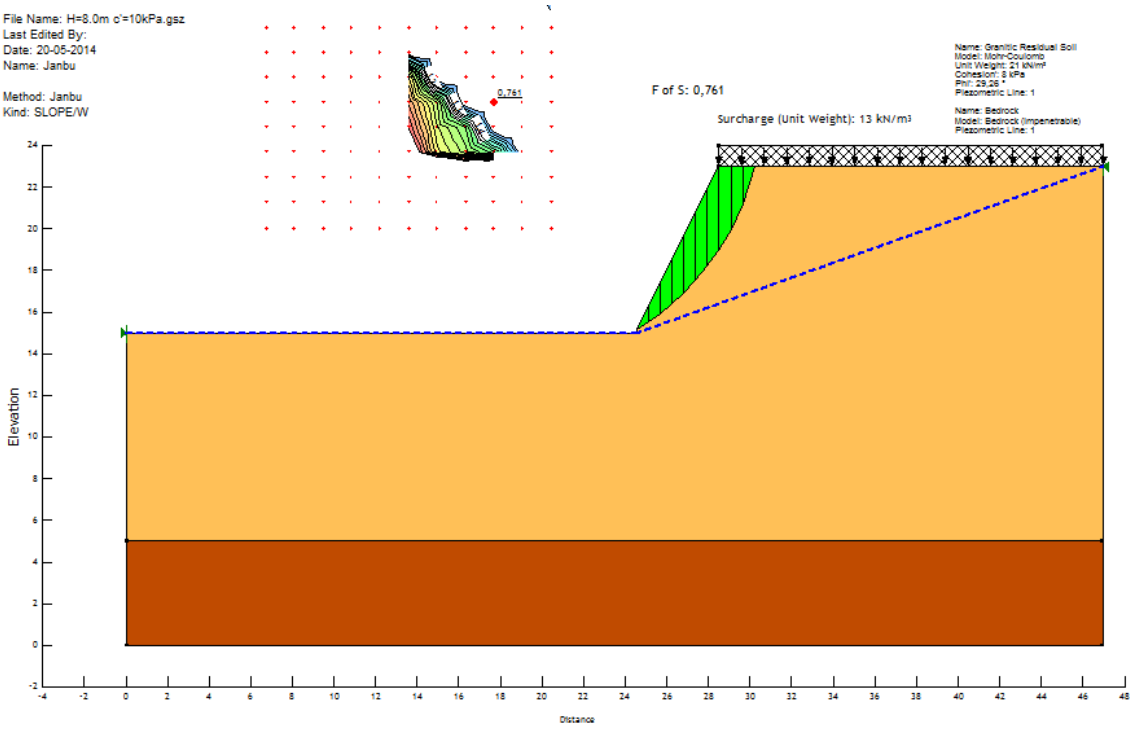
File Name: H=8.0m c'=10kPa.gsz
Last Edited By:
Date: 20-05-2014
Name: Janbu
Method: Janbu
Kind: SLOPE/W
0,761
F of S: 0,761
Surcharge (Unit Weight): 13 kN/m³
Name: Granitic Residual Soil
Model: Mohr-Coulomb
Unit Weight: 21 kN/m³
Cohesion: 8 kPa
Phi': 29,26 °
Piezometric Line: 1
Name: Bedrock
Model: Bedrock (Impenetrable)
Piezometric Line: 1
Elevation
Distance

C.4.3 High water table

Slope height 8.0m

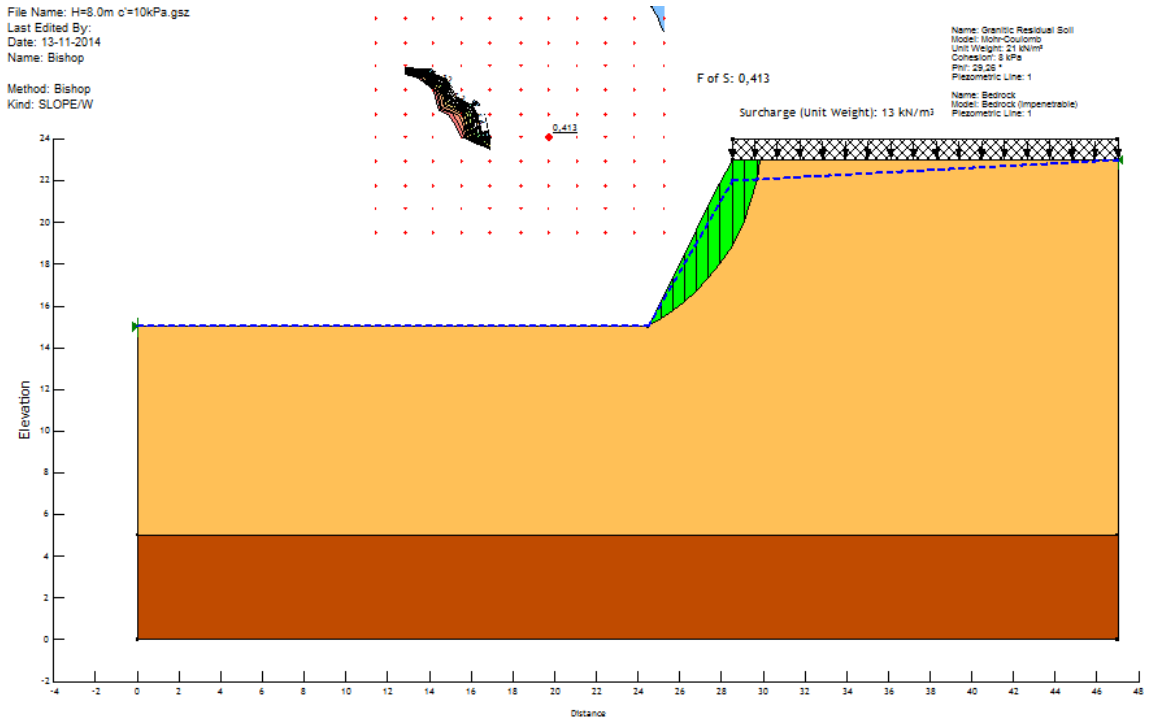

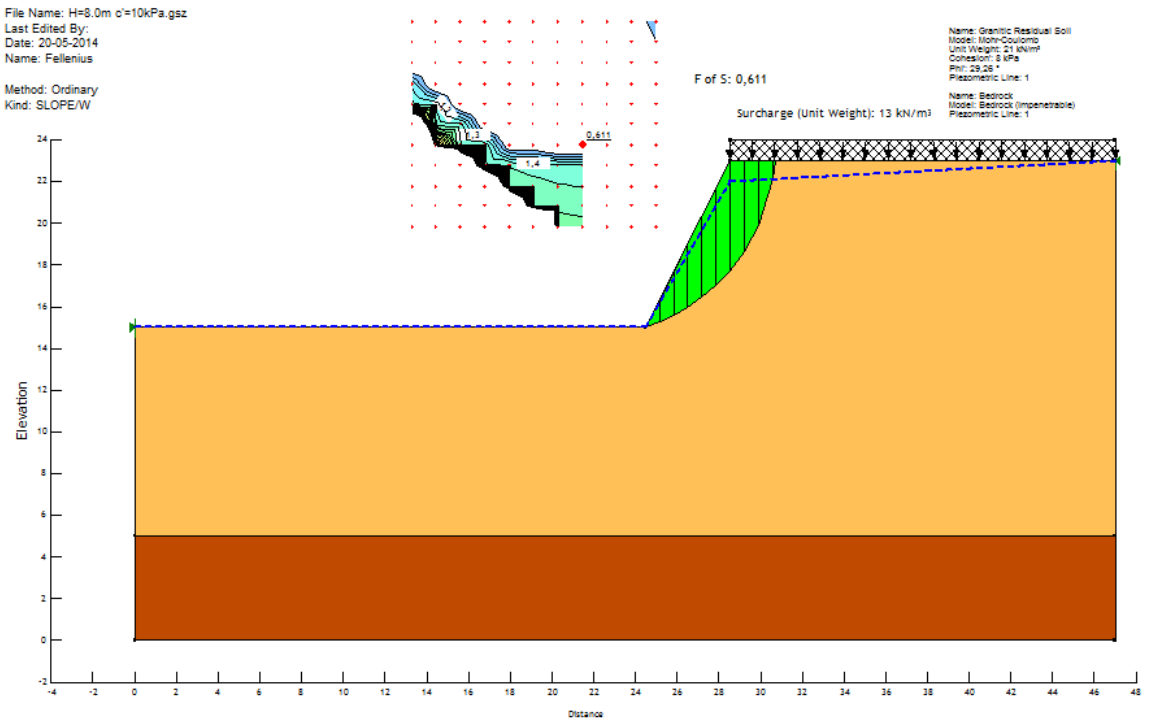

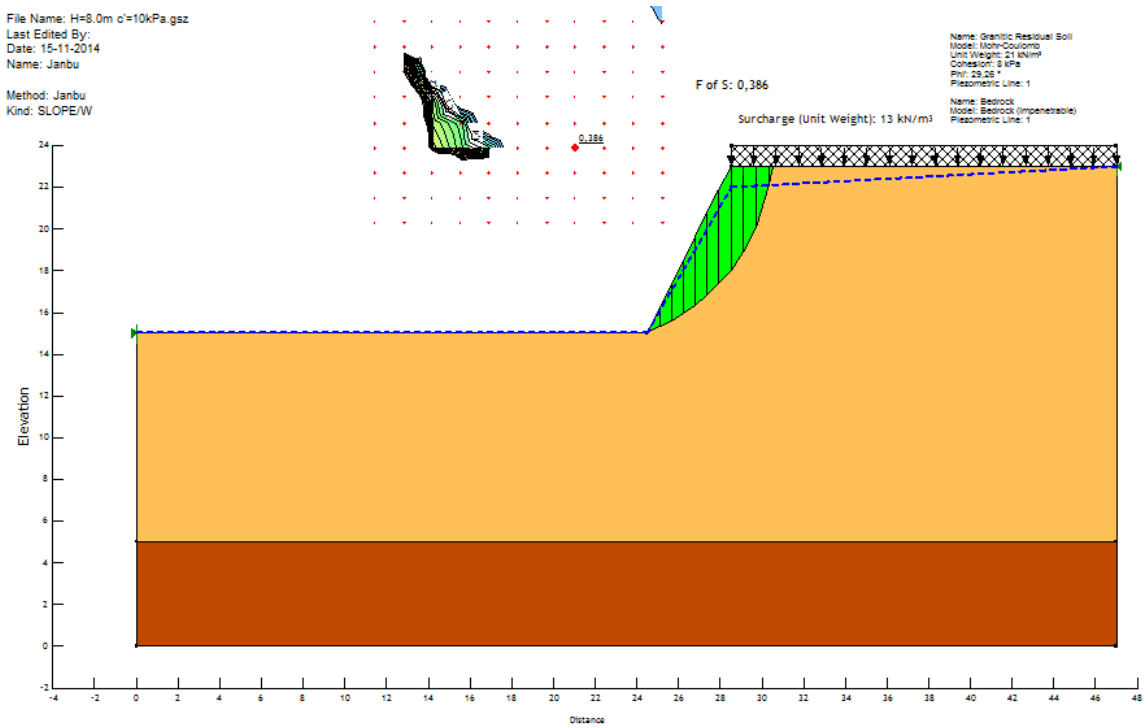
File Name: H=8.0m c'=10kPa.gsz
Last Edited By:
Date: 15-11-2014
Name: Janbu
Method: Janbu
Kind: SLOPE/W
F of S: 0,386
Surcharge (Unit Weight): 13 kN/m³
Name: Granitic Residual Soil
Model: Mohr-Coulomb
Unit Weight: 21 kN/m³
Cohesion: 8 kPa
Phi': 29,26 °
Piezometric Line: 1
Name: Bedrock
Model: Bedrock (Impenetrable)
Piezometric Line: 1
0,386
Elevation
Distance

Appendix D – Comparative analysis of FEM results

D.1 Effect of surcharge on slope's crest

Table D1. Reduction in MoS for changes in applied surcharge.

Reduction in MoS for changes in surcharge									
Slope height	Effective cohesion = 0kPa			Effective cohesion = 5kPa			Effective cohesion = 10kPa		
	Slope angle			Slope angle			Slope angle		
	1(V):2(H)	1(V):1.5(H)	1(V):1(H)	1(V):2(H)	1(V):1.5(H)	1(V):1(H)	1(V):2(H)	1(V):1.5(H)	1(V):1(H)
Applied surcharge = 5kPa							**No groundwater**		
5	20.0%	-	-	2.5%	1.6%	-	2.7%	2.7%	2.3%
8	12.7%	-	-	0.7%	0.8%	-	2.0%	1.2%	1.0%
Applied surcharge = 5kPa							**Low water table**		
5	17.1%	-	-	1.5%	1.2%	-	2.1%	2.2%	2.5%
8	7.6%	-	-	2.3%	2.8%	-	1.0%	1.0%	0.0%
Applied surcharge = 5kPa							**High water table**		
5	-	-	-	1.2%	-	-	1.9%	-0.4%	-
8	-	-	-	-	-	-	1.7%	-	-
Applied surcharge = 10kPa							**No groundwater**		
5	32.2%	-	-	5.6%	4.6%	-	6.2%	6.3%	4.7%
8	27.3%	-	-	3.0%	2.6%	-	3.7%	1.8%	1.6%
Applied surcharge = 10kPa							**Low water table**		
5	29.2%	-	-	4.9%	2.9%	-	6.3%	5.1%	5.0%
8	22.9%	-	-	4.0%	2.0%	-	3.5%	3.6%	2.7%
Applied surcharge = 10kPa							**High water table**		
5	-	-	-	3.9%	-	-	4.1%	4.6%	-
8	-	-	-	-	-	-	3.5%	-	-

D.2 Effect of groundwater level

Table D2. Reduction in MoS for changes in groundwater levels.

Reduction in MoS for changes in groundwater levels									
Slope height	Effective cohesion = 0kPa			Effective cohesion = 5kPa			Effective cohesion = 10kPa		
	Slope angle			Slope angle			Slope angle		
	1(V):2(H)	1(V):1.5(H)	1(V):1(H)	1(V):2(H)	1(V):1.5(H)	1(V):1(H)	1(V):2(H)	1(V):1.5(H)	1(V):1(H)
Applied surcharge = 0kPa							**Low water table**		
5	3.7%	-	-	6.9%	1.4%	-	8.2%	3.3%	-0.1%
8	5.6%	-	-	12.3%	4.1%	-	14.7%	5.6%	0.1%
Applied surcharge = 0kPa							**High water table**		
5	-	-	-	30.6%	-	-	29.1%	29.2%	-
8	-	-	-	-	-	-	35.5%	-	-
Applied surcharge = 5kPa							**Low water table**		
5	0.3%	-	-	5.9%	1.0%	-	7.6%	2.7%	0.0%
8	0.1%	-	-	13.8%	6.1%	-	13.8%	5.4%	-0.9%
Applied surcharge = 5kPa							**High water table**		
5	-	-	-	29.6%	-	-	28.5%	26.9%	-
8	-	-	-	-	-	-	35.4%	-	-
Applied surcharge = 10kPa							**Low water table**		
5	-0.5%	-	-	6.2%	-0.4%	-	8.3%	2.1%	0.2%
8	-0.1%	-	-	13.2%	3.5%	-	14.5%	7.4%	1.2%
Applied surcharge = 10kPa							**High water table**		
5	-	-	-	29.4%	-	-	27.5%	27.9%	-
8	-	-	-	-	-	-	35.1%	-	-